DOE/NASA/0261-1
NASA CR-168285
CTR 0747-84003

ADVANCED AUTOMOTIVE DIESEL ASSESSMENT PROGRAM

R. Sekar
L. Tozzi
Cummins Engine Company, Inc.

December, 1983

Prepared for
NATIONAL AERONAUTICS AND SPACE ADMINISTRATION
Lewis Research Center

Under DOE Contract DEN 3-261

for
U.S. DEPARTMENT OF ENERGY
Conservation and Renewable Energy
Office of Vehicle and Engine R & D

1. Report No.	2. Government Accession No.	3. Recipient's Catalog No
NASA CR No. 168285		

4. Title and Subtitle	5. Report Date
Advanced Automotive Diesel Assessment	December, 1983
	6. Performing Organization Code

7. Author(s)	8. Performing Organization Report No
R. Sekar R. Kamo L. Tozzi	
	10. Work Unit No.

9. Performing Organization Name and Address	11. Contract or Grant No.
Cummins Engine Company, Inc. Box 3005 Columbus, IN 47202	DEN3-261
	13. Type of Report and Period Covered
12. Sponsoring Agency Name and Address	Contractor Final Report
U.S. Department of Energy Office of Vehicle and Engine R&D Washington, D.C. 20585	14. Sponsoring Agency Code DOE/NASA/0261-1

15. Supplementary Notes

Monitoring Agency: NASA Lewis Research Center
21000 Brookpark Road
Cleveland, OH 44135
Mr. James C. Wood, Project Manager

16. Abstract

Cummins Engine Company completed an analytical study to identify an advanced automotive (light duty) diesel (AAD) power plant for a 3,000-pound passenger car. The study has resulted in the definition of a revolutionary diesel engine with several novel features. A 3,000-pound car with this engine is predicted to give 96.3, 72.2, and 78.8 MPG in highway, city, and combined highway-city driving, respectively. This compares with current diesel powered cars yielding 41.7, 35.0, and 37.7 MPG. The time for 0-60 MPH acceleration is 13.9 sec. compared to the baseline of 15.2 sec. Four technology areas were identified as crucial in bringing this concept to fruition. They are: (1) part-load preheating, (2) positive displacement compounding, (3) spark assisted diesel combustion system, and (4) piston development for adiabatic, oilless diesel engine. Marketing and planning studies indicate that an aggressive program with significant commitment could result in a production car in 10 years from the date of commencement.

17. Key Words (Suggested by Author(s))	18. Distribution Statement
Car Light Duty Vehicle Diesel Adiabatic Engine	Unclassified - Unlimited

19. Security Classif. (of this report)	20. Security Classif. (of this page)	21. No. of pages	22. Price*
Unclassified	Unclassified		

*For sale by the National Technical Information Service, Springfield, Virginia 22161

DOE/NASA/0261-1
NASA CR NO. 168285

FINAL REPORT

Advanced Automotive Diesel Assessment Program

by

R. Sekar
L. Tozzi

Principle Investigator: R. Kamo

Cummins Engine Company, Inc.
Columbus, Indiana

Contract No.: DEN 3-261

Sponsored by the Department of Energy

Monitored by NASA Lewis Research Center
Cleveland, Ohio

NASA Project Manager: James C. Wood

December, 1983

TABLE OF CONTENTS

TABLE OF CONTENTS (Continued)

FOREWORD

This final report covers all the analysis, design, drafting, and market studies conducted by Cummins and its subcontractors to fulfill the requirements of Contract DEN3-261 between the Department of Energy/NASA-Lewis Research Center and Cummins Engine Company.

The D.O.E. officers responsible for this program are Mr. A. A. Chesnes and Mr. E. W. Gregory II. Project Management was overseen by NASA-Lewis Research Center, Cleveland, Ohio. The NASA Lewis Research Center project manager was Mr. James C. Wood.

The Principal Investigator at Cummins was Mr. Roy Kamo and the Program Manager was Mr. Raj Sekar. The authors would like to acknowledge the valuable contributions of the following members of the Cummins team: Mr. D. M. Conner, Mr. R. E. Glasson, Mr. R. B. Jackson, Mr. P. C. McKavoy, Mr. D. L. Morin, Mr. P. R. Richart, Mr. G. L. Starr, and Mr. J. J. White. In addition, the authors would like to acknowledge the valuable contributions of the following subcontractors outside of Cummins for their significant contributions during this study: Mr. D. Davies and Mr. G. Peitch of Ford Motor Company, Mr. J. Wurm and Mr. T. Bulicz of the Institute of Gas Technology, Professor T. Priede of the Institute of Sound and Vibration Research, Mr. J. Edwards of Sir W. G. Armstrong Whitworth Ltd., and Mr. Michael G. May of Laboratoire de Recherches.

LIST OF FIGURES

LIST OF FIGURES (Continued)

LIST OF TABLES

LIST OF APPENDICES

D1

EXECUTIVE SUMMARY

The objectives of this analytical study were: (1) to select one advanced automotive diesel engine (A.A.D.) concept which would increase the tank mileage (mpg) of a 3,000 pound (lbm) passenger car from the present 35 mpg to at least 52 mpg; (2) to identify long term component research and development work required to bring the selected concept to fruition, and (3) to prepare a development strategy that will bring the selected concept to a prototype testing phase.

Cummins Engine Company has completed this study. The selected concept is a 4 stroke cycle, direct injection, spark assisted, advanced adiabatic diesel engine with positive displacement compounding plus expander and part load air preheating. The engine does not use a liquid coolant nor liquid lubricants. It is a 4 cylinder, in-line, 77 mm bore x 77 mm stroke, 1.434 liters displacement engine weighing 300 lb, and rated at 70 BHP at 3000 rpm. Installation dimensions are 621 mm length x 589 mm width x 479 mm height (24.4 inch x 22 inch x 18.9 inch)

The key aspect of this advanced diesel engine is the high temperature ceramic concepts which yields both in-cylinder efficiency improvements and a substantial improvement in available exhaust energy. This energy is recovered through a high efficiency helical screw type expander which is connected by belt to the crankshaft. The exhaust energy is also used to preheat the intake charge air. Analysis indicates this to be an excellent means of improving fuel consumption at part load. Based on the recommendation from Mr. Michael G. May, Laboratoire de Recherches, and earlier Cummins analyses, a spark assisted, high swirl, relatively low fuel injection pressure diesel combustion system is used. Oil-less operation of the engine results in reducing frictional and parasitic losses. The engine with all these features is predicted to have a BSFC of 0.275 lbm/bhp-hr (169 g/kw-hr) at rated power (70 bhp at 3000 rpm), an average BSFC of 0.260 lbm/bhp-hr (158 g/kw-hr) at cruising speed (55 MPH), and a minimum BSFC of 0.238 lbm/bhp-hr.

Ford Motor Company, under a subcontract to Cummins, prepared vehicle installation layout drawings with this engine installed in the 1984 TOPAZ vehicle. Also included in the vehicle drawings are the layouts of Ford's advanced designed Continuously Variable Transmission (CVT) and also their electronic distributor system.

Performance analysis of this engine and this Ford vehicle was completed using both the Cummins Diesel Cycle Simulation (DCS) and Ford's Vehicle Performance Analysis computer programs. The predicted combined metro-highway driving cycle is 78.8 mpg using city and

highway mileages of 72.2 and 96.3 mpg, respectively. The 0-60 MPH acceleration time is predicted to be 13.9 seconds. These values compare favorably to a baseline vehicle with a typical current indirect injection (IDI) diesel engine which gives 35.0 mpg (city), 41.7 mpg (highway), and 37.7 mpg (combined). The 0-60 MPH acceleration time for the baseline vehicle is 15.2 seconds.

Theoretical modeling of the predicted emissions for the A.A.D. indicates that: (1) the HC will be 0.13 gms/mile, (2) the CO will be 1.30 gms/mile, and (3) the particulates will be 0.18 gms/mile. These all compare favorably with the EPA Research Target Values for HC; CO; particulates of: 0.4 gms/mile; 3.4 gms/mile, 0.2 gms/mile respectively. However, the predicted value of NO_x for the A.A.D. is 1.65 gms/mile which is above EPA's Research Target for NO_x of 1.0 gms/mile. This is a potential problem. Hence, methods such as exhaust gas recirculation or retarded injection timing would have to be experimentally investigated in an effort to meet this target.

A complete development strategy was done to bring the A.A.D. engine through the proof of concept phase. This was done by Cummins and Ford primarily based on marketing and economic analyses. The conclusion developed here is that this advanced diesel engine would be a viable candidate for large 3000 pound luxury cars, light trucks, and vans. The market potential for these classes of vehicles is 156,000 to 546,000 per year assuming a dieselization rate of 5% to 15% by 1993. This study also concluded that a cost premium of $1500-1800 per vehicle is justifiable as an option price in the early stages, dropping rapidly to less than $1000. An aggressive schedule, with significant resource commitments, will lead to first production vehicles in 1993.

Ceramic technology development is critical to this advanced engine and is being worked on in other programs. The stress analysis done on the critical components in the A.A.D. engine using available ceramic data indicates that the engine would be successful. In addition to ceramics, the following long lead technology areas were identified and should be experimentally verified simultaneously with a prototype engine development program: (1) alternative piston designs for an oil-less, adiabatic, minimum friction engine, (2) a positive displacement compounding and expander system, (3) intake air preheating, (4) high swirl "fast" combustion system with ignition assist. These experimental verifications are important because of the lack of highly sophisticated analytical techniques. Emphasis of these experiments should be on emissions and durability characteristics of the A.A.D. engine and its major components.

1.0 INTRODUCTION

In June, 1982, a contract was awarded to Cummins by the Department of Energy (D.O.E.) through NASA-Lewis Research Center to identify an advanced automotive diesel powertrain that has the potential to meet or exceed the following criteria and to provide a development strategy for the same:

1. A 50% improvement in fuel economy in the Combined Federal Driving Cycle relative to the baseline diesel vehicle mileage of 35 mpg.

2. Reliability, life, and driveability comparable to automotive powertrains currently on the market.

3. Noise and safety levels that are currently legislated.

4. Initial cost and life cycle cost projections comparable to conventionally powered automobiles at the time of market introduction.

5. Federal emission research targets of 0.4, 3.4, 1.0, and 0.2 gms/mile for HC, CO, NOx, and particulates, respectively.

The following five subcontracts were awarded in order to assist Cummins in this study.

1. Ford Motor Company - (1) to assist in vehicle integration of the engine, (2) to provide consulting service regarding passenger cars and (3) to develop a market introduction strategy.

2. Institute of Gas Technology, Chicago - to analyze, design, and lay out a helical screw compressor and expander for this engine.

3. Institute of Sound and Vibration, Southampton, UK - to conduct a noise evaluation of the engine.

4. Mr. Michael G. May, Switzerland - to conduct experiments on a spark assisted diesel combustion chamber system .

5. Sir W. G. Armstrong Whitworth, UK - to study the feasibility of a 2 stroke-opposed piston engine concept for this potential application.

In order to conduct the study in an orderly manner, the program was divided into the following six subtasks:

Task I - Basic Powertrain Definition - Based on a literature survey and previous experience, Cummins will select three basic concepts for further analysis.

Task II - Powertrain Analysis - Brief performance analyses will be conducted on the selected concepts. Then, based on approved criteria, one concept will be chosen for further detailed study.

Task III-A & B - A. Vehicle System Characterization - The chosen engine system will be studied in detail including design drawings, performance analysis, and thermal plus mechanical stress analyses. Vehicle installation layouts will also be made. B. Cost estimates will be generated for the chosen design.

Task IV - Based on a market study, a long range development and marketing strategy will be prepared to bring the engine and vehicle to a prototype stage.

Task V - Critical long-term development R & D technologies relative to the engine will be identified.

Task VI - Monthly reports and a final report.

This final report contains all the essential aspects of the study. The material is presented essentially in the same order in which the tasks were carried out. The design, performance, and specification details of the chosen A.A.D. are presented in Section 4.1. Several of the individual studies done by various Cummins and subcontractor personnel are documented in the appendices. These appendices are briefly summarized at appropriate sections of the report. All the engine design layout drawings are presented in Appendix 6.

2.0 TASK I - BASIC POWERTRAIN DEFINITION

Cummins surveyed the various power plant options and compared their potential for meeting the objectives of this program. This section of the report documents the details covered.

2.1 Computation of Power Requirement

The first subtask was to compute the brake horsepower (bhp) needed to drive a 3000 lbm vehicle while also meeting the other requirements. This was found from fundamental vehicle dynamics that about 80 bhp is needed when using the 0-60 MPH acceleration criteria as the decisive factor. For cruising at 55 MPH, an engine horsepower of about 20 bhp was also found to be sufficient.

2.2 Candidate Engine Technologies

The following diesel engine systems and features were included in the survey and brief analysis:

- Two stroke opposed-piston swing beam engine
- Indirect vs. direct injection
- Adiabatic concept - different levels of internal insulation
- Turbocompound system
- Minimum friction design with oil-less operation
- Multifuel concepts
- Variable displacement
- Miller Cycle
- Different charge air systems
  - Turbocharger with waste gate
  - Positive displacement compressor and expander
  - Comprex Supercharger
- High pressure vs. low pressure injection systems
- Use of ceramics - coatings, composites, monolithic ceramics, etc.

The first cut preliminary evaluation of all of the above concepts was done for the following characteristics in that order of importance:

Fuel Economy (mpg), Emissions, Cost, Driveability, Size/Weight, Noise Level, Reliability/Durability and Multifuel Capability

2.3 Results of Basic Powertrain Definition

The survey of Task I resulted in three basic engine concepts considered most suitable for further study. These are:

1. Concept "A": - 2.5 litre, comprex supercharged, 3 cylinder engine with 18:1 compression ratio. Uncooled engine with Ford's Continuously Variable Transmission (CVT).

2. Concept "B": - 1.4 litre, 4 cylinder in-line, compression ratio 14:1

   - Adiabatic design, spark assisted diesel combustion concept (Figure 1)

   - Oil-less engine design for low friction requires a special piston with a crosshead (Figures 2 and 3)

3. Concept "C": - 1.1 litre, turbocharged, aftercooled, two stroke, opposed piston, swing beam engine, 4 cylinder,

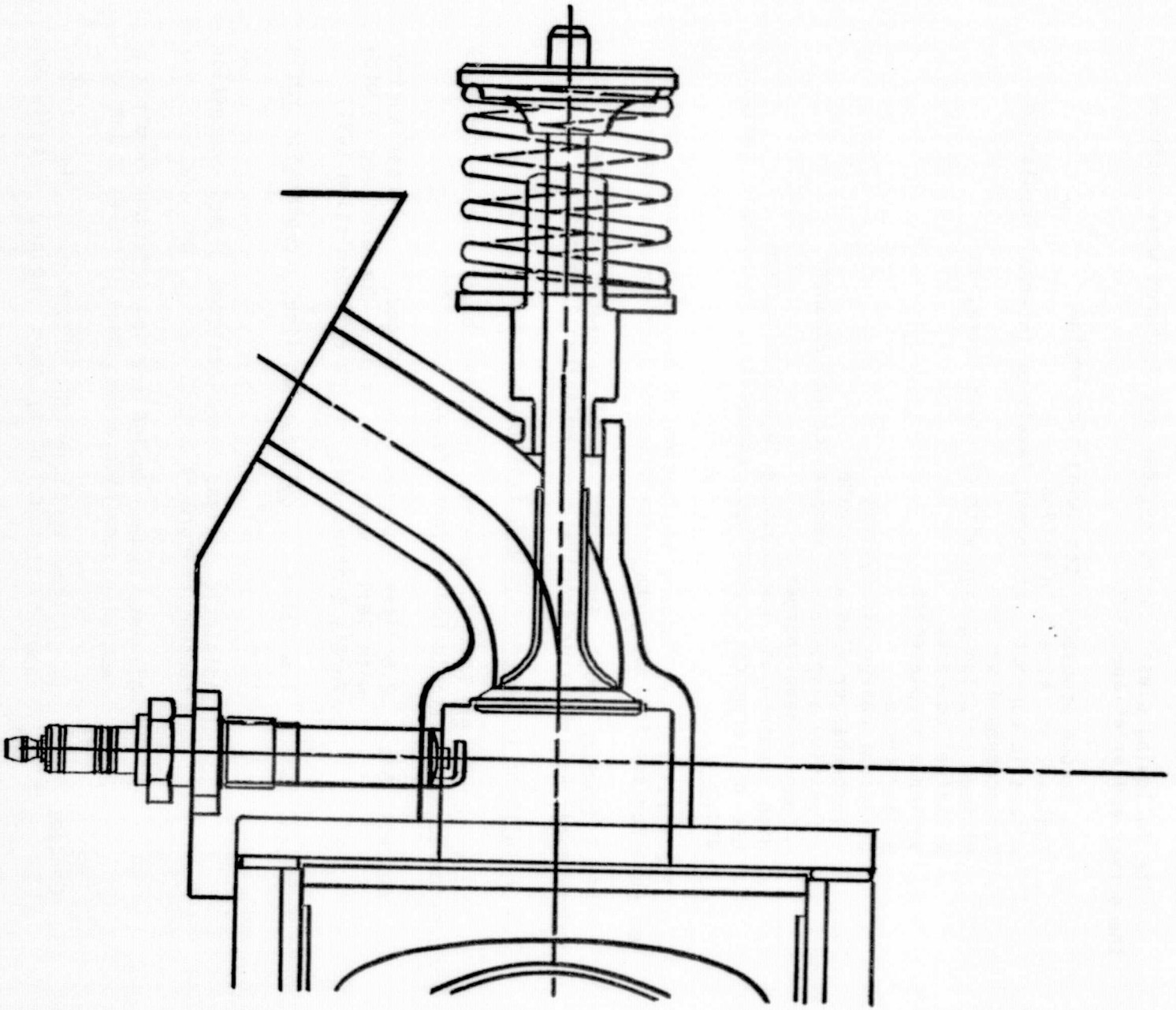

FIGURE 1. Combustion Chamber Configuration

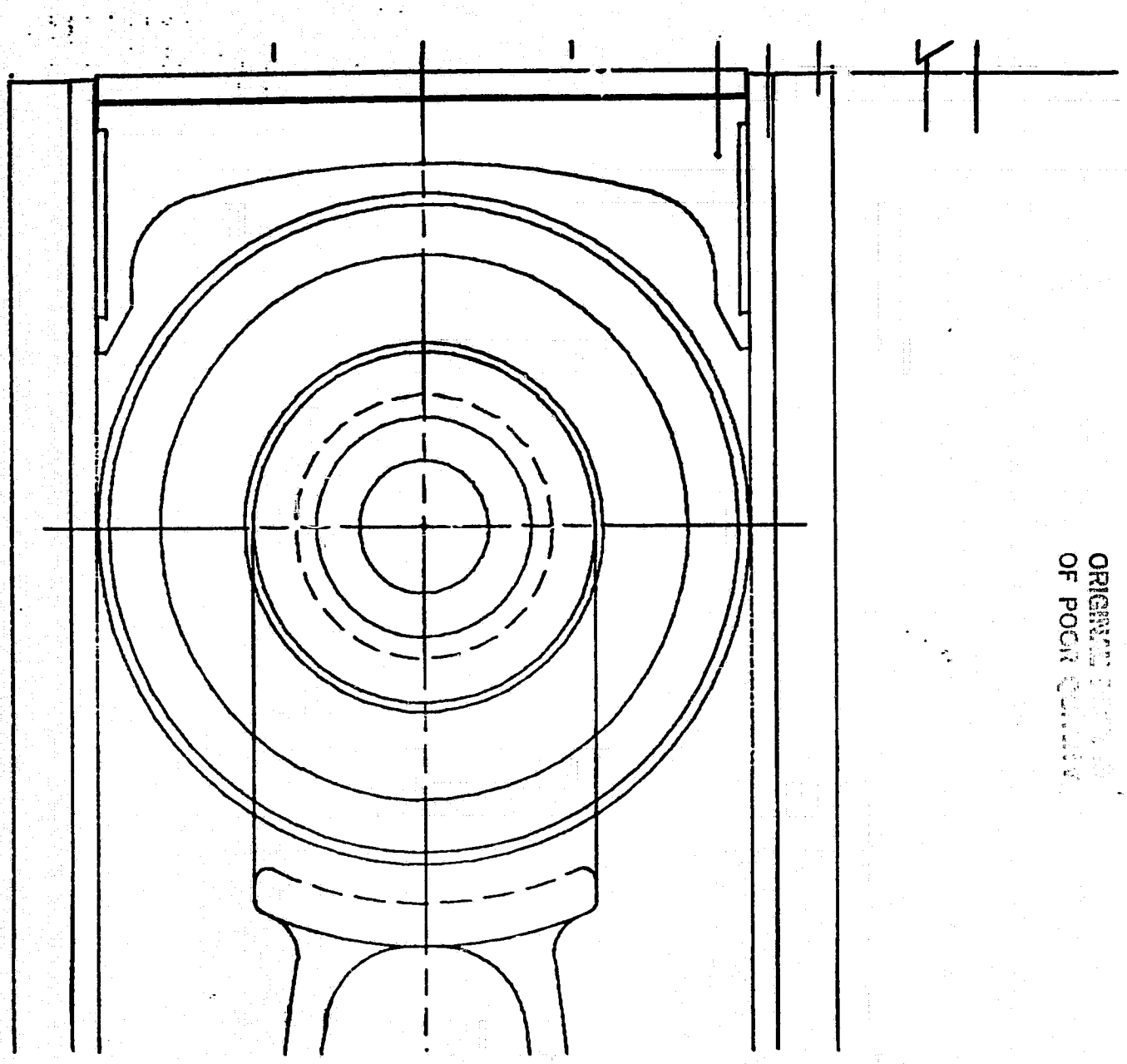

FIGURE 2. Piston with Rolling Cross - Head

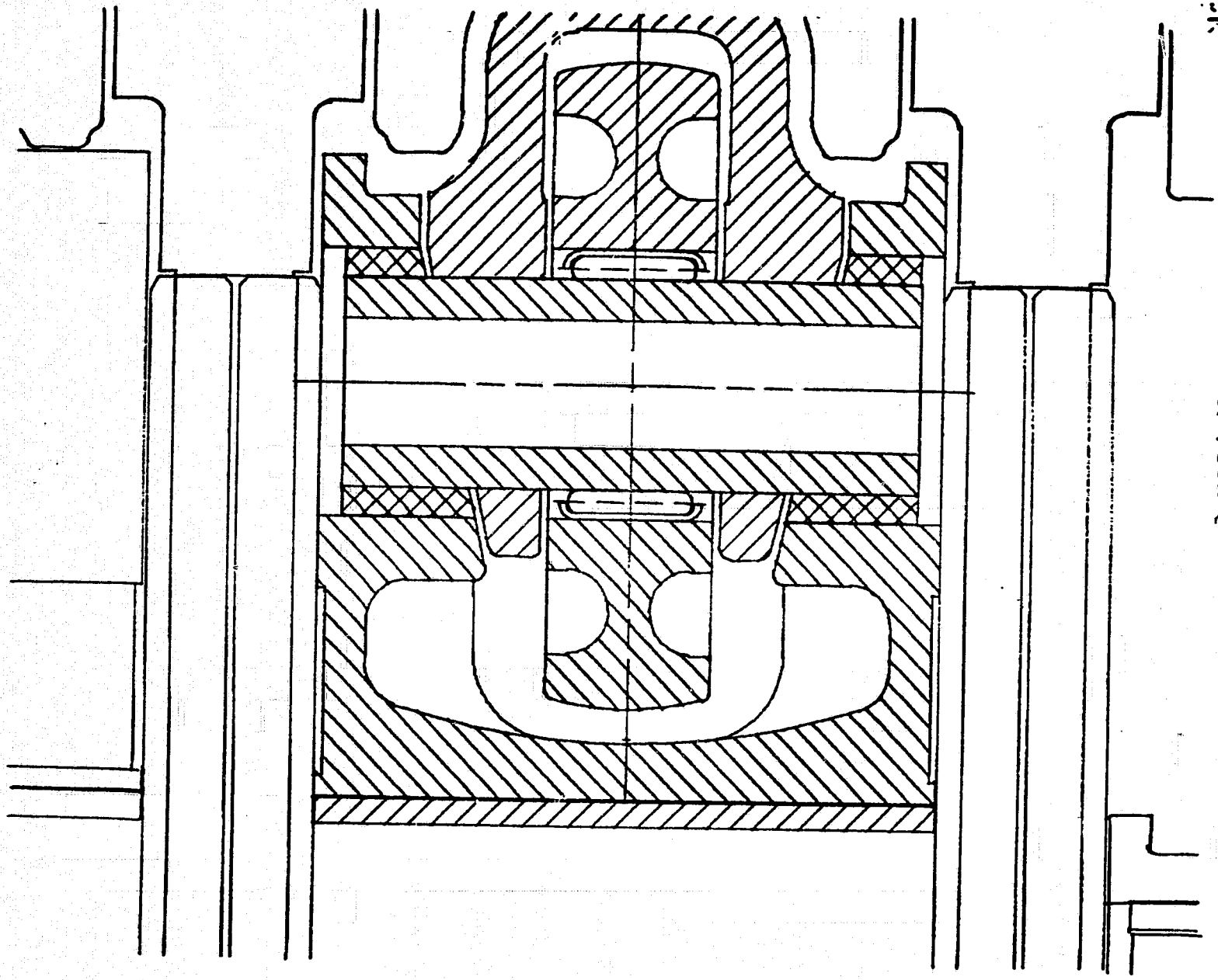

FIGURE 3. Cross - Section of Piston with Rolling Cross Head

compression ratio 14:1. This was analyzed by a subcontractor (Appendix 3).

No detailed quantified mathematical analysis was done in Task I. Engineering judgements, subjective evaluations, and published information were utilized in evaluating each concept for each of the eight criteria. The three concepts, A, B, and C, turned out to be equally good based on these qualitative evaluations.

3.0 TASK II - POWERTRAIN ANALYSIS

The main thrust of this task was to analyze the three concepts selected in Task I above. All three concepts were evaluated on the basis of the five criteria mentioned in Section 1.0. Task II was carried out as quantitatively as possible on a preliminary basis.

Preliminary fuel maps were generated using the Cummins Diesel Cycle Simulator (DCS) computer program (Ref. 1). DCS is a well proven computer analysis tool for 4 stroke, direct injection, turbocharged, diesel engines and has been successfully used at Cummins for both experimental as well as production engines. These fuel maps are shown in Figures 4 and 5 for Concepts "A" and "B" respectively. The fuel map for Concept "C" presented in Figure 6 was calculated by the subcontractor using the concepts discussed in Appendix 3. These fuel maps were provided to Ford. Together with the base vehicle characteristics, the continuously variable transmission performance curves, and these fuel maps, Ford utilized their Federal Driving Cycle Simulation computor program to obtain the preliminary estimates of mpg and driveability data for Concepts "A", "B", and "C".

The results are presented in Tables 1 and 2. Qualitative comparison of all the results in Tables 1 and 2 indicated that Concept "B" was the preferred approach based on a comparison using a linear average weight analysis technique. A baseline state-of-the-art turbocharged IDI diesel engine is also included in Table 1 for comparison purposes.

Since Concept "B" was selected as preferred, it will be the topic for the remainder of the main body of this final report.

3.1 Thermodynamic Cycle Analysis - Final Prediction for Concept "B"

Most of the thermodynamic analysis was done using the Cummins Diesel Cycle Simulator (DCS) (Ref. 1)*. This program was used in the "analysis mode" in which the engine geometrical features and air inlet conditions are specified with the engine performance and in-cylinder history printed as output. The geometrical features necessary for

---

* References are listed at the endd of the main body of the report.

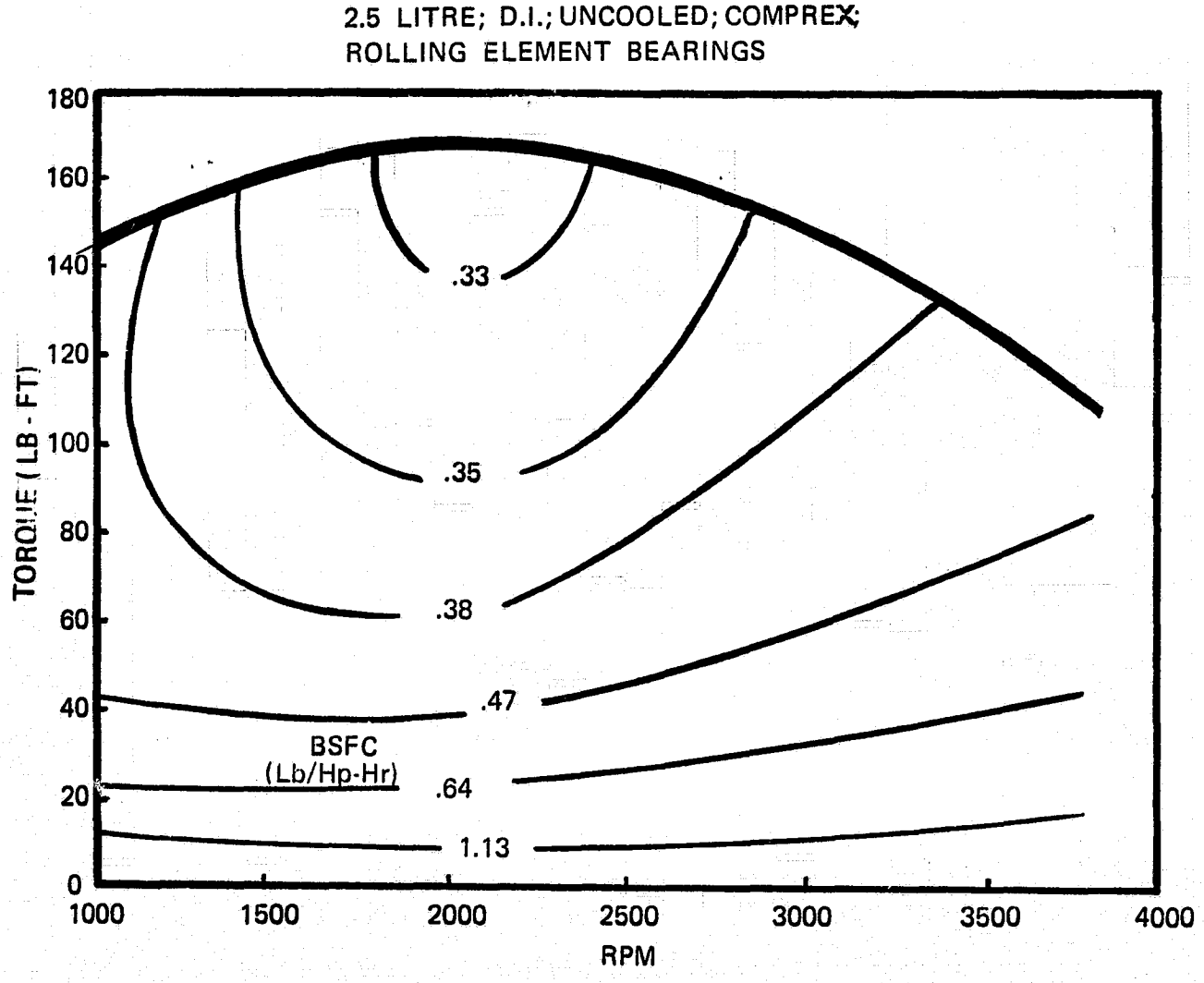

FIGURE 4. Concept "A" Engine Fuel Map - FINAL PREDICTION

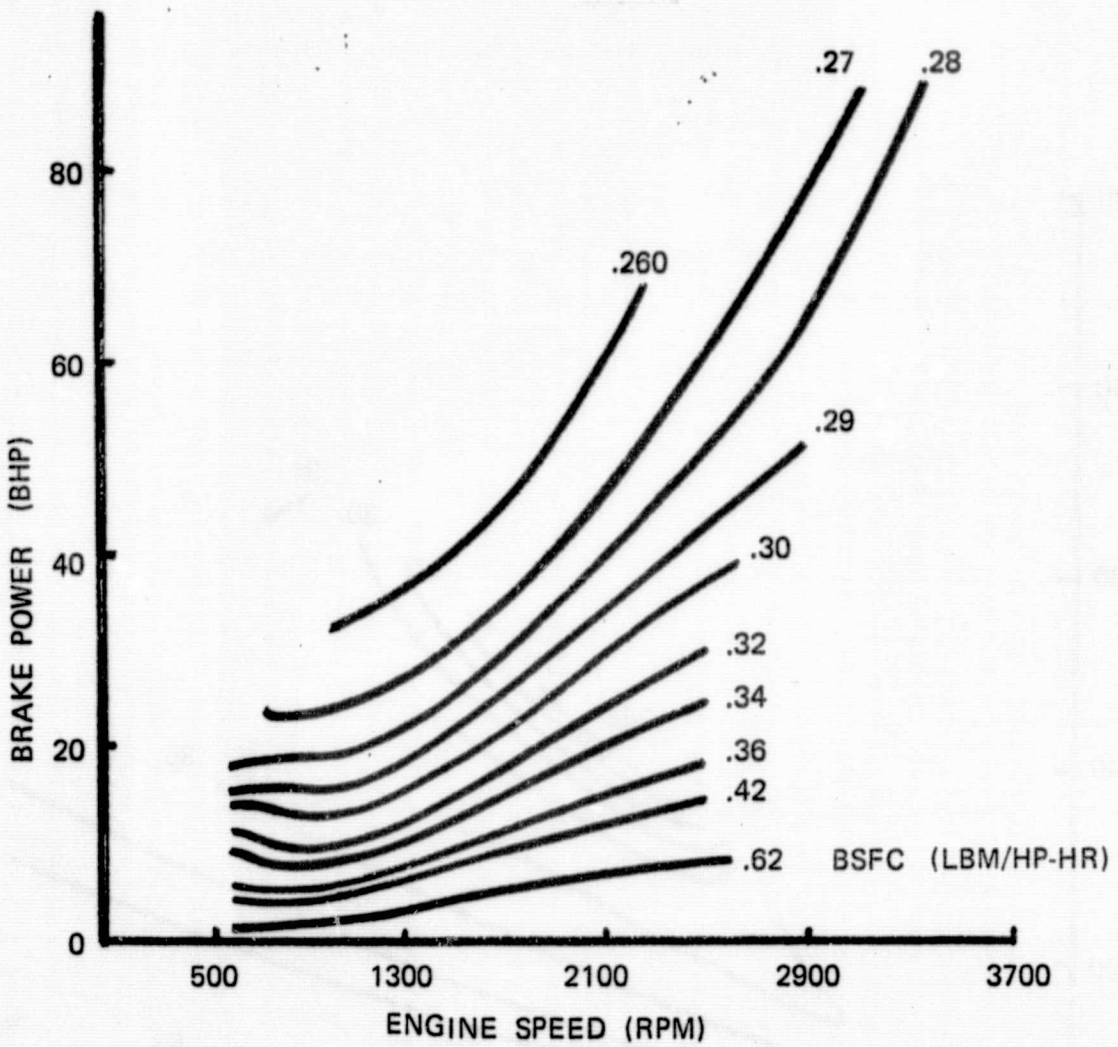

FIGURE 5. Concept "B" Engine Fuel Map - PRELIMINARY ESTIMATE

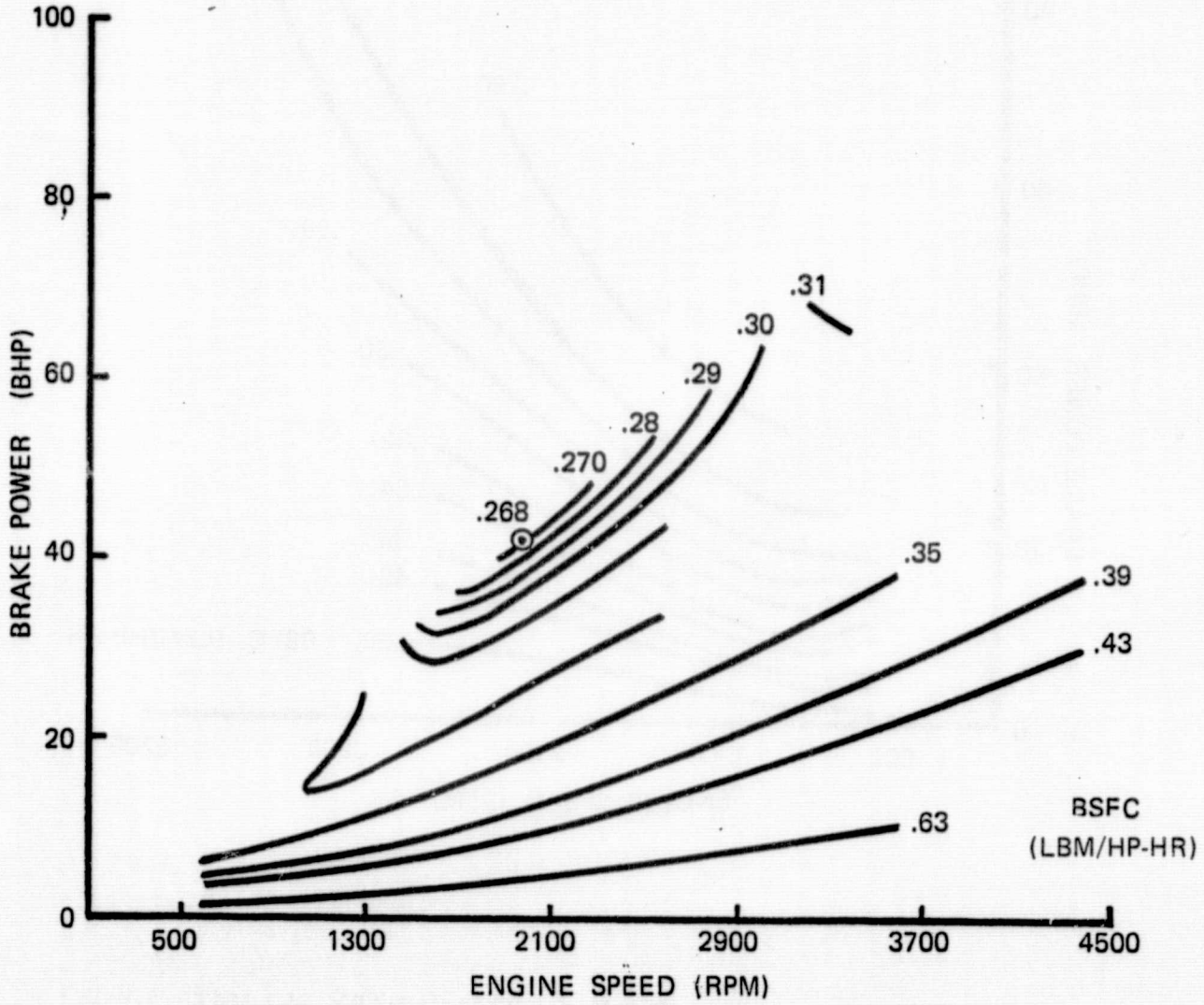

FIGURE 6. Concept "C" Engine Fuel Map - FINAL PREDICTION

TABLE 1. Comparison of Three Engine Concepts

EVALUATION CRITERIA	EPA RESEARCH TARGET	BASELINE I.D.I., TURBO-CHARGED DIESEL	CONCEPT "A" UNCOOLED ENGINE WITH COMPREX	CONCEPT "B" FOUR STROKE ADIABATIC ENGINE	CONCEPT "C" TWO STROKE OPPOSED PISTON ENGINE
1. FUEL ECONOMY IN COMBINED FEDERAL DRIVING CYCLE (MPG)	≥52.5	THEORECTICAL 35.0 MEASURED 37.7	PRELIMINARY ESTIMATE 46.7 FINAL PREDICTION 45.2	PRELIMINARY ESTIMATE 69.5 FINAL PREDICTION 78.8	PRELIMINARY ESTIMATE 53.0 FINAL PREDICTION 60.0
2. EMISSIONS - GMS/MILE					
HC	0.4	0.28	0.22	0.13	0.13
CO	3.4	1.33	1.30	1.30	?
NO_x	1.0	1.47	1.20	1.65	1.10
PARTICULATES	0.2	0.36	0.18	0.18	?
3. COST RELATIVE TO BASELINE	Comparable	100	115	120	120
4. DRIVEABILITY - TIME FOR 0 TO 60 MPH ACCELERATION (SECONDS)	15.0	15.2	13.4	12.6 (Preliminary Estimate)	15.0
5. (a) SIZE			Comparable 24" x 12" x 18½"	Comparable 22" x 12" x 18½"	Larger 17.7"x 25.2"x21.6"
(b) DRY WEIGHT (LBS)	Comparable To	325	284	300	308
(c) WET WEIGHT (LBS)	Baseline	354	292	300	316
6. NOISE DBA AT 3 FT.	90	92	88	88	88
7. RELIABILITY/DURABILITY MAJOR FAILURE					
B-10 LIFE	60,000 Miles	50,000 Miles	60,000 Miles	60,000 Miles	40,000 Miles
B-50 LIFE	100,000 Miles	>100,000 Miles	100,000 Miles	100,000 Miles	
8. MULTIFUEL CAPABILITY	Desirable	None	Good	The Best Available	Better

running the program are scaled-down versions of the Case-Cummins B-Series 3.9 Litre engine. The intake manifold pressures and temperatures are optimized at each load and speed to minimize fuel consumption (BSFC). The resulting intake and exhaust manifold temperature, pressure, and air flow history data were forwarded to the Institute of Gas Technology (IGT). The subcontract work by IGT was to design a screw compressor and expander to meet the intake and exhaust manifold pressure and temperature requirements. IGT varied the geometrical features of these components until these performance requirements were satisfied and predicted the efficiencies of these components. Based on these efficiency maps, a second final prediction iteration of the thermodynamic analysis was completed on Concept "B".

TABLE 2. Final Vehicle Performance Comparisons

Powertrain	Fuel Economy, MPG City	Highway	Combined	0-60 MPH Acceleration Time, Seconds
1. Baseline I.D.I. Diesel	35.0	41.7	37.7	15.2
2. Concept "A"	39.3	60.8	45.2	13.4
3. Concept "B"	72.2	96.3	78.8	13.9
4. Concept "C"	53.8	76.3	60.0	17.6

3.2 Powertrain Performance Trade-Off

Since Concept "B" included several novel features resulting in a significant improvement in vehicle performance this concept was analyzed at 4 levels of technology implementation in Appendix 1. Level 3 is considered to be a realistic and attainable combination of novel features. At this level, all the features are included in the engine to the optimum level (Appendix 1). The details of these also gives the sensitivity of engine performance to screw compressor

and expander efficiencies as well as to different heat release shapes. The advanced turbocompound engine study (DOE/NASA/4936-3, Ref. 3) predicts a fuel consumption improvement of 5.6% to 6.8% if a high efficiency screw compressor-expander is used in place of conventional turbocompound turbomachinery.

3.3 Engineering Cost Comparisons

Detailed cost estimates were done only for the selected concept, "B". However, rough cost estimates were made for all three engines based on discussions with the subcontractor and estimates from another program. This initial engine cost comparison is shown in Table 1. The vehicle cost and the life cycle cost estimates are discussed later in the report.

3.4 Risk Analysis of Engine Concept "B"

Concept "B" has several novel, experimentally unproven technologies. Ceramic manufacturing will also be a developmental area and must be researched further. At least four of these technologies have to be proven experimentally: (1) part load preheating, (2) screw compressor-expander design, (3) fast burning spark-assisted combustion system, and (4) piston design for adiabatic, oil-less engine. It has been concluded that a significant schedular risk exists if there is delay in developing any of these technologies. With significant and firm commitment by government and industry, this advanced adiabatic diesel could reach production by 1993. Major component risks are: (1) the screw machinery compounding system and (2) the piston design with ceramic cross head. If these two advanced components do not materialize, the fuel economy projected for this concept could drop by 24%. Also if a positive displacement screw machinery compounding system is absent the driveability will be very poor due to turbocharger lag.

The fuel injection in Concept "B" is accomplished by a Robert Bosch system with low injection pressure. This is compatible with Michael May's "fireball" high swirl combustion system. No special starting aid or changes in battery requirements are foreseen.

There are considerable uncertainties connected with ceramic coatings and other means of insulation for adiabatic concept. Even larger technical risk concerns the oil-less operation and the related piston design. The primary design has a ceramic wheel as a cross head. As the piston moves, this wheel rolls along the liner wall. A consultant conducted a study of propensity to skidding and damage to the adiabatic liner. The full report is in Appendix 2. The conclusion is that only experiments can conclusively prove whether this piston design will work effectively. Two alternate piston design are included for this engine (Figures 7 and 8). If the oil-less

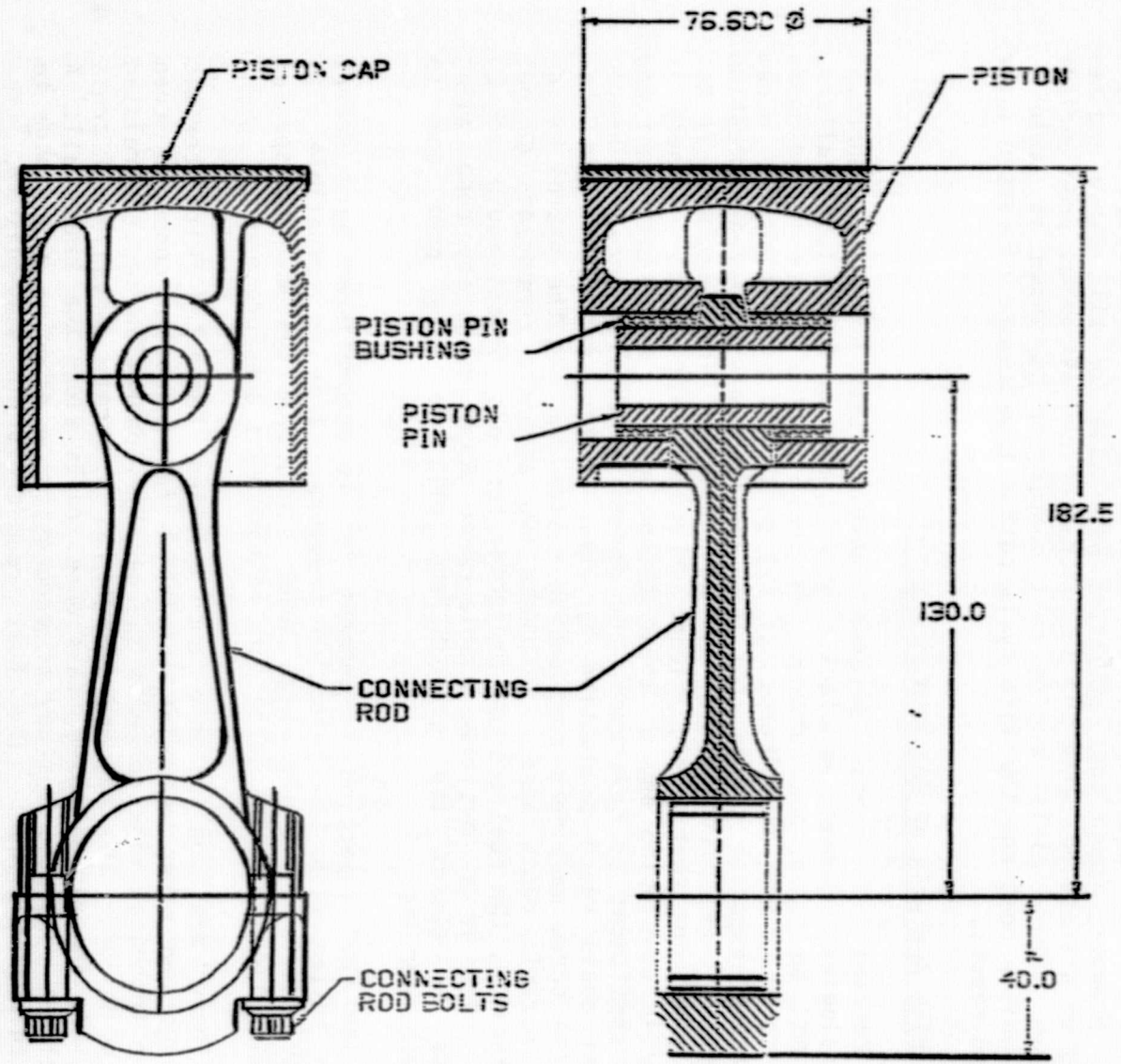

- NO CROSS HEAD
- TIGHT CLEARANCE (.038 mm Dia. Clearance with Liner)

FIGURE 7. A.A.D.Engine Piston - Alternative 1

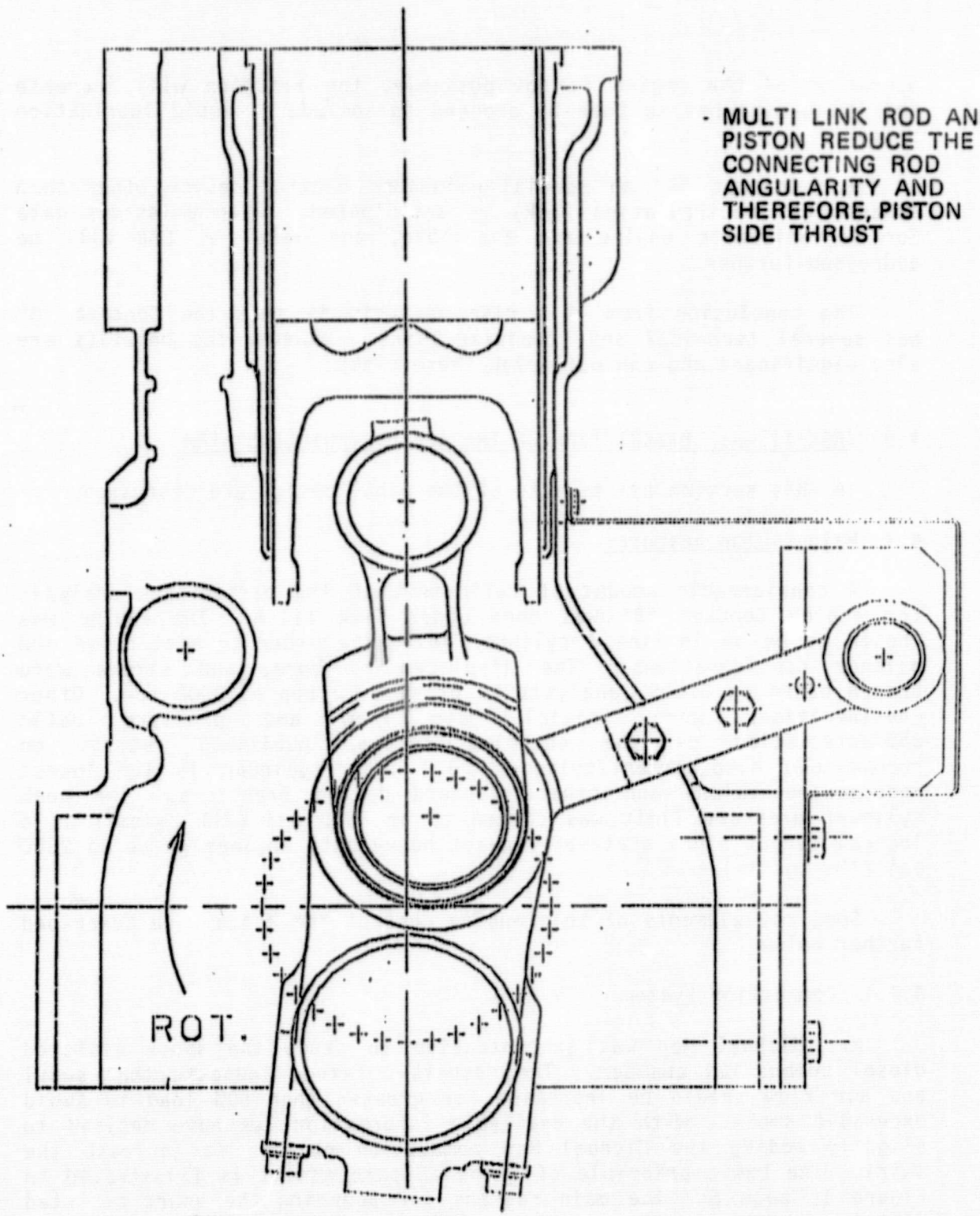

FIGURE 8 A.A.D.Engine Piston - Alternative 2

operation of the engine is not possible, the friction will increase and the design has to then be changed to include a liquid lubrication system.

For Concept "B" no special emissions control device other than exhaust gas recirculation (EGR) is anticipated. When emissions data for an adiabatic engine are available, the level of EGR will be addressed further.

The conclusion from this risk analysis is that the Concept "B" has several technical and schedular risks. However the benefits are also significant and can out weigh these risks.

4.0 TASK III-A: DESCRIPTION OF THE A.A.D. VEHICLE SYSTEM

In this section all aspects of the final design are discussed.

4.1 Main Engine Features

A considerable amount of refinement of the performance analysis for engine Concept "B" was done under Task III-A. The engine was chosen to be an in-line 4 cylinder design in order to meet noise and balance considerations. The displacement, bore, and stroke were chosen based on D.C.S. analysis to provide 70 bhp at 3000 rpm. Other considerations were initial mass flow and pressure ratio characteristics of the charging system, published reports on recommended displacement/cylinder (0.3 liter/cylinder is the lowest recommended value) and other standard design practices. The peak cylinder pressure limit was chosen to be 3000 psi (211 kg/cm^2) as a logical target since state-of-the-art heavy duty engines go up to 2500 psi (176 kg/cm^2).

Some key elements of this engine Concept "B" A.A.D. are described further below.

4.1.1 Combustion System

Mr. Michael May was subcontracted to study the spark assisted diesel combustion chamber. The results obtained indicate that swirl and air flow should be increased for greater than 50% load to avoid excessive smoke. With the available information, we have decided to slightly modify the Michael May combustion chamber to increase the swirl. The basic principle of using a spark assist is illustrated in Figure 1, page 6. The main reasons for adopting the spark assisted diesel combustion system are to obtain a faster heat release rate compared to normal diesels and to improve the multifuel capability range of this engine.

4.1.2 Positive Displacement Screw Compressor and Expander

Conventional turbochargers have poor efficiencies at part load and the "turbo lag" affects driveability. A positive displacement compressor and expander are used in this engine to overcome these two problems. The Institute of Gas Technology, which has experience in performance analysis and design of screw-type compressors and expanders, was subcontracted to design and predict the primary characteristics of this device for Concept "B". In addition to having a "flatter" efficiency characteristic, this device has a somewhat higher efficiency level compared to a turbocharger. The equipment is significantly larger than conventional turbochargers (compressor: 6 inch wide x 4 inch tall and expander: 9 inch wide x 7 1/8 inch tall) and occupies nearly 14 inch along the length of the engine.

4.1.3 Piston Design

One of the most severe problems anticipated in running an oil-less adiabatic engine is the piston-to-liner interface where excessive wear due to side thrust is anticipated. In order to minimize the side thrust on the interface, the piston design utilizes a wheel (or a rolling cross-head), as shown in Figures 2 and 3. This is a novel piston concept. Initial analysis indicates that the force exerted on the cylinder wall by the wheel is 2000 pounds. With this force, based on the curvatures of the cylinder and the piston wheel, it was determined that the maximum contact stress is 168,000 psi. This is well below the compressive strength of the ceramic material to be used for the liner and the wheel.

4.1.4 Part Load Air Preheating

Another key concept used in this engine is preheating of the inlet charge air using exhaust energy. Usually the thermal efficiency of a diesel engine at part load drops to half of full load value. This concept improves the part load performance.

4.1.5 Adiabatic and Minimum Friction Concepts

The most important aspect of this innovative diesel engine is the adiabatic concept. This concept is being evaluated in other TACOM programs on heavy duty diesels (Refs. 3, 6, and 12). Further developments in ceramic materials and processes should be the focus of future research. Especially for each adiabatic combustion chamber component, it is necessary to evaluate coatings, monolithic ceramics, and composites.

The adiabatic engine concept depends on insulating the internal surfaces of the combustion chamber and hot air passages. This reduces the heat loss to the cooling water in a conventional engine and improves the cycle efficiency slightly. Primarily, this increases the exhaust energy available for recovery in an external device such as a power turbine. In the A.A.D. engine, a high efficiency positive displacement screw expander generates power from the exhaust gas. A part of this expander output is used to drive the compressor and the rest is fed back to the crankshaft. The added benefit of the adiabatic concept is the total elimination of the cooling system.

The minimum friction concept consists of eliminating oil lubrication entirely and uses ringless, air bearing pistons. All rubbing surfaces such as cam lobes, rocker, and gears will use solid lubricants such as graphite. The main and rod bearings will use roller element bearings also lubricated with graphite. This results in significant reduction in friction and elimination of the oil system. This concept is also being studied under another advanced heavy duty diesel program.

This A.A.D. engine system design drawings are further described in Figures 9 - 12.

4.1.6 Distributor System

The distributor system used to energize the four spark plugs in this engine is Ford's most advanced electronic design that will be released in the 1985 model year on Ford cars. The distributor will be mounted near the end of the camshaft.

4.2 Main Vehicle Features

Ford used a production car, the Topaz, as its baseline vehicle for this evaluation. The characteristics of this vehicle are shown in the Ford subcontractor's report (Appendix 4). By utilizing the same vehicle for installing the advanced automobile diesel engine, the vehicle characteristics remain unchanged. The figures in Appendix 4 show the underhood views of the vehicle. Ford's report contains all the details of the vehicle related analysis. The elimination of the radiator allowed the hood line to be dropped. However, the drawings do not show the lower hood line. Ford conducted an analysis of this effect on the aerodynamic drag coefficient and vehicle performance. The results indicate that the drag coefficient could be reduced by 10%, resulting in a fuel economy improvement of 3% over the metro-highway combined cycle.

The vehicle uses a Continuously Variable Transmission (CVT) which is a proprietary Ford design. Figure 13 illustrates the more efficient matching of the CVT with the engine compared to a manual

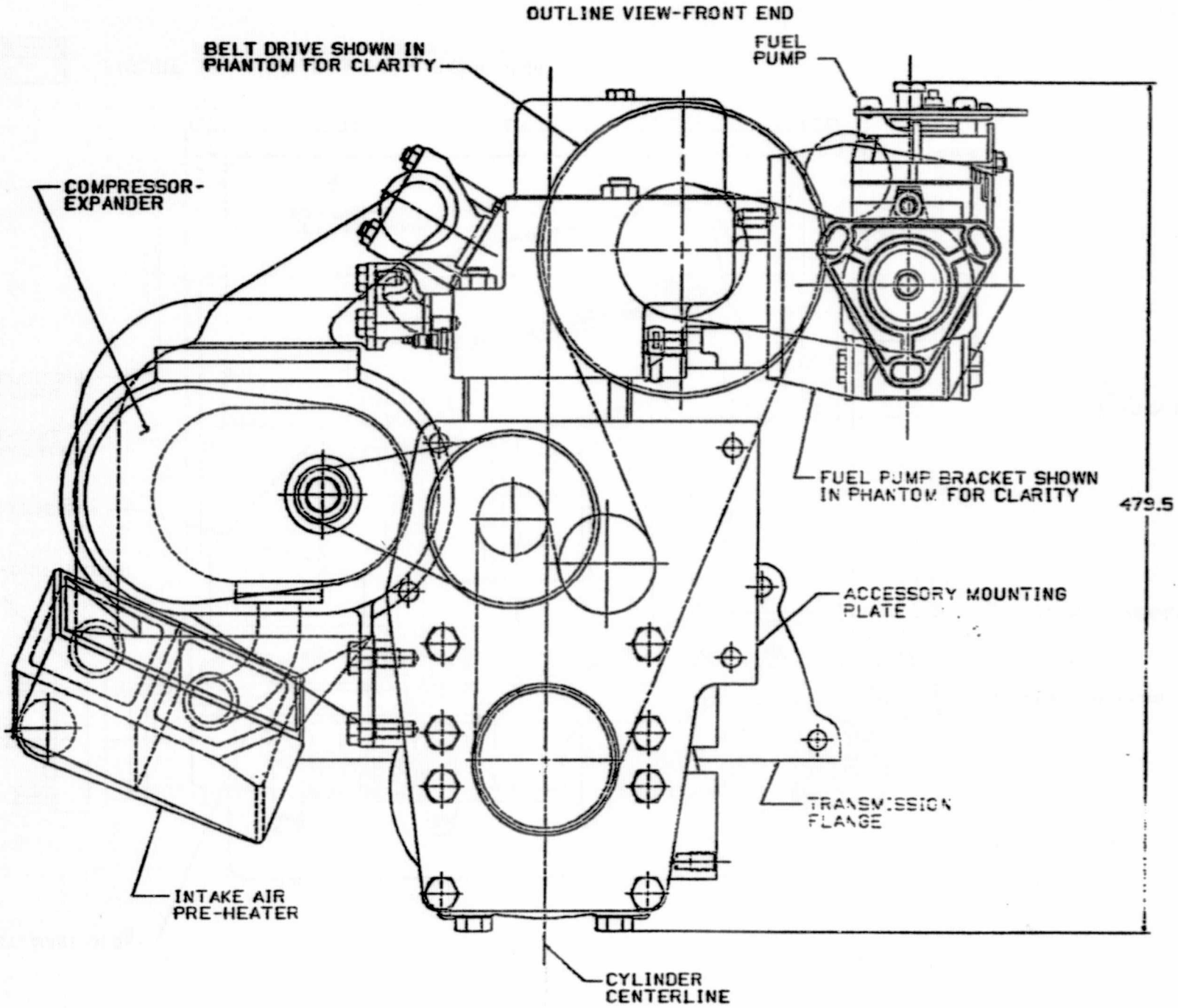

FIGURE 9. A.A.D. Engine Overall Front View

EXPANDER SIDE OUTLINE VIEW

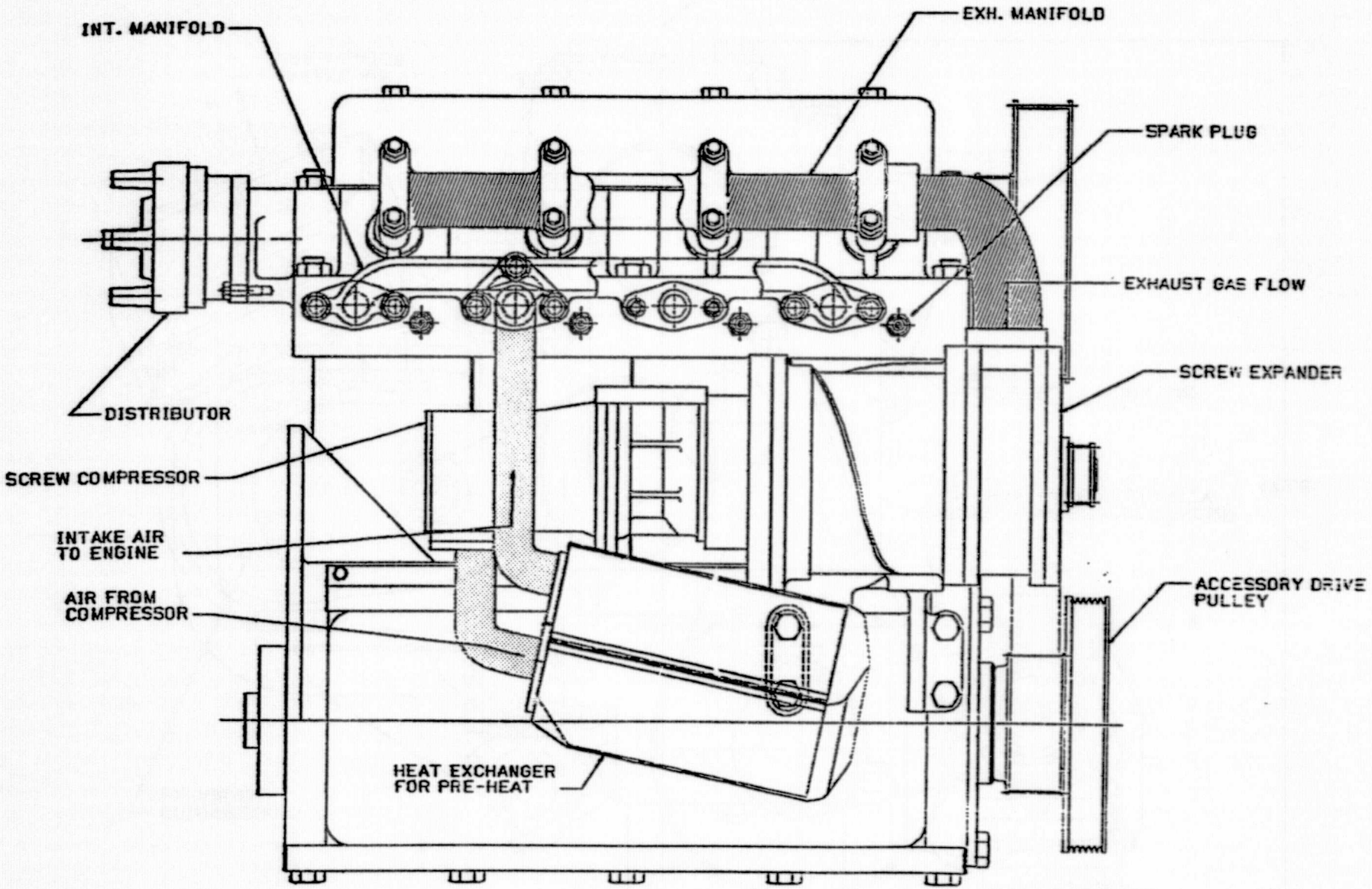

FIGURE 10. A.A.D. Engine Overall Side View

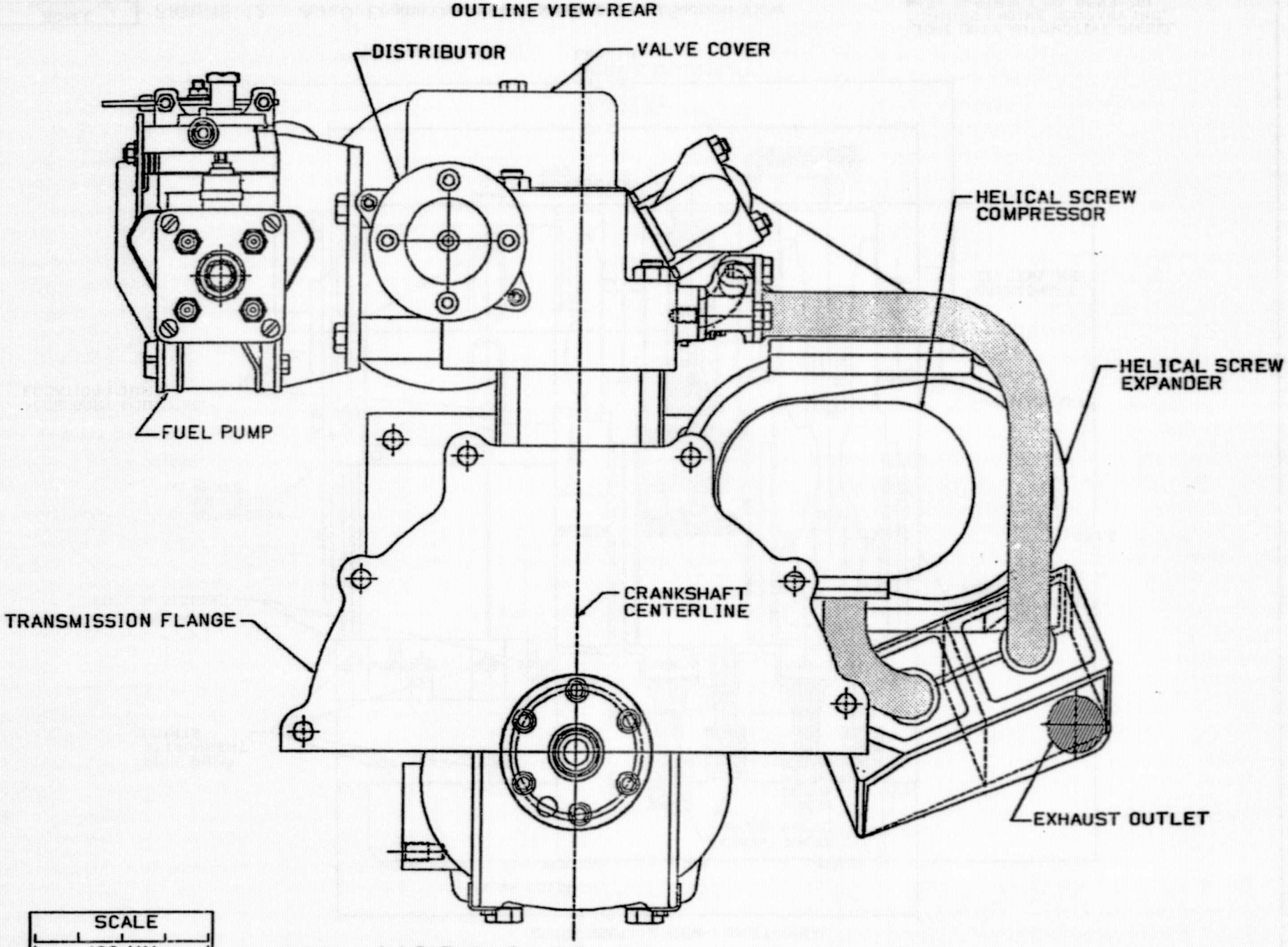

FIGURE 11. A.A.D. Engine Overall Rear View

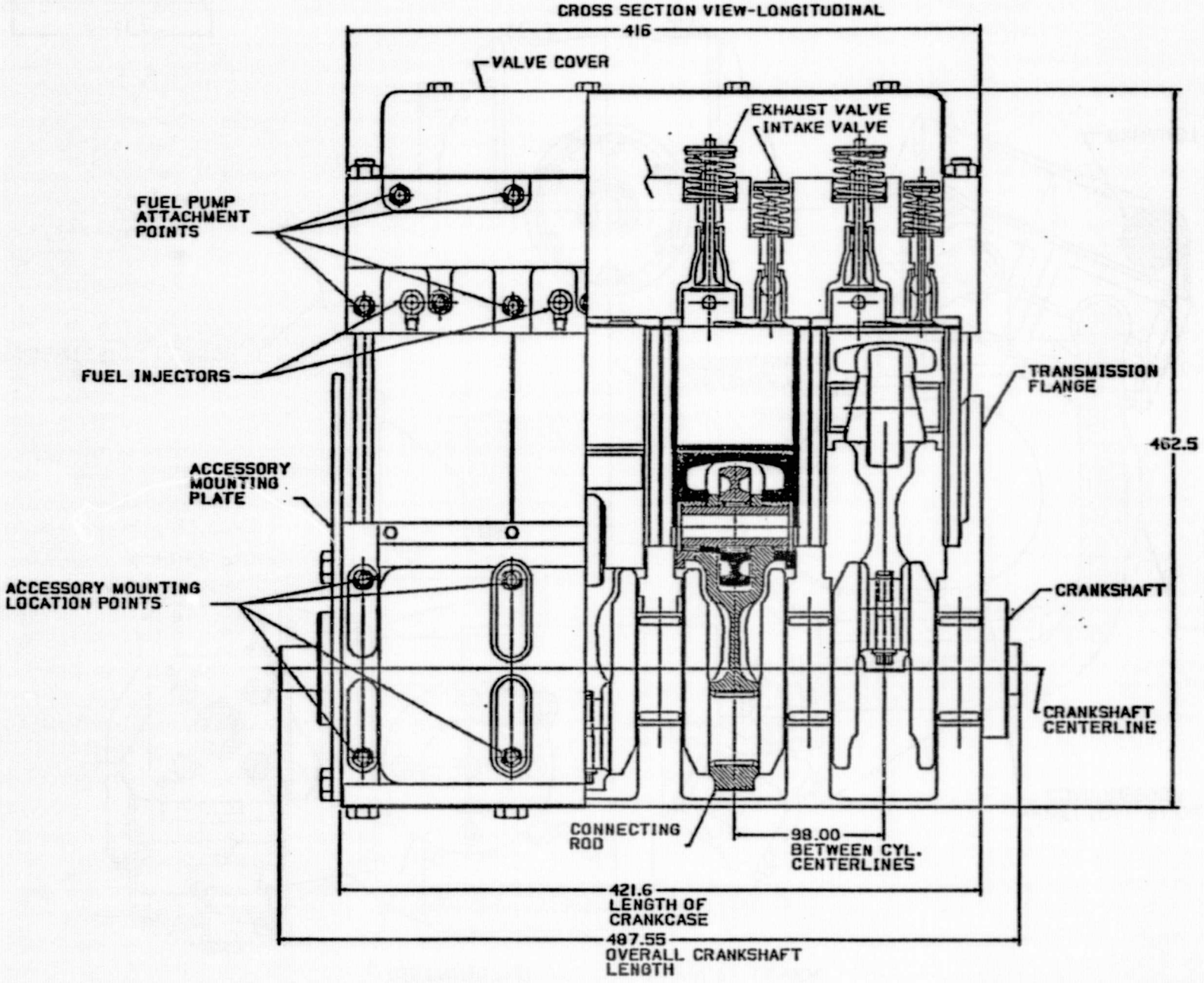

SCALE
100 MM

FIGURE 12. A.A.D. Engine Overall Longitudinal Cross Section View

LIGHT DUTY AUTOMOTIVE DIESEL
CUMMINS ENGINE COMPANY,INC.
NASA CONTRACT NO. DEN3-261
6-23-83 -C.A.D.D.- FIGURE NO. 5.

transmission. Basically, the transmission matches the road speed and load with the engine speed and load at the best BSFC points throughout the duty cycle. The BSFC map shown in Figure 14 is for an unknown car engine and is presented here to illustrate the operating principle of CVT. The details of the CVT design and performance are proprietary to Ford. According to Ford personnel, a prototype has been tested and the first generation CVT's will be in production in the next few years.

Since the engine does not have liquid cooling or lubrication systems, Ford analyzed several means of passenger compartment heating and recommended a fuel fired heater. This type of heating had been used in past Ford cars. The subcontractor report gives some of the details of the heating system. Since this is a proven method, no problems are expected.

4.3 Performance of the Engine and the Vehicle

The predicted fuel map of the engine is presented in Figure 14. Torque curve, BSFC, and bhp curves are presented in Figure 15. These fuel maps were forwarded to Ford for conducting vehicle performance analysis using their proprietary program to simulate the combined Federal Driving Cycle. The results are presented in Table 2. It can be seen clearly that the advanced diesel engine provides a significant improvement in fuel economy (mpg) and acceleration. The details of the assumptions, methodology, and sensitivity to various concepts included in the engine are discussed later in this section and in the appropriate appendices.

4.4 Emissions

There are no reliable analytical models available to predict the emissions characteristics of an adiabatic engine. However, based on data available from the heavy duty engine programs at Cummins, the key emissions characteristics were projected. The predicted in-cylinder conditions for this engine yield HC, CO, NOx, and particulate emissions of 0.13, 1.30, 1.65, and 0.18 g/mile respectively. For this study targets for HC, CO, NOx, and particulates are 0.4, 3.4, 1.0, and 0.2 gms/mile. The only problem area appears to be NOx due to the high cylinder gas temperatures. This could be solved by exhaust gas recirculation (EGR). Experimental measurements would be required to confirm accurately the emissions characteristics of the advanced diesel engine. Depending on the amount of EGR needed for NOx control, a particulate trap might be needed.

4.5 Driveability Considerations

The time to accelerate from 0-60 MPH for this car is 13.9 seconds compared to a target of 15.0 seconds and a current diesel car's time

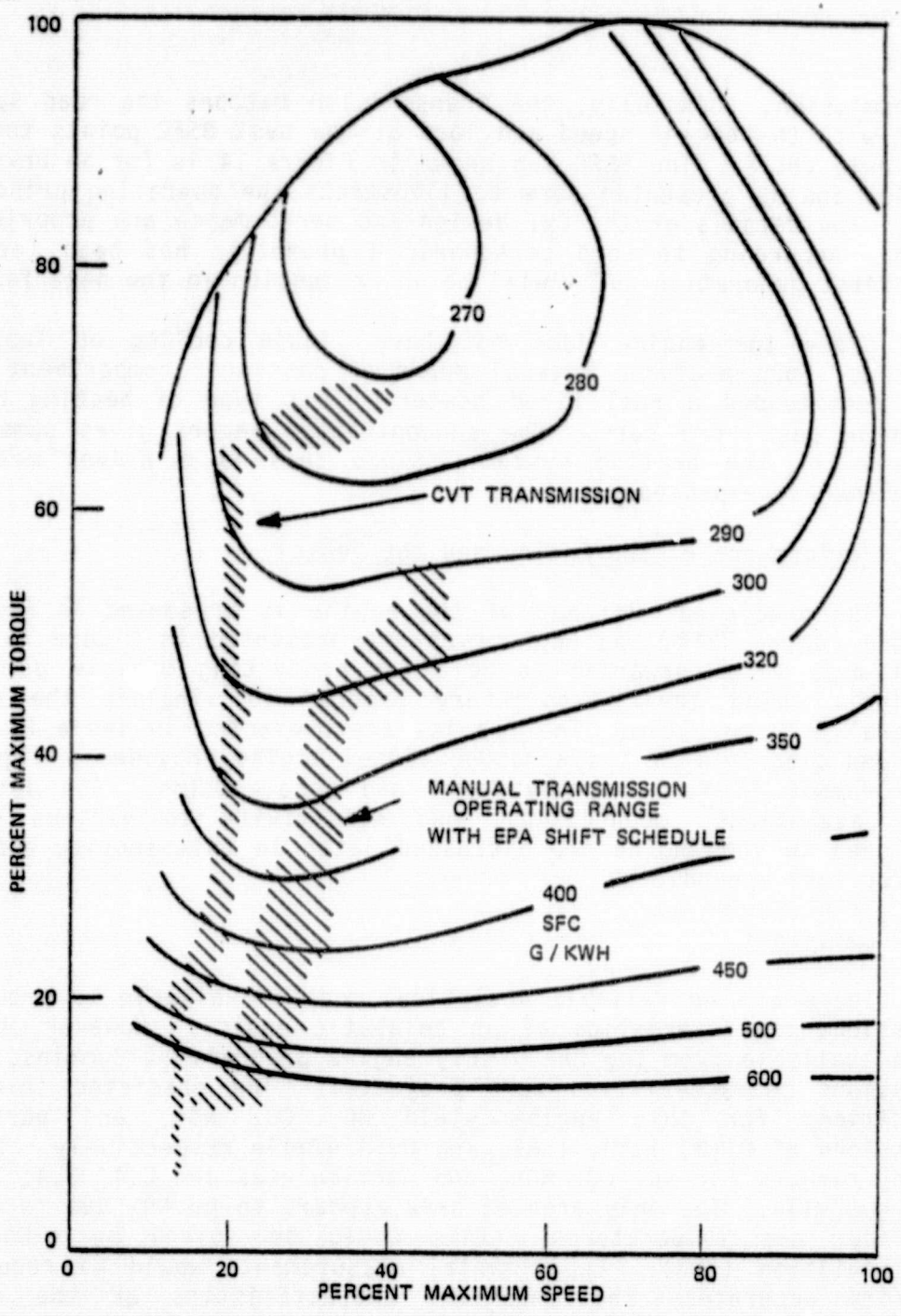

FIGURE 13. Operating Principle of Ford's Continously Variable Transmission (CVT)

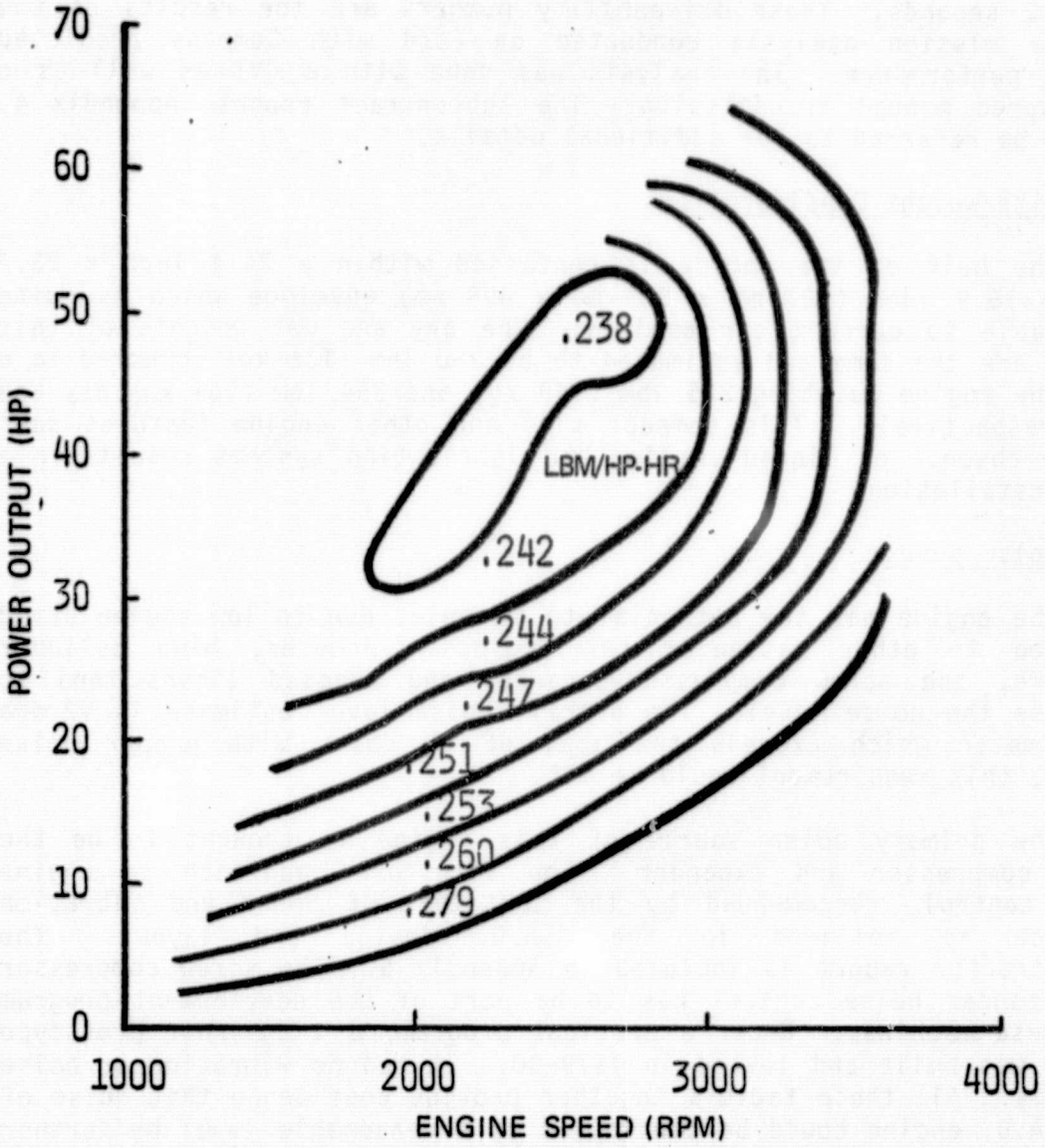

FIGURE 14. A.A.D. Engine Fuel Map

of 15.2 seconds. These driveability numbers are the results of the vehicle mission analysis conducted by Ford with Cummins predicted engine performance. The analysis was done with a CVT as well as a five speed manual transmission. The subcontract report, Appendix 4, should be referred to for additional details.

4.6 Size/Weight Considerations

The bulk of the engine is contained within a 24.4 inch x 23.2 inch x 18.9 inch (621 mm x 589 mm x 479 mm) envelope which is quite comparable to current car engines. The dry and wet weights of this engine are the same and estimated to be 300 lbm (136 kg) compared to a baseline engine weighing 325 lbm (148 kg) and 354 lbm (161 kg) dry and wet, respectively. This compact size and other engine features such as the absence of liquid cooling and lubrication systems results in a good installation.

4.7 Noise Level

The engine has the potential to be quiet due to low engine speed compared to other passenger car engines. However, high cylinder pressure, the screw compressor-expander and exposed liners tend to increase the noise level. The overall noise level estimate is 92 dba at 1 meter which exceeds the goal of 90 dba. With proper noise design, this requirement could be met.

The primary noise source of this engine is thought to be the screw compressor and expander. The structured approach to engine noise control, recommended by the Institute of Sound and Vibration Research is followed in the A.A.D. design and layout. The subcontractor report is included in Appendix 5. The screw compressor and expander noise control has to be part of the development program for these machines. Under a previous program, a 4 cylinder prototype engine was built and tested in 1979-80. It had no vibration or noise problems. All these factors together provide confidence that noise of the A.A.D. engine could be controlled to a reasonable level by further developing the optimum noise control design.

4.8 Reliability/Durability Considerations

The B-10* Life for major failures is judged to be at least 60,000 miles and B-50* Life is 100,000 miles. The design procedures adopted and the critical stresses compared to strengths of chosen materials for major components are very close to the Cummins proven heavy duty engines which typically have 250,000 miles durability. The unknown

---

*B-10 Life: 90% of the engines will not fail before 60,000 miles

*B-50 Life: 50% of the engines will not fail before 100,000 miles

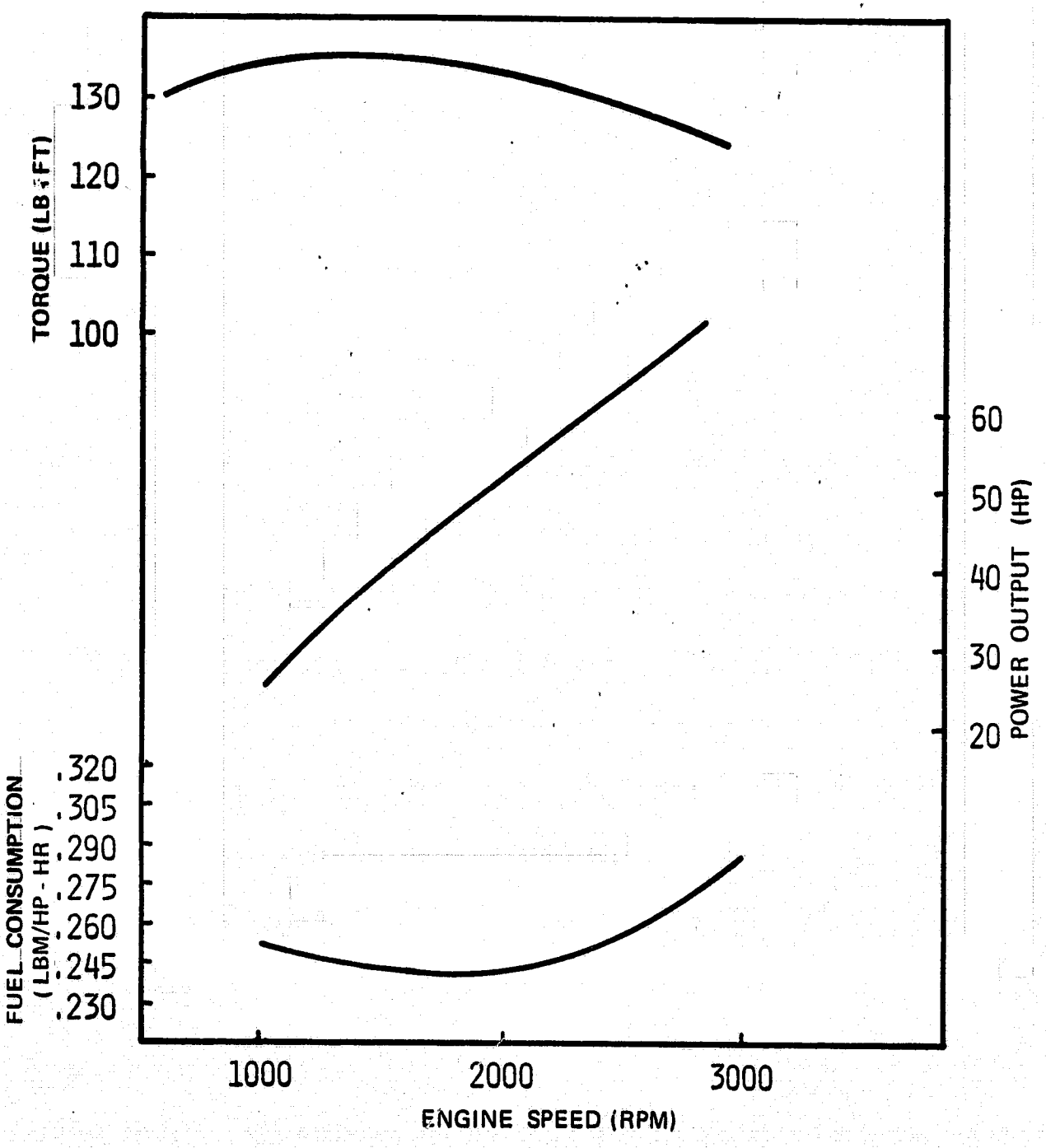

FIGURE 15. A.A.D. Engine Performance Curves

durability of ceramic coatings and components might bring this down. A considerable amount of research into ceramic components for engines is currently under way at several organizations in the U.S. and Japan. A statistically significant number of ceramic components have not gone through endurance testing up to now. The results of the few tests conducted, however, appear encouraging. The authors believe that with concentrated effort the ceramic components will be durable enough.

4.9 Multifuel Capability

In a previous Department of Energy funded study (Ref. 4), diesel engines with and without spark assistance were tested with fuels having a wide range of cetane numbers. The results indicate that the spark assisted diesel has an excellent potential for burning lower grade fuels compared to standard No. 2 diesel fuel. The hot combustion chamber in the A.A.D. makes it even more conducive for burning a wide range of fuels. Among the diesel and gasoline engines used for passenger car applications, the A.A.D. is considered to be the most promising in this respect.

4.10 Layout Drawings of the Vehicle, Engine and Major Engine Components

All the engine layout, assembly, and parts drawings were prepared in the Computer Aided Design and Drafting (CADD) system. These engine related drawings are numbered and included in Appendix 6.

Ford Motor Company used the Cummins drawings to prepare vehicle installation layouts. The gasoline engine in the 1984 TOPAZ car was removed and the A.A.D. engine was installed. A final set of installation drawings are included in Appendix 4.

4.11 Heat Transfer Analysis of Combustion Chamber Components

Finite Element Models (F.E.M.) were built for the cylinder head, piston (primary and alternate designs), and liner. Representative isotherm temperature plots of these components are shown in Figures 16 thru 18. Details of the models, assumptions, boundary conditions, and sensitivity analyses are presented in complete detail in the Cummins reports included in Appendix 8. These F.E.M. analyses proved to be extremely helpful in the design evaluation process. Initial analysis

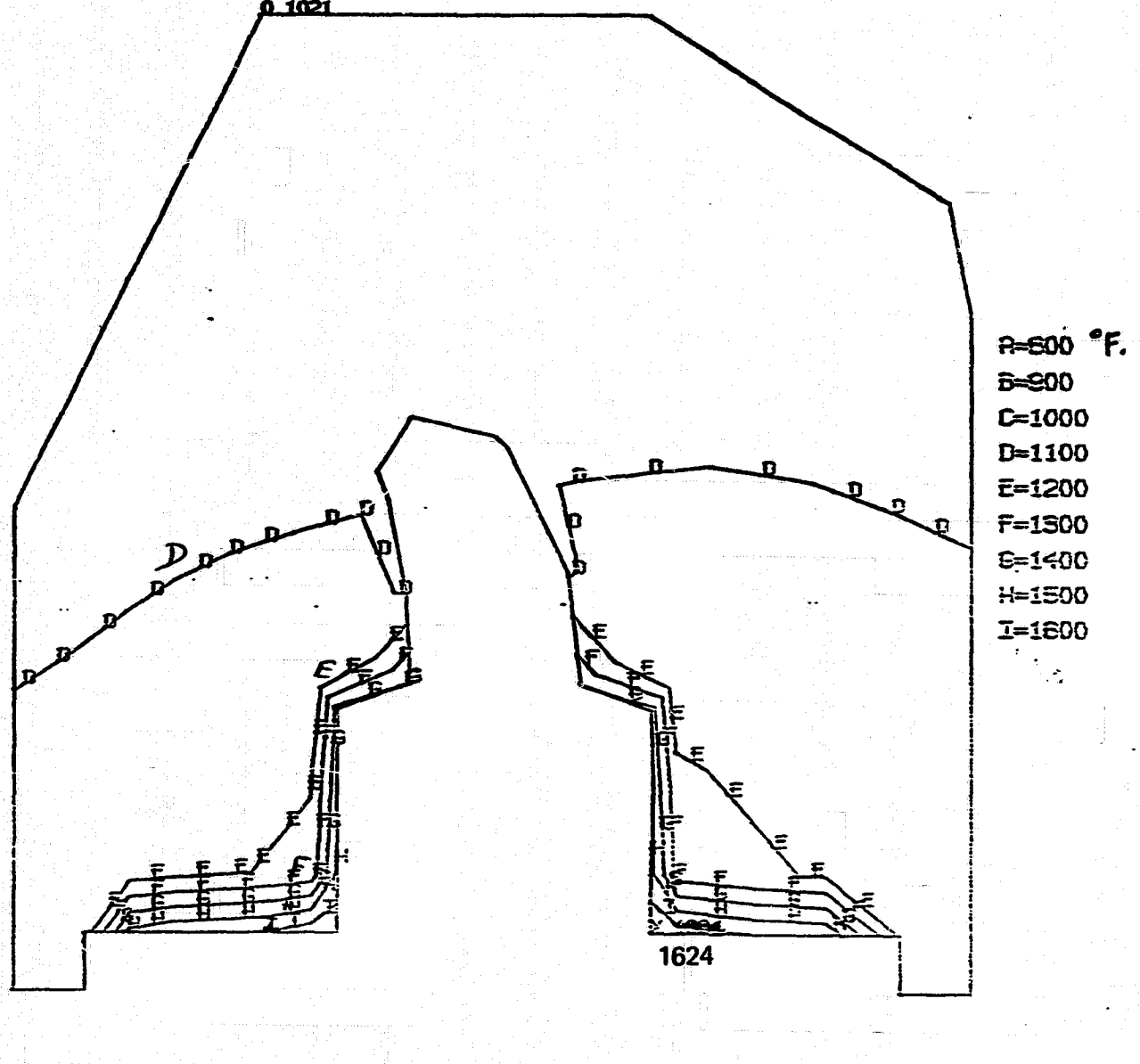

FIGURE 16. Example of Head Temperature Distribution

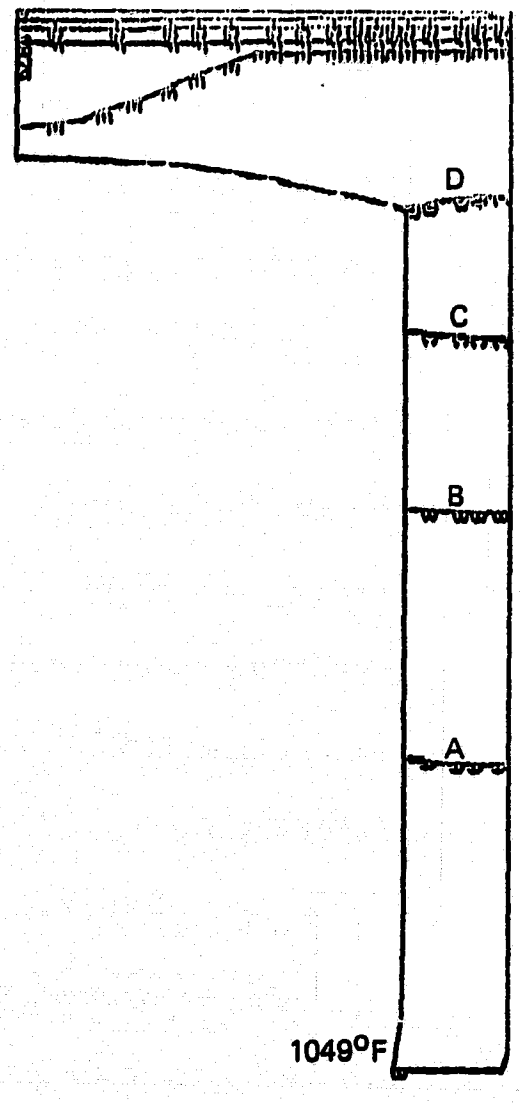

FIGURE 17. Example of Piston Temperature Distribution

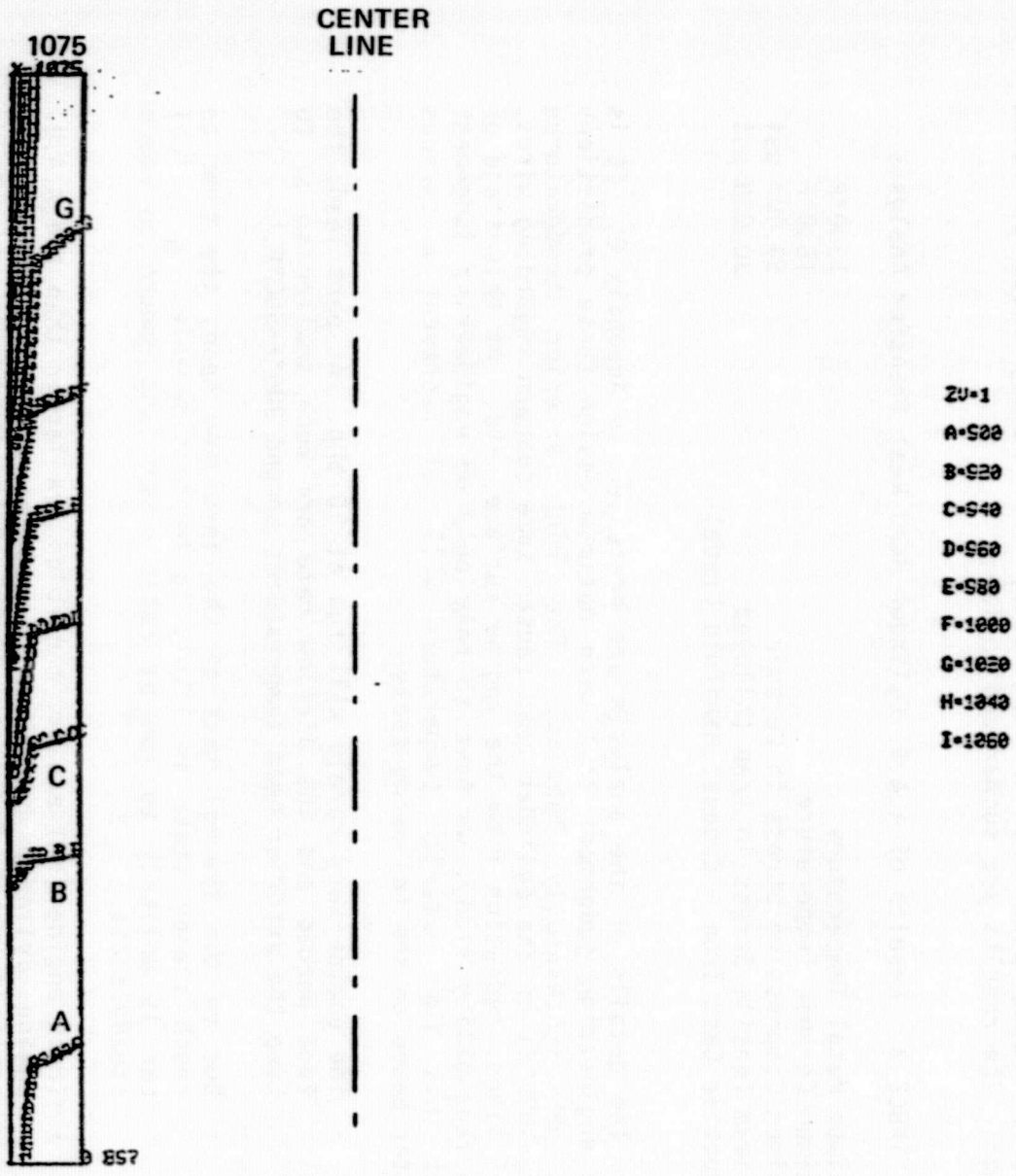

FIGURE 18. Thermal Analysis of Liner Section

indicated various component temperatures to be extremely high - clearly more than the transformation temperatures of the materials in the head and the piston. This resulted in a performance analysis iteration and a final rating of the engine of 70 bhp at 3000 rpm.

4.11.1 Cylinder Head

The purpose for doing this analysis was to determine the maximum component temperature, material specification, maximum tensile, and compressive stresses. The worst condition will be when the engine runs at rated power for a long time, i.e. steady state at rated power. The results are summarized in Table 3:

TABLE 3. Results of A.A.D. Cylinder Head Heat Transfer Analysis

Maximum Metal Temperature	1300°F
Maximum Ceramic Temperature	1680°F
Maximum Compressive Stress in Ceramic	59,000 psi
Maximum Tensile Stress in Iron (Alloyed Ductile Cast Iron - Exhaust Manifold Grade)	30,000 psi

The details of the analysis are presented in Appendix 8. It is our engineering judgement that with optimum design these predictions can be successfully handled. The high exterior temperatures (800-1000°F) of the cylinder head caused some concern regarding wires, fuel lines, radiation from the engine surface, etc. At this stage of the feasibility study, we have to rely only on engineering judgement that this high exterior temperature will not represent a serious factor based on the following facts:

- The engine very rarely will run at 70 bhp. At part load, the fuel burned and the airflow rate are much smaller so as to keep the exterior head temperatures around 300°F-500°F.
- Due to the thermal mass of the insulated head, the time to reach steady state is likely to be considerable. A typical car is unlikely to run at rated power long enough to reach steady state.
- Truck engine (NH) exhaust manifolds are larger than the A.A.D. engine cylinder head. The measured data on the exhaust manifold metal indicates 1000°F-1050°F temperatures. These run today without any significant underhood temperature-related problems.

No other than normal precautions such as keeping the wire, wire harness, and fuel lines away from direct contact with the cylinder head, are anticipated. If necessary, a radiation shield could be used for the cylinder head.

Based on this steady state analysis, it is concluded that the cylinder head design is feasible.

4.11.2 Piston

The A.A.D. adiabatic concept requires a piston-liner combination that does not have oil lubrication but rather utilizes solid lubrication. Based on Cummins/TACOM Minimum Friction Engine program experience, it is clear that even a small amount of side thrust caused by the angularity of the connecting rod will cause piston/liner scuffing. The maximum side thrust computed for a Cummins NH engine is 2600 lbm and for the A.A.D. it is 2000 lbm. So, some means of dealing with the scuffing problem is absolutely necessary. The primary piston design, shown in Figures 2 and 3, is a novel idea of using a rolling crosshead. The thermal analysis done on this piston is discussed in detail in Appendix 8. The results are shown in the table below.

TABLE 4. Results of Heat Transfer Analysis on the AAD Piston

Maximum Metal Temperature	1140°F
Maximum Ceramic Temperature	1434°F
Maximum Thermal Stress (at interface)	26,700 psi

It is our engineering judgement that the piston design considered is feasible from a thermal and mechanical stress view point even with these high temperatures that are predicted (Appendix 8). However, the rolling cross head in the piston is an untested concept. Due to the size of the rolling element, the roller might skid in the liner resulting in excessive wear or damage. An outside consulting firm, Tribolock, Inc., was asked to analyze the skidding characteristics of this piston. The consultant's report is included in Appendix 2. The summary of the consultant's report is as follows:

> The design does not contain any unsolvable fundamental problems. Skidding will most probably occur. However, a ceramic roller skidding in a ceramic liner will not be anymore harmful than a metal ring sliding on a metal liner; but some lubrication is necessary. Two solutions are possible: (1) a wheel made of a ceramic solid lubricant composite, or (2) a spring loaded

graphite stick rubbing against the wheel. The absolute answer to piston feasibility can only be determined by experiments.

Because of the serious questions regarding the practicality of the piston design, two more alternatives are also suggested. The tight fitting monolithic ceramic piston-liner combination is shown in Figure 7. The multilink connecting rod-piston is shown in Figure 8. Detailed analysis was not done for these two alternatives however. Detailed design and experimental evaluation of all the three concepts is recommended in a future study to confirm and select the most promising piston design.

In summary, the combustion chamber component temperatures are high compared to current standards. However, it is believed that with the use of ceramics, composites, or high temperature alloys and with the use of innovative designs the A.A.D. can withstand these operating temperatures.

4.12 Other Important Engine Characteristics

In this section, the following characteristics of the engine are discussed: materials, bearings, lubricants, seals, controls, fuel injection, and air charging system. A brief comment on producibility is also included in Section 4.12.7.

4.12.1 Materials

Extensive use of ceramics in the form of coatings, composites, and monolithics is necessary in the adiabatic engine. In addition wear resistant coatings are also needed since no liquid lubricant is available. Table 5 contains the materials to be used for major components of the engine. In addition to ceramics, combustion chamber components such as head, liner, piston, and valves will have to made of exhaust manifold grade high temperature alloyed ductile iron to withstand higher temperatures.

4.12.2 Bearings

All the crankshaft, camshaft and screw compressor-expander bearings are designed to be ceramic roller bearings. An example of this is shown in Figure 19. This approach was taken since rolling element bearings offer less frictional losses compared to conventional journal bearings. The rollers are ceramic and the races are steel. The solid lubricating comes from sacrifical graphite bearing cages and spacers. Similar hybrid bearings have been successfully tested for short duration in a heavy duty diesel engine at Cummins.

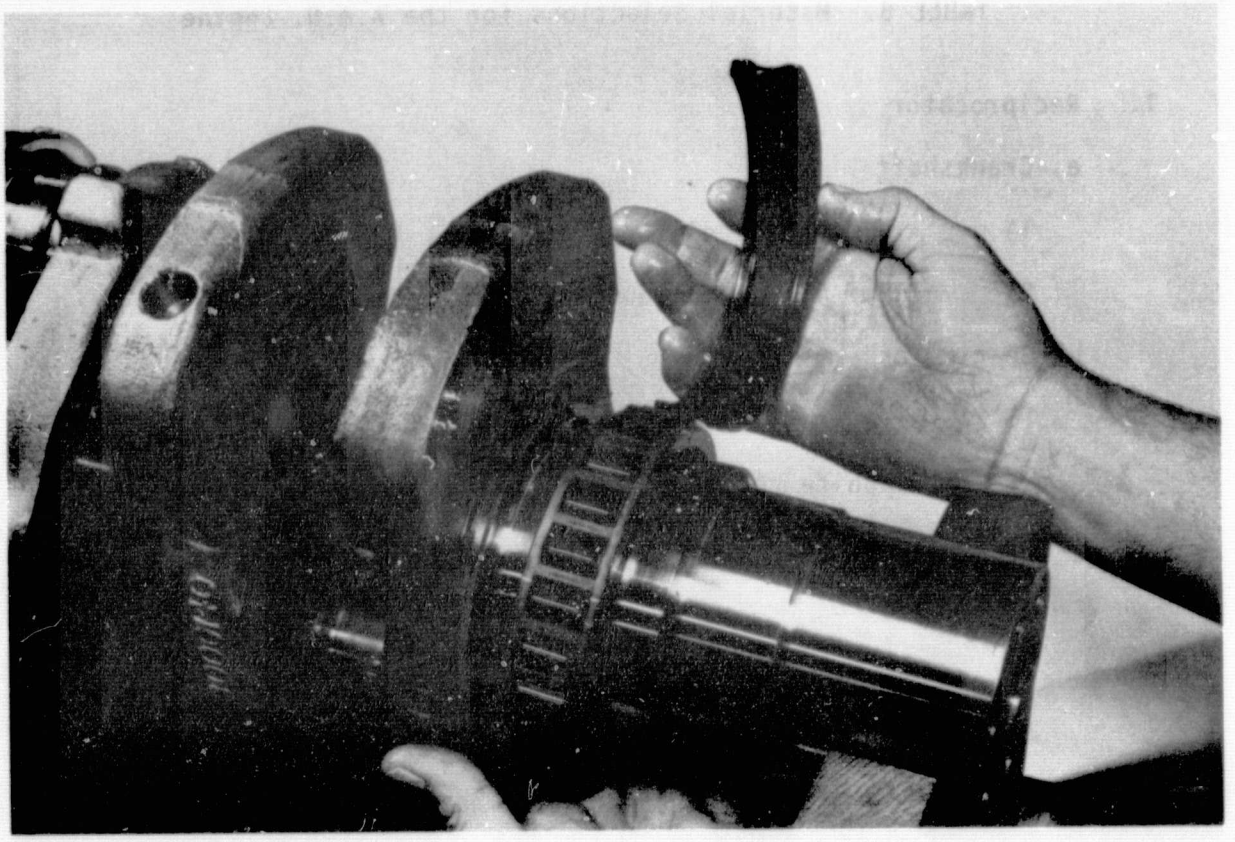

FIGURE 19. Photograph of Roller Element Bearing

TABLE 5. Material Selections for the A.A.D. Engine

1. Reciprocator
   a. Crankshaft
      1) AISI 1050 steel forging
      2) All fillets and journals - induction hardened
   b. Bearing assemblies
      1) Si_3N_4 rolling elements (Norton NC-132)
      2) Graphite retainers (cage)
      3) Outer race - through hardened M-50 steel
   c. Connecting rod
      1) Ductile iron casting
      2) Heat treatmented to Austempered condition
   d. Lower and upper crankcase and main bearing supports
      1) Estimated operating temperature 250°F
      2) Gray iron casting
   e. Capscrews
      1) Grade M12.9 steel (similar to Grade 8)
   f. Crankcase panel
      1) Stamped low carbon steel 1.5 mm thick
      2) Could be molded plastic depending on cost trade-offs
      3) Rubber U-shaped isolators
   g. Cylinder head studs
      1) Grade M12.9 steel

h. Piston pin

1) Hollow 5 mm wall thickness steel

2) Hardened M-50 steel

3) Could be lower alloy bearing steel if operating temperatures are low

i. Piston pin bushings

1) Si_3N_4-BN ceramic composite

2) Alternative - SiC fiber reinforced LAS-2 matrix (glass)

j. Piston wheel

1) Hot pressed Si_3N_4 (Norton NC-132)

k. Piston

1) Ductile iron casting

2) Ferritic or high temperature alloy may have to be used depending on maximum operating temperatures

3) Plasma sprayed ZrO_2 (0.015 inch) with Kaman Science SCA coating (0.005 inch); total thickness 0.020"

4) Monolithic, ZrO_2 with Y_2O_3 stabilized piston cap brazed to the ductile iron base. Cap thickness 3mm. Braze alloy: TiCuSil.

l. Rolling element bearing

1) Hot pressed Si_3N_4 (Norton NC-132)

m. Cylinder liner

1) Monolithic ZrO_2 with Y_2O_3 stabilized sleeve 3 mm thick in a gray iron liner 7 mm thick

2) May have to be an alloyed iron liner depending on operating temperatures

2. Cylinder Head

a. Cylinder head hot plate with intergral valve seats

1) Monolithic ZrO_2 6 mm thick

b. Exhaust port with intergral seat

1) Monolithic ZrO_2 6 mm thick

c. Valves

1) 751 one piece with plasma sprayed zirconia on face (0.75 mm thick) and on tulip of exhaust (0.75 mm thick)

d. Cylinder head gasket

1) Aluminized steel 1.5 mm thick

2) May change material depending on operating temperatures

3) Needs to deform to form gas seal

4) Oxidation resistant

5) Elevated temperature yield strength

e. Cylinder head

1) Grey cast iron

f. Camshaft

1) Assembled bearings and valve lobes on hollow shaft

2) Use powder metal bearings and valve lobes with impregnated solid lubricant

3) Brazed onto hollow shaft ground after assembly

4) Press spline into shaft end to run fuel pump

g. Rocker levers

1) Stamped steel with ZrO_2 inserts for sliding contact

2) ZrO_2 socket for valve stem

h. Valve guides

1) ZrO_2

2) Standard steel springs and steel retainers

4.12.3 Lubricants

There is no liquid lubricant in this AAD engine. All the solid lubricants used in this engine are expected to be calcium fluoride (CaF_2), molybdenum disulfide (MoS_2), or graphite. The operation of a diesel engine without liquid lubricants is being actively pursued by Cummins/TACOM. Development and testing of several alternate solid lubricants, including a means of replenishment, is of prime importance. As a fallback, synthetic high temperature oil lubrication is easy to accomplish and is being tested in Cummins/TACOM Adiabatic Engine Program.

4.12.4 Seals

No special problems are anticipated to seal engine combustion gases. A novel concept in seals is the absence of rings in the piston. The design includes a tight clearance between the piston and liner. This clearance is an order of magnitude smaller than in current production diesel engines. Monolithic ceramic piston and liner prototypes have been made which indicate that such tight clearances can be attained on a laboratory basis. The development of production machining of these concepts will be required.

4.12.5 Fuel System

The operating principle of the fuel system is illustrated in Figure 20. The fuel pump is a Bosch-type VE distributor pump. This is a standard production item currently available on the market. The injector is a pencil-type injector nozzle assembly shown in Figure 21. This injector is chosen due to its simplicity and a size that fits the combustion chamber properly. The layouts of the fuel pump and injectors are shown in Appendix 7. The addition of a ceramic seat might be needed at the injector tip to withstand high temperatures if they are determined to be excessive during testing.

4.12.6 Charge Air System

The charge air system of this advanced adiabatic diesel engine is novel. Due to high efficiencies of a helical screw machine at light loads and low speeds as well as full load operation it was selected instead of a conventional automotive size turbocharger. During

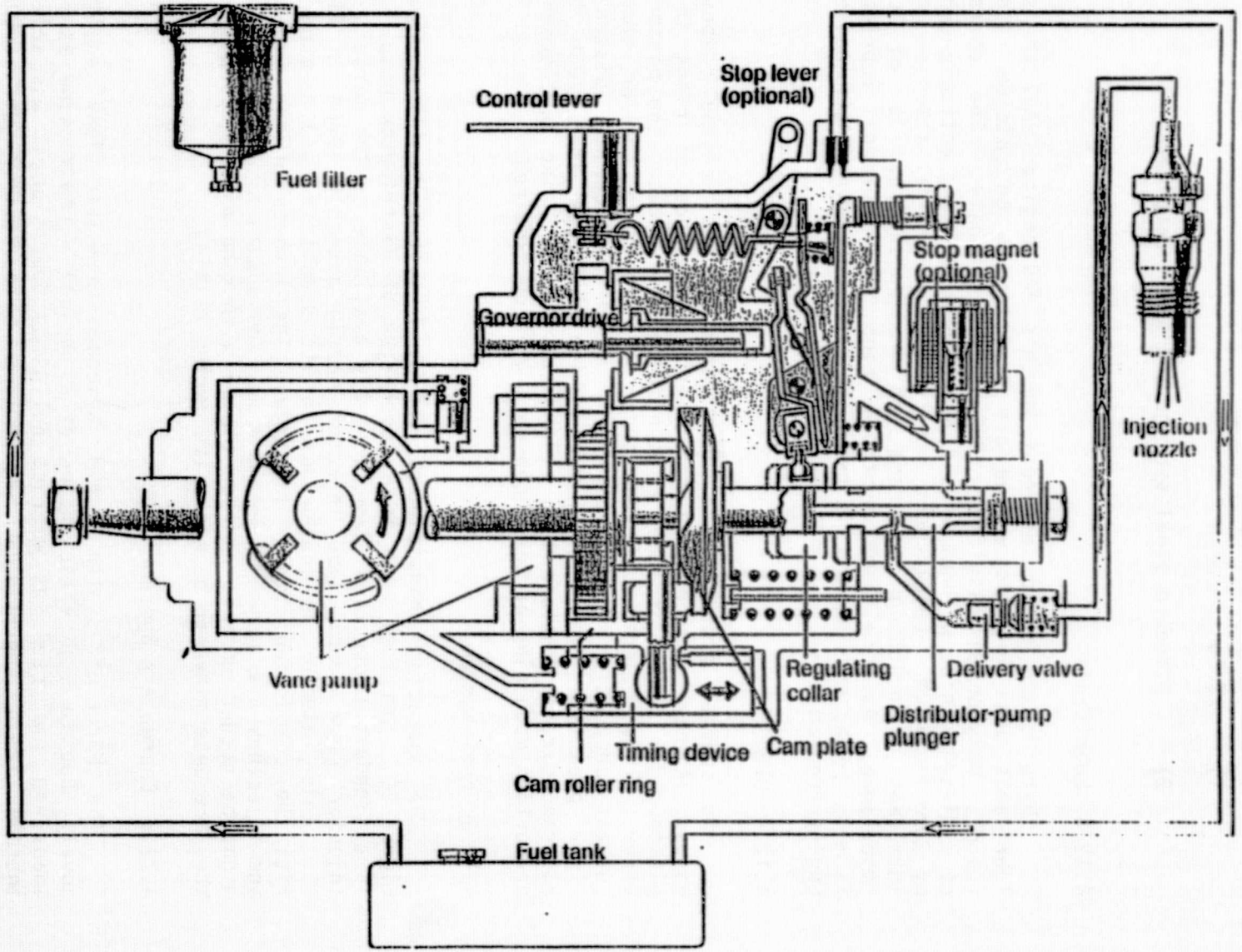

FIGURE 20. Operating Principle of a Diesel Fuel Injection System Incorporating the VE Distributor Type Injection Pump

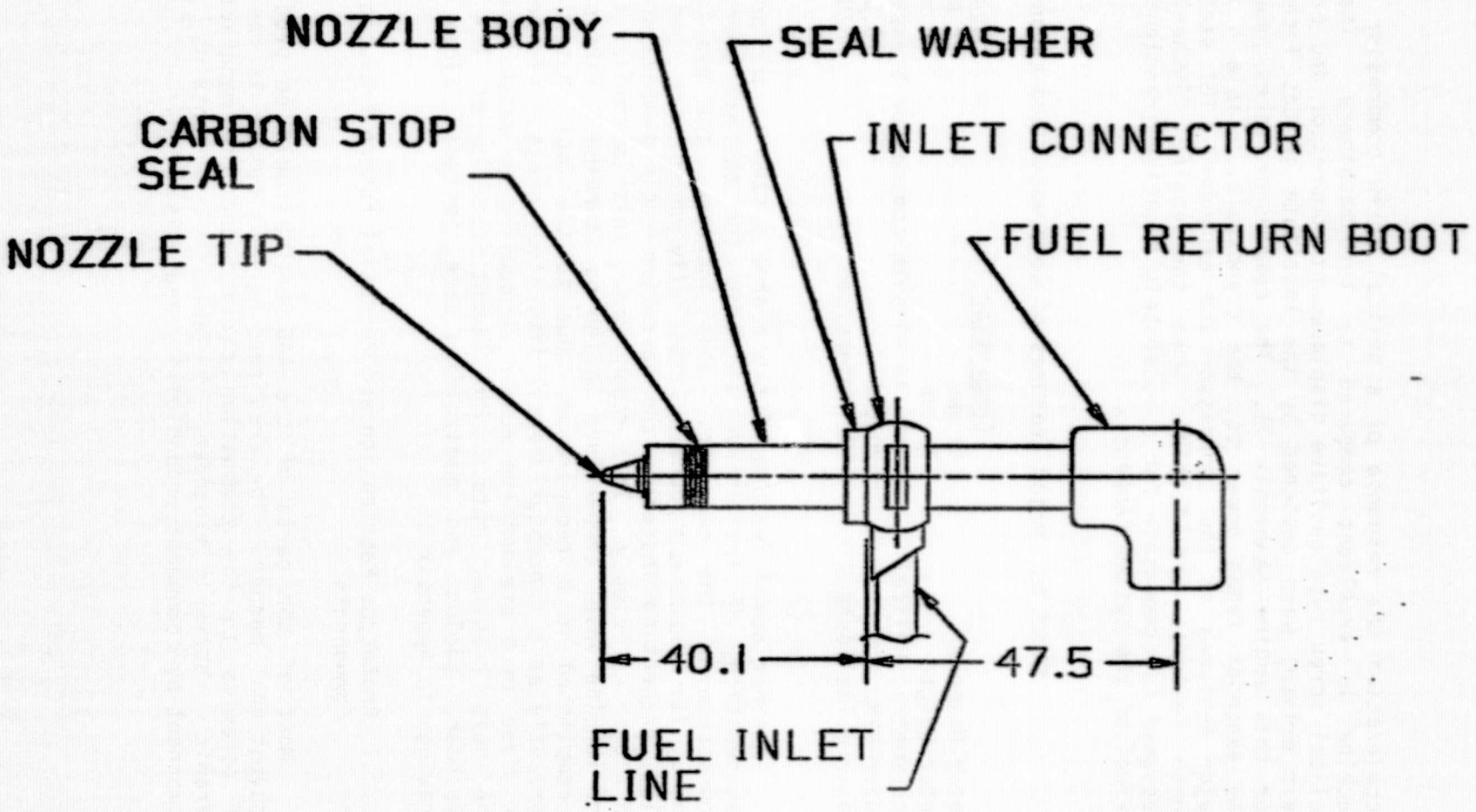

FIGURE 21. A.A.D. Fuel Injection Nozzle

acceleration the response of a helical screw compressor and expander machine is excellent compared to turbomachinery. Therefore, the helical screw type positive displacement compressor and expander (both belt driven) were designed by the Institute of Gas Technology (IGT) for this engine (Appendix 7). The compressor takes power from, and the expander feeds power to, the crankshaft. Table 6 contains the major features of the compressor and expander. IGT states that all these features are feasible when the engine flywheel is easily designed to compensate for a moderately negative transient performance effect of the system (Appendix 7).

TABLE 6. Major Features of Compressor and Expander

	Compressor	Expander
Rotor Diameter	62 mm	98 mm
Rotor Length	71 mm	98 mm
Unsymmetric Helical	Profile on both compressor & expander	
Rotor RPM	20,000	20,000
Maximum Tip Speed	102 meters/sec	200 meters/sec

Another novel feature of the charge system is the preheating (or regeneration) of the charge air with the thermal energy available downstream of the expander. This increases the available exhaust energy for engine compounding especially under part load conditions. Also, preheating increases the operating cycle temperatures resulting in higher efficiency. In a rough sense, this is similar to increasing the turbine inlet temperature in the gas turbine. This preheating is accomplished in a recuperator. Due to the fact that the A.A.D. is currently at a conceptual/feasibility study stage, this heat exchanger is sized in a preliminary manner by scaling an existing unit to meet the heat transfer rate. The layout details of the compressor, expander, piping and manifolding are included along with other drawings in Appendix 6.

4.12.7 Prototype Fabrication and Potential Future Producibility of Components

Most of the parts of the AAD engine could be produced in the conventional manner. The area needing development is the application of ceramics to the combustion chamber and the manufacture of the ceramic screw expander. Table 7 contains a brief component-by-component producibility analysis.

TABLE 7. A.A.D. Component Producibility Analysis

Description	Discussion
Camshaft	Existing Technology
Piston	Concern for bonding of sprayed-on PSZ or brazed monolithic ceramic cap
Piston Wheel & Bearing	Silicon nitride needle bearing cost
Conn. Rod	Existing Technology
Cylinder Block	Existing Technology
Main Bearings	Silicon nitride needle bearings - high cost
Cylinder Liners	Perpendicularity of ends to axis & overall length very critical - high cost due to precision & addition of 3 mm monolithic sleeve
Crankshaft	Existing Technology
Fuel System	Existing Technology - small PSZ insert may be required to protect nose of injector
Cylinder Head	Cast in ceramic core will require development for accuracy and bond. Accuracy required to grind valve seat and match port
Hot Plate	Contains integral intake valve seat and exhaust seats
Cam Bearings	Silicon nitride needle bearings - high cost
Intake & Exhaust Valves	Bonding concern for sprayed on ceramics durability
Rocker Levers	Bonding concern for sprayed on ceramics at long life
Exhaust Manifold	Will have to be designed to allow access to interior for spraying PSZ coating
Screw Expander	Requires redesign to reduce cost and improve producibility.

The concerns regarding producibility of components center around producibility of ceramic parts. Many institutions, government agencies, and researchers are currently working on making ceramic heat engine components. As far as this study program is concerned, it was assumed that all these efforts to manufacture ceramic parts would bear fruit in time to make prototype A.A.D. engines. The major problem areas at the moment are as follows:

- Bonding of ceramics to other material - especially using sprayed techniques.
- Availability and mature production costs of ceramics.
- Ability to cast the ceramic cores with required accuracy
- Realization that inspection is more critical - small fractures in ceramics tend to proliferate as compared to steel or cast iron
- Ceramics are only machined by grinding and used a 5 to 1 ratio cost penalty vs. hardened steel grinding.

Hence, it is estimated that producibility of prototype A.A.D. engines is feasible, but mass production capability depends on ceramic manufacturing technology developments and mature costs.

4.13 Major Component Dynamic Stress Analysis and Balance Analysis

This section of the report details the vibration and balance analysis of the crankshaft and the stress analysis done on the piston and connecting rod of this engine. Appendix 8 contains all the thermal and mechanical stress analyses of the cylinder head and piston.

4.13.1 Crankshaft

Cummins heavy duty engine crankshafts are fully fillet hardened and designed to an allowable maximum stress of 50,000 psi. The design life of the heavy duty engine crankshaft is 500,000 miles. The AAD engine crankshaft was designed for 100,000 miles. The design procedure is standard for fatigue life calculations. No special vibration or balance issues are expected to arise since this is a 4 cylinder engine having lower than conventional speed (compared to other automobile diesel engines). The crankshaft counterweights were determined by conventional procedures. The details of the crankshaft are presented in Appendix 6.

4.13.2 Connecting Rod

The A.A.D. engine connecting rod is conventional in design and the preliminary stress analysis indicates the proposed design dimensions are acceptable. This rod is not conventional in material since it is made of ductile cast iron instead of forged steel. The results of the analysis are summarized in Table 8.

TABLE 8. Results of Connecting Rod Stress Analysis

Rod Shank - Maximum calculated compressive stress is 50 ksi and is acceptable for material 3100.

Rod Bolt - Maximum calculated tensile stress at 50% overspeed is 59 ksi - grade 8 bolt with rolled thread is required for 10 mm bolt.

Rod Cap - For an assumed radial running clearance of 0.001 inch, the critical section of the cap is more than adequate with an 0.06 inch radius fillet.

Tight fit between rod bore and roller bearing cup will reduce alternating stress.

4.14 Engine Starting Characteristics

This spark assisted, advanced adiabatic diesel engine is expected to be superior to any of the current diesels and at least equal to any gasoline engine in terms of ease of starting. Current diesels generally have higher capacity batteries and a glow plug. This advanced diesel will not require a larger battery than currently used for a diesel powered car. In addition, glow plugs are not needed. This significant advantage and cost reduction comes about because of the following three factors:

1. Spark assisted combustion
2. Low friction and low reciprocating mass
3. No liquid lubricant or coolant to warm up

4.15 A.A.D. Engine System Advantages

One primary advantage is the elimination of the radiator and cooling system. It becomes clear from the vehicle layout drawings shown in Appendix 4 and 6 that the vehicle hood line could be lowered by about 38 mm (1.5 inch) compared to the current design of the TOPAZ

car. Ford estimated this would result in a reduction in the drag coefficient of 10% and the improvement in fuel economy could be 3% (Appendix 4). The actual advantage of the change in the hood profile may be nominal however. The front grill could not be completely closed due to the fact that the air conditioning coil and transmission oil cooler must be in front. Electrical fans will be used for these coolers. Hence a design change in the TOPAZ car would be required to realize this 3% potential fuel economy improvement.

Another major system advantage lies in the servicing of the car. Crankcase oil and filter changes and coolant checks are all totally eliminated. These advantages result in major cost advantages as well as selling points for this engine (Appendix 4). In addition, the absence of water passages in the block results in virtual elimination of the block. The liners can be exposed except for noise control purposes. The engine structure is thus much simplified.

5.0 Task III-B - Vehicle Cost Analysis for Design Concept "B"

Cummins prepared a preliminary cost estimate of this engine compared to a typical current automobile diesel. Cummins Advanced Manufacturing Personnel who made this estimate have an excellent data base and prior experience in component and assembly cost - both material and labor - for current diesel engines. The layout drawings, producibility analysis, and material selection guidelines were all used in estimating component-by-component relative costs. The total engine cost was used by Ford for estimating the initial cost of the car as well as life cycle cost. Table 9 contains the Cummins estimate of the engine cost. Two major uncertainty items are the cost of application of ceramics and the cost of the screw compressor-expander. These uncertainties result in an error band of 40% in the engine cost estimates. The most optimistic and pessimistic projections, respectively, yield $700 and $1000 increase in the initial cost and $900 and $195 savings in life cycle cost (Appendix 4). Discussions with screw machine manufacturers indicate that with a simpler design, advanced manufacturing techniques and mass production, the compressor and expander costs could be reduced by 50% compared to the current projections. If this comes true, there is a real possibility that the initial cost could be only $300-$500 higher than a current diesel and the life cycle cost savings would be about $500-$1400. Due to the high fuel economy and absence of oil, the total savings in petroleum use will be very large.

TABLE 9. Preliminary Manufacturing Producibility Cost Estimates for the A.A.D. by Cummins

(Proposed 1.4 liter A.A.D. - 4 cylinder - 1000 engines per day vs. typical 1.4 litre current engine design - 4 cylinders - 1000 per day)

A.A.D. PARTS		Costs (1982 Dollars) A.A.D.	Typical Current
Component Description	Discussion	Design	Design
Camshaft	20 mm tube-P.M. brazed lobes & brg. journals located in cyl. head	$21	$25
Cam Sprocket	Timing Belt Drive - powder metal or formed	$6.50	$20
Piston	Cast iron-same as exhaust manifold sprayed on PSZ .010 in. on O.D. - brazed on 3mm thick PSZ monolithic cap - bushing silicon nitride tapered - chrome oxide dip (.005 in. thick)	$38	$24
Piston Wheel	Silicon Nitride Cylinder	$32	--
Piston Bearing	Silicon Nitride Bearings	$48	--
Piston Pin	Hollow-press fit in fork of rod	$4	$4
Connecting Rod	Austempered ductile iron - carries piston pin, piston, & piston wheel	$30	$30
Cylinder Block	Actual 2 pc. crankcase - top half carries seat for bottom of cylinder liner & top half of mains - bottom half is lower mains & replaces oil pan with casting - cast iron	$105	$118

A.A.D. PARTS		Costs (1982 Dollars) A.A.D.	Typical Current
Component Description	Discussion	Design	Design
Caps-None		--	$14
Main Bearing Shells	Needle bearings 2 halves - silicon nitride	$125	$12
Main Bearing Capscrews	(10) M-12's - Grade 12.9	$5	$5
Side Panels	2 fabricated - covers side of crankcase from upper crankcase to lower crankcase	$6.50	--
Cylinder Liners	Cast iron with 3mm PSZ shell-grind ends for precision - 7mm iron	$60	$20
Fire Ring	Steel (aluminized) 1.5mm	$4	$1.50
Crankshaft	Steel - induct, HDN journal - forged	$62	$62
Injector	Pencil type - "STANADYNE"	$32	$28
Crank Sprocket	Powder metal or formed	$4	$4
Idler Pulleys	Speed reduction - PM or formed	$8	$8
Spark Plugs		$2	--
Cylinder Head	Cast in PSZ ports - valve throats & seats - combustion chamber in head (2 valve head)	$135	$70
Cam Bearings	Spray face with PSZ	$50	$6
Intake Valves	Plasma sprayed	$14	$6
Exhaust Valves	Spray face and stem (or solid ceramic)	$21	$8

A.A.D. PARTS		Costs (1982 Dollars) A.A.D.	Typical Current
Component Description	Discussion	Design	Design
Studs (C'Case to Head)	(10) M-12's - Grade 12.9	$12	$6
Rocker Levers	Fabricated (rocking) (coat PSZ) PSZ button	$18	$12
R.L. studs	Treat with PSZ	$4	$2
Cam Followers	Not needed	--	--
Vibration Damper	Rubber with pulley	$12	$12
Flywheel Housing	None needed - OEM supply hookup	--	--
Flywheel	None needed - OEM supply hookup	--	--
Accessory Drive Housing	None needed	--	--
Exhaust Manifold	Spray interior with PSZ	$18	$8
Screw Expander & Compressor		$800	$130 - Turbo
Heat Exch.	3 in. x 6 in. x 6 in.	$11	--
Intake Mfd.	Cast Iron	$8	$6
Oil Cooler	None Needed	--	$18
Lube Pump	None Needed	--	$23
Oil Pan	None Needed	--	$18
Rocker Housing Cover	Fabricated	$4	$4
Water Pump	None required	--	$12

A.A.D. PARTS		Costs (1982 Dollars) A.A.D.	Typical Current
Component Description	Discussion	Design	Design
Hot Plate		$12	--
Fuel pump	Robert Bosch	$130	$130
Fan Hub Support	None required	--	$8
Front Support	In Crankcase	--	--
Starter	Ford Transmission	--	--
Subassembly		$18	$18
Assembly		$18	$25
Test		$12	$14
Electronic Ignition Module	From Ford	--	--
Alternator		--	--
Subtotal		$1890	$911.50
	(Misc. Capscrews, Gaskets, Lines, Covers, Seals, etc.)	$95	$91
TOTAL		$1985	$1002.50

If a decision is made to follow through with this engine into prototype and production stages, the cost analysis should be periodically revised as new information on ceramic costs and screw machine costs becomes available. Table 10 contains the summary results of the cost study by Cummins and Ford.

TABLE 10. Summary of Cost Analysis by Cummins and Ford

Current Estimate	Estimate	Error Band of Estimate +	Error Band of Estimate -
A.A.D. Base Engine Cost	$2,000	0	$300
A.A.D. Vehicle Cost Premium	$2,127	$ 80	$680
Life Cycle Cost Savings	$ 195	$705	-0
Optimistic Future Cost Reduced Version of AAD			
A.A.D. Base Engine Cost	$1,300	$200	-0
A.A.D. Vehicle Cost Premium	$1,400		
Life Cycle Cost Savings	$ 500	$900	-0

5.1 Engine Cost Trade-off Analysis

Since the single most important item that increases the engine cost is the screw compressor-expander system, it was decided to briefly analyze the cost vs. performance trade-off for the following three charge air systems:

Case 1. Conventional turbocharger with waste gate
Case 2. Cummins turbocompound system with power turbine, gear train, and fluid coupling
Case 3. Advanced diesel with positive displacement compounding

Cost studies at Cummins on various programs resulted in estimates of cost of the three systems listed above as $130, $680, and $820, respectively, over a naturally aspirated diesel engine.

The Diesel Cycle Simulation (DCS) analysis of a small waste gated turbocharger in a diesel engine predicted a brake specific fuel consumption (BSFC) of 200 gms/kW-hr (0.330 lbm/bhp-hr) with compressor and turbine efficiencies estimated at 75% each. With positive displacement screw compounding, this BSFC decreased to 175 gms/kW-hr (0.289 lbm/bhp-hr). This represents an improvement of 12.5% at rated power. At a part load point, this improvement goes as high as 30%. Since a light duty vehicle operates at part load for a significant portion of the duty cycle, a fuel economy degradation of 25% was assumed if the A.A.D. engine used a conventional turbocharger with waste gate. An advanced turbocompound engine is expected to provide a 10% improvement in fuel economy over conventional turbocharged diesels.

The advanced adiabatic diesel engine has 0-60 MPH acceleration time of 13.9 seconds as computed by Ford's duty cycle analysis program. This fast response is due to the charge system being belt driven by the crankshaft. Reference 5 indicates that the response

difference between a 70 bhp and 85 bhp 4 cylinder engine is about 4.4 seconds. Since compounding provides about 12.5% increased rated bhp, it was calculated that case 1 with the conventional wastegated turbocharger would have 3.1 seconds worse acceleration time compared to case 2 having a conventional turbocompound engine, and case 1 would be worse by 1.6 seconds than case 3 with the positive displacement screw compound system (Ref. 5). These approximations result in a cost trade-off as shown in Table 11.

TABLE 11. Cost-Benefit Trade-Off of Positive Displacement Screw Compounding

System	Unit Cost Increase	MPG	0-60 MPH Acceleration Time (Seconds)
1 Conventional Wastegated Turbocharger	$130	59.1	17.0
2 Conventional Turbocompound	$680	65.0	15.5
3 Positive Displacement Screw Compound System	$820	78.8	13.9

It becomes clear that on an initial cost analysis basis, the conventional wastegated turbocharger cost is less than the other two compounding systems. This is mostly due to the number of years of development that have gone into refining the turbocharger for mass production. With additional engineering, all three systems could be made to meet the acceleration requirements. While the absolute costs of turbocompounding and positive displacement screw compounding could be brought down with concentrated cost reduction and mass production efforts; relative to the turbocharger, this compounding system will always be more expensive since they have many more parts. Hence, is the increased cost justified on a total life cycle basis? On a 100,000 miles life cycle cost basis, the A.A.D. with the positive displacement screw compounding has a savings of $156 compared to the A.A.D. with a conventional turbocharger because of fuel economy. The conclusion is the compounding is justified.

Though there are several uncertainties regarding the cost of the A.A.D. at this time, it appears to be a viable and feasible engine worth developing further.

6.0 Task IV - A.A.D. Powertrain Long Range Development and Marketing Strategy

The A.A.D. development strategy was based on a market and economic study by Cummins and Ford. The summary of the study is presented here while full details of assumptions and trends are presented in Appendix 9.

6.1 Vehicle Costs

The economic analysis suggests that future large/luxury cars (3000 lbm curb weight) would be the best automobile class for the A.A.D. Performance and economy potentials are an excellent match for this class. In addition, large/luxury cars should offer a somewhat easier packaging opportunity than the smaller classes. Lastly, cost sensitivity is not as great in this class as in others, thus offering a somewhat more lenient engine cost premium target.

Compact light trucks are also excellent candidates for the A.A.D. The economic analysis is identical with that of large/luxury cars. A.A.D. performance and economy potentials are very attractive in this class of vehicle.

The target production for the A.A.D. powered vehicle is 1993, assuming R&D efforts could start in 1984 and uninterrupted commitment will be available.

6.2 Potential Volumes

Volumes are based on Cummins' car and light truck market forecasts, segmentation, and dieselization rate assumption.

1993 Car Market	12,000,000 units/year
Domestic Share	75%
Large/Luxury Share (domestic)	20%
Dieselization	5-15%
Diesel Large/Luxury Cars	90,000-270,000 units/year
1993 Light Truck Market	3,500,000
Domestic Share	75%
Compact Share	50-70%
Dieselization	5-15%
Diesel Compact Light Trucks	66,000-276,000
A.A.D. Market Potential Principle Candidates	156,000-546,000

6.3 Manufacturing Cost Premium

Although an option price for the AAD engine in the $1500-$1800 range is economically justified, we feel that most customers respond to more than merely "rational" buying stimuli. With this in mind, we have made a professoral judgement and set an option price target of $1,000. Given the pricing target, we recommend a near-term manufacturing cost premium of $1,000 over the equivalent gasoline engine and reducing to $500 the manufacturing cost premium as quickly as technology and volume growth permit.

6.4 Project Schedule

Because of the new technologies included in the A.A.D., a 9-year development schedule is visualized. If the program starts in January 1984, production availability of 1993 model year vehicles with the A.A.D. is possible. This is an aggressive schedule requiring significant commitments by participants. Key dates include:

Activity	Timing
. Engine company demonstrate prototype multicylinder engine	End of 1985
. Vehicle companies demonstrate complete prototype power train	Middle of 1988
. Order long lead tooling	Early 1990
. Job #1 (1993 Model Year)	3Q 1992

A development strategy in greater detail through proof-of-concept testing of prototype power trains was developed. The overall schedule shown in Table 12 is based on a 1993 model year launch of the AAD powered vehicle and was developed jointly by Cummins and Ford. This is a very aggressive schedule requiring parallel efforts in several phases of the program. The program visualized involves mostly component and system development and testing, which will result in engines being tested in vehicles by the middle of 1988. The engine development strategy presented here follows the actual processes that Cummins went through in the latest projects: the L-10 and B series Case-Cummins engines.

Key events that should take place, many of them simultaneously, up to mid-1988 are summarized below.

TABLE 12. Proposed Project Schedule

	Start	Finish
- Analytical Study	6/82	7/83 (Completed)
- Experimental verification of four critical technologies	1/84	9/86
- Detail design and drafting of the components for 1.4 liter engine	1/84	6/84
- Procure components for A.A.D.	1/84	12/84
- Component Tests	6/84	8/85
- Engine tests for BSFC, Emissions	7/85	12/85
- Vehicle design, procurement of nonstandard components	1/85	3/86
- Vehicle tests for proof of concept	5/86	8/88

The pacing item is the progress in ceramic manufacturing methods. A considerable amount of funds and efforts is currently being applied in this area by the government and private organizations. The progress should be continuously monitored as part of this program.

7.0 Task V - Identification of Long Lead Technology Development Requirements

Four important technologies incorporated in the AAD engine/power train need to be developed and experimentally verified. These are:

1. Piston development for oilless, adiabatic engine
2. Positive displacement compound charge air system
3. Preheating concept
4. Combustion system with positive ignition assist

Even though ceramic manufacturing technology development is the pacing critical path item, it is not over emphasized here since it is

already receiving considerable attention and has a good chance of success.

These four technologies should be developed prior to, or at least concurrent with, the development of the engine for prototype testing. All these technologies have beneficial effects on light, medium, and heavy duty engines to varying degrees. Only the preheating concept will have pronounced impact on light duty engines and less impact on heavy duty engines. Development of these technologies is critical to the ability of the A.A.D. engine to realize its full benefits. In order to speed up the process, a parallel effort to finalize the engine design is recommended while these four technology development programs are being completed. Appendix 10 contains a description of efforts needed to develop and test these advanced concepts. Ideally, a single cylinder test rig and a multicylinder test rig should be set up and hardware design, procurement, and test of the concepts be conducted in these test rigs.

CONCLUSIONS

Overall, the A.A.D. is a feasible diesel engine. It is a high payoff high risk concept and requires aggressive schedules and resource commitments. The marked improvement in fuel economy projected for the A.A.D. represents one of the best means of reducing the petroleum based fuel and oil consumption while maintaining a good commercial position for the automotive manufacturers. The authors project that this engine can be taken to the prototype stage simultaneously with experimental evaluation of the critical technologies identified in this report.

LIST OF REFERENCES

(1) A. S. Ghuman, M. A. Iwamuro, and H. G. Weber, "Turbocharged Diesel Engine Simulation to Predict Steady State and Transient Performance", ASME Publication No. 77-DGP-5 (1977).

(2) L. Tozzi, R. Sekar, R. Kamo, and J. C. Wood, "New Perspectives for Advanced Automobile Diesel Engine", Inter-Society Energy Conversion Engineering Conference, Orlando, Florida (August 1983).

(3) J. L. Hoehne and J. R. Werner, "The Cummins Advanced Turbocompound Diesel Engine Evaluation", DOE/NASA/4936-2 (December 1982).

(4) R. Kamo, T. Yamada and T. Nakagaki, "Synfuel Modified Diesel", Final Report U.S. Dept. of Energy, Contract No. B-A0763-A-P (May 1982).

(5) G. M. Cornetti and C. Bassoli, "Fiat Diesel Engines Database", U.S. Dept. of Transportation, Report No. DOT-TSC-1424 (December 1980).

(6) M. C. Brands, J. R. Werner, J. L. Hoehne, and S. Kramer, "Vehicle Testing of Cummins Turbocompound Diesel Engine", SAE Paper No. 810073 (1981).

(7) R. F. Steig and W. S. Worley, "A Rubber Belt CVT for Front-Wheel Drive Cars", SAE Paper No. 820746 (1982).

(8) F. J. Weinberg, K. Hom, A. K. Oppenheim, and K. Teiehman, "Ignition by Plasma Jet", Nature 272, 341-343 (1978).

(9) B. Myers, R. Landingham, P. Mohr, and R. Taylor, "A Topping Cycle for Coal Fueled Electric Power Plants Using the Ceramic Helical Expander", EPA-ERDA Symposium on the Environmental and Energy Conservation, Denver, Colorado (1975).

(10) G. Cerri, "Regenerative Supercharging of Four Stroke Internal Combustion Engines", SAE Paper No. 830507 (1983).

(11) D. W. Tryhorn, "New Turbocharging System for Two-Stroke Cycle Diesel Engine", SAE Paper No. 700075, Sir W. G. Armstrong Whitworth and Company Limited (1970).

(12) R. Kamo and W. Bryzik, "Cummins/TACOM Adiabatic Engine", SAE Special Publication SP-571, Pages 21-34 (Feb. 1984).

D2

N85 13237

APPENDIX 1

DETAILED PERFORMANCE ANALYSIS OF THE A.A.D. - CONCEPT "B"

R. SEKAR
L. TOZZI

I. INTRODUCTION AND SUMMARY

New concepts for engine performance improvement are seen thru the adoption of (a) heat regeneration techniques, (b) advanced methods to enhance the combustion, (c) higher efficiency air handling machinery, such as the positive displacement helical screw expander and compressor. Each of these concepts plays a particular role in engine performance improvement.

First regeneration has a great potential for achieving higher engine thermal efficiency through the recovery of waste energy. Although the concept itself is not new (this technique is used in the gas turbine), the application to reciprocating internal combustion engines is quite unusual and presents conceptual difficulties. The regeneration can be considered as a simple way to recover exhaust energy. It consists of transferring the heat from the exhaust to the intake by means of a heat exchanger. When the intake temperature is higher, then less fuel is required for given maximum in-cylinder temperature conditions, but more energy has to be spent to compress the hotter charge. Therefore, the improvement in thermal efficiency is not obvious. As it will be explained later, an improvement in the engine thermal efficiency can be obtained if proper values for boost pressure, intake temperature, and reciprocator compression ratio are implemented along with the utilization of an expansion device to convert exhaust gas energy into mechanical power. In this way, the entire engine may be regarded as hybrid, formed by a reciprocator plus a compression device, a recuperator, and an expander device (Figure 1).

The second important area is better control of the combustion process in terms of heat transfer characteristics, combustion products, and heat release rate. If a stratified temperature distribution (hot core and cold periphery) is induced in a low swirl chamber, the amount of heat rejected during the combustion process can be significantly reduced. This implies that more energy can be converted into mechanical work. In the same fashion, if a fast heat release curve can be realized (Figure 2), a higher compression ratio can be used for the same peak cylinder pressure limitation, improving the engine's thermal efficiency. Furthermore, hydrocarbon and nitric-oxide formation can be controlled through better mixing and by means of proper concentration of active radicals like nitrogen (N) and Oxyhydic (OH). Evidence of beneficial effect of the radicals on the formation of NOx and particulates is found in the current literature (Reference 1).

Finally, the third area for performance improvement is in the adoption of high efficiency air handling machinery. In particular, positive displacement helical expander and compressor (Ref. 3) exhibit an extremely high efficiency over a wide range of operating conditions. This becomes very important when the hybrid engine concept is implemented. More than 30% of the reciprocator power is delivered by the expander at part load conditions (TABLE 1). Boost pressure ratios of about 4.0 are required.

TABLE 1

Work Split Between the Reciprocator and the Compound System

Load %	RPM	Reciprocator Power (HP)	Expander Power (HP)	% of the Reciprocator Power
100	2500	70	17	25
	2000	56	13	23
	1000	27	5	19
75	2500	51	12	24
	2000	43	9	22
	1000	21	4	19
50	2500	35	11	31
	2000	28	9	32
	1000	13	4	28
25	2500	25	9	34
	2000	19	7	34
	1000	9	3	28

In order to evaluate the potential of each technique, a numerical computation was performed by means of a computer program simulating the diesel engine cycle. This program , called Diesel Cycle Simulation (DCS), was developed at Cummins Engine Company. The program can be used to simulate any steady state operating condition of a single cylinder four stroke diesel engine. Particular attention was devoted to the specific power and to the specific fuel consumption as well as temperatures and pressures induced within the combustion chamber. These data were subsequently used to determine stress and thermal load in critical components such as the piston, head, and cylinder liner. DCS was also used to optimize intake temperature, intake pressure, and exhaust pressure. Results in terms of power and fuel economy corresponding to different conditions of load and engine speed were used to generate the engine fuel consumption map.

The calculation of exhaust emissions in a new engine without an experimental correlation leads to inaccurate speculations. In fact, any combustion model needs to be calibrated with experimental data. Furthermore, the large number of parameters involved in a new advanced combustion system cannot be included in a general combustion model. However, thermodynamic considerations can produce a reasonably accurate qualitative picture especially for the nitric oxides and hydrocarbon formation. Principle factors considered in the emissions analysis were the increased ignition temperature and the presence of a positive ignition device.

II. DIESEL CYCLE SIMULATION (DCS) DESCRIPTION

The reciprocator is divided into three thermodynamic subsystems, (1) intake manifold and intake port, (2) engine cylinder, (3) exhaust manifold and exhaust port (Figure 3). The calculations are made by using mass and energy conservation equations along with the state equations (momentum effects are not included). Discrete crank angle increments are considered throughout the 720° crank angle degree cycle, and integration of the appropriate variables compute the full cycle engine performance.

The engine heat transfer process is described by simplified models. The ideal gas law and thermodynamic equilibrium are assumed at all times for all subsystems. Within each control volume homogeneous mixtures of air and combustion products are assumed. Mass averaged temperatures are used in the analysis; therefore, no effects of high temperature burning zones are considered. The heat transfer model is simplified by assuming one dimensional heat transfer. The cylinder wall temperatures are updated at the end of each iteration based on one dimensional energy balance in the wall.

The combustion process is simplified by assuming that combustion products are homogeneous and at thermodynamic equilibrium at all times. Either the heat release curve or the cylinder pressure data must be entered in the program. The values of density, viscosity, specific heat, and conductivity are those of air instead of products of combustion. The friction model consists of two submodels. The first one accounts for rubbing friction and is based upon motored engine test data. The second accounts for pumping losses and is given by the cylinder pressure integral over the intake and exhaust process.

The DCS computer program can operate in four different modes (Figure 3): 1) manifold conditions known, 2) black box turbocharger, 3) detailed turbocharger maps, and 4) cylinder pressure analysis. The first three modes are essentially different boundary conditions placed on the reciprocator and are explained in Figure 3. Mode 4, cylinder pressure analysis, affects the closed cycle calculations only and is used to calculate an apparent heat release rate from experimental cylinder pressure, rather than calculating cylinder pressure from a fuel burning curve as is done in operating modes 1, 2, and 3.

Cummins has validated the DCS against a wide range of direct injection (DI) diesel engines of varying ratings, and good general agreement has been obtained. The DCS has been found to be particularly useful in predicting both the direction and the magnitude of changes in performance as engine parameters and operating conditions are altered. (Ref. 1)

For the work reported here, the DCS input has been adjusted to account for an insulated combustion chamber, fast heat release, and variable intake manifold pressures and temperatures.

The baseline engine simulated in this study was obtained by scaling down a Cummins 4T-390 DI light duty diesel engine with a power rating of 27-34 HP/cylinder. Details of the simulated engine are given in TABLE 2.

TABLE 2

Engine Geometry

The engine dimensions entered in the computer for the diesel cycle simulation (DCS) are as follows:

Intake Manifold Inside Diameter	= .687 in.
Intake Manifold Length	= 2.0 in.
Intake Manifold Outside Diameter	= .937 in.
Intake Port Inside Diameter	= .707 in.
Intake Port Length	= 4.0
Intake Port Outside Diameter	= 1.0 in.
Exhaust Manifold Inside Diameter	= 1.01 in.
Exhaust Manifold Length	= 5.01 in.
Exhaust Manifold Outside Diameter	= 1.31 in.
Exhaust Port Inside Diameter	= 1.00 in.
Exhaust Port Length	= 3.94 in.
Exhaust Port Outside Diameter	= 1.30 in.
Cylinder Bore Diameter	= 3.03 in.
Connecting Rod Length	= 7.56 in.
Cylinder Liner Outside Diameter	= 4.60 in.
Connecting Rod Bearing Diameter	= 3.12 in.
Equivalent Piston Skirt	= 1.85 in.
Cylinder Head Surface Scale Factor	= 1.00 in.
Piston Surface Area Scale Factor	= 1.1 in^2
Exhaust Valve Flow Area Scale Factor	= 1.0 in^2
Intake Valve Flow Area Scale Factor	= 1.0 in^2
Piston Ring Contact Height	= 0.601 in.
Intake Valve Radius	= 0.83 in.
Piston Stroke	= 3.03 in.
Accessory Bearing Length per Cylinder	= 0.25 in.
Total Main Bearing Length per Cylinder	= 1.78 in.
Number of Valves per Cylinder	= 2
Accessory Bearing Shaft Diameter	= 2.03 in.
Engine Block Main Bearing Diameter	= 4.50 in.

III. ADVANCED TECHNOLOGIES FOR PERFORMANCE IMPROVEMENT

The major areas defining the performance of an engine are: (1) engine configuration, (2) thermodynamic conditions, (3) combustion process, (4) air handling system, and (5) mechanical friction.

1. Engine Configuration

a) Rated Power: The contract specifies that the 3,000 lbm vehicle must be capable of accelerating from 0 MPH to 60 MPH in 15 seconds. This determines the rated power requirement which is obtained by running the vehicle simulation computer program several times until the

desired acceleration is obtained. The figure generated by this computation, and considering the use of a continuously variable transmission (CVT), was 70 HP which resulted in an acceleration of about 14 seconds.

b) Displacement: This parameter is automatically defined by the rated power, the mean effective pressure (BMEP) and the engine speed (rpm). High BMEP yields high specific power, which is desirable; but at the same time, the thermal and mechanical loads increase as well. Therefore, the strength of the material used for the fabrication of the engine defines the maximum BMEP level. The light duty engine structure uses common materials to which some ceramic components are added to insulate the combustion chamber. A thermal analysis of the critical components (piston, cylinder head, and liner) showed that the absence of any form of cooling results in about a 25% increase in metal temperature and consequently the induced thermal stress is higher. For this reason, a maximum BMEP level of 240 psi was considered a reasonable value. To reduce the rubbing friction, the rated engine speed was reduced to 3000 rpm. The relation between power (P), mean effective pressure (BMEP, psi), speed (rpm), and displacement (D, litre) is the following:

$$D = \frac{P * 13230}{BMEP * rpm}$$

From this equation and corresponding to the rated values of power, BMEP and rpm, the displacement is calculated to be 1.4 litre.

As far as the bore/stroke ratio is concerned, the actual trend is to consider square configuration. In fact, long stroke tends to have high surface to volume ratio which increases the heat losses. On the other hand, large bore can originate stagnation pockets in which the flame can get quenched causing an increase in hydrocarbon emissions. The bore and stroke dimension corresponding to 1.4 litre displacement and to four cylinders is 77 mm (3.03 in.).

c) Number of Cylinders and Engine Layout: For a given displacement, the increase of the number of cylinder improves the smoothness and the power output through better capability of running at higher rpm. The efficiency, on the other hand,tends to deteriorate. This is due to the increase of the surface to volume ratio which causes an increase in heat loss and in rubbing friction. Another negative aspect concerns the combustion process. A small combustion chamber increases the possibility of fuel impingement against the walls resulting in flame quenching and consequently, worse emissions characteristics. The cost and the length of the engine increase too. In the range of .9-1.5 litre, three cylinder, in-line appears to be very attractive. None is marketed at present; but Datsun is working on a 3 cylinder 1.0 litre diesel engine, VW has a 1.2 litre aluminum 3 cylinder diesel engine, and Elko has recently published a paper about a 3 cylinder DI 1.4 litre diesel engine. However, the three cylinder solution presents an inherent unbalance which can probably be controlled by using a counterbalance shaft. The only problem, that cannot be eliminated, is the high torque fluctuation. This causes stronger vibrations and higher noise levels. Therefore, the

four cylinder engine was selected. As far as the layout is concerned, the in-line type is the most common one. The alternative would be the horizontally opposed piston configuration adopted by Alfa Romeo, but this presents the problem associated with long, high pressure injection lines. The V configuration offers a very compact package but presents a small secondary unbalance couple and a more complex head design. For these reasons, the four cylinder in-line engine has been chosen for this design. The chosen engine configuration for the advanced light duty diesel engine is as follows:

Displacement	1.4 litre
Bore	3.03 in.
Stroke	3.03 in.
Number of Cylinders	4
Layout	In-line
Rated Power	70 HP

2.0 Thermodynamic Operating Conditions

If one of the main goals is to increase the engine thermal efficiency, then the thermodynamic conditions under which the engine operates become extremely important. The following criteria must be considered:

a) High combustion temperature: The thermal efficiency for a Brayton cycle can be written:

$$(1)\ \eta = \left(1 - \frac{T_{min}}{T_{max}}\right) \frac{T_{max} - T_{ign}}{T_{max} - T'_{ign}} \cdot \frac{1}{C_{eff}} \times \left(1 - \frac{1 - \varepsilon_{eff} C_{eff}}{1 - \frac{T_{min}}{T_{max}} CR^{\frac{\gamma-1}{\gamma}}}\right)$$

where (Figure 4):

T_{min} = the cycle's lowest temperature which is limited by the ambient temperature.

T_{max} = the cycle's highest temperature which is limited by the materials used in the fabrication of combustion chambers, cylinder head, piston, and cylinder liner.

T_{ign} = the ideal temperature at which combustion occurs. If spontaneous type of combustion has to be initiated, then T_{ign} must be higher than the self-ignition temperature corresponding to the particular ignition pressure.

T'_{ign} = the real temperature at which combustion occurs which is higher than T_{ign} because of the heat transfer into the charge and the heat production during the compression stroke.

C_{eff} = the adiabatic compression efficiency and is represented by the following formula:

$$\eta = \frac{\Delta H \text{ ideal}}{\Delta H \text{ real}}$$

where ΔH ideal is the increase of enthalpy corresponding to adiabatic compression and Δ H real is the increase in enthalpy during compression.

ϵ_{eff} =the adiabatic expansion efficiency and is represented by the following formula:

$$\eta = \frac{\Delta H \text{ real}}{\Delta H \text{ ideal}}$$

where ΔH real is the decrease in enthalpy corresponding to the real expansion and ΔH ideal is the decrease in enthalpy corresponding to an adiabatic expansion.

CR = the volumetric compression ratio which defines, for the same heat input, the maximum pressure and temperatures of the cycle.

γ = the specific heat ratio (C_p/C_v) which is a function of the thermodynamic conditions and of the gas chemical composition.

From eq. (1), it is clear that higher thermal efficiency corresponds to higher T_{max}. High combustion temperatures can be accomplished by using high input energy and high compression ratio. High energy input is limited by the amount of air that can be introduced into the engine. The breathing capability of the engine can be improved by using a forced charge system (turbocharger or supercharger). The engine boost pressure creates an increase in engine back pressure, in the case of the turbocharger, and reduces the power output in the case of the supercharger. In both cases, boosting the engine results in a loss of efficiency which can be compensated by the higher maximum in-cylinder temperature and pressure obtainable with a higher boost level. This implies the existence of an optimum boost pressure for any particular engine. If the mechanical connection between the engine and the charge system is removed and substituted by a thermal connection (Ref. 4), which consists of a gas turbine bottoming cycle, then boost pressure will be obtained without any loss in efficiency as in the previous case. The problem associated with this concept is the higher exhaust temperature needed to produce the required boost pressure level.

As will be discussed later, the numerical analysis performed by means of the Cummins Diesel Cycle Simulator (DCS) predicted an optimum boost level range between three to four, depending upon the load conditions.

The main factor considered in the evaluation of the engine was the duty cycle. Figure 5 shows the Environment Protection Agency (EPA) Urban Driving Cycle in terms of fuel consumed versus time and load. This plot clearly shows that most of the time and most of the fuel is consumed at very light load. In this condition, the engine thermal efficiency is usually very low, because of the low in-cylinder temperatures and pressures. Based on this consideration, a method to improve the engine efficiency at part load without sacrificing acceleration capability, was identified and applied to this engine.

In order to increase the in-cylinder pressures and temperatures to the maximum values for best efficiency, it has been shown that it is necessary to increase either the amount of fuel introduced into the cylinder per stroke, or the compression ratio. In a part load situation, the amount of fuel cannot be varied for obvious reasons; therefore, the only alternative would be to increase the compression ratio. If this solution is adopted and high in-cylinder pressures and temperatures are established at part load, then full load operations become extremely difficult since pressure and temperature cannot be too much higher than at part load. This results in a poor acceleration capability which is undesirable.

TABLE 3 gives the values of intake pressure and temperature used in the DCS computer simulation corresponding to different operating conditions. These values have been obtained from an optimization study shown in Figure 6, where the variation of BSFC has been related to the intake manifold temperature. It is important to note that higher intake temperature is needed at lower load. The engine air charging system was designed by IGT (Appendix 7) to meet these requirements.

TABLE 3

Optimum Intake Pressures and Temperatures

RPM	Load %	Intake Temp. (°F)	Intake Press. (PSIA)	Air Mass Flow (LBM/MIN)
3000	100	450	46	7.8
3000	75	700	56	9.2
3000	50	840	50	6.5
3000	25	1140	63	8.5
1000	100	450	46	3.1
1000	75	700	56	3.3
1000	50	840	50	2.4
1000	25	1140	63	2.8

As was anticipated, the temperature decreases from 1150°F at part load to 450°F at full load. Similarly, the pressure decreases from 63 psi at part load to 46 psi at full load.

The high part load intake temperatures and pressures will result in moving up the thermal cycle to higher temperatures and pressures; consequently, more heat will be added at higher temperatures and better thermal efficiency will be accomplished.

b) Low Exhaust Gas Temperature: As is well known, the efficiency for a thermal engine is given by the ratio:

$$\frac{Q_{in} - Q_{out}}{Q_{in}}$$

Q_{in} = heat added
Q_{out} = heat rejected

From this relation, one can infer that for the same Q_{in}, a reduction in Q_{out} will increase the thermal efficiency of the engine.

In order to obtain an improvement in efficiency, the preheated cycle exhaust gas temperature must be low enough so that the amount of heat rejected is less than the amount of heat added. One of the most critical parameters affecting the performance of the preheated cycle is the reciprocator compression ratio. In fact, from the formula:

$$W_{comp} = M C_p T (P_R^{\gamma - 1} - 1)$$

where:

W_{comp} = compressor work
M = mass flow rate of air
C_p = specific heat at constant pressure
T = intake temperature
P_R = pressure ratio
γ = C_p/C_v

It is clear that the energy necessary to compress a certain mass of air increases with the intake air temperature and the compression ratio. The higher the compression work, the smaller the net work, or the difference between expansion work and compression work. But the net work is also equal to the difference between heat added and heat rejected. Therefore, for the same heat addition, higher compression work implies higher heat rejected; consequently, less thermal efficiency. A solution to this problem consists of reducing the reciprocator compression ratio such that the corresponding value of the heat rejected is lower than the case without preheating. On the other

hand, to accomplish high in-cylinder pressures, a higher boost level is necessary. Hence, the reciprocator compression ratio and boost pressure have to be optimized in relation to the intake temperature necessary for the improvement in thermal efficiency.

c) Low Heat Loss During Power Stroke: As will be shown later, several levels of insulation have been tried for best thermal efficiency. The presence of insulated material, inside the engine combustion chamber, results in two effects. One consists of an increase of the energy converted in mechanical work during the power stroke. The other effect consists of an increase of the exhaust gas energy. This leads to a linear improvement in BSFC as shown on computer runs for increased insulation.

Another effect of the in-cylinder thermal insulation consists of noticeable degradation in volumetric efficiency. The Diesel Cycle Simulation results are presented in Figure 7 and represent the effect of different insulation levels.

The degradation of the volumetric efficiency is caused by the higher thermal capacity characteristic of the insulating material. The higher the heat stored in the in-cylinder components during the power stroke, the higher the amount of heat transferred to the fresh charge during the intake stroke. Table 4 shows the relationship between volumetric efficiency and heat rejection reduction. When the insulation is such that to reduce 65% of the heat loss during the power stroke, then the volumetric efficiency drops from about 94%, for the cooled case, to about 79% for the insulated case. The loss in volumetric efficiency causes more energy to be absorbed by the charge system; consequently, less work will be recovered by the compound system. This will result in a deterioration of the overall BSFC whose variation with the insulation thickness will not be linear any more. As is shown in Figure 11, the curve has a "knee" at 65% reduction in heat rejection. Beyond this value, no significant improvement in BSFC can be obtained.

TABLE 4

Effect of Heat Rejection Efficiency on Volumetric Efficiency

Heat Rejection Efficiency (%)	Volumetric Efficiency Reduction (%)
92	0
91	20
90	40
82	60
55	80

d) Low Energy Expenditure During Compression: As was shown at the beginning of this section, the indicated net work is given by the difference between the expansion work and the compression work. The latter can assume different values depending upon the type of transformation. In particular, an adiabatic compression requires the

highest amount of energy, whereas an isothermal compression requires the lowest energy expenditure. The equation that represents the adiabatic compression work is given by:

$$W_{comp} = m \frac{C_p T_{in}}{\eta_c} \left(P_R^{(\gamma - 1)} - 1\right)$$

where: m = mass of air compressed

C_p = specific heating value at constant pressure

T_{in} = temperature at the start of compression

P_R = compression pressure ratio

γ = specific heating values ratio

η_c = adiabatic compression efficiency

From this formula, one can infer that the dependence with the temperature is linear whereas the dependence with the pressure ratio is not. Consequently, to compensate for a large increase in temperature, a small decrease in pressure is sufficient. This concept is used in the application of the preheating technique where part of the exhaust gas energy heats the intake charge. The engine compression ratio was reduced from a very high value to 14:1 and the intake temperature was raised up to 1150°F at part load conditions. To insure high in-cylinder pressures, the boost was increased up to four atmospheres. In essence, the compression work was significantly reduced by adopting a two stage compression with preheating in between, as compared to the one stage compression preceded by the heating of the intake. A qualitative schematic of the cycle arrangement is given in Figure 8. From this figure, it is clear that the ΔH required in the two stage compression is lower than for the single stage compression.

e) Positive ΔP Across the Engine: Figure 9 shows a typical indicated P-V diagram of a turbocharged diesel engine. From this figure, it is possible to distinguish two regions bounded by the points representing the in-cylinder condition. When the sequence of the points is allowed to run along the curve clockwise, then, for definition, the work is positive (delivered by the engine); otherwise, the work is negative (absorbed by the engine). Consequently, the area "A" is positive and represents the work produced by the engine, whereas area "B" is negative and represents the work necessary to induce the air into the cylinder during the intake stroke and to push it outside during the exhaust stroke. This negative work is called "pumping". The higher the pumping losses, the smaller the work delivered, and the worse the engine efficiency.

To reduce the pumping losses, it is necessary that the difference between intake pressure and exhaust pressure is as small as possible. If

the intake pressure is higher than the exhaust pressure, then the area "B" becomes positive and the pumping is no longer a loss, but useful work.

This particular charge air system results in a positive ΔP across the engine. It is obvious that higher boost pressures require more compression energy; therefore, less energy will be available for compounding. But in the case discussed in the previous paragraph and relative to the two stage compression with preheating, the positive ΔP across the engine maximizes the thermal efficiency. This implies that the disadvantage in reducing the amount of energy that can be compounded is overcome by the positive pumping work.

3. Combustion Process

In an internal combustion engine, the combustion process assumes a critical role affecting the entire cycle thermal efficiency and thus critically affects fuel economy. In fact, the heat addition process is completely controlled by the way in which the fuel burns. Fast burning rate results in constant volume heat addition; on the other hand, a slow burning rate results in constant pressure heat addition. Another important factor is where the combustion occurs with respect to the piston top dead center (TDC). It is well known that if more fuel is burned around TDC, the energy conversion will be more efficient. Figure 2 shows a comparison between a typical fast and long duration diesel combustion and a hypothetical short duration combustion. The differences between the two are that the first results in a nearly constant volume heat addition which imposes a lower volumetric compression ratio, for a given peak cylinder pressure limitation, and induces higher peak cylinder temperatures. The lower compression ratio limits the thermal efficiency. Furthermore, higher in-cylinder temperatures increase the amount of heat transferred to the cylinder walls not only due to the increase in ΔT but also because a high temperature diffusive flame produces high concentration of carbon particles (soot) which have very high emissivity and produce a significant increase of the heat lost by radiation. Because of the low in-cylinder thermodynamic conditions, late heat addition produces low thermal efficiency. Hence, it is important to optimize the heat release rate and the heat release shape relative to TDC.

4. Air Handling System

As already pointed out in the heat balance analysis, part of the exhaust gas energy can be converted into mechanical power to boost the intake pressure and to augment the reciprocator power through a mechanical drive to the engine crankshaft. In this case, the exhaust gas energy conversion is mainly affected by fluid mechanic losses due to the real behavior of the gas which undergoes irreversible processes. The type of machine and its design have a significant effect on the efficiency of the transformation. In particular, the efficiency variation with the engine load and speed depends upon the type of machine. Positive displacement helical type of compressors and expanders are characterized by flatter adiabatic efficiency curves (Appendix 7, IGT

Report). On the other hand, the top efficiency value depends only on the design accuracy. This means that regardless of the type of machine one can get high adiabatic efficiency if the design of the ducts, through which the gas flows, is such to create minimum flow dynamic losses.

It is obvious that the higher the air handling system efficiency, the more exhaust gas energy can be recovered. Table 5 shows the sensitivity of the overall engine efficiency to the air handling system efficiency. This plot was obtained by running the DCS computer program with different compressor and expander efficiencies. Depending upon the engine load, the percentage of compound HP with respect to the total available exhaust HP can vary between 61% and 37% as shown in TABLE 6. Therefore, if the air handling system adiabatic efficiency is 100%, then all the energy expressed in (2) can be converted into mechanical work. If the efficiency is 80% (η_{adb} = .8) and one indicates with W*.8 the amount of energy converted by the compound system with B*.8 the amount of energy converted by the charge system, then the overall work delivered by the engine will increase by the quantity W*.8 from which one can infer that efficiency decreases linearly with the air handling system adiabatic efficiency (η_{adb}).

TABLE 5

Effect of Compressor and Expander Efficiency on AAD Engine BSFC

Compressor and Expander Combined Efficiency	Compound Engine BSFC lbm/HP-hr)
76	0.24
74	0.25
70	0.25
64	0.26

TABLE 6

Percentage of the Compound HP with Respect to the Available Exhaust HP

Engine Load	Engine HP	Available Exhaust HP	Compound HP	Compound HP % Exhaust HP %
100	70	39	24	61
75	53	39	17	43
50	35	37	15	40
25	18	35	13	37

As will be discussed later, an average benefit of 7% can be attributed to the use of an improved air handling system.

In this study, a performance map of a hypothetical positive displacement helical expander and compressor was considered. Performance analysis of the helical machinery was conducted by the Institute of Gas Technology (IGT). They based their study on the currently available literature. They used all the necessary information to build a first approximation mathematical model. This was a one dimensional steady state semi-empirical model which makes use of certain coefficients experimentally obtained by other authors. Leakage problems related to clearances between rotors and the casing were the major issues in the formulation of the problem. Figure 10 shows the computer predicted helical expander and compressor efficiency. From this plot, one can infer that the advantage of this type of machinery lies in a higher value for the adiabatic efficiency and in a small sensitivity to the engine load and speed variation.

This important characteristic results in a low end torque which, as it is well known, greatly improves the engine performance. Furthermore, the lower rotational speeds allow a belt driven expander and compressor to be used.

The absence of a compound model in the computer cycle simulator necessitated adjustment of the calculated BSFC according to the formula:

$$BSFC_{new} = BSFC_{old} \frac{HP_{new}}{HP_{old}}$$

where, $BSFC_{new}$ = the new engine efficiency value that accounts for increased output power

$BSFC_{old}$ = the old engine efficiency value that doesn't account for the additional net power delivered by the expander to the engine crankshaft through the belt.

HP_{new} = the sum of the reciprocator power plus the total expander work minus the compressor work

HP_{old} = the power delivered by the reciprocator.

The discussion of the validity of the assumptions and results is presented in the IGT final report.

5. Mechanical Friction

A recent study conducted by Ford Motor Co. has shown that depending upon the engine load, the percentage of the rubbing friction in a light duty engine, with respect to the total indicated output power, is approximately 4% at full load and 8% at part load. Therefore, if part of this friction is reduced, a considerable improvement in efficiency may be accomplished especially at part load operation.

Lubrication in an adiabatic engine is a major problem. Studies are being undertaken on new liquid lubricants with increased stability at high temperatures and high ring contact pressures. However, solid lubricants and/or gas lubricants are preferable solutions.

The advantages of the rolling piston cross head, piston gas bearings, and solid lubricated roller bearings are considered here. Quantitative evaluation remains to be made of the adiabatic, oil-less, minimum friction engine concept.

It is generally agreed that in a heavy duty diesel engine, 50% of the mechanical friction can be attributed to the piston. The remaining 50% is due to friction in the valve train, crankshaft, crankpin, and wrist pin. By using a hydrostatically gas supported piston-liner assembly and solid lubricated hot pressed silicon nitride (HPSN), hybrid roller bearings, the following reduction in engine friction was measured:

Piston/Rings	72% reduction
Con. Rod & Crank	81% reduction

Therefore, a realistic projection might be the following:

- 6.0% fuel economy improvement at part load

- 3.0% fuel economy improvement at full load

Based on this information, efficiency value estimated from the DCS analysis was adjusted by reducing the amount of friction calculated depending upon the engine load and according to the following formula:

$$BSFC_{new} = BSFC_{old} \frac{BMEP}{IMEP - RFMEP} \qquad (3)$$

where:

$BSFC_{new}$ = the new efficiency value that accounts for reduction in friction

$BSFC_{old}$ = the efficiency value calculated by DCS

BMEP = the brake mean effective pressure

IMEP = the indicated mean effective pressure

RFMEP = the rubbing friction mean effective pressure.

Therefore, according to the previous figures, the percentage reduction in rubbing friction is 76%. This means that the calculated value of RFMEP was reduced by 76% and used in equation (3) to generate the corrected value of BSFC.

III. RESULTS

As already pointed out, this analytical study was conducted by means of a diesel cycle simulation (DCS) computer program developed at Cummins Engine Company, Inc. Furthermore, the simulation results were adjusted to account for reduced friction and a compound device. Proper thermal conductivity values for the piston, liner, cylinder head, valves, and intake/exhaust manifolds were used. They were obtained by considering the type and thickness of the ceramic insulation and by correlating them with some extrapolated experimental single cylinder engine results. TABLE 7 shows the thermal conductivity values used in the computer simulation.

TABLE 7

Thermal Conductivity Values Used in the Simulation
Btu/(ft-hr-°R)

	Ceramic	Metal
Exhaust Valve	.2	10
Cylinder Head	.5	25
Intake Valve	.5	25
Cylinder Liner	.5	25
Piston	3.5	60

To account for waterless conditions, an overall external convective constant was estimated and a good agreement with the experimental data was obtained.

According to the engine configuration discussed in Part III, a complete design of the engine was performed and the necessary geometrical specifications showed in TABLE 2 were used for the computer simulation. The valve schedule was optimized for best fuel economy at light load operations.

Different heat release curves were input in the program corresponding to different load conditions. In particular, due to the part load preheating technique, higher ignition temperature is established at light load and more favorable heat release curve was assumed to occur. TABLE 8 shows the three heat release curves input in DCS relative to full, part, and light load engine operations.

TABLE 8

Heat Release Rate Curves Used in AAD

Load	Firing Pressure (Bar)	Firing Temperature (°C)	Ignition Delay (MS)	Heat Release Shape
Full	57	1200	.1	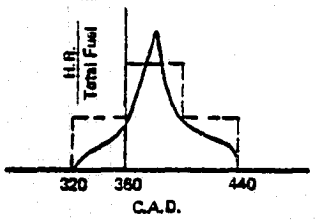
Part	60	1600	.04	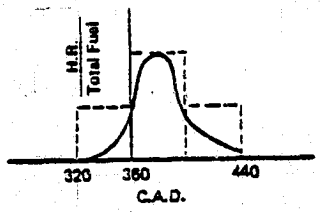
Light	78	2300	.02	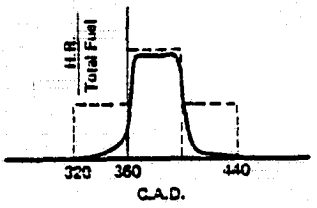

The air/fuel ratio and the boost pressure were adjusted for a maximum peak cylinder pressure of 3000 psia. This resulted in maximum BMEP and temperature of 220 psi and 350°F, respectively. The corresponding stress induced under these conditions was evaluated by a finite element computer program and detailed results are presented in the stress analysis part.

SENSITIVITY TO THE TECHNOLOGY

As already pointed out in Part III, several technologies need to be implemented in order to improve the performance of the existing automobile diesel engine.

First, the engine performance was defined in terms of acceleration capability, fuel economy, emissions, and the major factors affecting them were identified in magnitude and shape of the torque curve, engine BSFC, and relative fuel map The torque curve shape mainly depends upon the engine breathing characteristics at different engine loads and speeds. Therefore, charge air system efficiency and part load prehating were identified as the principle technologies affecting the engine acceleration capability.

The engine BSFC as already explained in Part III is directly affected by many factors. These can be influenced by technologies such as: (a) heat rejection reduction by in-cylinder insulation and consequent exhaust heat recovery, (b) high cylinder pressure, (c) proper heat release curve as a functon of crank angle, (d) charge system efficiency, and (e) percentage reduction in rubbing friction. On the other hand, the fuel map shape strictly depends on the enigne breathing characteristics (charge system efficiency map and part load preheating). Furthermore, the high boost pressure, low reciprocator compression ratio technique resulted in more effective part load preheating; therefore, it was considered to be effective on the fuel map shape.

Nitric-oxides, hydrocarbons, and particulate emissions were directly related to the air/fuel ratio, to the heat release curve shape, and to the heat rejection level. TABLE 9 summarizes this discussion.

Six emerging technolgoies were applied, one at a time, to the baseline engine. Therefore, the improvements were caused by the particular technology and depends only upon the assumed performance of the baseline engine.

TABLE 9

Factors Affecting Engine Performance and Emissions

Acceleration	Fuel Economy	Emissions
- BMEP	-adiabatic-compound	-charge air system effectiveness
- Chage Air System Efficiency Map	-cylinder pressure	- combustion process
- Part Load Preheating Effectiveness	- combustion process - charge air system efficiency map - minimum rubbing friction	- adiabatic

A literature review was conducted in order to establish the most realistic reference of an automobile diesel engine. Two different approaches could have been taken. The contract considers the state of the art production automotible diesel engines presently used in a 3000 lbm car. These are cooled indirect injection diesel engines with an acceleration of 0-60 MPH in 15 sec., a fuel economy of 37 MPG and complying with current emissions regulation. This appendix considers the state of the art prototype minimum cooled, direct injection diesel engine prototype. Examples of these engines are given by Elsbett, Wosvager, and Komatsu. The performance of a 1.4 litre, 70 HP, direct

injection, semi-adiabatic engine has an acceleration of 0-60 MPH in 15 sec. and a fuel economy of 43 MPG. This is an experimental engine and could be thought of as first level improvement over our IDI baseline.

In order to simplify the explanation of the effect of each technology on the engine performance, three technology levels were established:

1. First Technology Level:

   - Adiabatic Compound Concept
   - High Cylinder Pressure
   - Controlled Combustion Process

2. Second Technology Level:

   - First Technology Level
   - High efficiency Charge System
   - Minimum Rubbing Friction

3. Third Technology Level:

   - Second Technlogy Level
   - Part Load Preheating

FIRST TECHNOLOGY LEVEL

a) Adiabatic Compound Concept

The heat rejection reduction adopted by the so-called minimum cooled or semi-adiabatic diesel engine is about 25%, and usually the engines do not include any exhaust energy conversion system. The adiabatic engine concept, as it is conceived at Cummins, implements about 65% heat rejection reduction; consequently, the presence of an exhaust energy recovery device is more appropriate. For this reason the considered technology includes both the adiabatic and compound concept. Furthermore, the adiabatic technology itself doesn't lead to significant performance improvement, and the full potential can be exploited with the use of an exhaust energy recovery device. In this study the presence of a positive displacement expander, directly connected to the engine crankshaft, insured the recovery of the left over exhaust gas energy after boosting the engine.

The implementation of this technology resulted in an increase of the in-cylinder energy conversion and in an increase of the exhaust gas temperature. However, the in-cylinder parts thermal load also increased. TABLE 10 summarizes the differences between an advanced minimum cooled direct injected diesel engine and an adiabatic compounded diesel engine.

TABLE 10

Minimum Cooled vs. Adiabatic Engine

	Minimum Cooled	Adiabatic Compounded
maximum exhaust gas temperature	1100°F	1800°F
maximum in-cylinder parts temperature	1100°F	1600°F
Minimum BSFC	.340 lbm/HP-hr	.308 lbm/HP-hr
volumetric efficiency	91%	79%

It is clear that about 9% improvement in the minimum value of b.s.f.c. can be obtained with a 65% reduction in heat rejection and with a compound system adiabatic efficiency of 70%. This produces 60% increase in maximum exhaust gas temperature, and reduces the volumetric efficiency by 13%.

Figures 11 and 12 compare the fuel maps of to the semi-adiabatic engine and the computer simulation of the adiabatic-compounded Cummins' engine. The shape of the iso-BSFC curves is now different and the BSFC value itself is lower. The improvement goes from 10% at full load (high BMEP) to 4% at light load. This is due to the fact that at light load there is no left-over exhaust energy to recover and the improvement in thermal efficiency is due to the reduction in in-cylinder losses (see Part III).

b) High Cylinder Pressure

For a given heat release curve, different reciprocator compression pressures result in different peak cylinder pressures (PCYLP). Figure 13 shows the DCS prediction of the effect of a high PCYLP on the engine BSFC. It appears that the relationship is linear and that an increase in PCYLP from 2000 PSIA to 3000 PSIA improves the BSFC from .340 lbm/hp-hr to .330 lbm/hp-hr. This is an improvement in BSFC of 3% for 50% increase in PCYLP.

Part load conditions are still characterized by low cylinder pressure. Therefore, no improvement in efficiency can be accomplished. This implies that the engine fuel map will have lower b.s.f.c. values at high loads and no significant changes at light loads.

The implementation of both technologies brings the minimum b.s.f.c. value from .340 lbm/hp-hr to .298 and improves the fuel map values as shown in Figure 14.
#

c) Controlled Combustion Process

The implementation of a hypothetical, controlled combustion process, generating a heat release curve similar to that shown in Figure 2, resulted in an improvement of the minimum BSFC of about 4%, (i.e. from .340 lbm/HP-hr to .326 lbm/HP-hr).

It was assumed that different heat release curves occurred at different engine load. In particular, at light load, the higher ignition temperature was assumed to result in more favorable combustion process. Consequently at light load 2% BSFC improvement was obtained.

The implementation of all the three advanced technologies so far discussed, resulted in an improvement of the BSFC from .340 lb/hp-hr to .289. As in the previous cases, when the shape of the fuel map changed, the b.s.f.c. values improved as shown in Figure 15. This fuel map was run through a computer program simulating the EPA duty cycle for a 3000 lbm car, with a drag coefficient of C_x=.37, a frontal area of 26 ft^2, and equipped with a continuously variable transmission (CVT). The resulting acceleration performance remained unchanged, since the rated power was unchanged, and the fuel economy improved from 43 MPG to 50 MPG.

This particular engine configuration was identified as a first level of technology, and represented a first step toward a high performance diesel engine.

As far as the effect on exhaust emissions is concerned, the lack of a reliable combustion model prevents any sort of valid exhaust emission prediction. Generally, the increased charge temperature at the start of injection could have two opposite influences on NO_x production. An important source of NO_x is the rapid burning of the fuel vaporized and mixed during the ignition delay period. The shorter delay period, due to the higher temperature, will result in less NO_x formation by this mechanism despite the increase in vaporization rate. Later in the combustion process, the generally increased temperature and pressure, resulting from insulation, will both increase the NO_x formation rate and postpone the point at which the NO_x formation reaction is quenched.

It is very difficult to judge which of the two mechanism will prevail during the real engine operations. The previous assumption of smooth combustion process, consisted in a significant reduction of the amount of fuel burned instantly as the mixture formed during the ignition delay period. This could prevail on the second mechanism and the overall NO_x production could decrease.

Experimental data on a single cylinder uncooled engine, shows an increase of the specific NO_x. On the other hand new perspectives in

advanced combustion systems, offer a potential for NO_x reduction in insulated engines. As far as the NO_x production for the first technology level engine should comply with the Federal Regulation. Unburned hydrocarbon emissions should be reduced by the increased wall and gas temperature. This will produce higher oxidation rates and reduce the chances of flame quenching.

As far as particulates formation is concerned, the increased gas temperature postpones the point at which soot oxidation reaction is quenched. On the other hand, the formation of soot by pyrolisis may be accelerated by the higher temperature. Fortunately in this case, single cylinder test data shows a clear drop in particulates for an adiabatic engine as compared to a standard water-cooled engine (see Figure 16).

SECOND TECHNOLOGY LEVEL

a) High Efficiency Charge System

This technology is now considered in addition to the first level. Figure 10 shows the values for the computer predicted helical expander and compressor adiabatic efficiency as a function of engine load and rpm. These values were used to replace the conventional performance maps of a turbocharger similar to the one used by the Elko's engine.

The results obtained are shown in Figure 17. The new fuel map presents a larger minimum BSFC island, or flatter torque curve with about 30% increase in low end torque, and lower values of BSFC The latter improvement ranges between 9% to 6%, going from full load to light load. The minimum BSFC is now .266 lbm/HP-hr, which is about 8% lower than the first technology level engine's BSFC, .289 lbm/HP-hr.

b) Minimum Rubbing Friction

As in the previous case, the benefit of this technology was added to the performance. As already pointed out in part III, the results of a previous experimental investigation conducted at Cummins were used to adjust the friction predicted by DCS. The resulting BSFC values were improved by 3% at full load and about 6% at very light load. The shape of the fuel map improved and the minimum b.s.f.c. became 0.257 lb/bhp-hr (Figure 18). This fuel map was run through the same computer program simulating the light duty cycle discussed previously and relative to the same automobile characteristics. The rated power was maintained constant at 70 Hp, and no improvements in the acceleration performance were obtained. The fuel economy prediction is 58 MPG. The second technology level fuel map is shown in Figure 18.

As far a emissions are concerned the increase in low end torque allows lower engine speed for the same duty cycle. This implies higher A/F ratio and lower combustion temperature, which will be certainly beneficial for both NO_x and particulates reduction. TABLE 11 summarizes the performance results relative to first and second level of technology.

TABLE 11
Performance and Emissions Summary of Two Technology Levels of the AAD

	Acceleration	Fuel Economy	NO_x	HC	Soot
Uncooled D.I. engine (3 Speed Automatic)	0-60 MPH 15 Sec.	43 MPG	acceptable	acceptable	acceptable
First Technology Level (Adiabatic, Compound, High Cylinder Pressure, Controlled Combustion Process)	0-60 MPH (CVT)	52 MPG 13.9 Sec.	acceptable	acceptable	acceptable
Second Technology Level (First Level Plus High Efficiency Charge System and Minimum Friction)	0-60 MPH (CVT)	62 MPG 13.9 Sec.	Lower	Lower	Lower

THIRD TECHNOLOGY LEVEL

a) Part Load Preheating - Hybrid System

As in the previous two cases, the benefits of this technology were added to those previously discussed.

As already explained in Part III, the light duty cycle relative to a passenger car is such that most of the fuel is burned at part load (Figure 5). In this condition the in-cylinder pressure and temperature are not high enough to accomplish high reciprocator efficiency and good compound system utilization. To solve this problem and increase the overall engine efficiency an original technique, called part load preheating, was adopted. The reciprocator compression ratio was reduced from 24 to 13.5 and the maximum boost pressure ratio was increased from 2.4 to 4.2, and exhaust gas energy was used to preheat the compressed air before entering the reciprocator. Figure 19 shows the optimum pressure and temperature necessary upstream and downstream of the reciprocator for a fuel economy improvement. Two cases are presented, one full load conditions and the other is light load conditions at 1000 rpm. Low temperatures and pressures characterize the full load operation (i.e. 450°F and 46 psia, A/F = 24), whereas high temperatures and pressures characterize the part load operation (i.e. 1150°F and 63 psia, A/F = 34).

The effect of this technique on the fuel map consisted in enlarging the low BSFC island, and in improving the part load BSFC by about 30%. This fuel map is shown in Figure 20 generated a fuel economy of about 77 MPG over the combined EPA driving cycle. No change in acceleration resulted, since the rated power was kept constant at 70 Hp. The engine performance curves are presented in Figure 21.

The increased in-cylinder temperature at part load might increase the production in NO_x. Therefore, the implementation of a controlled combustion system, as previously discussed, appears to be extremely important for the reduction in NO_x.

CONCLUSIONS

The three levels of technology identified in the performance analysis of the advanced automotive diesel engine are based on three fundamental concepts:

a) High temperature and pressure operation and exhaust gas energy recovery.

b) Controlled constant pressure combustion process.

c) Modified thermal engine cycle.

The implementation of the first two concepts to the first level of technology characterized by an acceleration time of 14 seconds, a fuel economy of 50 MPG and an acceptable emission level. The minimum BSFC was of .289 lbm/HP-hr compared to the baseline of .340 lbm/HP-hr.

As a following step this particular engine arrangement was integrated with a higher efficiency air handling system and with the minimum rubbing friction technology. In this way a second level of technology was established and a significant improvement in performance was obtained. The fuel economy increased to 58 MPG and better emissions were foreseen. The minimum BSFC obtained in this condition was of .266 lbm/HP-hr.

A third step consisted in the modification of the engine thermal cycle in a hybrid cycle with part load preheating. This allowed a significant improvement in part load engine BSFC, which resulted in a fuel economy of 77 MPG and the minimum engine BSFC of .238 lbm/hp-hr. The increased part load in-cylinder temperatures raise some concerns relative to an excessive NO_x production. Therefore, one can conclude that the key factor for engine fuel economy is higher temperature operations, through a more effective thermodynamic cycle. This will probably lead to emission problems, which, however, can be solved by adopting an advanced controlled combustion system .

1. LOW COMPRESSION RATIO RECIPROCATOR
2. POSITIVE DISPLACEMENT EXPANDER
3. POSITIVE DISPLACEMENT COMPRESSOR
4. HEAT EXCHANGER
5. BELTS
6. CONTROL UNIT

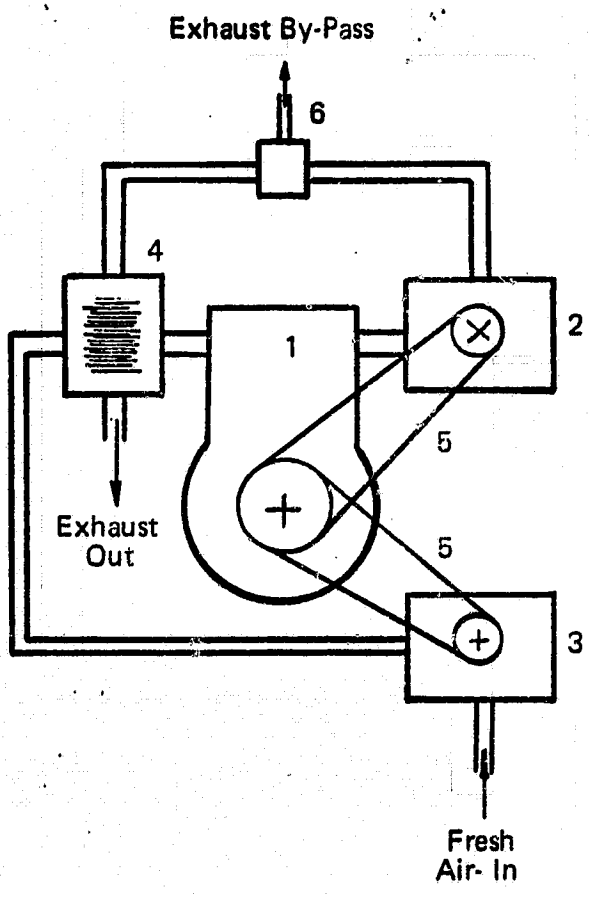

FIGURE 1. SCHEMATIC OF A COMPOUNDED RECIPROCATOR

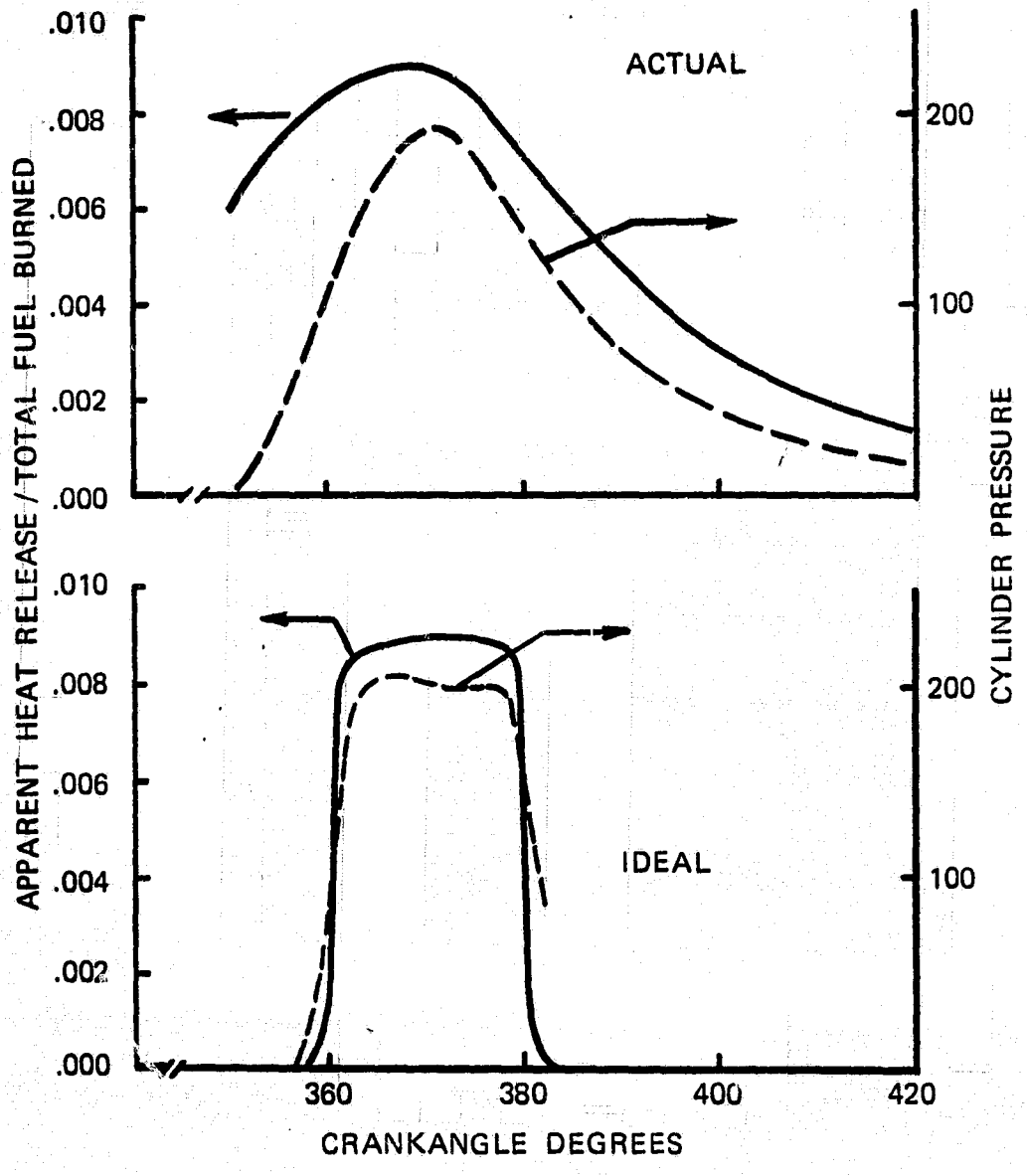

FIGURE 2. ACTUAL AND IDEAL, SHORT DURATION HEAT RELEASE PROCESSES

C-2

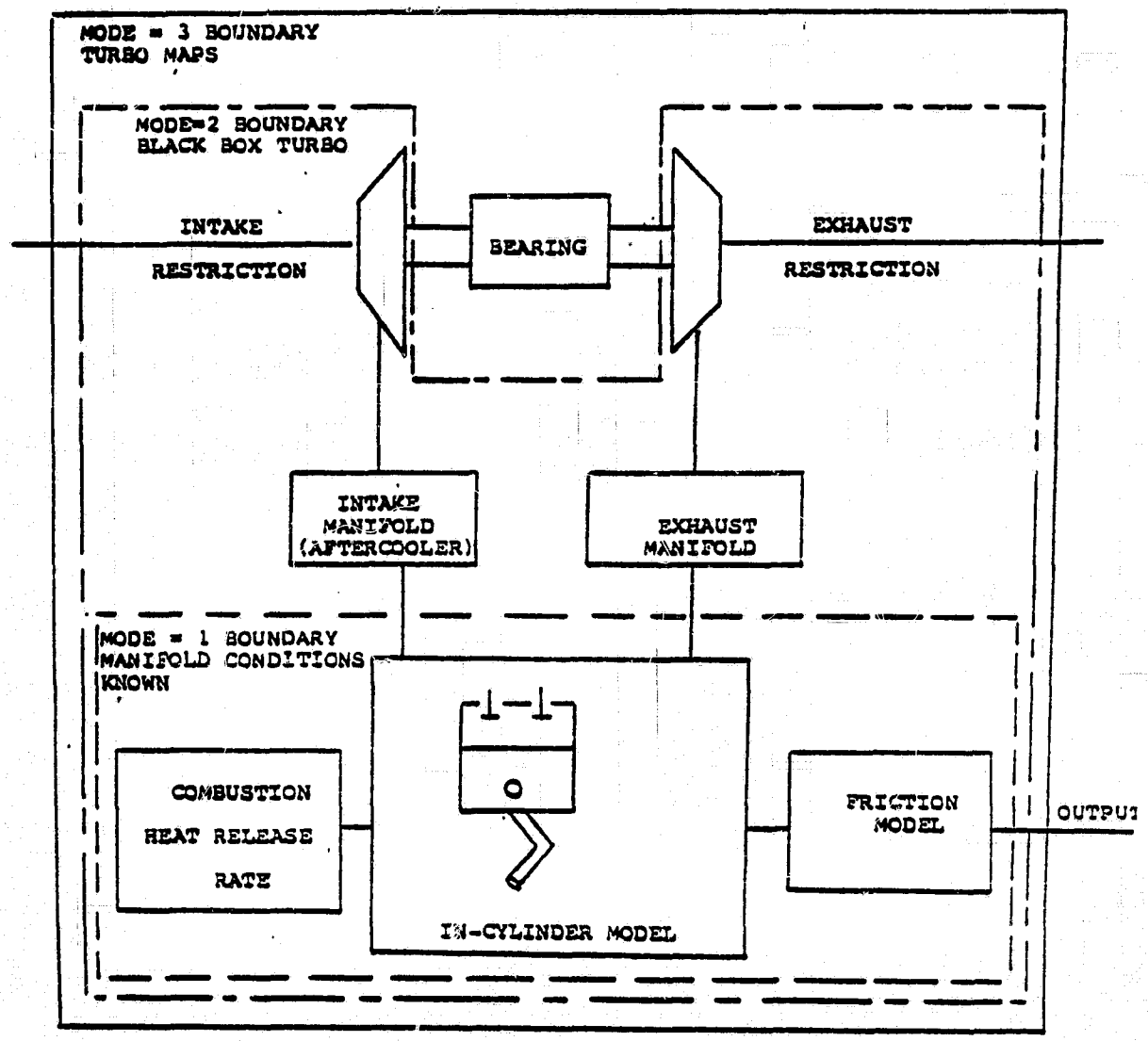

FIGURE 3. OPERATING MODES OF THE DCS

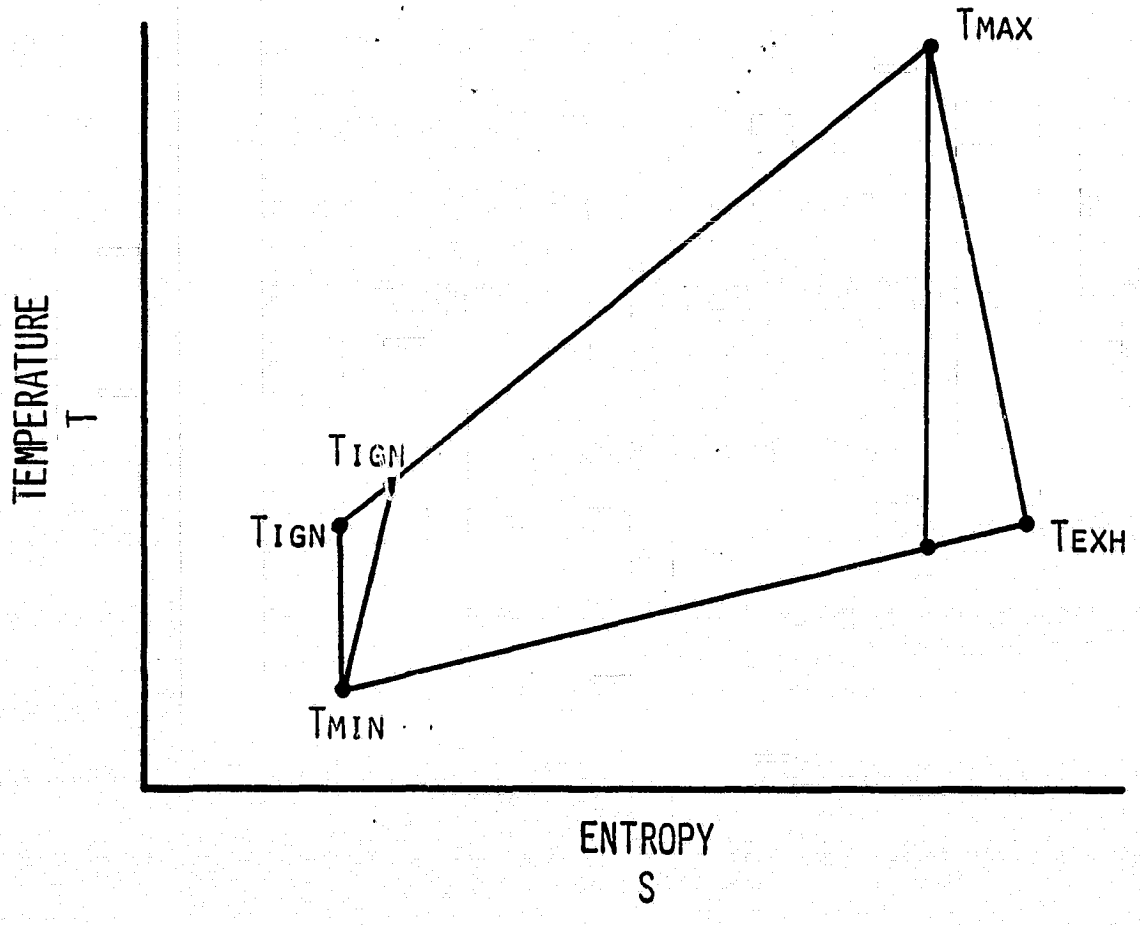

FIGURE 4. TYPICAL BRYTON CYCLE

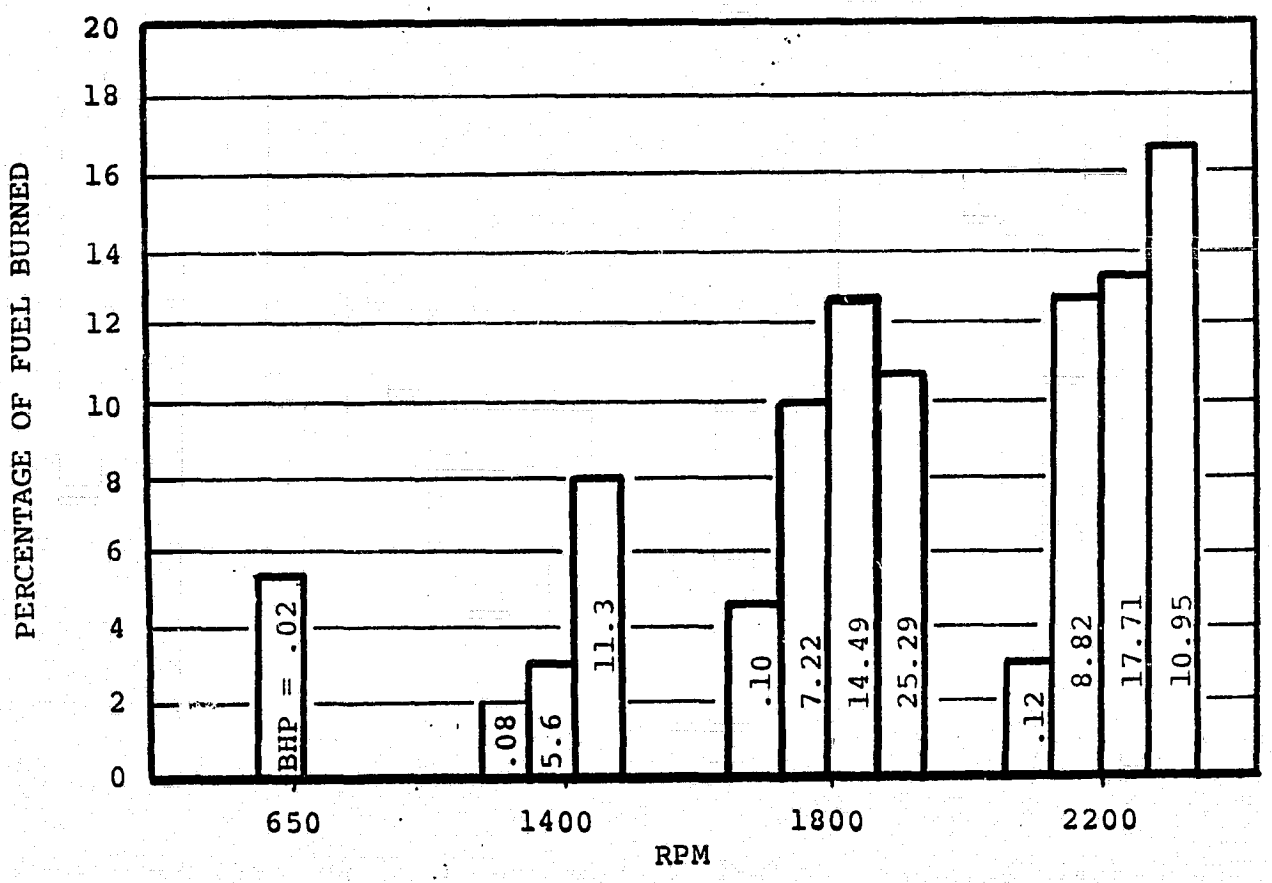

FIGURE 5. EPA DRIVING CYCLE

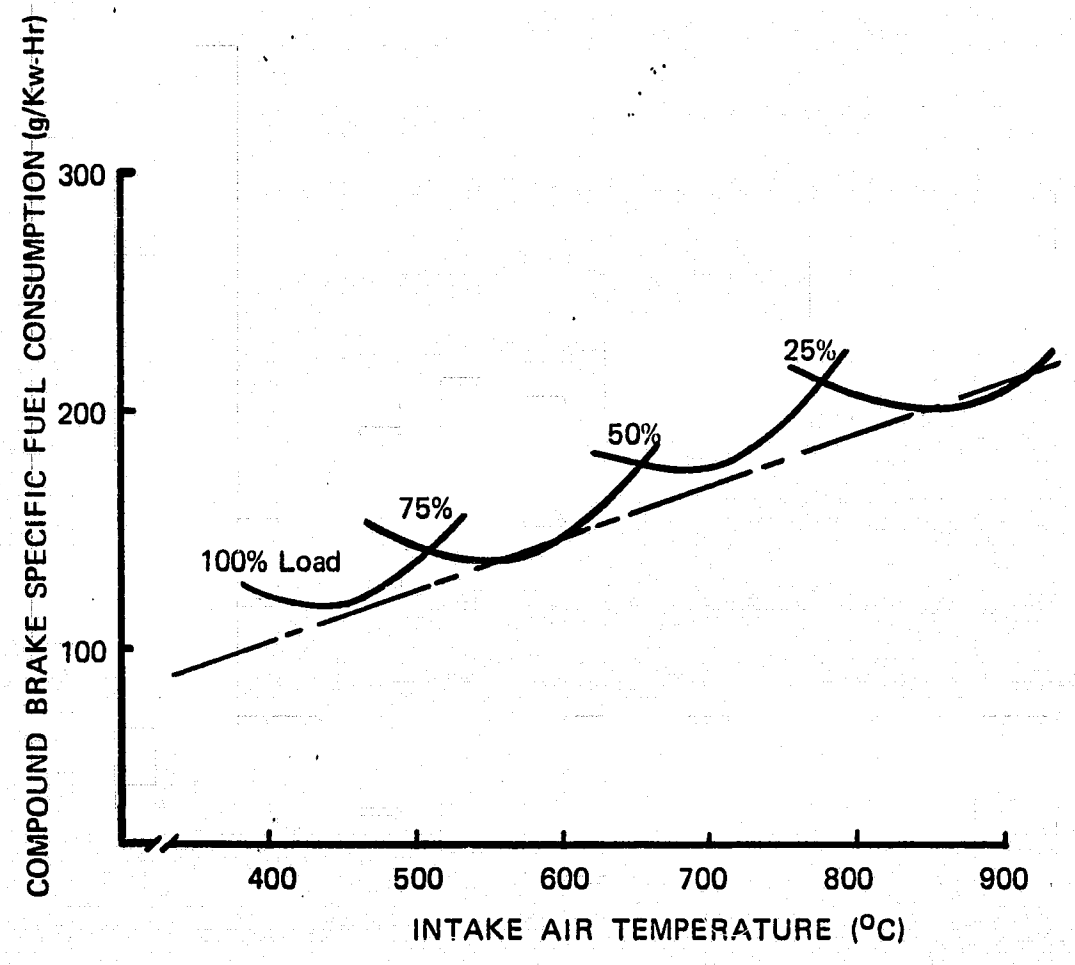

FIGURE 6. OPTIMUM INTAKE AIR TEMPERATURE

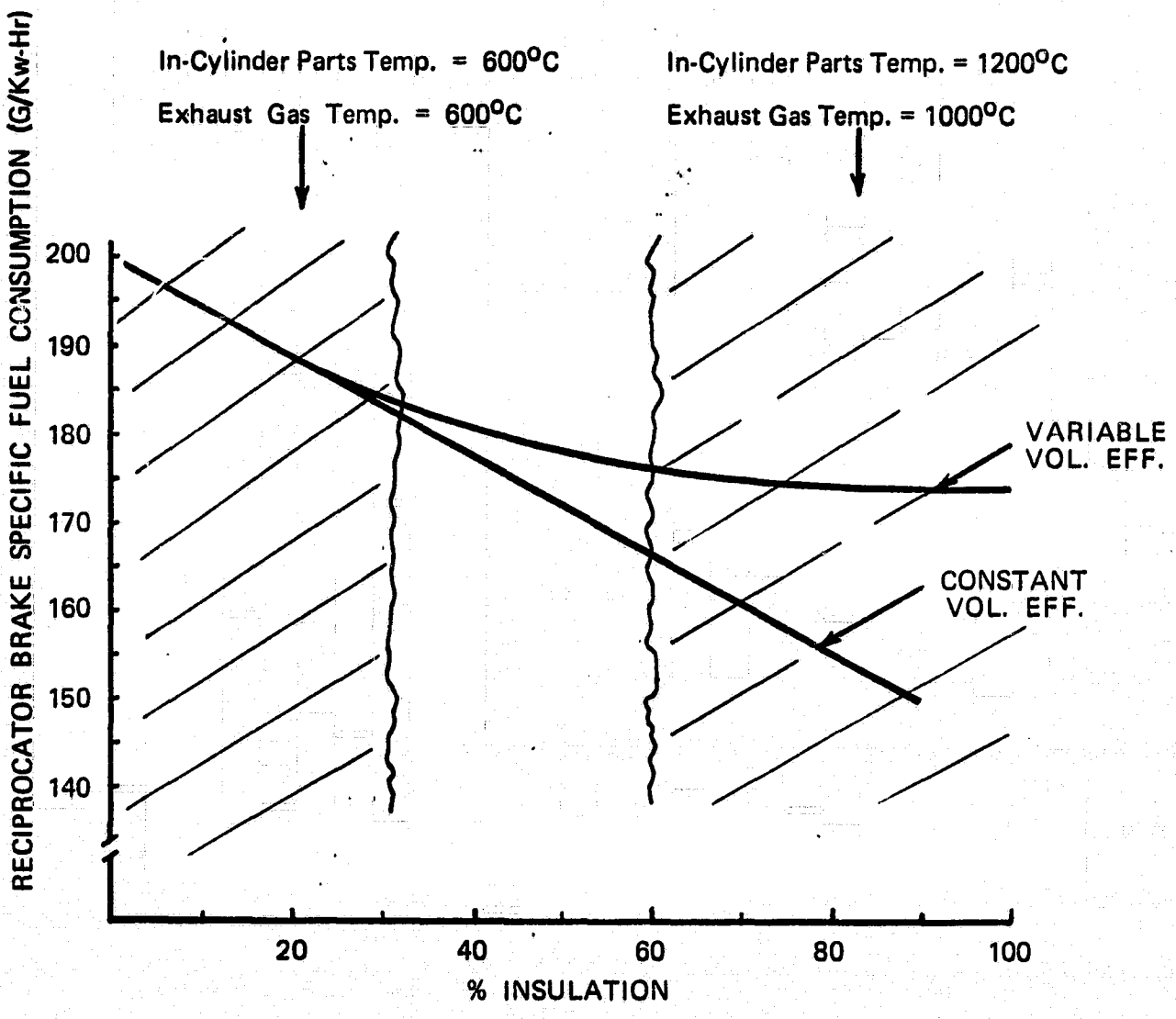

FIGURE 7. EFFECT OF INSULATION ON BSFC

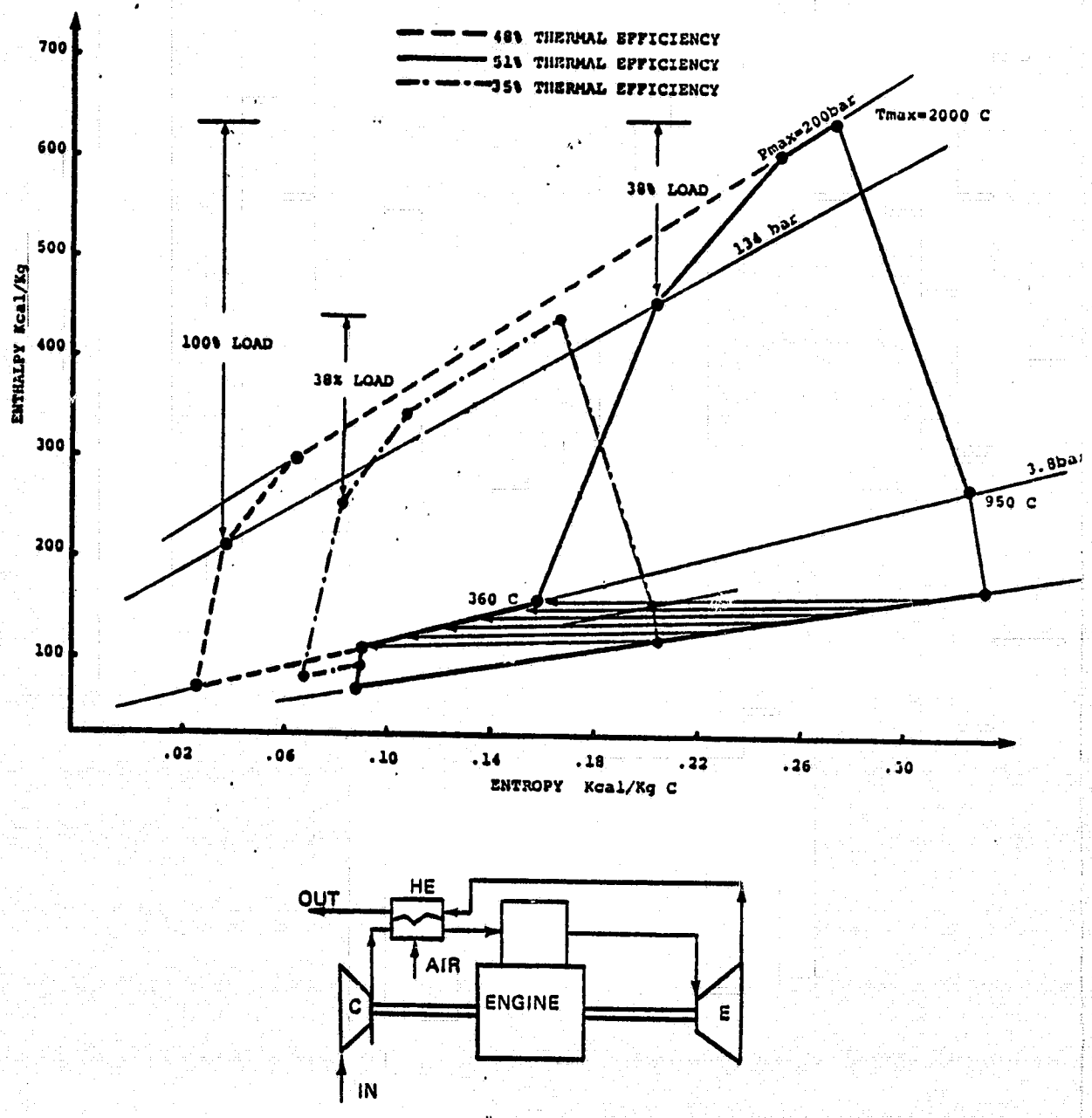

FIGURE 8. PART LOAD PREHEAT CONCEPT

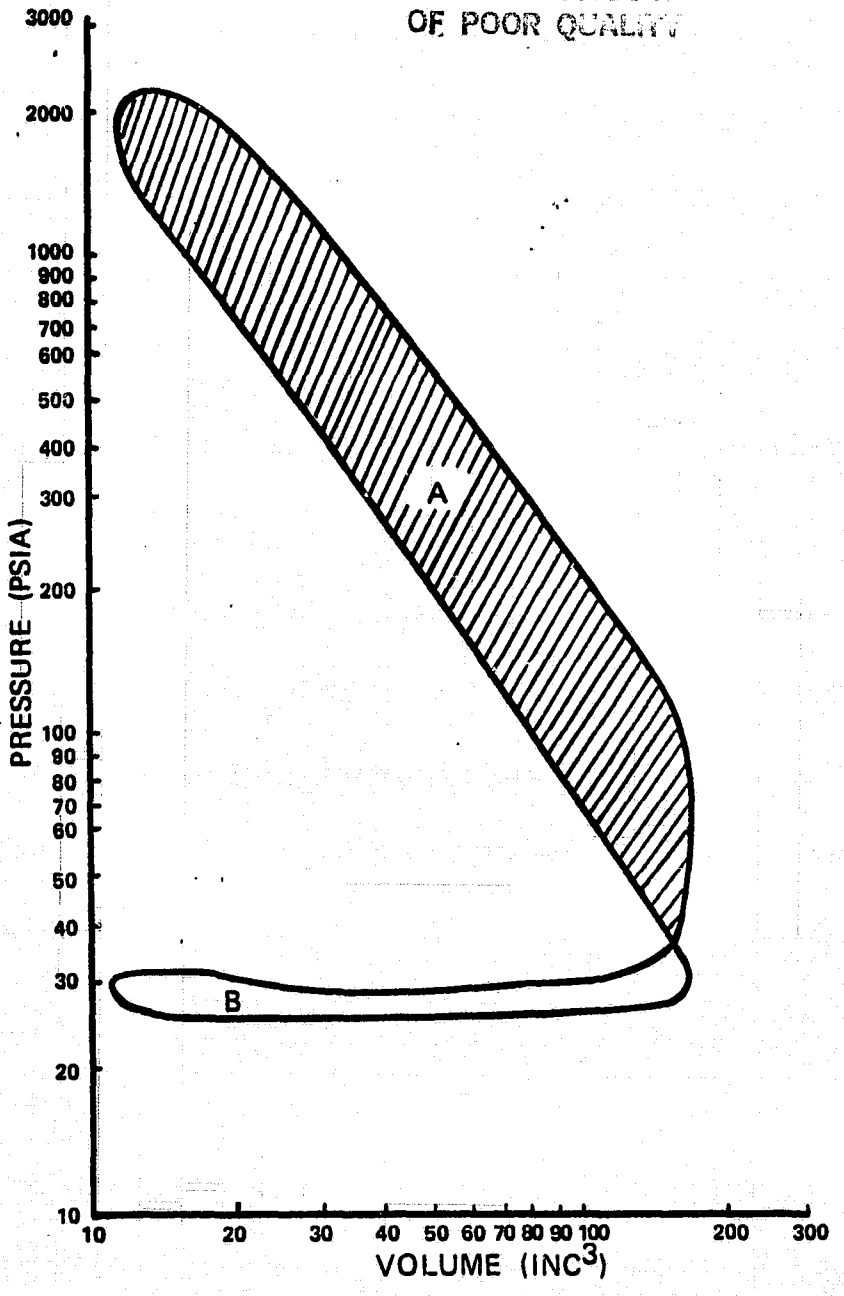

FIGURE 9. TYPICAL DIESEL P-V DIAGRAM

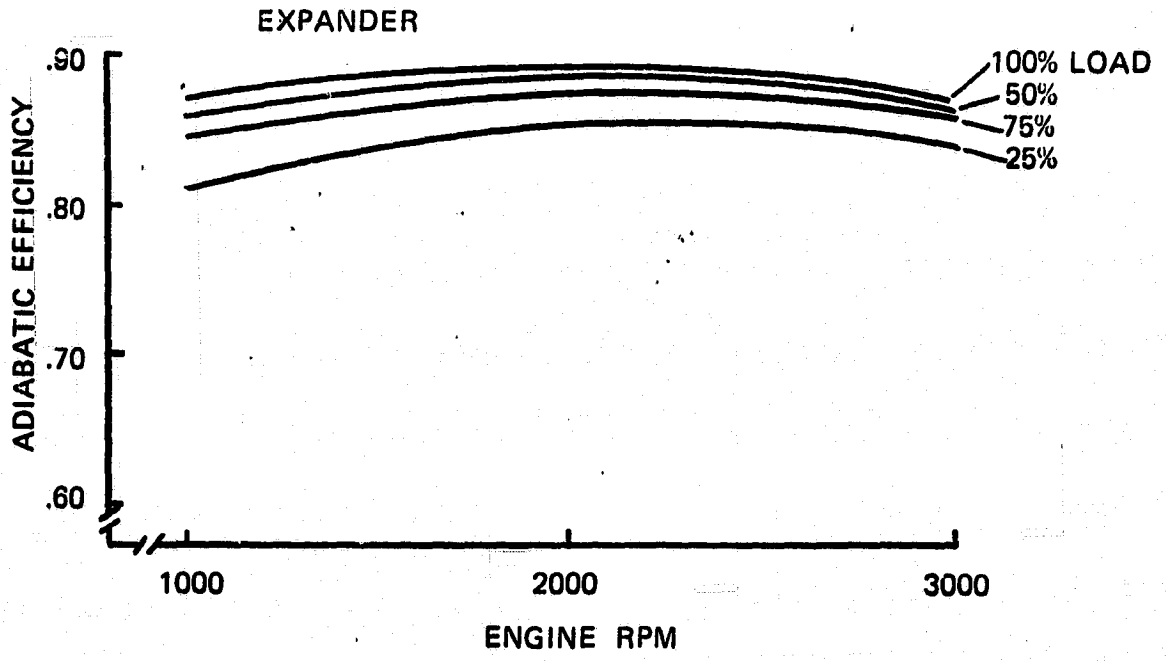

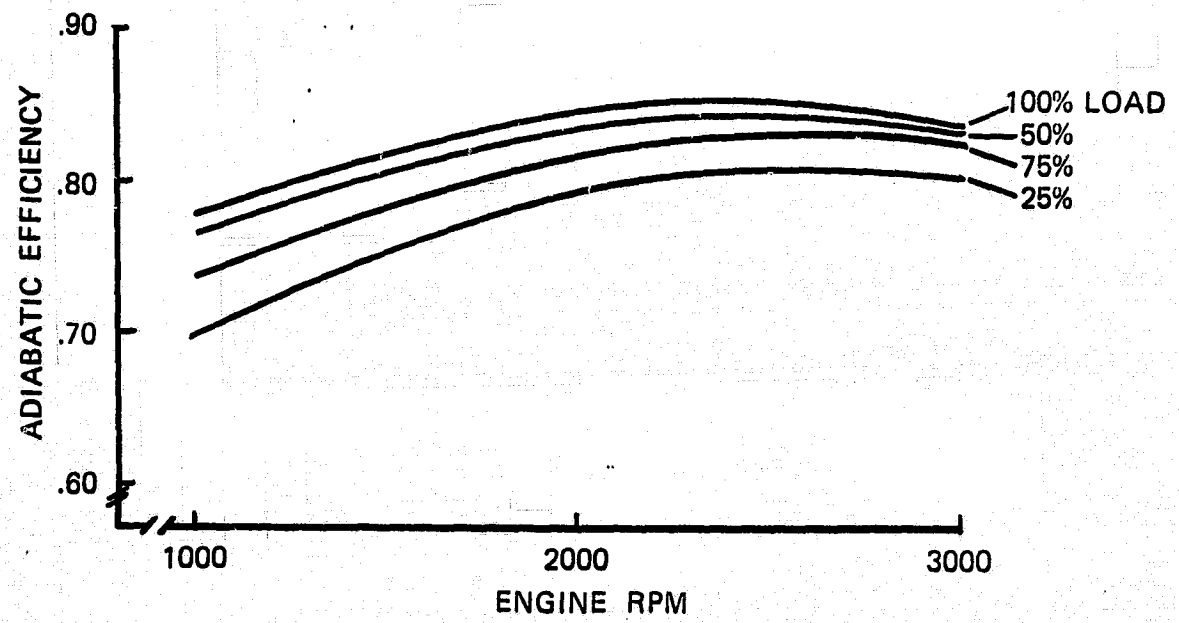

FIGURE 10. EFFICIENCIES OF THE A.A.D. ENGINE SCREW MACHINES

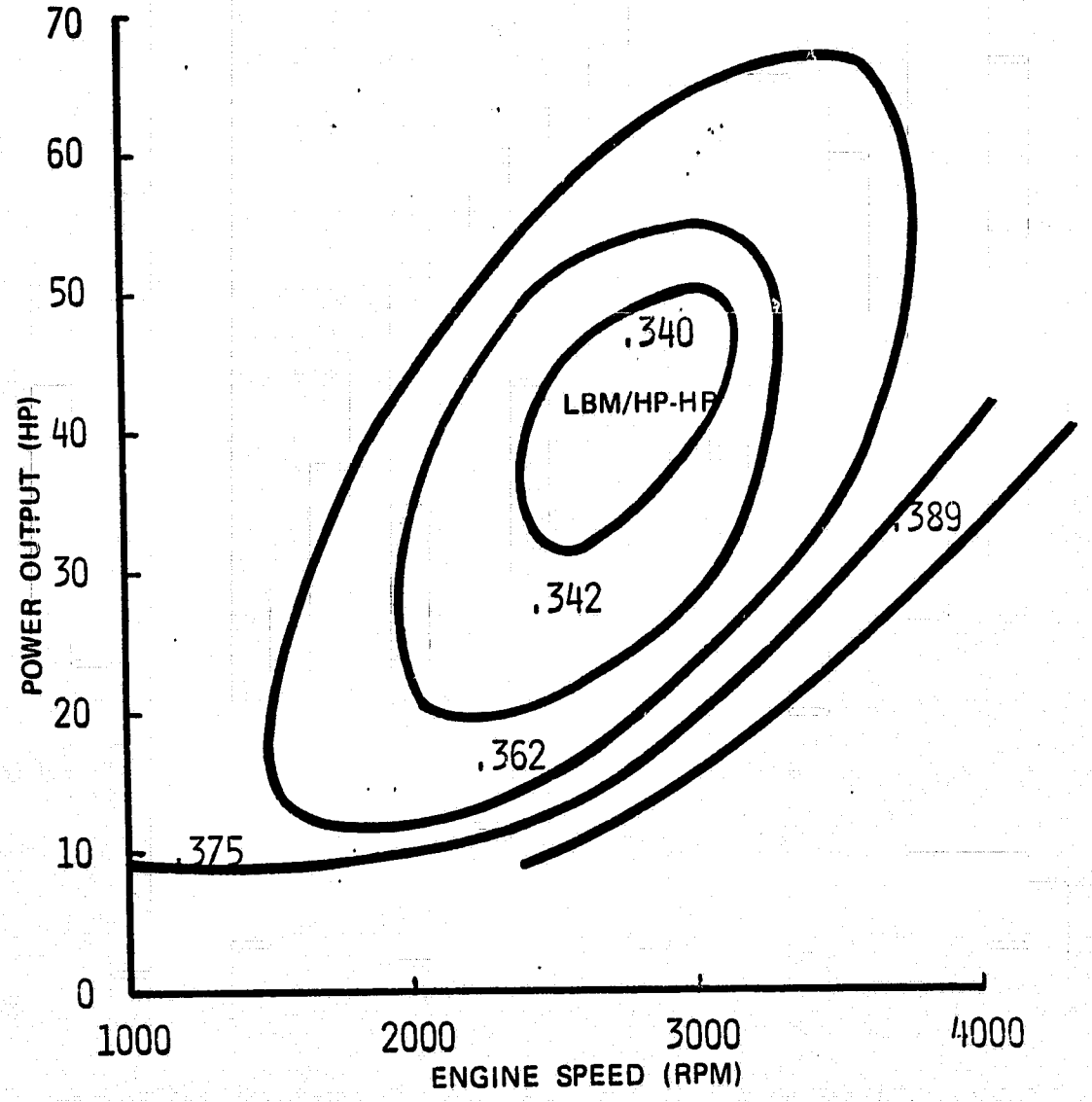

FIGURE 11. SEMI - ADIABATIC ENGINE FUEL MAP

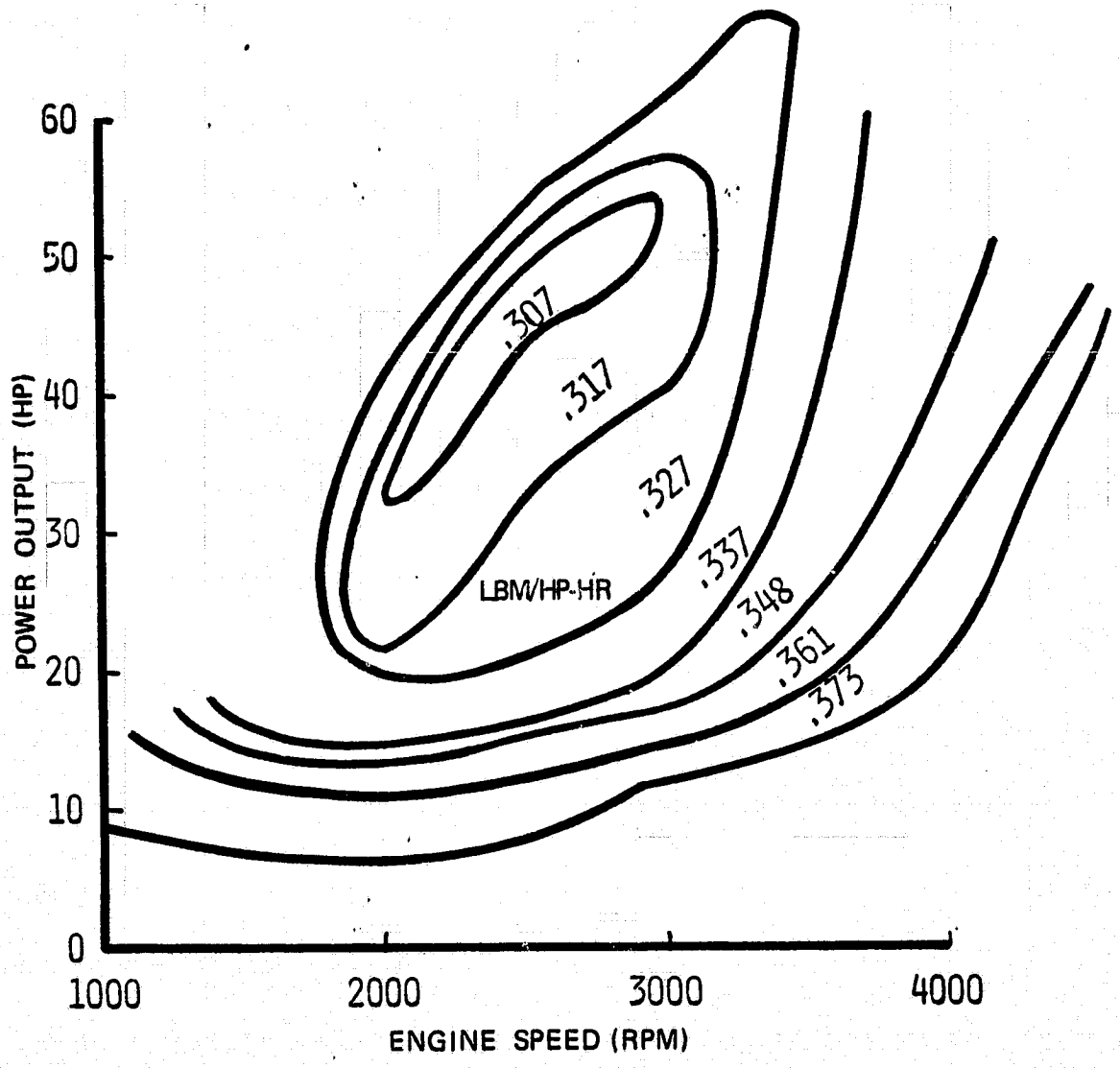

FIGURE 12. ADIABATIC COMPOUND ENGINE FUEL MAP

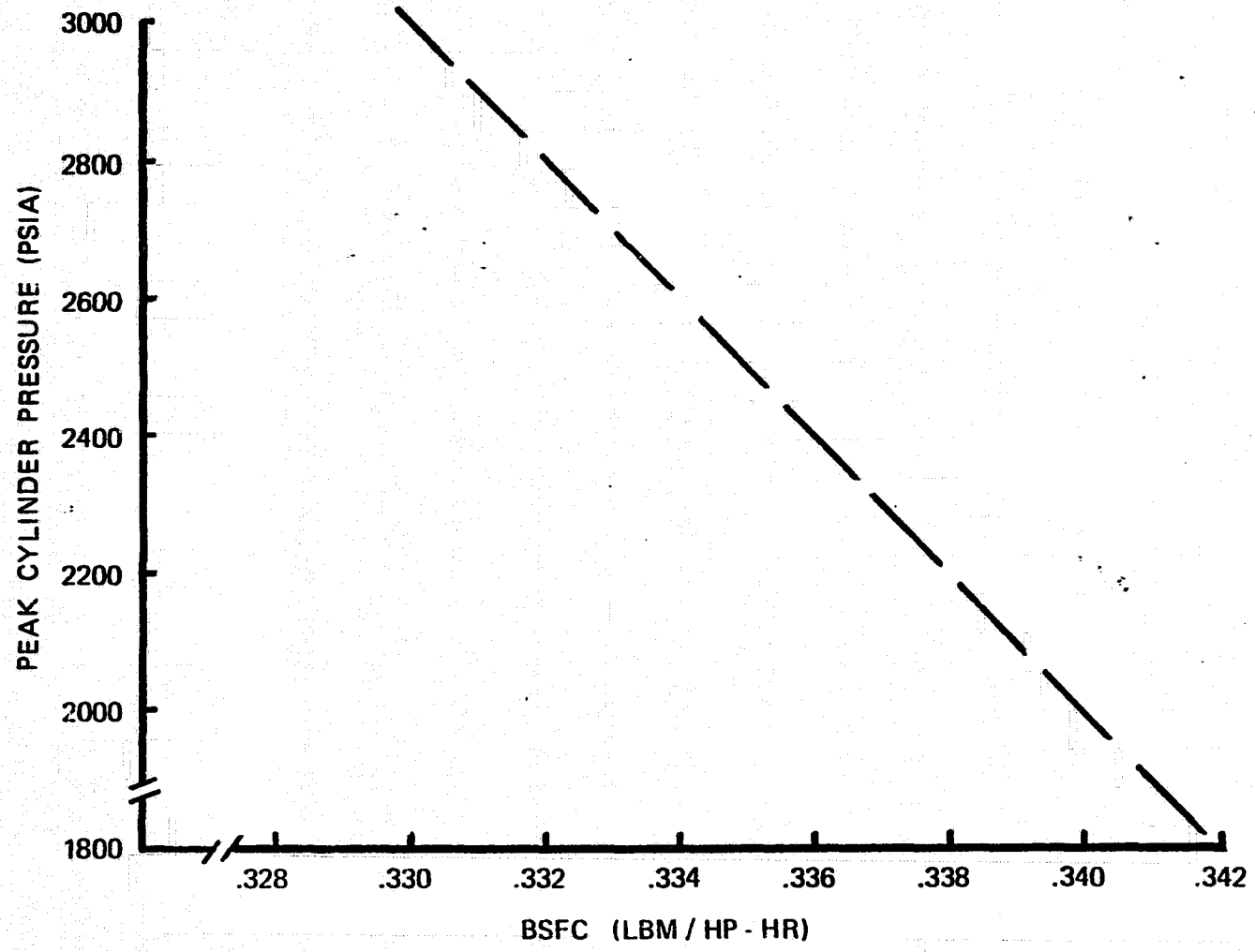

FIGURE 13. EFFECT OF PEAK CYLINDER PRESSURE ON BSFC

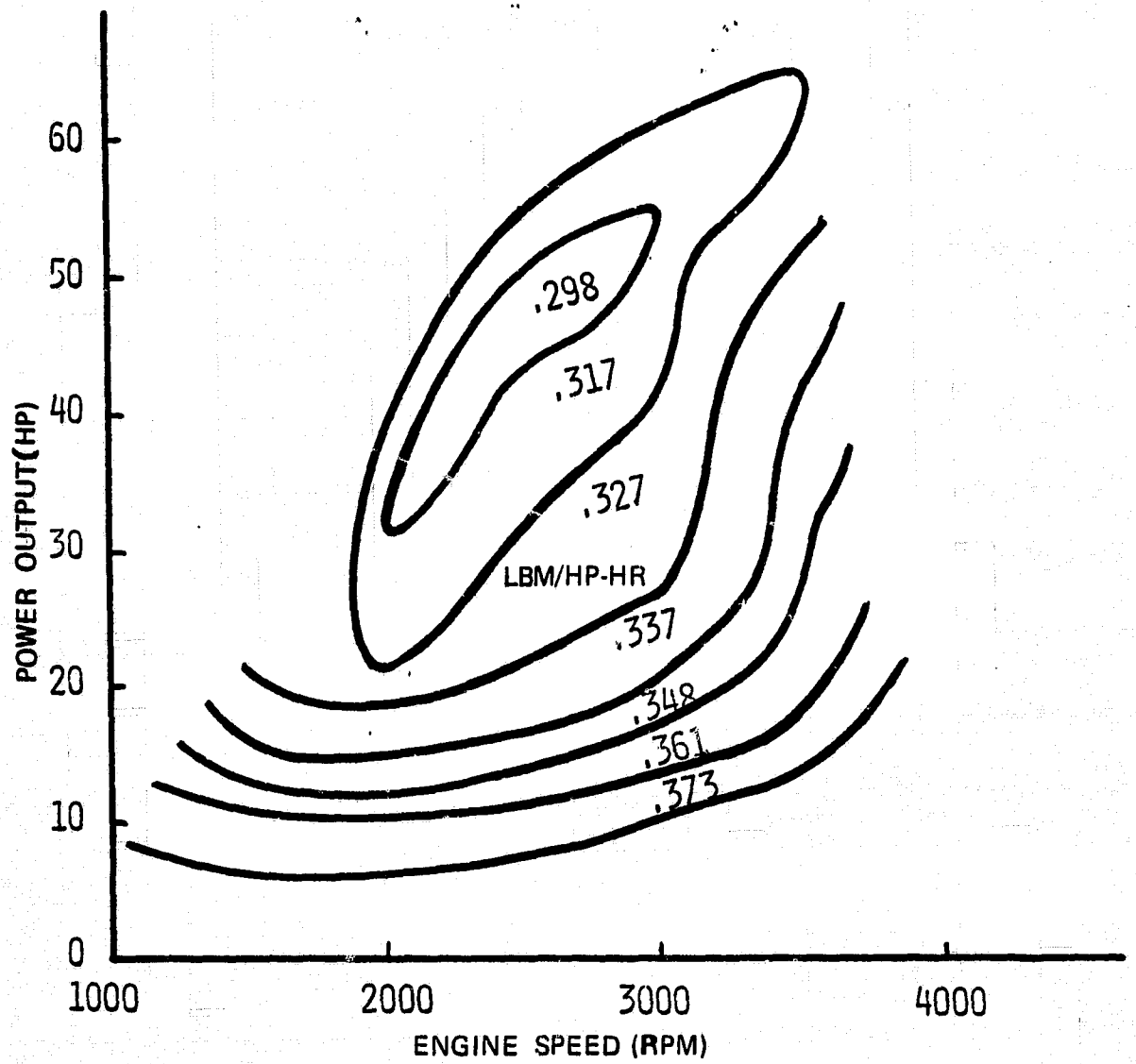

FIGURE 14. FUEL MAP OF HIGH PRESSURE ADIABATIC ENGINE

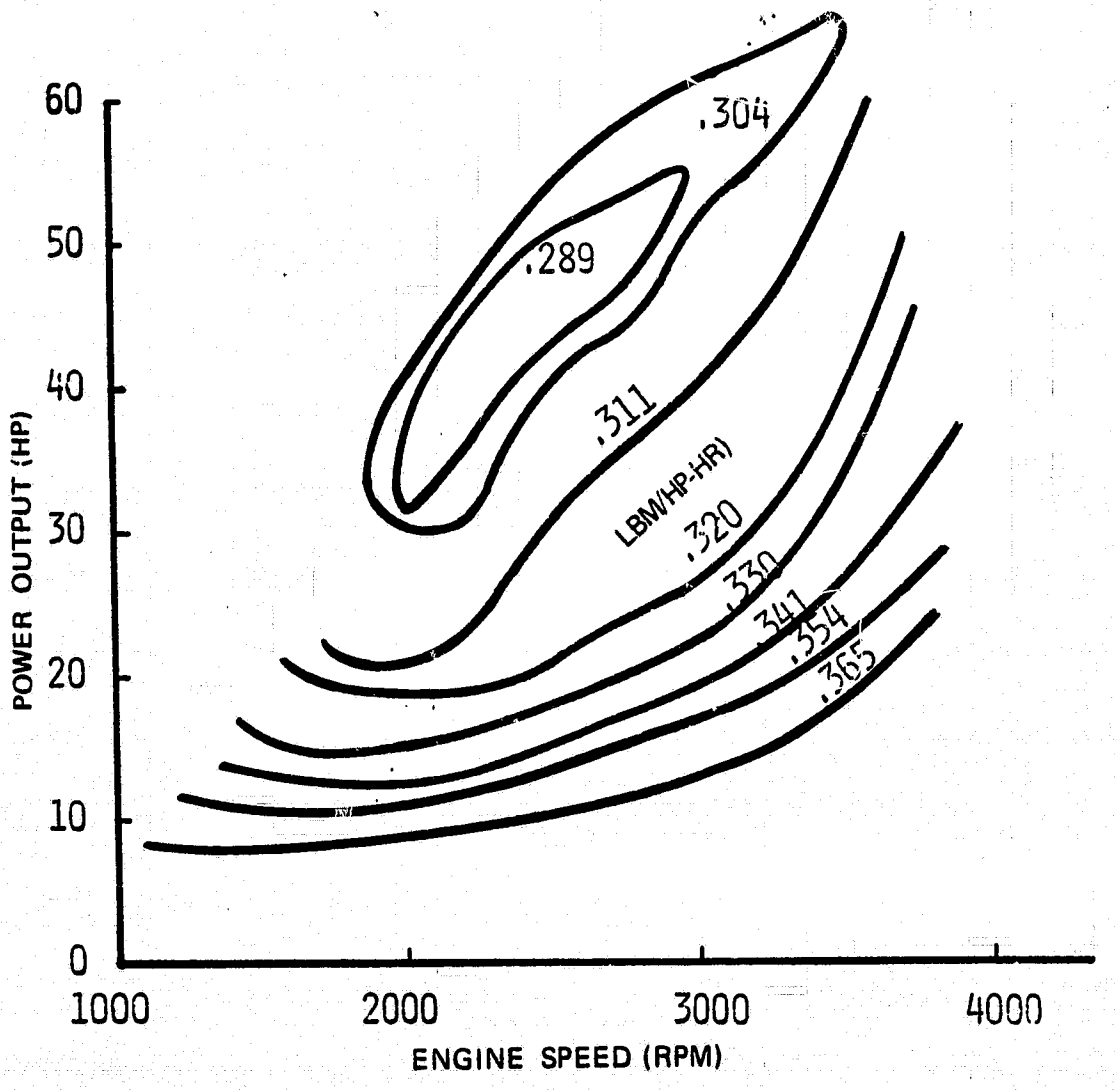

FIGURE 15. FUEL MAP - FIRST TECHNOLOGY LEVEL

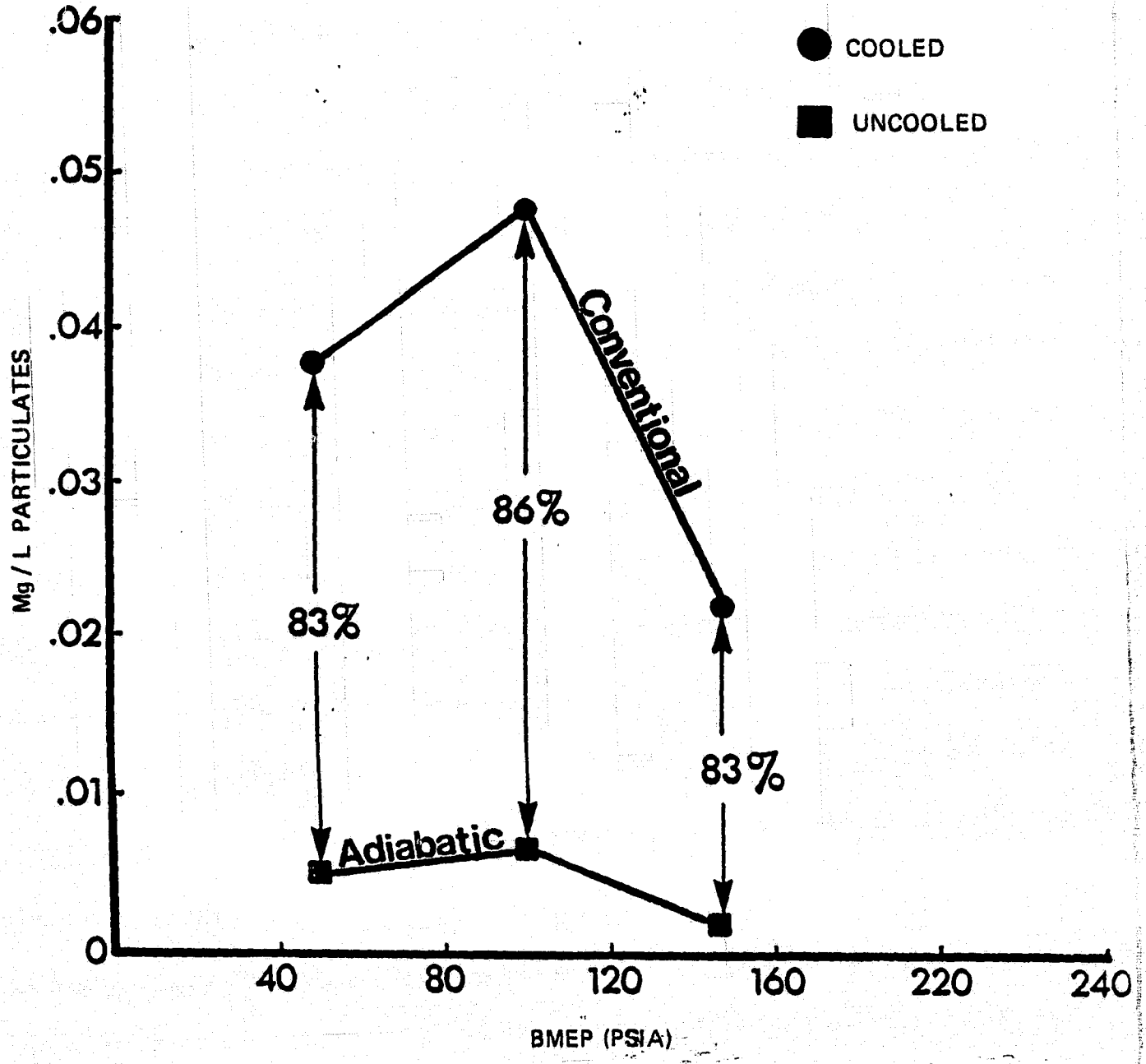

FIGURE 16. ADIABATIC VS. CONVENTIONAL ENGINE RELATIVE CARBON PARTICULATE LEVELS

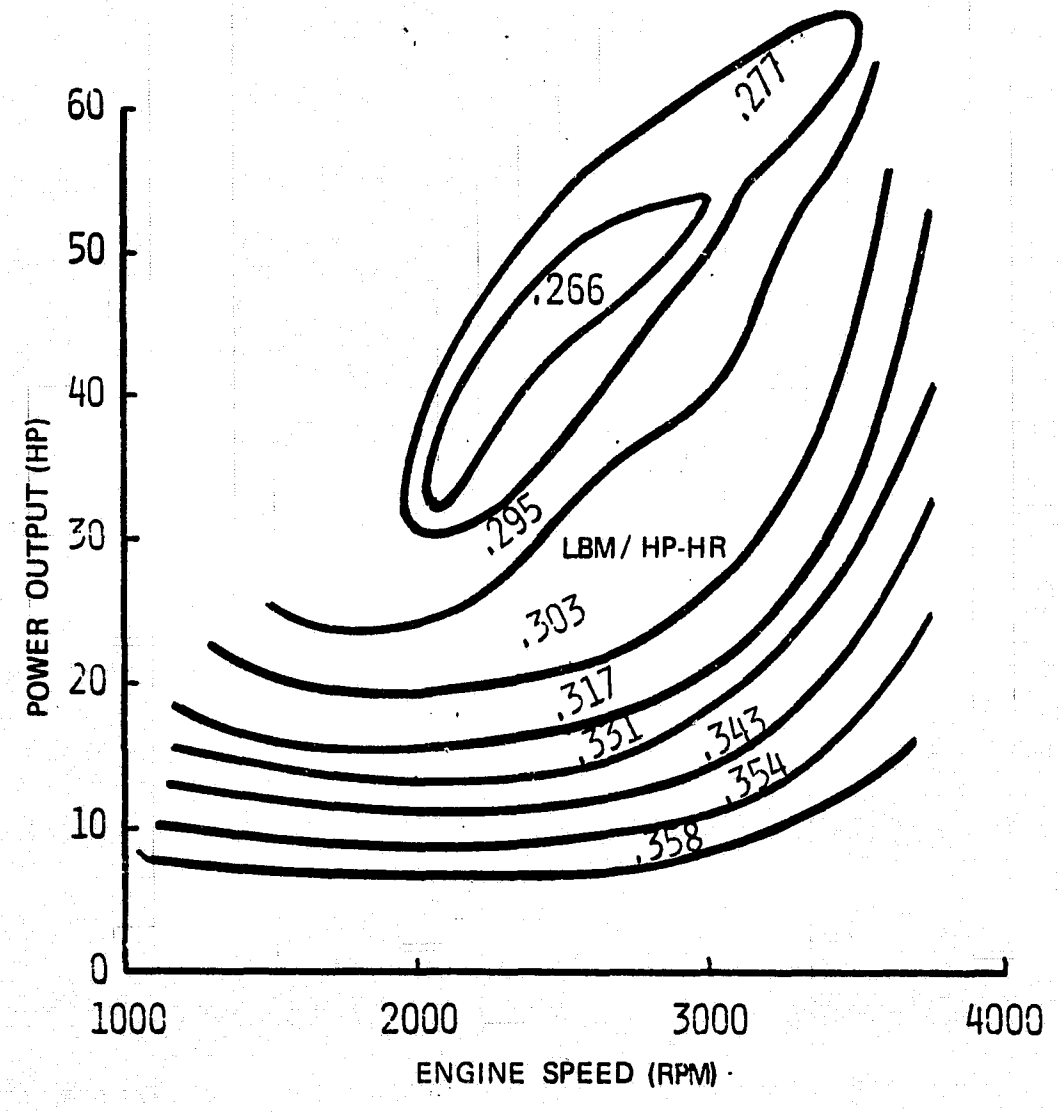

FIGURE 17. EFFECT OF HIGH EFFICIENCY CHARGE SYSTEM ON THE FIRST TECHNOLOGY LEVEL FUEL MAP

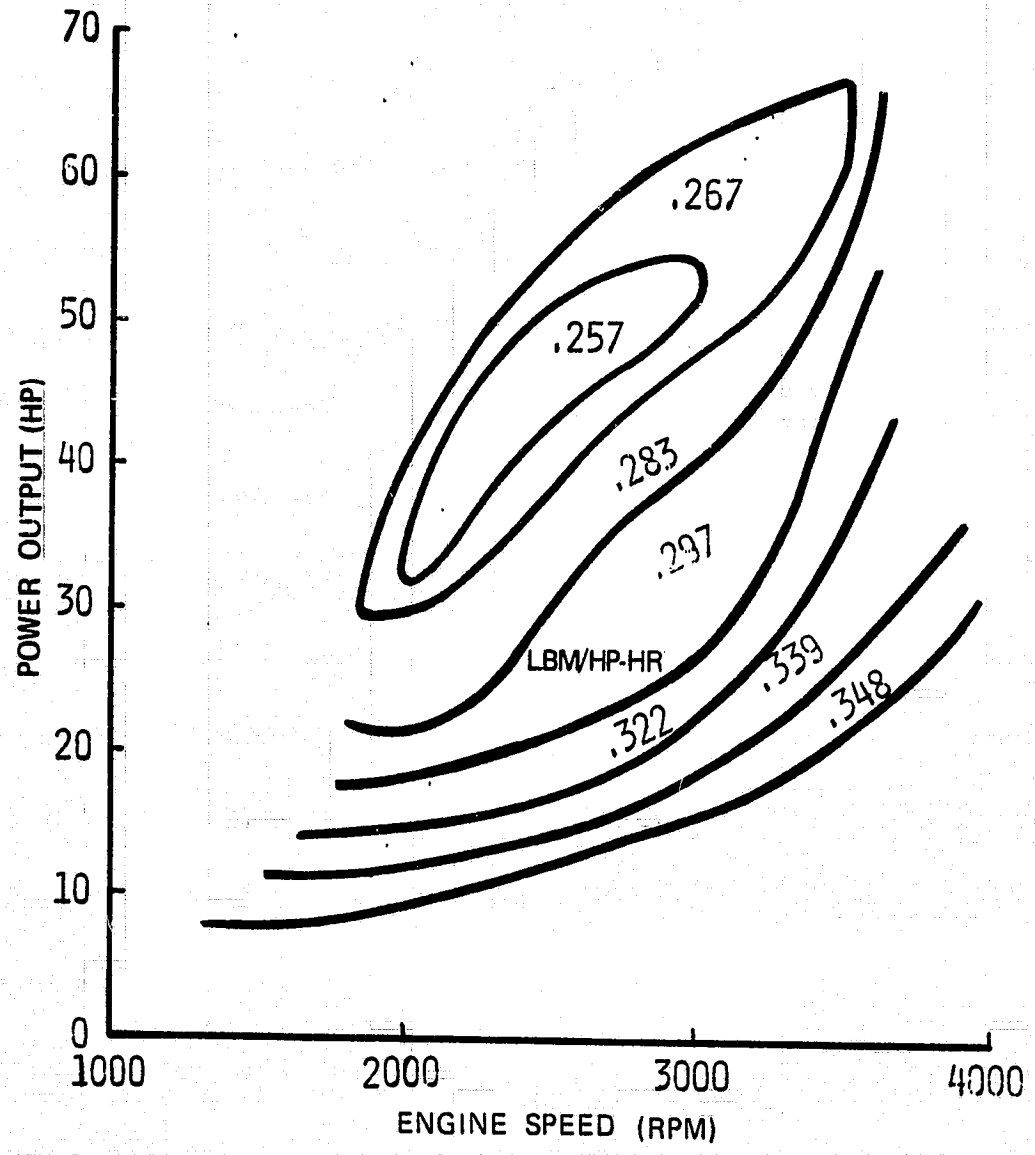

FIGURE 18. SECOND LEVEL OF TECHNOLOGY FUEL MAP

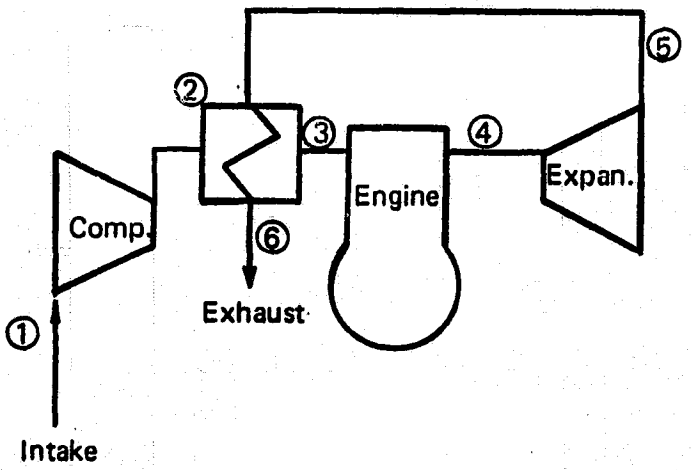

	FULL LOAD 70 HP	PART LOAD 15 HP
$\dot{m}$ =	8 LBM/MIN	3 LBM/MIN
①	120 °F ; 13 PSIA	SAME
②	426 °F ; 49 PSIA	559 °F ; 63 PSIA
③	450 °F ; 46 PSIA	1000° F ; 60 PSIA
④	1800 ° F; 56 PSIA	SAME
⑤	1100 ° F ; 19 PSIA	SAME
⑥	980 ° F ; 17 PSIA	570 ° F ; 17 PSIA

FIGURE 19. FULL AND PART LOAD THERMODYNAMIC CONDITIONS

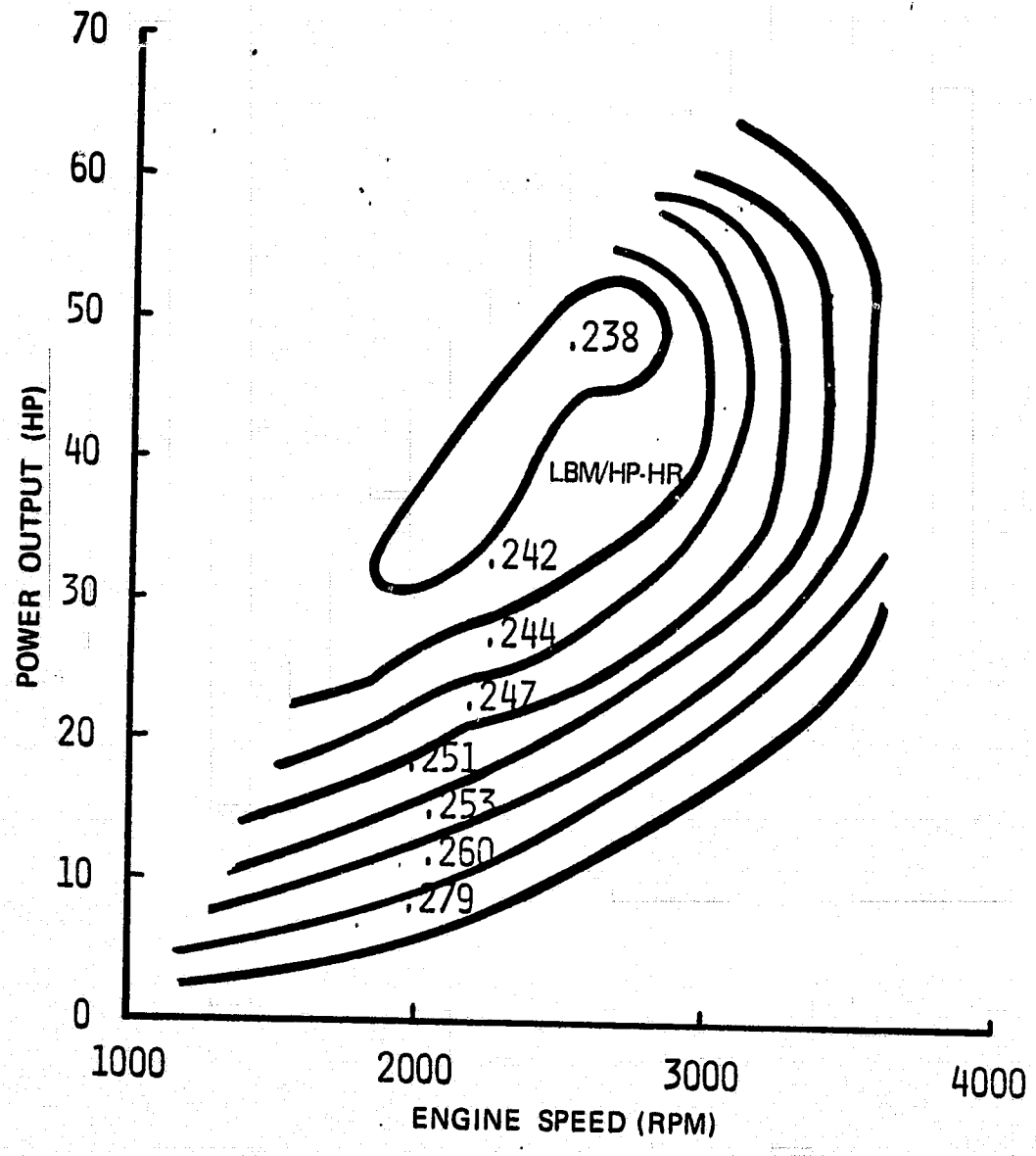

FIGURE 20. THIRD TECHNOLOGY LEVEL (A.A.D.) FUEL MAP

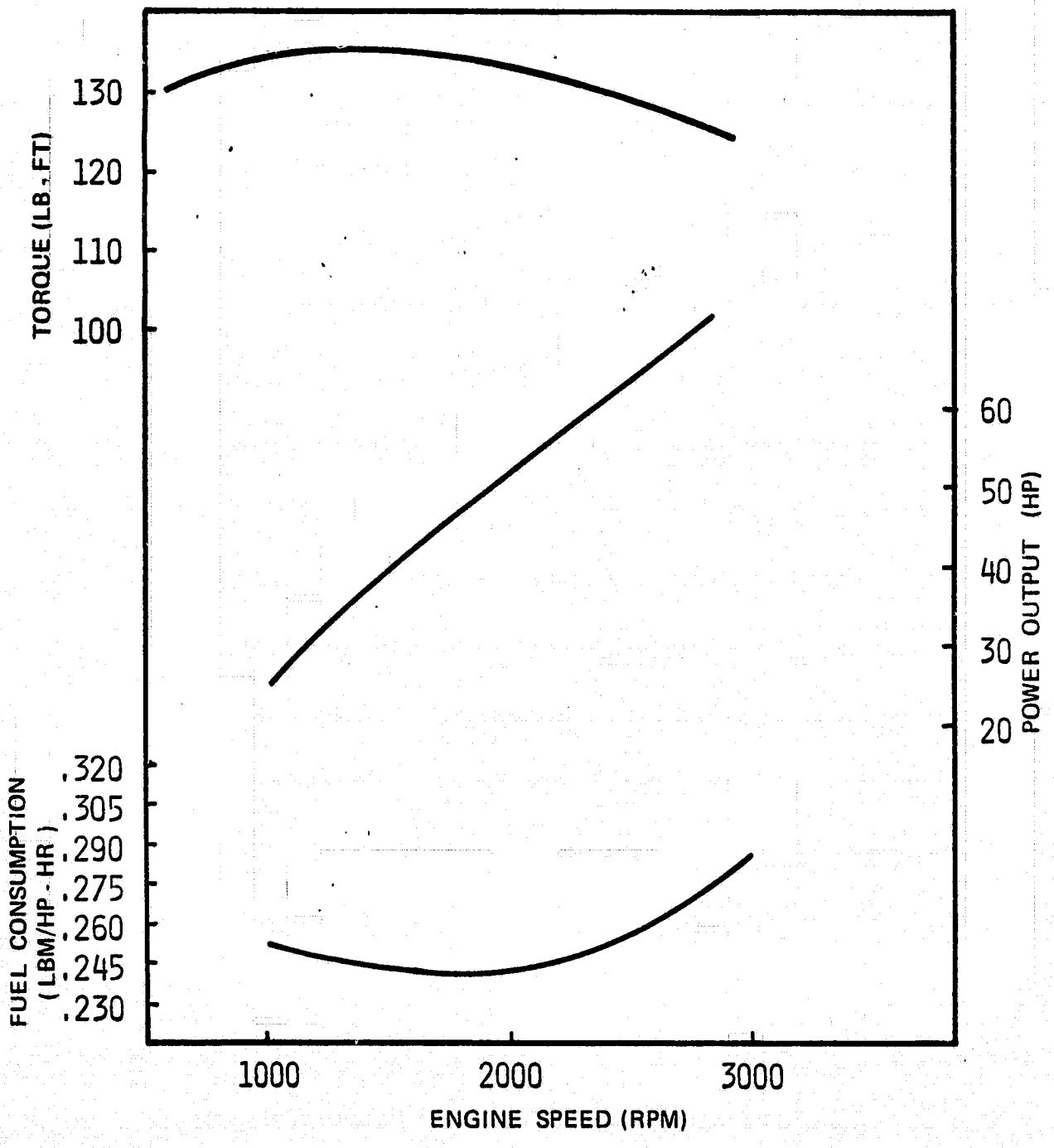

FIGURE 21. A.A.D. ENGINE PERFORMANCE CURVES

D3

N85 13238

APPENDIX 2

ROLLER CROSSHEAD ANALYSIS

Mr. Donald Wilcock
Tribolock Inc.

1.0 INTRODUCTION AND SUMMARY

This report concerns an analysis of the frictional behavior of a roller crosshead configuration. This configuration consists of a piston which carries at the wristpin position a roller of large diameter which can roll on the cylinder liner surfaces. The report covers a preliminary assessment of whether the roller can roll on the cylinder liner without skidding, and what, if any, are the tribological implications of this approach to a dry lubricated design.

The rotational speed of the roller must change during the stroke if it is not to slip on the cylinder liner. The maximum value of angular acceleration occurs at top dead center and bottom dead center.

If the traction force on the rim of the roller, which is the product of the normal force due to piston side load and the coefficient of friction, is not sufficient to drive the roller through the necessary angular acceleration, sliding will occur. At 1,000 rpm, it appears that there will be a definite area of slip near each end of the stroke. The length of the area of slip may be of the order of 1/8 inch at each of these points.

In addition to this inertia-generated slip, there will be continual slip over the engine stroke in the contact zone between the roller and the liner. The contact zone, which is elliptical, will exhibit 2 lines of pure rolling, plus an area at the center of the elliptical contact which is sliding in one direction and 2 areas at either end of the elliptical contact zone which are sliding in the opposite direction. This phenomenon is clear to see, as an example, following operation of a ball bearing without adequate lubrication. Distressed areas in the slip zones mentioned above are apparent.

The side load vs. crank angle data supplied for this preliminary analysis do not include side forces due to the inertia effects in the piston-connecting rod-crank shaft system. In order to allow for this, the maximum load in the cycle was corrected by adding about 20% to it and arriving at a maximum side load of 2,000 lbf. In order to keep the contact ellipse within the bounds of the 20 mm wide roller in the preliminary design, it will be necessary to reduce the roller cross radius a significant amount below the radius of the cylinder liner. This can be done without imposing unreasonable Hertz stresses on the contact zone.

The two types of sliding which will occur in the contact areas of the roller-cylinder liner contact zone, one within the contact ellipse and the other at the ends of the stroke, appear to dictate the requirement for the presence of a solid lubricant on the surfaces at all times. Since one can expect any reasonable solid lubricant coating to be worn away long before a typical engine life is attained, it is recommended that part of the development program should include a study of various means of replenishing the solid lubricant wear, if possible automatically.

2.0 ROLLER PROPERTIES

The specific gravity of silicon nitride, the roller material, is 3.26. Based on this, the mass density is calculated in equation (1).

$$\rho = \frac{3.26 \times 0.03613}{386} = 0.000305 \text{ lbm-sec}^2/\text{in}^4 \qquad (1)$$

The moment of inertia of a hollow cylinder is given by equation (2)

$$I = \pi \rho L (R_1^4 - R_1^4)/2 \qquad (2)$$

Applying this equation to the dimensions of the roller, some of them estimated from the rough drawing, gives the following table:

R_1	R_2	L	I
1.510	1.225	0.787	0.00111
1.224	0.980	0.363	0.00023
0.980	0.630	0.787	0.00029

Total I = 0.000163 $\frac{\text{inch - lbf}}{\text{sec}^2}$

This is for a wheel with a pinched in center and a 20 mm width at the outer rim and at the inner hub. The value calculated is 84% of the wheel inertia if there are no cutouts in the cross section.

2.1 Track Width vs. Rim Radius

An available computer code for the calculation of the parameters of a Hertzian contact was used to investigate the size of the contact ellipse under a load of 2,000 lbs. The cylinder radius was taken as 1.5160 in. and the effect of various radii on the half width of the contact zone was calculated and is plotted in Figure 1.

The lower curve in Figure 1 shows the half width as a function of the radius of the lower rim which is assumed to have the radius in the circumferential direction of 1.515 and the cross radius as shown in the figure. The upper curve in Figure 1 indicates the maximum Hertz stress times 10^{-5}.

Figure 1 shows that the cross radius cannot be greater than 1.505 inches to keep the contact ellipse within the width of the roller. At this radius, the Hertz stress is 130,000 psi. In order to provide a margin for misalignment and for wear, it is recommended that the cross radius be made 1.480 inches at which position the maximum Hertz stress is 178,000 psia.

The track will, of course, be narrower during most of the cycle where the loads are lower than 2,000 lbs., and where the hertz stresses will be correspondingly lower.

3.0 KINEMATICS

Let us define the following variables:

ℓ – connecting rod length

r – crank radius

V_s – piston linear velocity

Θ – crank angle from TDC

ω_1 – crank angular velocity, $d\Theta/dt$

From the geometry of a crank driven piston, the piston velocity is given by:

$$V_B = \omega_1 r \sin\Theta \left[1 + \frac{r\cos r}{(\ell^2 - r^2 \sin^2\Theta)^{1/2}} \right] \qquad (3)$$

The linear piston acceleration is then given by differentiating V_B, to obtain equation (4):

$$\frac{dV_B}{dt} = \omega_1^2 r \left\{ \cos\Theta + \frac{\cos 2\Theta}{A^{1/2}} + \frac{\sin^2\Theta \cos^2\Theta}{3/2} \right\} = \omega_1^2 \; rB \qquad (4)$$

where

$$A = (\ell/r)^2 - \sin^2\Theta \qquad (5)$$

Letting β be the angular velocity of the roller, the angular acceleration of the roller is given by:

$$d\beta/dt = \dot{\beta} = \frac{1}{R} \left(\frac{dVB}{dt}\right) = \omega_1^2 (r/R)\, B \qquad (6)$$

where

R is the roller radius.

The torque equilibrium for the roller may then be written as:

$$F_T R = I \omega^2 (r/R) B \qquad (7)$$

noting that in this case the stroke r is equal to the roller radius, R, the tangential force required to accelerate the roller is given by the following equation:

$$F_T = I \omega^2 B/R \qquad (8)$$

4.0 REQUIRED FRICTION COEFFICIENT

Assuming that the side force, F_s, is known at any given crank angle, the coefficient of friction necessary to change the roller speed is given by the ratio, F_T/F_S. In the following table, this ratio is calculated for the range of crank angles from 180 to 360 degrees.

0 (deg.)	B	F_T	F_s	F_t/F_s
180	-0.704	8.30	0	∞
202 1/2	-0.710	8.37	49	0.17
225	-0.700	8.25	100.5	0.082
247 1/2	-0.597	7.04	169	0.042
270	-0.310	3.65	264	0.014
292 1/2	0.169	1.99	409	0.005
315	0.714	8.42	642	0.013
337 1/2	1.138	13.42	866	0.015
360	1.296	15.27	0	∞

This table was constructed for the inertia of 0.00163, and for ω= 104.7 radians per sec. corresponding to 1,000 rpm. A roller radius of 1.515 was assumed.

Since a coefficient of friction of 0.1 to 0.15 can be assumed if a solid lubricant is used in the track and on the roller surface, it is evident from this table that at 1,000 rpm, the roller should be driven in synchronism over most of the stroke. However, at the ends of the stroke, there will not be sufficient side force to provide the necessary driving torque and slipping or skidding will occur.

Two other points should be noted. One is that since the tangential force is a function of the square of the speed, at 1,500 rpm the required friction coefficients are increased by a factor of 2.25 which will increase the portions of the stroke over which skidding will occur. At 3,000 rpm, the friction coefficients required to drive the roller are increased by a factor of 9 over the above table which suggests that skidding would occur over the much broader range from 180 to almost 270 degrees. The second point is that for larger diameter cylinders, the traction force required will increase as the third power of radius (inertia will increase as r^4 but this is divided by the radius as shown in equation (8)). While the side force can be expected to increase in proportion to the piston area, or as the radius squared, the net result is that the friction force will increase in proportion to the cylinder diameter so that the range of stroke over which skidding occurs will increase.

In order to explore further the behavior near the ends of the stroke, further data on the side force in the end of the stroke sections was obtained.

The friction coefficients required to drive the roller in the region from 180 to 225 degrees are shown in Figure 2. Curves for 1,000 rpm and 3,000 rpm are shown. In addition to the crank angle scale on the abscissa, a second scale is shown giving the distance of the piston from the bottom dead center. This shows that at 1,000 rpm the distance over which skidding will occur, assuming that it starts at $f = 0.15$, is 0.2 inches at 1,000 rpm and over 1/2 inch at 1,500 rpm. The distance approaches 1.5 inches at 3,000 rpm.

5.0 TRIBOLOGICAL IMPLICATIONS

There are two types of sliding which will occur in this design of engine. One is gross sliding near the ends of the stroke, where the roller acceleration required is the highest and the side force available to load when roller against the side of the cylinder is the lowest. The second kind of sliding is that which will occur within the Hertzian contact ellipse area.

Fortunately, from the standpoint of wear of the roller, the cylinder, or both, the sliding or skidding (which will occur near the ends of the stroke at moderate speeds) occurs in areas where the side load is small. As a result, the amount of wear that will occur will at least be minimized since wear can be roughly equated to the product of sliding velocity and load. As the engine speed increases, the area of gross sliding increases rapidly.

Sliding within the contact zone must occur, as was briefly discussed in Section 2.0. Here, the wear effects will be the most severe over the portions of the stroke where the side load is the highest and where consequently the contact ellipse is the largest. Both of these factors will maximize the product of slip velocity and, load and hence wear. Furthermore, since wear will not occur, at least initially, in the rolling contact zones between the forward slip and reverse slip portions of the contact ellipse, the stress pattern can be expected to change as wear occurs with the result that the rolling areas will become overloaded and will eventually suffer damage due to fatigue spalling as the result of rapidly increasing Hertz stresses.

6.0 PISTON DESIGN

In the absence of piston rings, the piston will be fitted very closely to the cylinder in order to avoid blowby. If the piston skirt is also made tight there may be a problem of assuring that the roller will indeed transmit the load and that the piston skirt remains free.

For this reason, it is recommended that the piston skirt area be cut back from 5 to 10 mils in order to permit free roller action. The top one inch or so of the piston can be maintained with a tight clearance and provide the necessary seal from the combustion chamber. The distance between the upper one inch section and the wristpin location will provide some flexibility in location for the two actions to take place. However it may be desirable to increase this distance somewhat in order to avoid cocking of the piston so much as roller wear may occur.

7.0 RECOMMENDATIONS

If it is decided to develop this concept of an adiabatic engine, there are a number of recommended tasks which should be carried out in order to assure proper piston/cylinder performance. These are briefly outlined below.

- Run an experimental single-cylinder mockup of the piston roller cylinder combination. Since the main interest is in the lower range of forces at the ends of the stroke, a motored operation should be satisfactory. Experiments should be run with and without the solid lubricant coatings, and with a chrome oxide roller, chrome oxide liner combination as well as the silicon nitride/chrome oxide liner combination. The roller should be instrumented so that its instantaneous speed can be sensed and monitored as a function of crank angle position. The track should be examined in detail, as well as the surface of the roller after various periods of operation, varying from about half hour up to at least one hundred hours.

- Conceive and test methods of lubricant transfer to the roller surface or to the cylinder wall.

- Prepare a computer code that will predict the total kinematic operation of the roller piston and predict the wear pattern as a function of the wear coefficient.

- Model the roller track situation in a simple test rig, and determine the wear coefficient.

- Support a more fundamental program aimed at gaining an understanding of the mechanism of lubricant transfer, and the relative merits of various methods of feeding lubricant to a moving part.

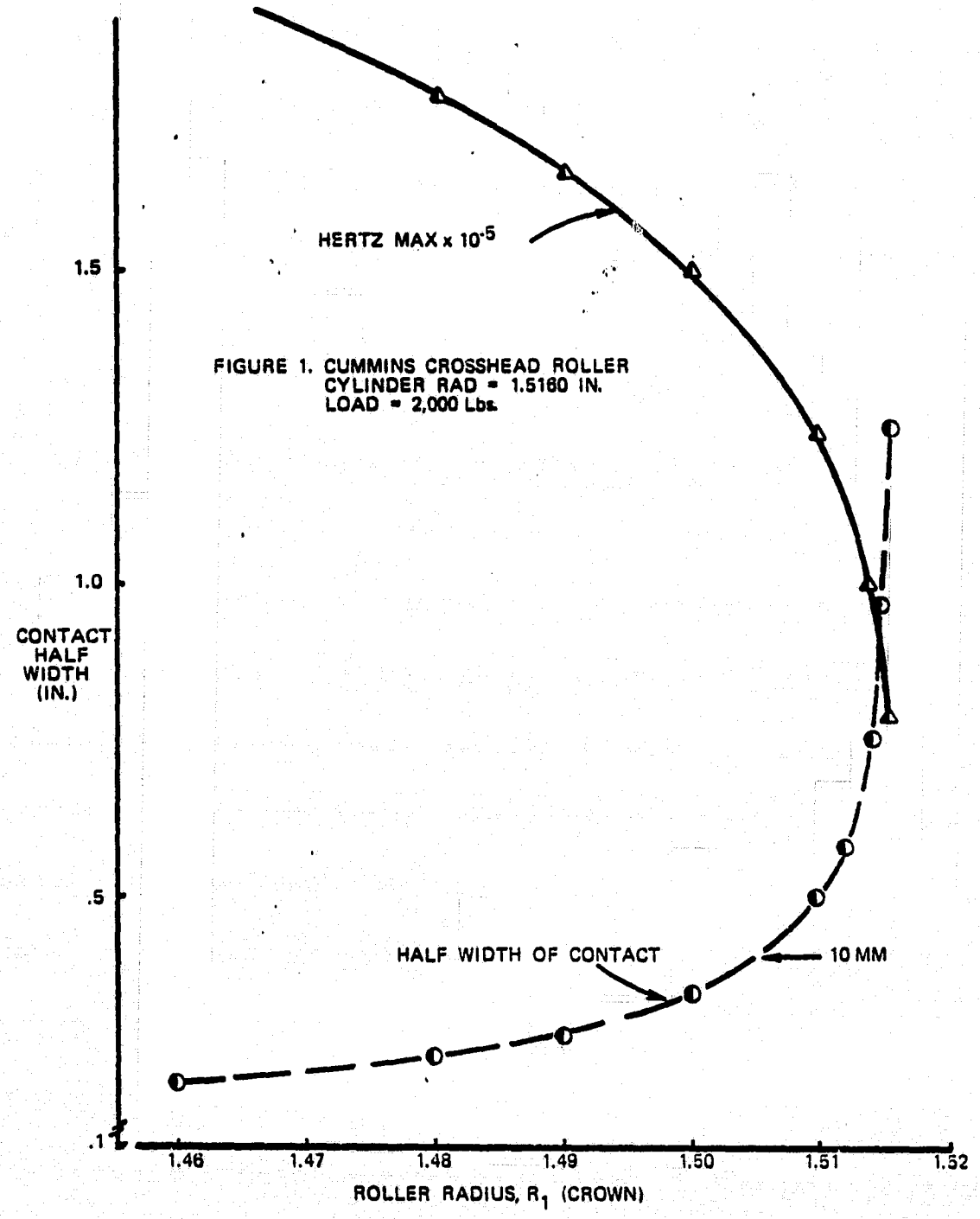

FIGURE 1. CUMMINS CROSSHEAD ROLLER
CYLINDER RAD = 1.5160 IN.
LOAD = 2,000 Lbs.

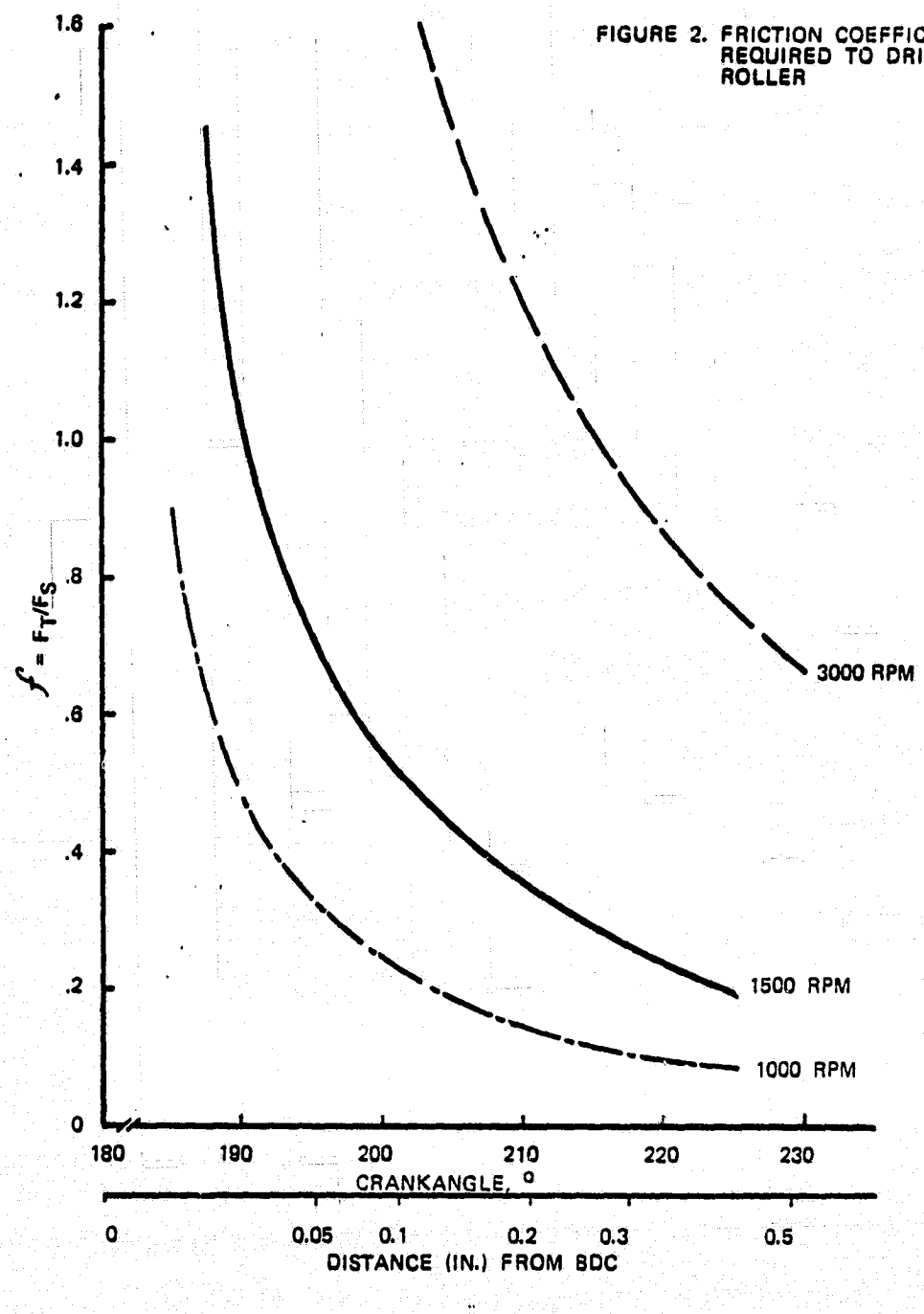

FIGURE 2. FRICTION COEFFICIENT REQUIRED TO DRIVE ROLLER

D4

APPENDIX 3

A STUDY OF THE ARMSTRONG WHITWORTH SWING BEAM ENGINE FOR AUTOMOTIVE APPLICATION

SIR W.G. ARMSTRONG WHITWORTH & COMPANY (ENGINEERS) LTD.
277, ABERDEEN AVENUE, SLOUGH, BERKSHIRE, ENGLAND

The introduction of ceramics to those parts suffering high thermal loading has been successfully demonstrated by Cummins, and there is no question that the 100 kw (134 hp) naturally aspirated engine of the future will be developed to produce up to 300 kw (402 hp) by the application of turbocharging or its equivalent.

However, at the 60 - 80 kw (80 - 107 hp) size needed for the economic automotive engine, scaling down the 300 kw (402 hp) is beset by the laws of scale. The conventional four stroke diesel has not been shown to be successful at the small high speed engine size.

The opposed piston two stroke engine does not suffer the same laws of scale and engines in the low power range have already been marketed successfully.

The half litre/cylinder Armstrong Whitworth Swing Beam Engine is the latest to be designed with the automotive market in mind. Its low noise structure and balanced linkage system coupled with advantages for easy start and potential use of low grade fuels, derived from its variable compression ratio and slow piston motion, qualifies it for the application.

This engine concept is not just a design. Many development testing hours have been carried out, and the results show that it has the potential for more advanced development.

The application of ceramics to the components of the O.P. engine will be easier than those needed for the four stroke, and the advantages will be the same.

In addition, the most important advance to look for from ceramic in the O.P. engine is that of its potential to run without piston or liner lubrication. The O.P. engine type has always had limitations regarding oil loss to exhaust through the ported liner and in thermal limitation from materials that have restricted its potential of high specific output.

The unlubricated ceramic liner concept favors the Swing Beam configuration due to its lower piston side thrust forces. This feature lends itself ideally to introducing the short crosshead type piston with piston rod seals which would exclude crankcase oil from the cylinder.

Ceramics will also extend the power linits on the engine. Increased exhaust temperatures will compensate for the lower efficiency of the small turbocharger and so reduce blower power and raise thermal efficiency.

A two cylinder ceramic crosshead Swing Beam engine of about 1 litre capacity incorporating the basic Swing Beam features has been studied and outputs of 150 psi BMEP to 220 psi BMEP over a speed range of 2000 rpm to 4000 rpm looks a reasonable target with turbocharging.

This performance has been predicted using basic characteristic curve of isfc and exhaust temperature plotted against imep.

It was most advantageous that in making the predictions a known engine performance was used as a starting point.

A table of progressive stages of turbocharging showed that by allowing the exhaust temperatures to rise to 750°C, a pressure of 2 atmospheres and reduced scavenge blower resulted in a predicted performance of 205 psia BMEP and 0.318 lbm/hp-hr specific fuel consumption. It should be noted that the starting point that led to this performance was not particularly good (80 psi BMEP and .45 BSFC) and the figures would be

substantially improved by the better combustion quality anticipated from the use of ceramic - levels of smoke and emission will also be reduced.

Developments are going on with scavenge blowers utilizing the engine's flywheel which is seen as the next important breakthrough for the two stroke diesel. Servo operated fuel systems also have been run which would give injection characteristics well suited to the (DI) O.P. engine.

If the same percentage of improvement predicted could be achieved over the whole load and speed range then a vehicle which was normally getting 37 mpg with a 2.5 litre engine would get 53.8 mpg from a 1 litre engine developing the same power - a further improvement being had from the reduced engine weight.

It is estimated that the approximate size of the engine will be Height 550 mm (22 inches), Width 640 mm (25 inches), Length 450 mm (18 inches), and dry weight 140 Kgs. (309 lbm).

D5

N85 13240

APPENDIX 4

ADVANCED AUTOMOTIVE DIESEL ENGINE SYSTEM STUDY

FORD MOTOR COMPANY
RESEARCH STAFF
DEARBORN, MICHIGAN

TABLE OF CONTENTS

SUMMARY

Cummins Engine Company has a NASA-administered contract (DEN 3-261) with the Department of Energy to conduct a conceptual study of an Advanced Automotive Diesel engine. Ford Motor Company is a sub-contractor to Cummins with the tasks of calculating the fuel economy and performance of a vehicle using the various engine concepts considered by Cummins, also, to prepare installation drawings of the selected engine in a vehicle, to estimate the approximate vehicle initial and lifetime costs and to assist in developing a market strategy. This report presents the results of the work done by Ford.

The recently introduced front wheel drive 1984 Ford Tempo/Mercury Topaz was the vehicle selected as representative of the 3000 lb. test weight baseline vehicle specified in the contract. All of the engine concepts were evaluated in this vehicle over the EPA urban (or metro) and highway driving cycles using computer models of the engine and vehicle in a Ford computer program. To incorporate an automatic transmission and yet maximize economy and performance, with an engine that has a limited speed range from idle to maximum, a typical continuously variable transmission (CVT) was included in the powertrain.

The engine concept selected for vehicle installation was a supercharged 1.4 liter, 4 cylinder spark assisted Diesel of 14:1 compression ratio. A compounding unit consisting of a Lysholm compressor and expander is connected to the engine crankshaft by a belt drive. The inlet air charge is heated by the expander exhaust gas via a heat exchanger.

Four levels of technology achievement on the selected engine concept were evaluated, from state-of-the-art to the ideal case. This resulted in the fuel economy increasing from 53.2 mpg to 81.7 mpg, and the 0-60 mph time decreasing from 17.6 seconds to 10.9 seconds. The table below summarizes the results.

Technology Level	1	2	3	Ideal
CFDC*(mpg)	53.2	61.7	79.2	81.7
0-60 mph (sec.)	17.6	13.1	11.4	10.9

Because of the elimination of the need for radiator cooling air and the compactness of the powertrain which permits a recontouring of the vehicle hood, it was estimated that a 10 percent reduction in drag coefficient would be possible. This would be expected to result in a 3 percent improvement in the CFDC mpg. In the case of the 3rd level of technology achievement, this would improve the fuel economy from 79.2 mpg to 81.6 mpg.

No problems were encountered in the packaging of the engine in the vehicle. A commercially available fuel fired heater was specified for heating the passenger compartment. This was installed on the vehicle bulkhead.

* Combined Federal Driving Cycle

The costing study was undertaken on broad engineering estimates and is of a preliminary nature. Uncertainties on the design content and on the costs likely to be achieved in high volume production produce considerable range for the estimates.

The baseline vehicle selected is a gasoline engine powered 1984 Ford Tempo/ Mercury Topaz. The cost of parts removed from the vehicle were tabulated and subtracted from an estimate of the costs of the Advanced Automotive Diesel system. Initial costs of the diesel-powered vehicle were estimated to be at a premium of $2127 with an uncertainty of +$80 to -$680. Life cycle costs were calculated over a 100,000 mile period and included equal scheduled maintenance costs of the gasoline and diesel engine and fuel costs based on improvement in fuel economy from the baseline 35 mpg (as specified in the contract) to the 81.6 mpg of the 3rd level of technology achievement with account being taken of the reduction in vehicle drag coefficient. Based on a fuel cost of $1.20 per gallon, the life cycle cost of an Advanced Automotive Diesel engine could be less than that of a conventional gasoline engined car (assuming 35 mpg) by $195, with a possible range from $875 to $115.

Marketing strategy was discussed with Cummins and covered the following areas:

- Car market segmentation
  - Current and future vehicle size, fuel economy, performance, sales rates.
- Planned/expected product functional improvements.
- Corporate average fuel economy.
  - Current and future outlook and significance
  - Methodology
- Diesel market
  - Current Status
  - Customer purchase reasons
  - Vehicle usage data
  - Current and future payback logic/methodology
  - Penetration forecasts

INTRODUCTION

This report covers the work done by Ford Motor Company as a sub-contractor to Cummins Engine Company under a government DOE/NASA contract (DEN 3-261) to conduct a conceptual study for an Advanced Automotive Diesel engine.

The sub-contract comprised the following basic tasks:

- Evaluate different engine concepts, as defined by Cummins, for performance and fuel economy in a vehicle over the combined Federal driving cycle.
- Define a vehicle and provide system installation drawings for the selected engine concept.
- Assist in determining cost differentials for the selected engine concept in comparison with a conventional powerplant.
- Collaborate with Cummins in developing a tentative market strategy for introduction of the selected engine concept in a vehicle.

The principal objectives of the DOE/NASA contract were:

- Fuel economy of a 3000 lb. test weight vehicle to be improved 50 percent relative to a baseline vehicle mileage of 35 mpg over the combined Federal driving cycle.
- An acceleration capability of 0-60 mph in 15 seconds.
- Estimate the initial cost and life cycle cost projections compared to conventionally powered automobiles.

The recently introduced, front wheel drive vehicles, 1984 Ford Tempo/Mercury Topaz were selected as the vehicles in which to make the vehicle installation and the performance and fuel economy projections since they are in the weight class specified by the contract. To provide for an automatic transmission and yet maximize the fuel economy a typical continuously variable transmission (CVT) was included in the powertrain.

A proprietary Ford computer program was used to determine performance and fuel economy over the combined Federal driving cycle with both a CVT and 5 speed manual transmission. Computer models of the vehicle and CVT were available at Ford, and fuel island maps were supplied by Cummins for each engine concept.

Cost estimates were made by subtracting the total variable cost of all items removed from a standard gasoline-powered production vehicle (not fuel injected) and then adding the estimated costs of new items. Life cycle cost estimates were based on a total mileage of 100,000 and assumed that the fuel used in the baseline vehicle was equal to the cost of Diesel fuel.

1.0 Vehicle Specification

The 1984 Ford Tempo/Mercury Topaz were selected for this study, these are actual production vehicles which have the same test weight as the NASA baseline vehicle and a comparison between the vehicles is shown in the table below. The vehicle is currently powered by a 2.3 litre gasoline engine and is offered with either a manual or automatic transmission. Although the baseline vehicle is specified with an automatic transmission, this study will consider both an automatic (in this case a continuously variable transmission) and a 5-speed manual transmission.

For the installation studies, engine compartment drawings and accessory drawings of both standard production and limited production or prototype components have been used. The continuously variable transmission represents current industry state-of-the-art prototypes.

For the performance and fuel economy analysis the characteristics of the Ford Tempo and accessory loads were readily available in company computer files. A proprietary computer program developed by Ford Research which has the capability of evaluating vehicles with continuously variable and conventional transmissions was used in this study.

Comparison of 1984 Tempo with Baseline Vehicle

	NASA Baseline Vehicle	1984 Ford Tempo
Inertia Test Weight Class (lbs.)	3000	3000
Wheelbase (ins.)	109.5	99.9
Frontal Area (sq. ft.)	21.5	20.6
Drag Coefficient	Not specified	0.37
Final Drive Ratio	2.70	3.33
Tires	ER78-14	P175/8R13XA4 (and other options)
Transmission	3-speed automatic	See results of study with AAD powertrain.
0-60 mph accel. time (secs.)	15.0	
Fuel economy-CFDC (mpg)	35	

2.0 Engine System Definition

2.1 Engine Concept Evaluation

Three engine concepts were evaluated for fuel economy and performance in a Ford Tempo vehicle by using the Ford developed computer program (See Section 3.0 of the main body of the report for the description of the concepts used - i.e. A,B, and c). Each concept was evaluated with a 5-speed manual transmission and a CVT. Data on each engine concept was provided by Cummins Engine Company in the form of "fuel island maps" and computer matrix print-outs. This print-out data was used as supplied with no modifications. Accessory loads for a power steering pump and an alternator charging at 8 amps were stored in the computer files so that the appropriate losses were deducted from engine power to provide the net input power to the transmission. Idle speed was selected at 500 RPM but will depend on NVH characteristics of final engine/transmission.

The results of the vehicle performance and economy calculations are given in the table below. The fuel economy over the Combined Federal Driving Cycle (CFDC) is calculated from the following formula:

$$CFDC = \frac{1}{\frac{0.55}{(0.95)M} + \frac{0.45}{H}}$$

where M = fuel economy over the EPA metro (or urban) driving cycle for a hor engine (mpg)

H = fuel economy over the EPA highway driving cycle for a hot engine (mpg)

To allow for the cold start included in the metro driving cycles, an estimated decrease of 5% of the hot start fuel economy was used i.e. E.P.A. Metro driving cycle (average of cold and hot start) = 0.95 M (hot start)

Concept	A		B		C	
Transmission	Man*	CVT**	Man.	CVT	Man.	CVT
M (mpg)***	37.4	39.3	51.4	60.1	52.0	53.8
H (mpg)	54.4	60.8	71.8	85.9	70.4	76.3
CEDC (mpg)	42.1	45.2	57.0	67.2	57.1	60.0
0-60 mph	14.3	13.4	14.3	12.6	16.6	17.6
0-2 sec. dist.(ft.)	24.8	25.5	24.2	25.6	20.3	17.2
0.4 sec. dist. (ft.)	90.2	94.5	89.0	96.0	77.9	64.9

Concept B is clearly the superior choice which gives 67.2 mpg on the CFDC and a 0-60 mph time of 12.6 seconds when used with the CVT.

2.2 Sensitivity Evaluation

The preliminary screening of concepts in Section 2.1 above indicated the superiority of Concept "B". In this section the effects of variable levels of technology applied to concept B are evaluated. Fuel island maps for each level of technology were supplied by Cummins. The stages of technology are defined as follows.

1st level -- a state-of-the-art adiabatic diesel engine

2nd level -- an advanced adiabatic diesel engine with compounding

3rd level -- the same as level 2 with the addition of charge air preheating and minimum friction.

Ideal -- the same as level 3 with technology improvements extended to the limits

The table below summarizes the improvements in performance and fuel economy resulting from each level of technology for both a 5-speed manual transmission and a CVT.

Tech.Level							Optimistic Achievable		Future Tech. Gasoline
Transmission	Man.*	CVT**	Man.	CVT	Man.	CVT	Man.	CVT	Engine
M (mpg)	47.1	48.4	47.0	56.6	74.0	72.7	78.3	74.9	40 (45)†
H (mpg)	62.5	65.8	66.3	75.2	95.4	96.4	101.1	99.8	70 (79)†
CFDC (mpg)	51.3	53.2	52.3	61.7	79.7	79.2	84.4	81.7	50 (56.5)†
0-60 mph	20.8	17.6	15.8	13.3	13.7	11.4	13.1	10.9	
0-2sec.dist.(ft.)	22.7	23.6	24.5	26.3	24.6	26.8	24.7	26.8	
0-4sec.dist.(ft.)	78.9	83.8	86.6	97.7	89.4	102.7	90.7	103.4	

As can be seen the fuel economy with the CVT increases up to 81.7 mpg, and 0-60 mph time reduces to 10.9 seconds with the "optimistic acievable" level of technology. It must be understood that this level includes long-range high risk development requiring extended laboratory prove out.

* Manual 5-speed transmission, shift schedule (15/25/40/45 mph)
** CVT optimally shifted
*** Diesel fuel 7.1 lbm/gal.

The final column of figures gives an indication of levels of fuel economy that could be attained by future gasoline engines with CVT using anticipated technological improvements under development at this time. After compensating for the higher energy content of Diesel fuel (13 percent higher than gasoline), the comparative economy, on an equivalent energy basis, of the gasoline engines will be within 30 percent of that for the 3rd level of technology.

3.0 Vehicle System Definition

3.1 Powertrain System

The selected engine concept for vehicle installation was the 1.4 liter, 4 cylinder, adiabatic Diesel engine. It is highly supercharged by means of a positive displacement Lysholm compressor/expander compound unit, the net power into or out of the compounder is transmitted through a belt drive connected to the engine crankshaft. The engine drives through a continuously variable transmission (CVT).

Since this is an adiabatic engine that operates without lubricating oil, there is no need for either a coolant radiator or an engine oil cooler. However, provision must still be made to permit air to flow to the air conditioner condenser coils and possibly a transmission oil cooler.

Standard automotive accessories must be included in the powertrain package i.e. an alternator, power steering pump and an air conditioner compressor. Because the engine is a spark assisted Diesel, an ignition system as well as a fuel injection pump is required. An auxiliary vacuum pump is also necessary to provide for the vacuum driven vehicle controls, etc.

3.2 Passenger Compartment Heating

A vehicle with a powerplant that is not water cooled and does not have lubricating oil obviously cannot use the standard passenger compartment heating system. Possible alternatives for consideration are:

- Engine exhaust heat
- Engine casing heat
- External fuel fired heater
- Electric resistance heater
- Air conditioner/Heat pump system

The capacity of the heating system must be such as to deliver 260 BTU/min. as derived from the following specifications under steady state conditions:

Ambient temperature 0°F
Vehicle speed 30 mph on a 0 percent grade
Fan delivery of 100 cfm
Air delivery temperature 125°F

At 30 mph it was estimated that the selected engine will be delivering 40 lb.-ft. torque at 720 rpm. The engine housing temperature was estimated to be 200°F (average) and the engine exhaust temperature was estimated to be 550°F at a mass flow rate of 2.8 ppm.

The heat contained in the exhaust gas is more than adequate to supply 260 BTU/min. However, to utilize engine exhaust heat requires some form of heat exchanger. Two basic types of heat exchanger are possible. One is stationary with an element or matrix fixed in the path of the gas flow and therefore susceptible to plugging, fouling and corrosion due to the particulates and exhaust deposits. The other type is a rotating, counter flow heat exchanger which is self cleaning, however, there is some carryover of exhaust gas into the heated air. This would necessitate at least one more heat exchanger to transfer heat to the passenger compartment. Both of these systems would create a back pressure on the engine.

Engine casing heat is a possible means of acquiring heated air. The powerplant could be essentially encapsulated and the air surrounding the engine ducted to the passenger compartment. Calculations, assuming a surface at 200°F with an area of 2.25 sq. ft. and with an air film thickness of 0.5 ins., indicated a heat transfer of only 36 BTU/min., insufficient for this application.

A tried and tested method for heating is by means of an external fuel fired heater. A separate air circuit provides for combustion of the fuel and a heat exchanger transfers the heat to the passenger compartment air. An overall efficiency of 75% at full load can be obtained with current commercial type heaters. So far there is no known EPA emissions policy covering this type of installation.

An electric resistance heater has the attraction of almost instantaneous heat with no direct contamination of the atmosphere and no additional heat exchangers. However, the alternator would be prohibitively large, it is estimated that a 4.5 KW alternator running at 7 times engine speed would be about 10-12 ins. dia. and 14-16 ins. in length.

By making modifications (probably extensive) to the engine driven air conditioning system, a heat pump could be developed for providing heat (and cooling) to the passenger compartment. The disadvantage to this approach is that air conditioning would have to be a standard feature of the vehicle thereby significantly increasing the initial cost of the vehicle.

A summary of the above systems is provided in the table below. After weighing the advantages and disadvantages noted in the above discussion, it is recommended that an external fuel fired heater be considered for initial vehicle installation studies. The other likely approaches such as exhaust heat utilization and the heat pump would require further analysis and design evaluation going beyond the scope of this program to explore their possible cost effectiveness.

It should be noted that there is a penalty associated with the use of an external fuel fired heater. For example, if the heater were operated at the maximum rate and for 10 percent of the time for the full driving cycles, the fuel economy would be reduced as shown in the table below for the 3rd level of technology.

	No Heater	With Heater at Max. Rate	
		100% of driving cycle	10% of driving cycle
M (mpg)	72.7	56.3 (-23%)	70.6 (-3%)
H (mpg	96.4	83.3 (-14%)	94.9 (-2%)
CFDC (mpg)	79.2	63.8 (-19%)	77.3 (-2%)

Summary of Passenger Compartment Heating Schemes

System	Heating Rate BTU/Min.	Remarks
Conventional System	260	Heat exchanger core 6 x 8 x 2 ins.
Engine Exhaust Heat Utilization	260	Additional heat exchanger. Increases engine back pressure. Potential fouling & corrosion problems.
Engine Casing Heat -Encapsulated Engine	36	Would require supplemental heater.
External Fuel Fired Heater	260	Efficient conversion of fuel energy. No present emissions policy.
Electric Resistance Heater	260	Alternator size, 10 ins. Dia. x 14 ins. long
Heat Pump (Includes A/C System)	260	High development cost. Increases initial vehicle cost.

3.3 Powertrain Installation

Installation studies were conducted with a front wheel drive 1984 Ford Tempo/ Mercury Topaz vehicle and the engine design provided by Cummins.

The study involved defining the packaging envelope within the Tempo after removal of the conventional gasoline engine, transmission and accessories including radiator. Location of the Cummins engine with the CVT transmission was determined by the required positions of the output shafts from the transmission. This resulted in the engine crankshaft center moving 37 mm forward of the position for the conventional engine. Three views of the installation package are shown in Figures 3.3.1 and 3.3.2. at the end of this report. A new front engine support bracket had to be designed to attach to the engine crankcase since loads could not be taken through the ceramic cylinder liners. The two rear supports were off the CVT and were essentially the same as for the conventional engine.

Standard automotive accessories are included in the powertrain package i.e. alternator, power steering pump and an air conditioner compressor. The latter two accessories are bracket mounted to the engine crankcase and driven by a polyvee belt. The alternator is bracket mounted off the power steering pump bracket and driven by a V belt from that pump. An auxiliary vacuum pump is necessary to provide for vacuum driven vehicle controls. This is an electrically driven unit mounted on a bracket attached to the front cross member.

Because the engine is a spark assisted Diesel, an ignition system as well as a fuel injection pump was required. The ignition system is a typical unit with the distributor being mounted on the cylinder head and directly driven by the camshaft at the end opposite to the accessories. The location of the distributor permits a short run for the ignition wires and provides for the most clearance available between the wires and the hot exhaust manifold. A Robert Bosch fuel pump as specified by Cummins is mounted on the side of the cylinder head and driven by a cogged belt from the camshaft at the camshaft drive end.

The heater for the passenger compartment air is a commercially available unit that is shown mounted to the vehicle bulkhead. It is quite probable that in production this heater would be integrated into the vehicle bulkhead design and the heating system.

Due to the smaller height of the engine a lower hood line by about 1 1/2 ins. would appear possible, see figure 3.3.1 at the engind of this report. It is estimated that with a re-contoured hood line and the elimination of radiator cooling air that the vehicle drag coefficient might be lowered by 10 percent.

A 10 percent reduction in drag coefficient is expected to improve the fuel consumption by 2 percent over the metro driving cycle, by 5 percent over the highway driving cycle and by 3 percent over the combined Federal driving cycle. This would result in combined Federal driving cycle for the 3rd level of concept B to be improved from 79.2 mpg to 81.6 mpg.

4.0 Cost Analysis

A complete cost analysis includes the difference in cost of ownership between a conventional gasoline engined vehicle and the Cummins engined vehicle over a total of 100,000 miles of operation. The essential items which would be different between the two vehicles are initial cost, scheduled maintenance and repairs, and fuel costs.

4.1 Initial Vehicle Cost

The initial vehicle cost is arrived at by subtracting the variable costs of the items deleted from the standard production package and adding the best estimates of the costs of the new equipment. The costs of the parts that are deleted are known with some accuracy, however, the costs of the added parts are not accurately known and they are expressed as estimated costs with an error band to allow for uncertainties.

The table below lists all of the equipment that is deleted from the standard production vehicle. The total variable cost of these items is about $1500.

Base Engine
Engine Cooling System
Fuel Charging
Exhaust Emissions Controls
Evaporative Emissions Controls
Electronic Engine Controls
Heating Components
Automatic Transmission

Estimated costs of items to be added to the vehicle were based on a volume of 230,000 units per year at 1983 prices and are given in the table below:

	Estimated Cost ($)	Variance +	Variance -
Base Engine *	2000	0	300
Vacuum Pump	12	0	0
Heater	815	0	300
CVT Transmission	800	80	80
	3627	80	680

The initial premium cost of an AAD vehicle therefore is $(3627-1500) = $2127 (with a variance of -$680 to +$80). Obviously, major items of uncertainty are the cost of the AAD engine and the cost of the passenger compartment heater in mass production. It is also assumed that no special exhaust treatment is required for the AAD except for EGR/NOx control. If particulate control is required, cost increases for the AAD system would be necessary.

4.2 Scheduled Maintenance and Repairs

The difference in costs due to scheduled maintenance between a 1984 conventional vehicle and an AAD-powered vehicle over 100,000 miles of operation is the necessity of oil and anti-freeze changes for the conventional vehicle. Assuming oil and filter changes every 10,000 miles at a retail cost of $21.50 per change and anti-freeze changes every 30,000 miles at a retail cost of about $50 results in the following scheduled maintenance cost.

Oil & filter changes	10 x 21.50 =	$215.00
Antifreeze changes	3 x 50.00 =	150.00
		$365.00

Warranty repair costs will be assumed to be the same for both powerplants, including the fuel systems.

Vehicle and powertrain weights are assumed equal, as well as battery requirements. This is contingent on meeting the design objectives of an all ceramic diesel, to avoid the extra battery weight normally found with conventional diesels.

4.3 Fuel Costs

Fuel costs are very much dependent upon the cost of oil, this is a variable dependent upon many factors, such as supply and demand, local, state and federal taxes, international cartels and, of course, the competitive position of the oil companies. For this analysis, it is assumed that the baseline vehicle and the selected engine are operating on the same type of fuel costing $1.20 per gallon.

Baseline vehicle at 35 mpg for 100,000 miles
fuel cost = $3428

AAD vehicle at 81.6 mpg for 100,000 miles
fuel cost = $1471

4.4 Life Cycle Cost

The cost of ownership difference between a 1984 conventional 3000 lbs. vehicle running on fuel of equal cost to Diesel fuel and the AAD running on Diesel fuel at 1983 economics is shown in the following table.

* Base engine cost developed by Cummins based on preliminary designs.

	1984 Conventional Power	AAD Power
Initial cost premium ($)	-	2127 (-680 to +80)
Scheduled maintenance and Repair difference ($)	365	-
Fuel costs over 100,000 miles @ $1.20 per gallon ($)	3428	1471
	3793	3598 (-680 to +80)

To summarize, the life cycle cost for 100,000 miles of operation of the AAD powered 3000 lb. vehicle is less than that for a 1984 conventional powered vehicle by $195. This saving could be as much as $900, in round figures.

5.0 Marketing Stragegy

In this section the general subject of the automobile market was reviewed with Cummins personnel. Specific assistance provided included two revisions of a draft marketing strategy, developed by Cummins and summarized as follows:

- Car Market Segmentation — In today's car market shares are split about 30 percent each for Subcompact and Intermediate segments and about 20 percent each to Compact and Large/Luxury segments. Those segment shares are not expected to change significantly in the next ten years although minicars might achieve a 5% penetration that would come out of the Subcompact segment. Vehicle curb weight range in 1983 runs from about 1750 lbs. to 4250 lbs. By 1993, this range probably will run from about 1400 lbs. to 3400 lbs.

- Planned/Expected Product Functional Improvements — Fuel economy will remain a high priority, and future engine and vehicle functional improvements are expected to contribute to increased fuel economy and also provide improved performance. For gasoline engines, the current round of combustion improvements (i.e. fast burn) will be followed by more advanced concepts which will contribute to improved efficiency as electronics allow more optimal control of the engine and transmission. Multipoint fuel injection and improved central fuel injection will be used for all SI fuel metering. Downsizing, decreased chassis friction, improved aerodynamics, and transmission improvements also will contribute to significantly improved vehicle fuel economy. Direct injection for diesel engines should offer a 10-15 percent improvement over IDI diesel engines. Semi-adiabatic and adiabatic diesels will be an emerging trend.

- Diesel Market — Increased "dieselization" is not required to meet foreseeable CAFE requirements, but there always will be some demand for diesels. Today's depressed diesel market, currently under 3% of new car sales, illustrates the emotionalism involved in the purchase of an automobile. At current pricing, most diesel options would not pay back on a strict financial assessment over a three-year period and the current pricing and availability of gasoline have cut deeply into diesel sales. Other factors working against diesel sales include the poor reputation of early gasoline-engine-derived car diesels, generally poor performance relative to gasoline-engined cars, diesel odor, and increased maintenance.

  Ford is continuing to examine the diesel on a strict financial basis -- calculating a present value of savings and expenses associated with diesel ownership. Cummins was provided sample output from a model that compared forecasts of fuel pricing, option purchase pricing, and vehicle resale value against estimates of customer driving habits. The model then can output an estimated percentage of customers for which a diesel would be a rational financial decision. Clearly not all, perhaps even few, customers are making "rational" financial decisions relative to their automobile so the payback percentage is considered an upper bound on diesel penetration (neglecting fuel availability/pricing crises). Diesel car penetration in the early 1990's presently is projected at 5 to 10 percent.

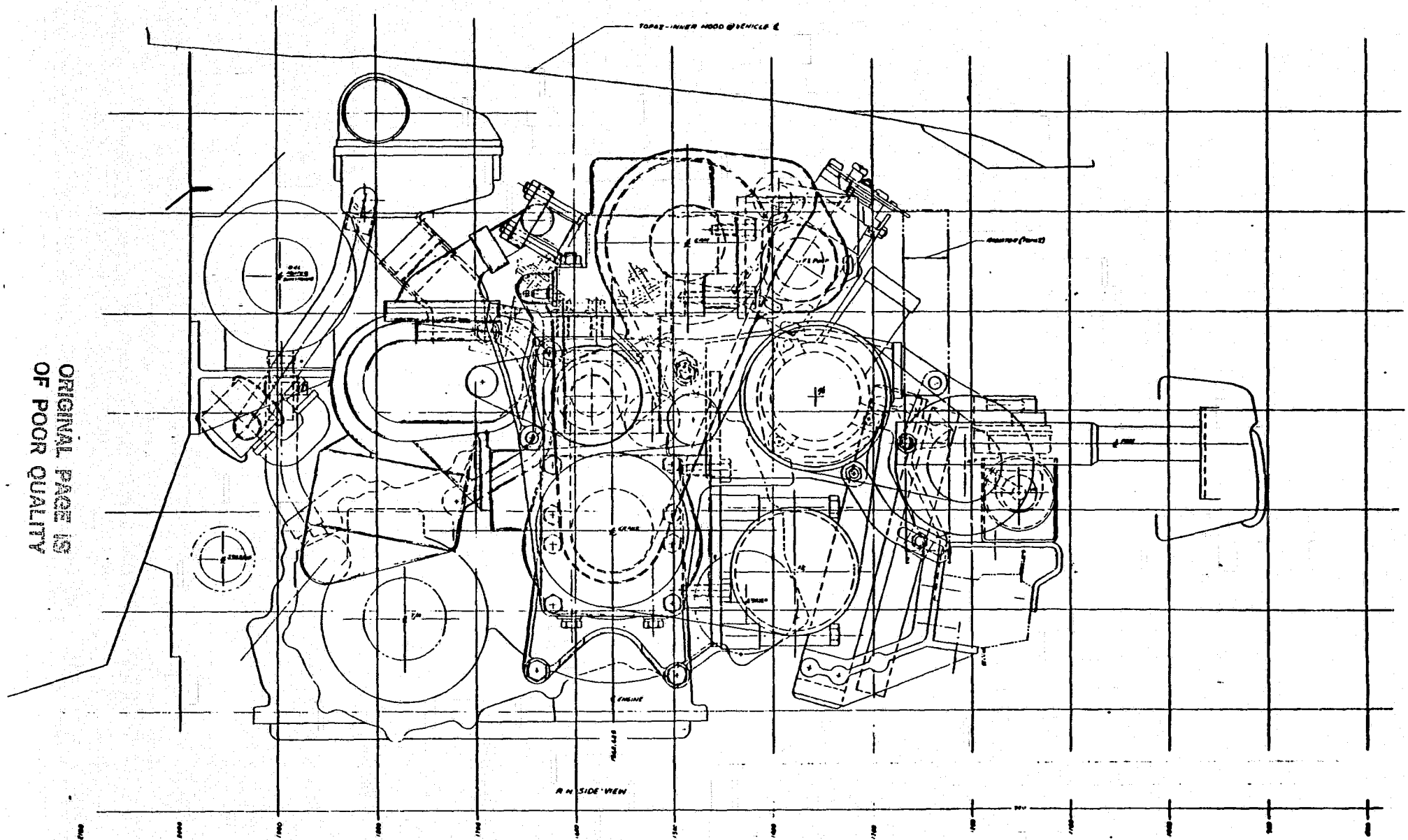

FIGURE 3.3.I. Front wheel drive installation of advanced automotive diesel engine

ORIGINAL PAGE IS
OF POOR QUALITY

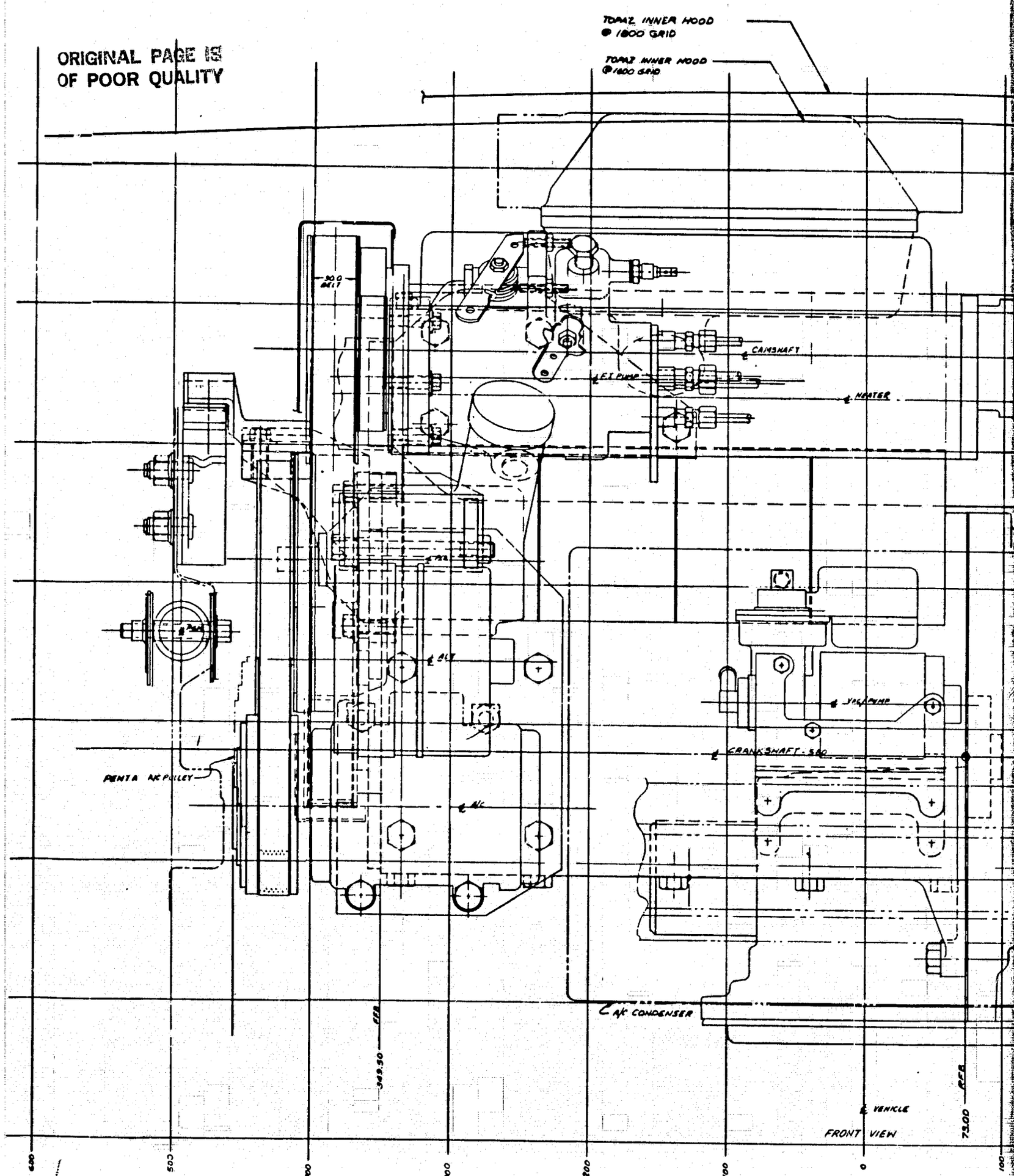

FOLDOUT FRAME

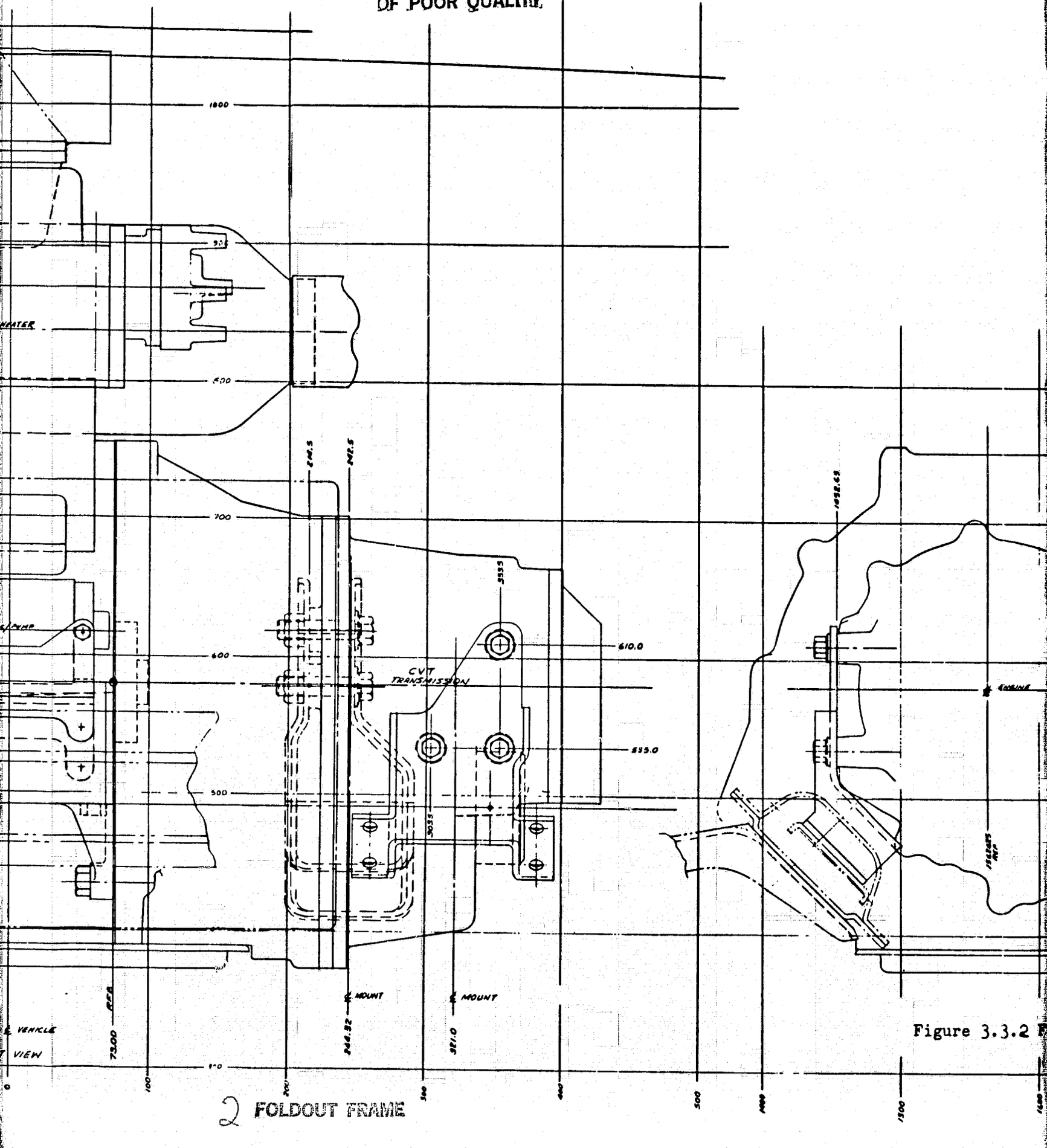

Figure 3.3.2 F

2 FOLDOUT FRAME

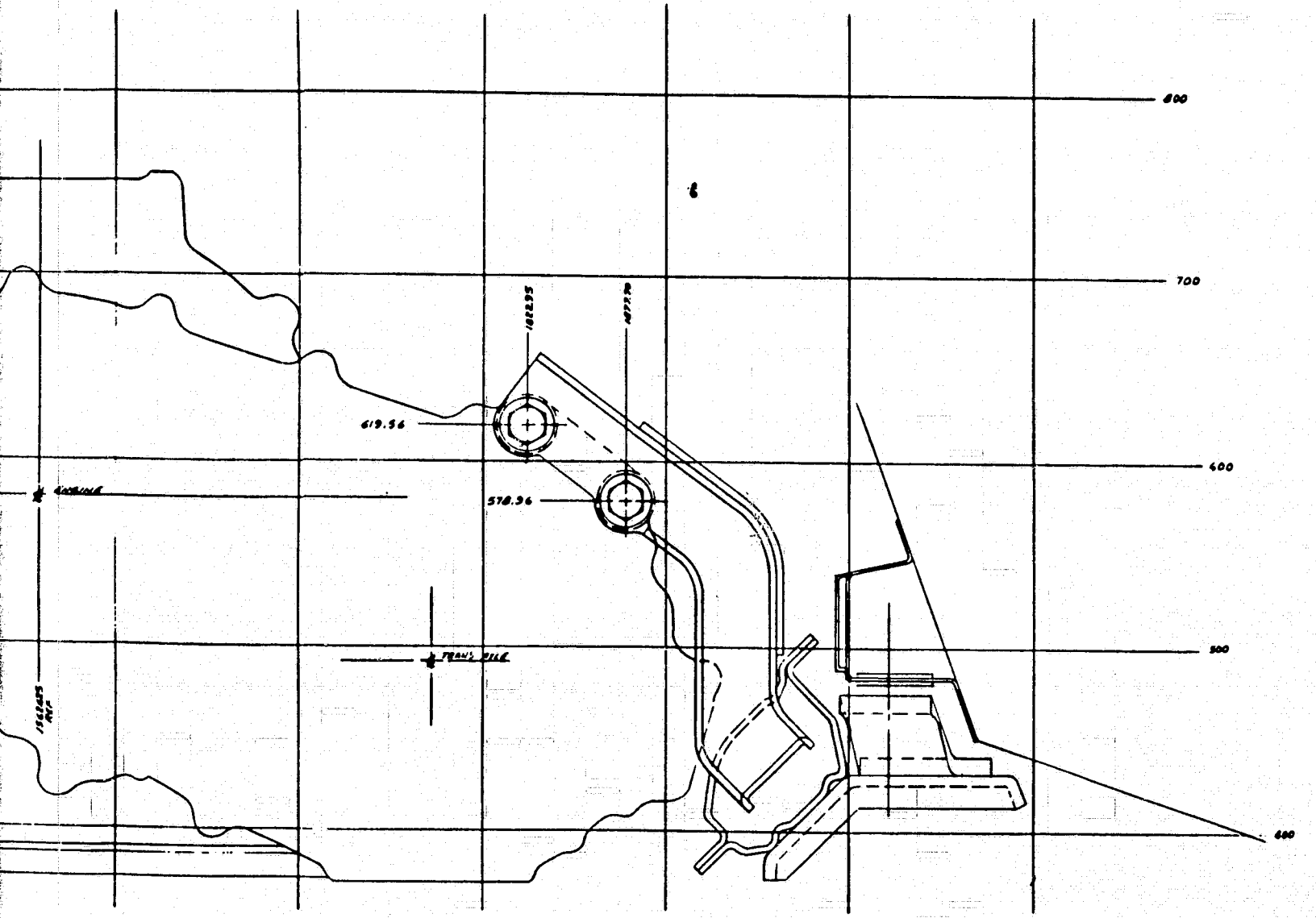

e 3.3.2 Front Wheel Drive Installation of Advanced Automotive Diesel Engine

D6

APPENDIX 5

A.A.D. ENGINE NOISE EVALUATION

INSTITUTE OF SOUND AND VIBRATION RESEARCH
SOUTHAMPTON, U.K.

1. INTRODUCTION

The report covers the critique of the various characteristics of the engine design influencing noise and attempts to indicate areas where attention is required to obtain a noise acceptable engine for car application.

Comments are made on the schematic drawing No 01317 received on 9th May 1983 and engine specification as communicated earlier.

2. ENGINE SPECIFICATION

2.1 Bore x stroke 77mm x 77mm
2.2 4 Cylinder in-line
2.3 Adiabatic design (no cooling)
2.4 Combustion system D.I. 4 stroke
2.5 Max power 80BHP at 3000 rpm
2.6 Peak cylinder pressure 3000 psi
2.7 Positive displacement compounding with screw type compressor and expander
2.8 No lubrication oil. Solid lubrication for some components, Roller bearings. Air bearings between pistons and liners.
2.9 One integral head

3. COMBUSTION SYSTEM AND RESULTANT ENGINE EXCITING FORCES

3.1 Consideration of Combustion System

From the head section, Figure 1, it is clear that the design utilizes the basic principle of the "fireball" gasoline engine high compression lean burn (HCLB) adapted for diesel operation incorporating spark assisted ignition.

The specification states that peak pressures of 3000 psi (204 bar) are considered. This is about three times higher than the pressures encountered in present production Ricardo Comet V chambers. The combustion chamber suggests a design incorporating high turbulence and therefore, it is expected that smooth cylinder pressures will be achieved similar to those of highly turbocharged conventional open chamber engines. Based on available experimental data, a pressure diagram which would be probable in the proposed engine is shown in Figure 2. In this diagram, combustion starts at around 10° ATDC. Figure 2 also shows for comparison, the optimum pressure development from a noise point of view, which can be achieved from a current I.D.I. chamber. In this case the peak pressure is about equal to that of the compression pressure and combustion starts

at around TDC and the whole combustion process takes place at constant pressure - the ideal diesel cycle.

3.2 Assessment of the level of Combustion Excitation and its Effect on Noise

Harmonic analysis of the assumed cylinder pressure diagram at the rated speed of 3000 rpm full load and its comparison with the conventional I.D.I. system of the same bore diameter, in the frequency range up to 4000 Hz, is shown in Figure 3. The spectra are expressed in terms of the actual force in Newtons on a dB scale. The spectra show that in the proposed engine the combustion excitation is considerably higher:

At low frequencies up to 250 Hz	10dB (A)
from 350 - 450 Hz	7dB (A)
from 500 - 800 Hz	14dB (A)
from 1000 - 1250 Hz	4dB (A)
from 1500 - 3000 Hz	8dB (A)

Examination of the spectra show that there are two main problem regions of significance to diesel engine radiated noise. These are particularly from 500 to 1000 Hz and also in the high frequency region from 1500 Hz upwards.

If these levels of combustion force were to be applied to a structure of conventional design a noise spectrum at 1m distance from the side would probably resemble that shown in Figure 4. (Assuming that the engine structure has linear characteristics). As can be seen the spectrum is dominated by a huge peak between 400 and 1000 Hz. This is the region of fundamental engine horizontal bending which could cause considerable problems in a car installation. Overall engine noise is increased by 16dB(A) due to direct combustion force alone. The effect of increased pressure on mechanical noise would be additive.

3.3 Characteristics of Combustion and Inertia Exciting Forces

The sketch shows the forces applied to the main bearings of a 4 cylinder engine.

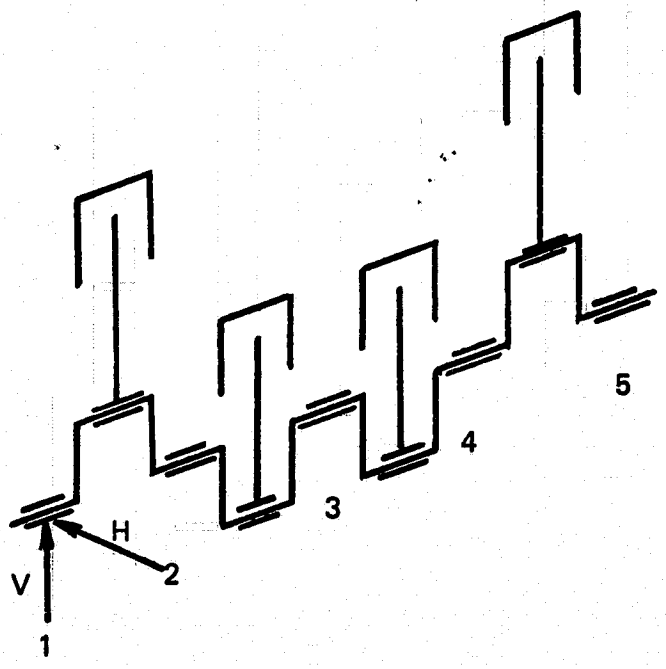

Assuming a reciprocating weight for piston assembly and connecting rod, the reactive forces due to inertia and combustion, on the vertical and horizontal components of the main bearings (Nos 1, 2 and 3) have been calculated at 3000 rev/min full load. These diagrams are shown in Figures 5 to 7 inclusive. A firing code of 1, 3, 4, 2 has been assumed.

From the diagrams it can be seen that bearings 1 and 5 display a single peak of 48KN in the force over two revolutions. On bearings 2 and 4 there are two peaks of 38KN separated by 180° over the two revolutions, thus representing non-symmetrical excitation. The centre bearing receives the peak value of force of 30KN but the force peaks are symetrically displaced by 360°. These distributions are typical to 4-cylinder engines but should be considered when designing a comet engine, that is,

care should be taken to react the forces at number 2 and 4 bearings – the proposed design is symmetrical.

The spectra of vertical force components at the bearings are shown in Figures 8 to 10 inclusive. The corresponding force spectra in the horizontal direction are shown in Figures 11 to 13.

The levels of horizontal excitation is, in overall terms, about 20dB lower than the vertical. The horizontal stiffness of the engine, however, is considerably lower than the vertical stiffness and severe excitation of the fundamental bending mode can be expected. Again, in overall terms the spectral characteristics show that at bearings 1 and 5 the force spectra density is higher than at 2 and 3. At 11° bearing 3, because of the symmetrical double force pulses, spectral density is halved while at bearing 2 and 4, due to non-symmetrical force pulses, the spectra show groupings of harmonics which influence the noise spectra in such a way that strong firing components tend to be impressed on the radiated noise spectrum.

3.4 Experimental Evidence of the Effect of Peak Cylinder Pressure on Engine Noise

The effect of peak gas pressure in a motored engine was considered using compression pressure as a means of engine excitation, thus resulting only in mechanically induced noise. Investigations which were carried out at ISVR showed a pronounced effect of peak gas pressure over the range from 60 to 1250 psi which is particularly marked at low engine speeds. These data can be used to extrapolate and determine the likely increase of mechanical noise when the peak gas pressure is raised to a value of 3000 psi.

Figure 14 shows the experimental results at 1000, 2000 and 3000 rev/min extrapolated to 3000 psi. To a first approximation the indications are that there is a linear relationship between noise and log peak pressure:

at 1000 rev/min	$I \alpha p^{1.4}$
at 2000 rev/min	$I \alpha p^{1.1}$
at 3000 rev/min	$I \alpha p^{0.65}$

The expected increase over the value of a normally aspirated I.D.I. engine is:

3.2 dB(A) at 1000 rev/min
2.5 dB(A) at 2000 rev/min
1.5 dB(A) at 3000 rev/min

Due to the higher combustion pressure the engine mechanical noise is likely to increase and will be particularly significant at low speeds. Predicted motoring noise is shown in Figure 15.

As stated in Section 3.2 direct combustion noise will increase dramatically due to higher pressures and at 3000 rev/min could be still higher due to mechanical noise by 1.5dB(A), because of lack of direct experimental evidence of the behaviour of small engine structures under exceptionally high loading conditions. However, the values quoted must be regarded as indicative only and not absolute.

4. COMMENTS ON NOISE CHARACTERISTICS ON ENGINE STRUCTURE DESIGNS

4.1 Basic load carrying structure

From the drawing study the engine construction is symmetrical. This is usually a beneficial feature for noise control as some adverse vertical bending modes are restrained. A particularly attractive detail of the symmetrical design is the through bolting arrangement for main journal bearing support and cylinder head. This helps avoid high local distortion at points of high stress and also increases the bending stiffness of the upper bearing diaphragms by pre-stressing.

The crankcase design incorporates an integral bearing beam below the throw of the crankshaft in the form of a crankframe as in an earlier ISVR design which was found, together with a sheet metal cover over the lower part of the engine, to be a successful noise control feature. Vibration measurement taken on the ISVR beam showed that inspite of its massive structure, levels were high. This however was not significant because the beam was enclosed by the lower one-piece sheet metal cover. On the Cummins design the beam is of extremely light construction (figure 16). It has

been demonstrated by many researchers that the axial movements of bearing caps of a conventional engine under firing loads are high even though they are restrained to some extent by the crankcase walls. The Cummins crankframe will have exceptionally high vibration levels. This will introduce two specific problems - Firstly direct noise radiation from the bottom of the engine and secondly transmission to the side covers. The mounting arrangements for the covers themselves are good at the lower deck of the cylinder block, but the insulation is insufficient at the bearing beam base.

The horizontal bending stiffness of the design is weak. This is augmented by the separate cylinder liners and the lack of real stiffness of the bearing beam. The likely bending frequency will be very low around 550 Hz and as previously stated will be readily excited by engine horizontal forces.

The vertical stiffness is likely to be low, again for the reasons affecting the horizontal stiffness, but the actual frequency is less predictable.

A serious problem when installed in a vehicle could be lack of drive line stiffness at the rear plate engine block interface. The design is weak in both the horizontal and vertical directions.

4.2 Internal Structure

All shafts and journal bearings for crankshaft and camshaft run in rolling elements (Figure 17). There is scant experimental evidence to assess the behaviour of rolling element bearings with respect to transmission of forces with a high frequency spectral content. What little there is suggests that the difference between the transmissibility of element and plain bearings is small. It is therefore suggested that this aspect will not prove to be an adverse feature of the design.

However, the problem associated with rolling element bearings is self generated high frequency broadband noise resulting from inaccuracies of element roundness and aberration of the mating surfaces. From this point of view, great care must be taken of bearing quality to prevent generation of high frequency noise. Any noise problem here is likely to be manifested at high speed as the noise intensity increases in proportion to the fifth power of rotational speed.

Regarding the piston design, the novel feature using an element race to reduce side thrust friction is an unknown quantity, (Figure 18). One possible feature is that the force is applied at a finite area on the liner which could cause local distortions large enough to generate complex liner vibration modes. Another possible feature is that the point of contact will be a fulcrum about which the piston can tilt and impact at top and bottom with the liner as the side forces change direction. This latter point is closely associated with the qualities of the air bearings between the pistons and the liners. However, no design details are given of this arrangement.

The relative proportions of the main journals and crankpins result in an overlap of 10mm. Because of the extreme pressures acting at the pins these will be large deflections of the crankshaft webs which will lead to axial vibration of the crankshaft nose and consequential noise radiation from the front pulley. It would be beneficial to increase the overlap by increasing pin diameters to counteract this tendency.

4.3 Timing Drive

Insufficient detail is given to comment constructively on this feature. It is assumed that it is a toothed belt drive. If so the tight radius at the idler wheel is a likely source of noise generation.

4.4 Camshaft and Fuel Pump Drive

The design shows that a distributor jerk type fuel injection pump is driven directly from the rear of the camshaft. The camshaft is driven via a toothed belt at the front. Thus torque to the pump is applied through the free length of the camshaft. The natural frequency of oscillation of the camshaft is in the region of 1000 Hz. The pump repetition frequency is 100 Hz at top speed and is therefore not likely to present a direct resonance phenomenon. However, the torsional stiffness of the shaft is low and as the pumping rates and pressures must be very high to deliver the fuel for the designed performance there is likely to be a wind-up of the camshaft at each impulsive pumping load. This will have the adverse effect of exciting the shaft at its natural frequency and can result in erratic injection timing and variable rate. The fuel injection pipes are also much longer than that normally recommended for high rates of injection.

4.5 Noise Characteristics of Screw Expander/Compressor

There are two problems associated with noise of this type of unit:

(a) compressor air-inlet noise
(b) casing radiated noise

The compressor delivery noise, unless a waste gate is incorporated, does not present a problem as the engine itself is always a sufficient attenuator. The exhaust noise, however, will contain the expander rotor fundamental frequency with its harmonics of considerable level which may cause certain problems in engine silencer design.

From the study of the engine timing and compressor drive system of the engine, the following information can be deduced:

1) compressor speed at engine rated speed of 3000 rev/min.

2) Symmetrical rotors - rotor diameter 78mm.

3) Tip speed of rotor at engine rated speed is 270 ft/sec.

4) No specification is given regarding the number of lobes per rotor. It is therefore assumed that the common figure of four is chosen.

The main component of rotary positive displacement compressor noise is produced by rotor rotation. The rotor boundaries present to the incoming air a surface which undergoes extremely rapid change of shape and velocity similar to that of a flexible diaphragm, which has an amplitude of fluctuation of several inches.

The delivery pressure has only a small effect on noise. It is caused by fluctuating leakage from the high pressure delivery side resulting in an increase of high frequency noise affecting the level of the high frequency part of the spectrum and thereby changing the characteristics of the noise and only changing the actual level by a small amount. Depending on the rotor design, another source which can sometimes be prominent is due to high pressure air which is trapped between the meshing rotors. This can, in some cases, substantially increase the noise with delivery pressure.

Figure 19 shows the noise at one meter from the air inlet of a screw type compressor of equivalent size to the Cummins design. The maximum tip speed of this compressor as tested was 160 ft/sec. Since there is a straight line relationship between tip speed and noise emitted, the line can be extrapolated to determine the level of the inlet noise at 270 ft/sec. This can be seen as 123.5 dB(A).

In regard to the characteristics of noise, the spectrum will contain rich harmonic density above the fundamental which can also be augmented by cavity resonances of the blower which depends on physical dimensions and shape.

The frequency of the fundamental, according to speed varies from 900 to 2667 Hz, which falls clearly within the engine structure resonance range and therefore may present problems.

A silencer of substantial size will be required if it has to deal with the compressor fundamental, i.e. according to engine speed from 900 to 2667 Hz.

5. CONCLUSIONS

The engine has a potential to be quiet because a low rated speed is chosen. For this reason, the rapid rise of noise with speed which occurs in engine from 2500 rev/min upwards due to bearing impacts will be minimized. Offsetting this advantage is the high peak gas pressure which is likely to result in high levels of both combustion and mechanically induced noise.

Careful consideration is required in cover design, namely crankcase enclosure, and the stiffness of the integral beam which ideally should be fully enclosed. Some thought is also necessary to increase the drive line stiffnesses.

The location and drive of the fuel injection pump is likely to be the cause of serious combustion problems. It is strongly recommended that the design is reconsidered to mount the fuel pump at the front end of the camshaft near the point where it is driven.

The expander/compressor will constitute a significant source of noise which, apart from silencing problems of the air intake and direct casing radiation, can also excite the basic elements of the load carrying structure.

The exposed cylinder liners are an unknown quantity with the proposed high cylinder pressures. It is probable that some form of block cover will be required over this area.

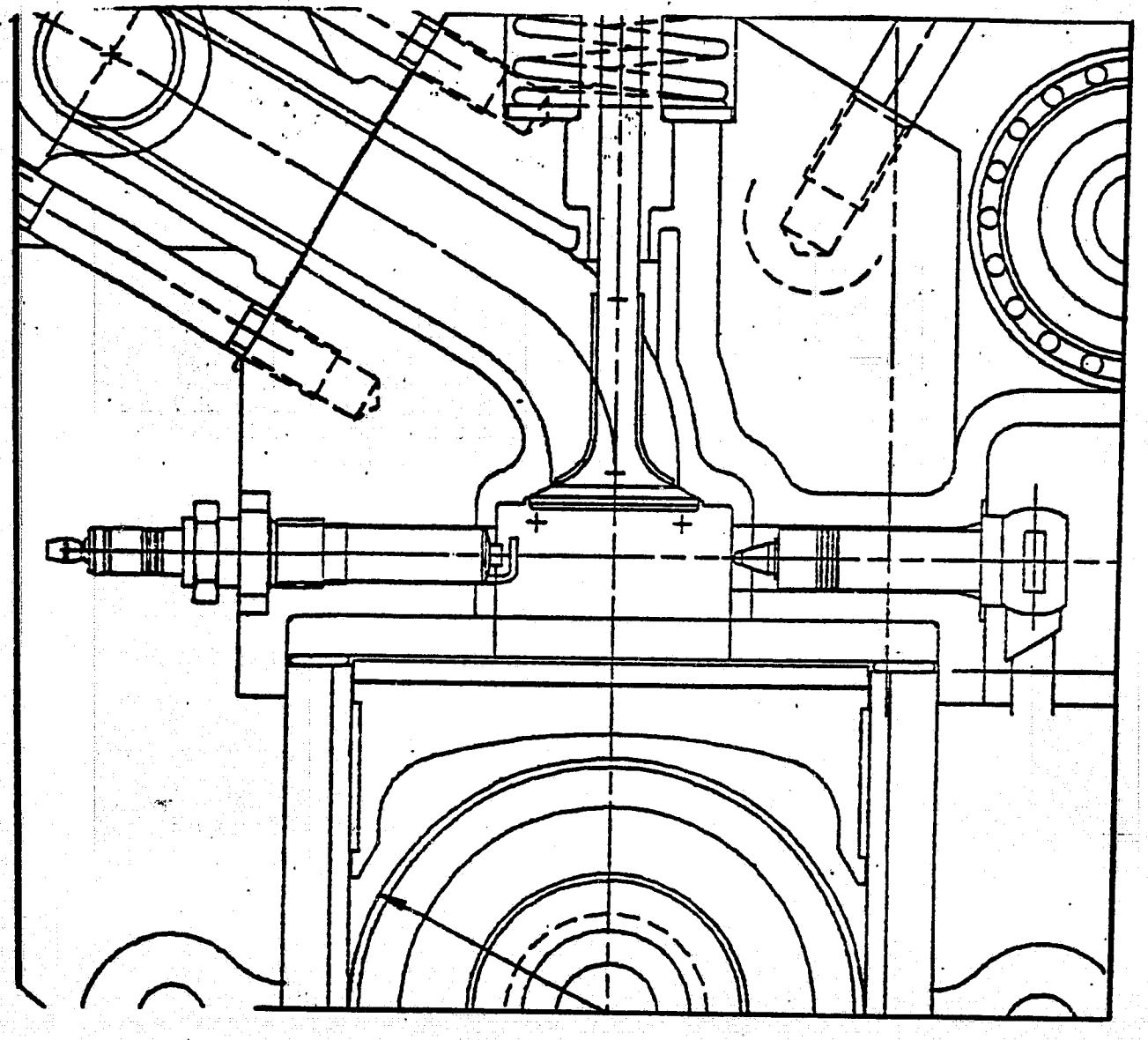

Fig 1 Combustion chamber details

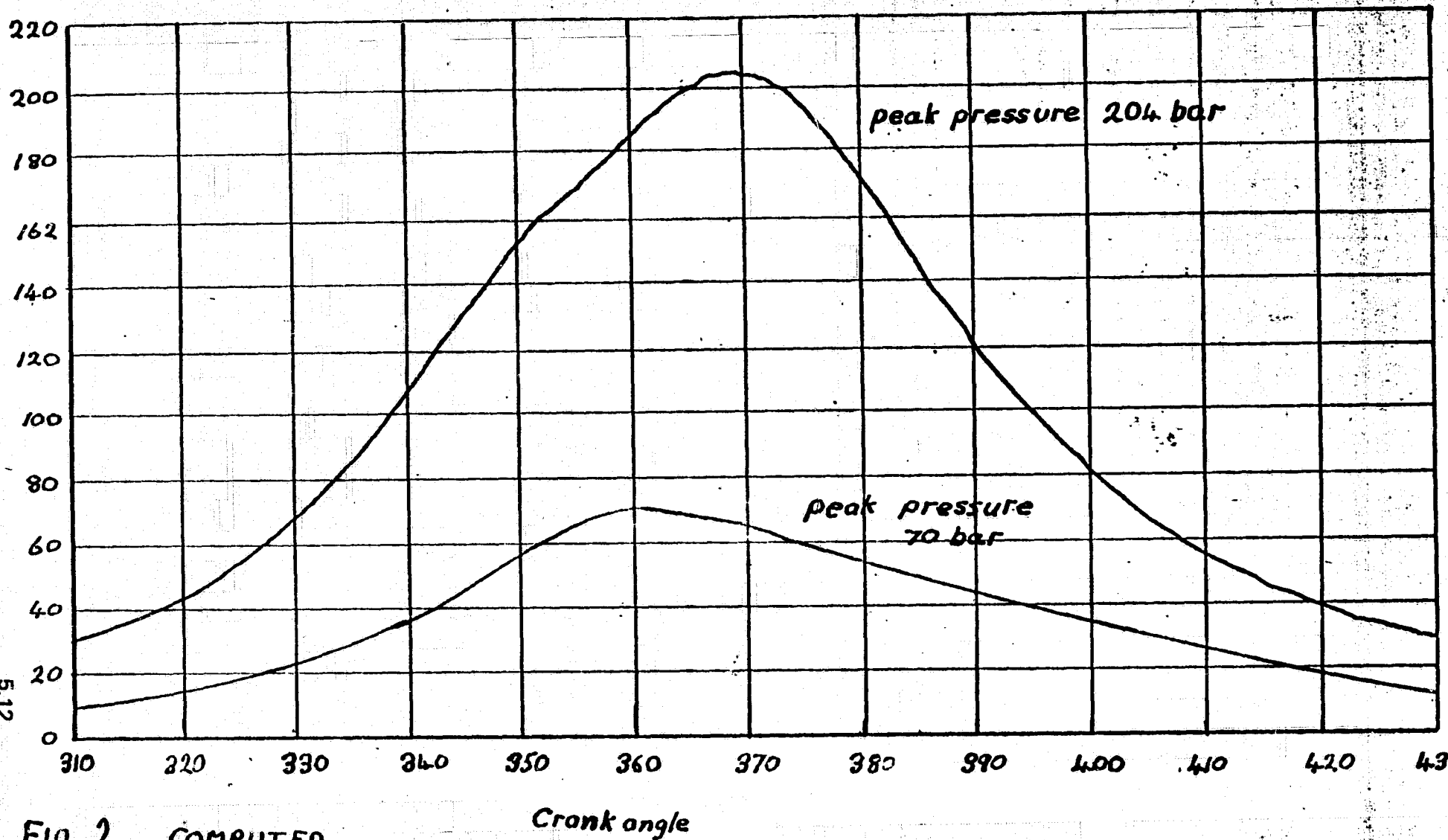

Fig. 2 COMPUTED

CYLINDER

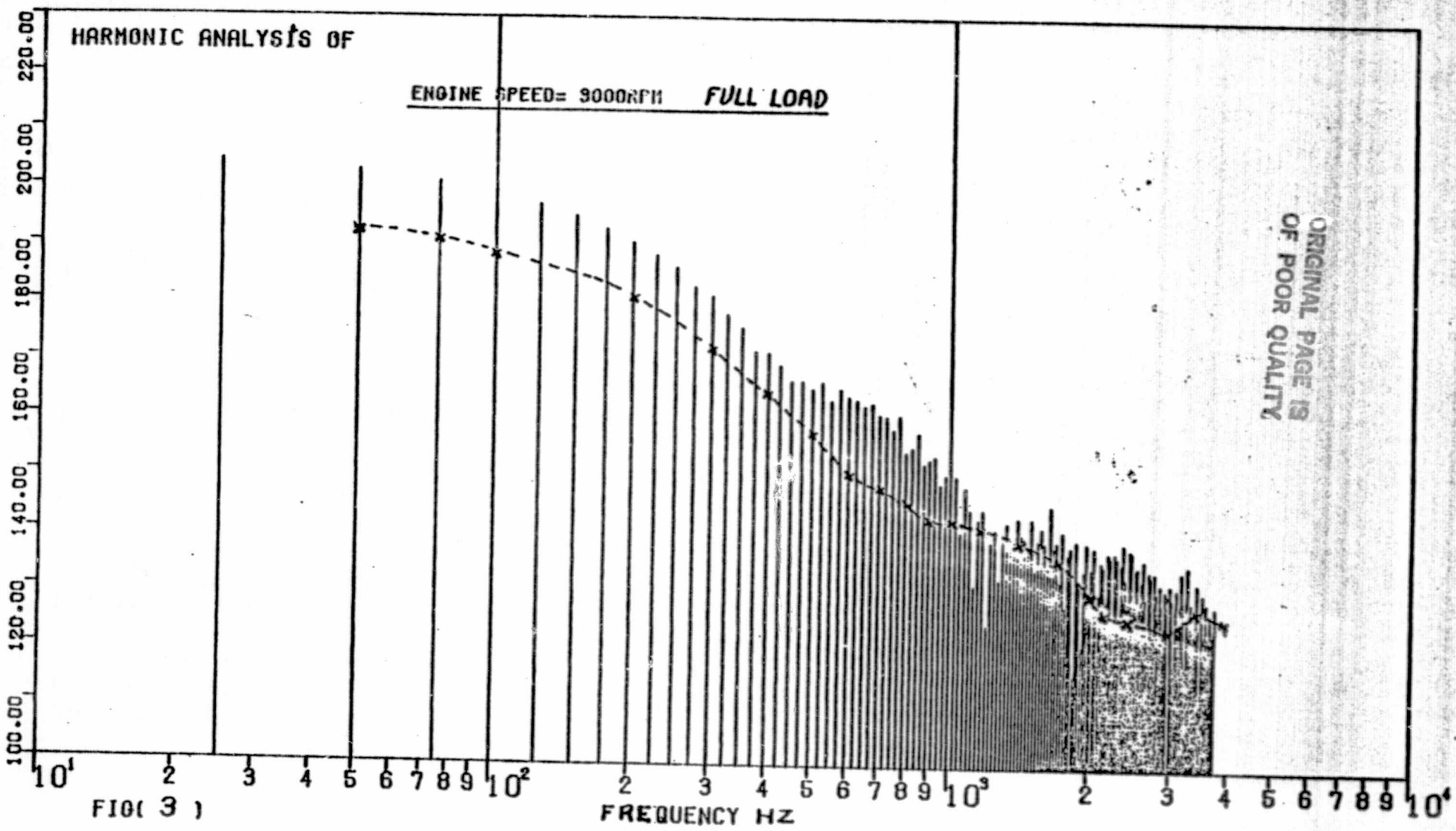

FIG(3)

5.13

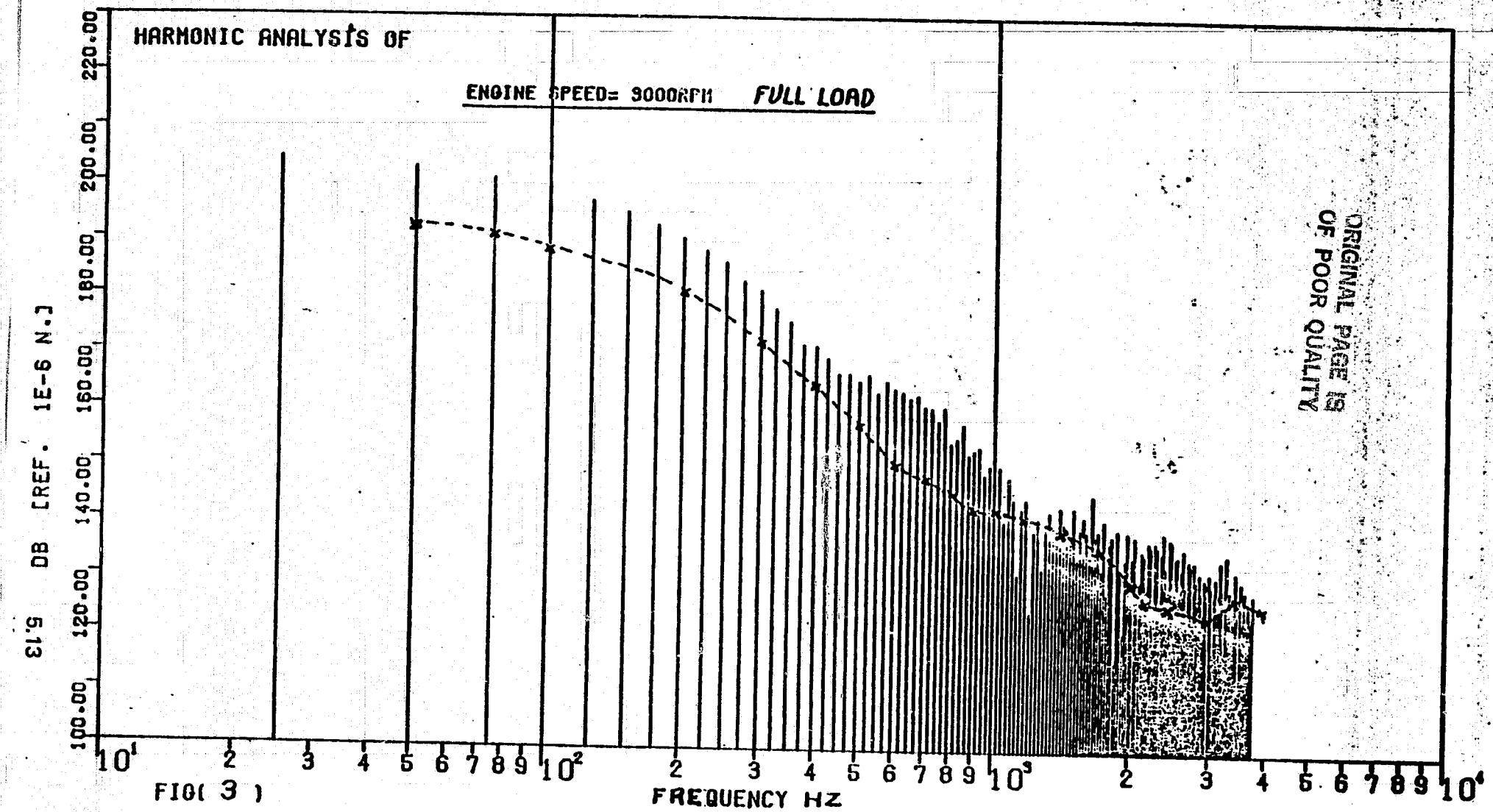

FIG(3)

ORIGINAL PAGE IS
OF POOR QUALITY

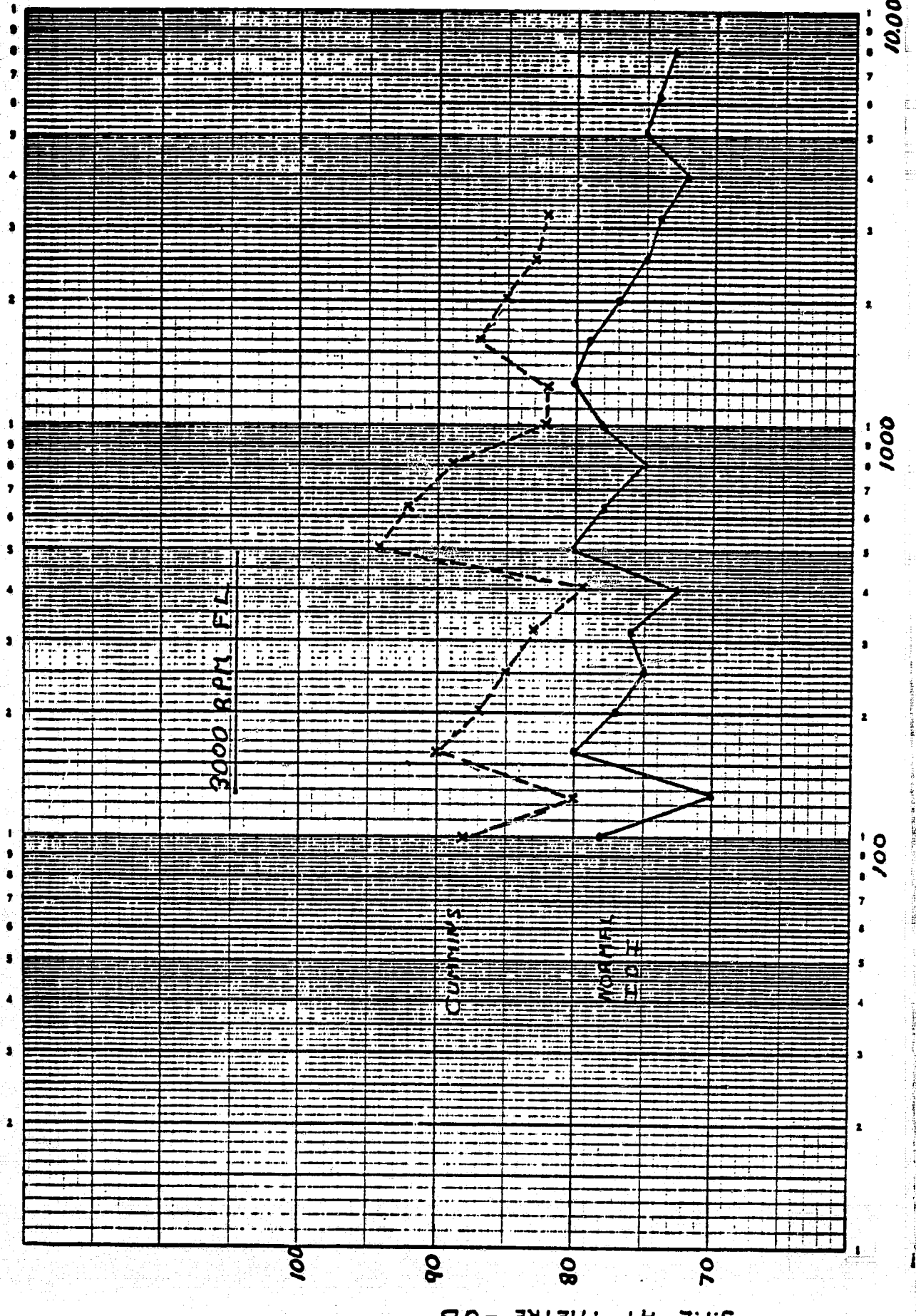

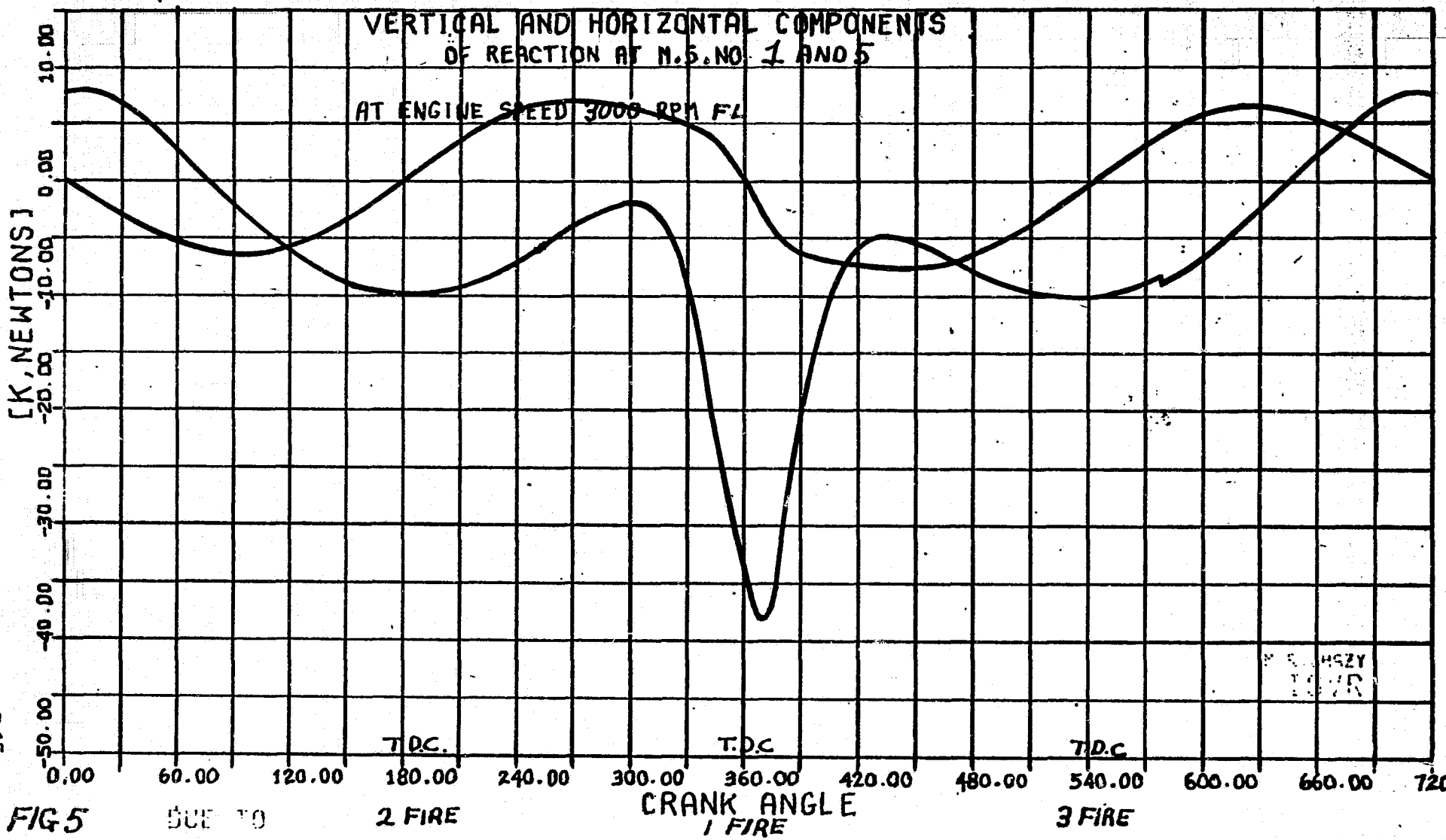

FIG 5 DUE TO

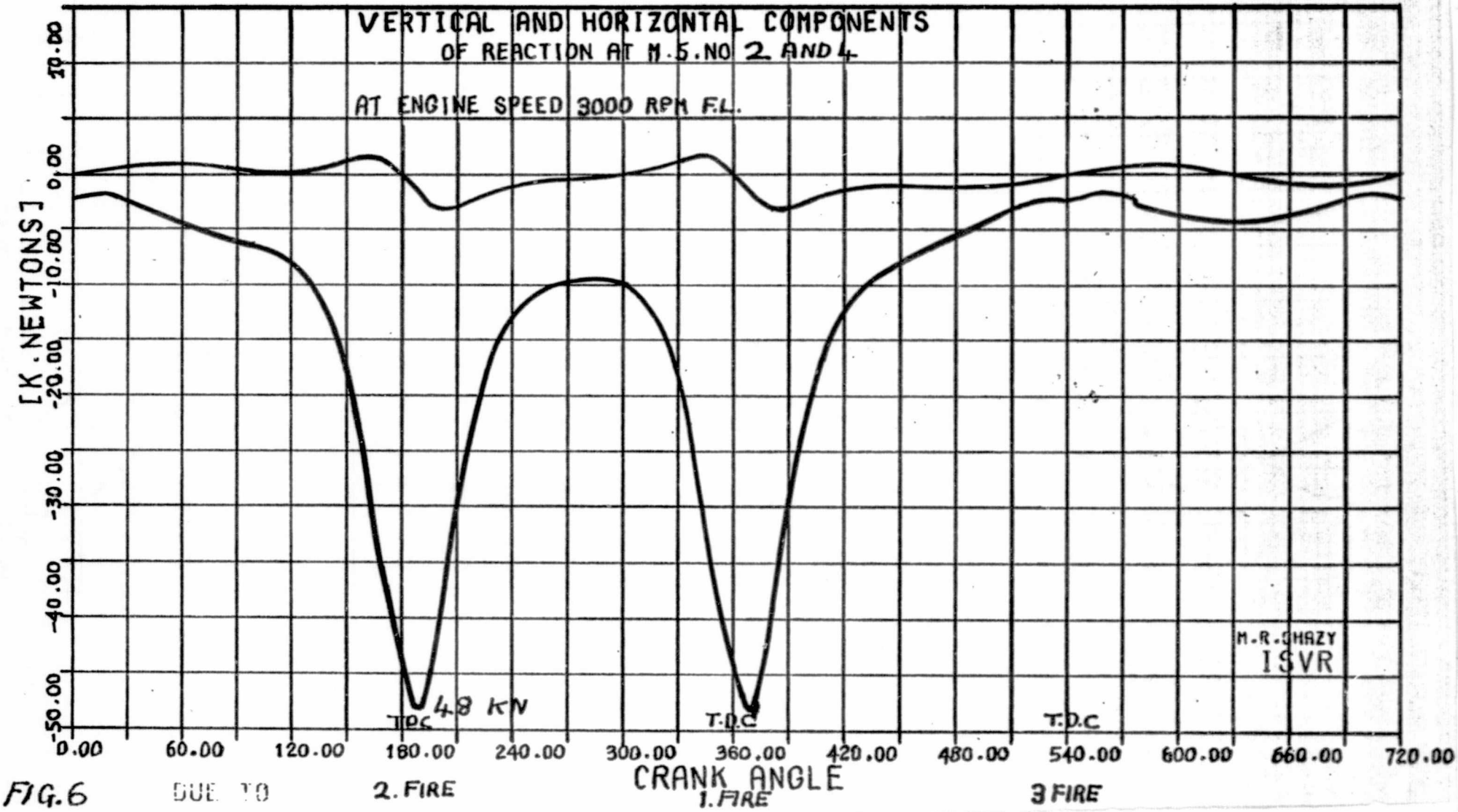

FIG.6 DUE TO

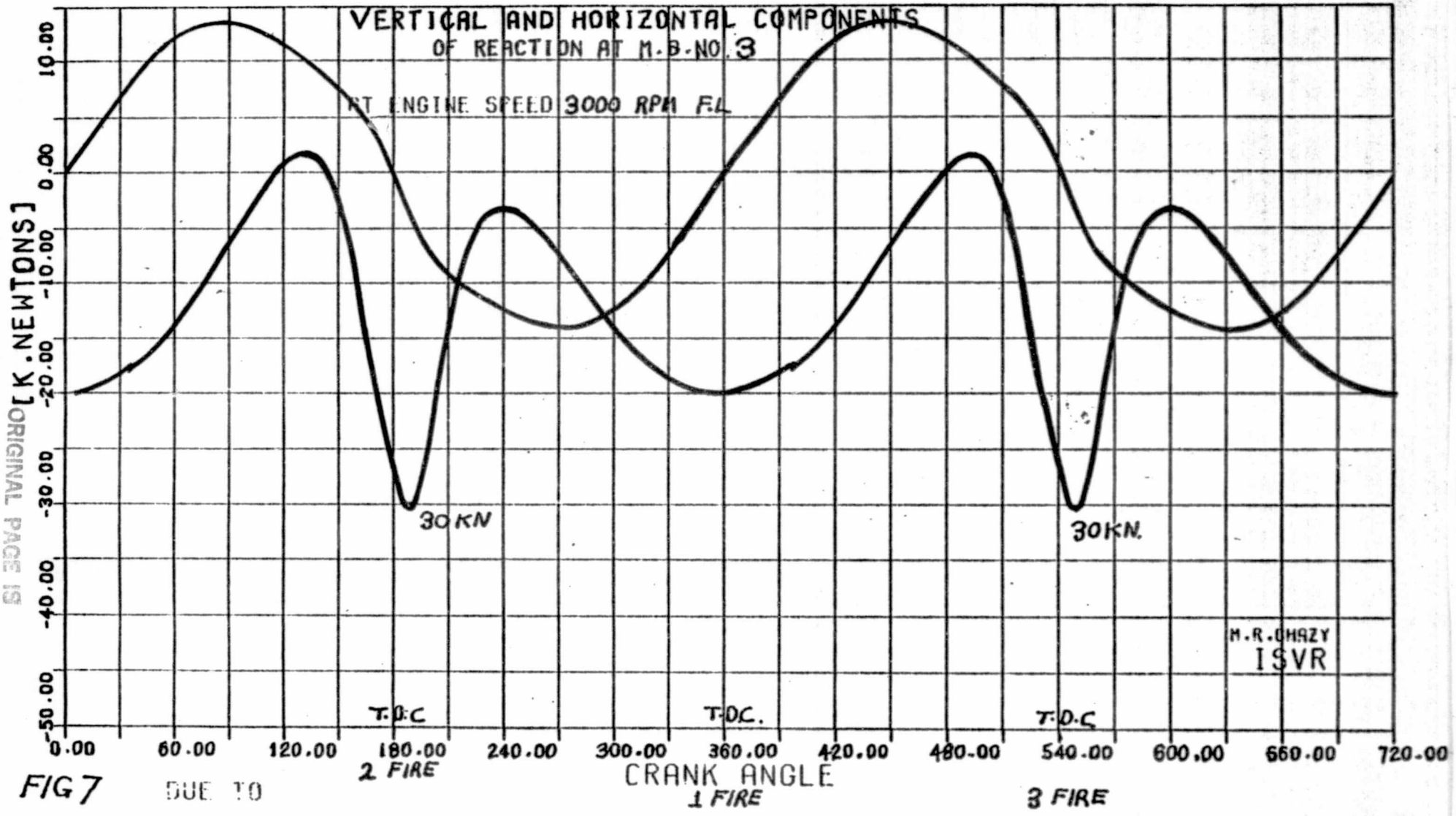

FIG 7 DUE TO

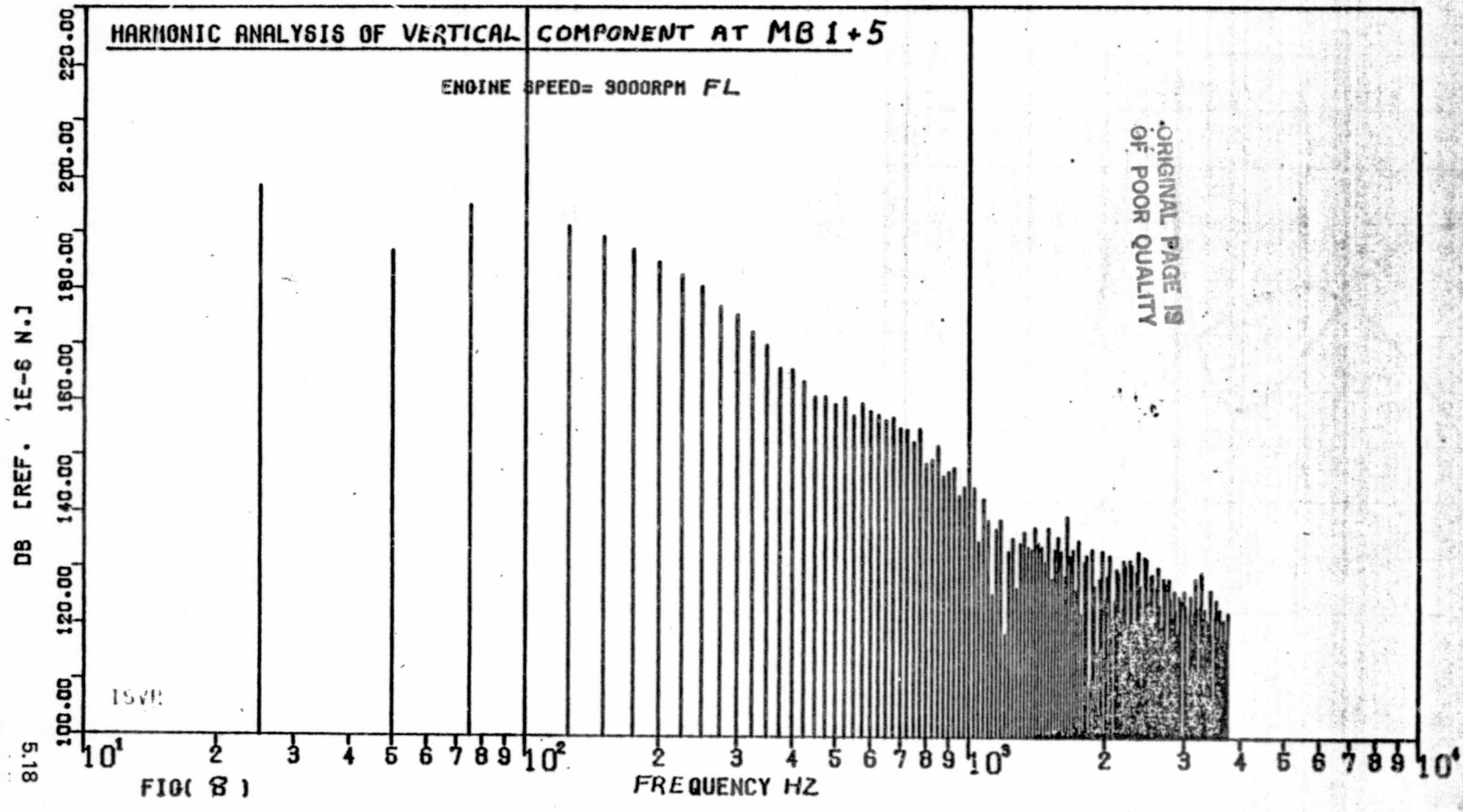

FIG(8)

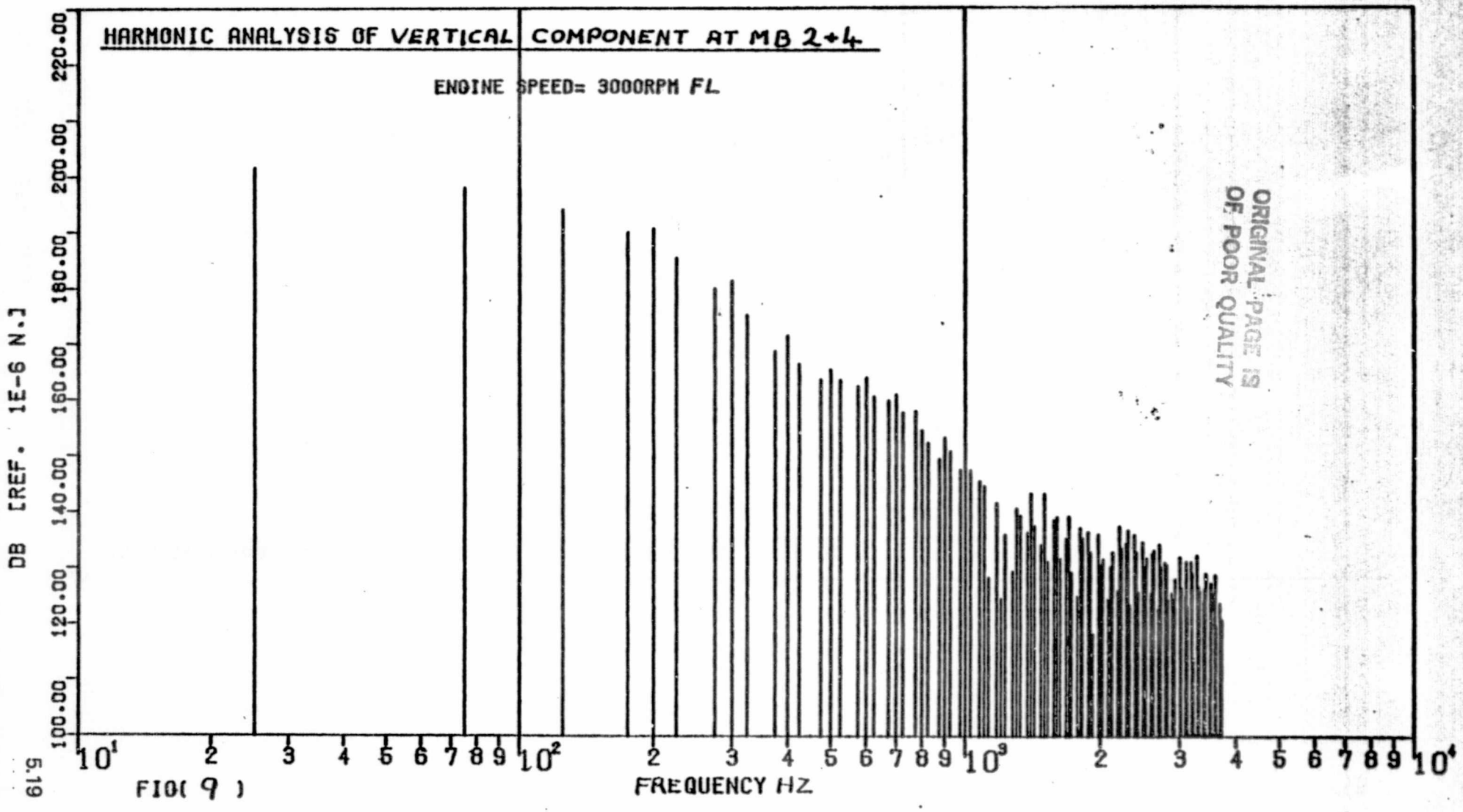

FIG(9)

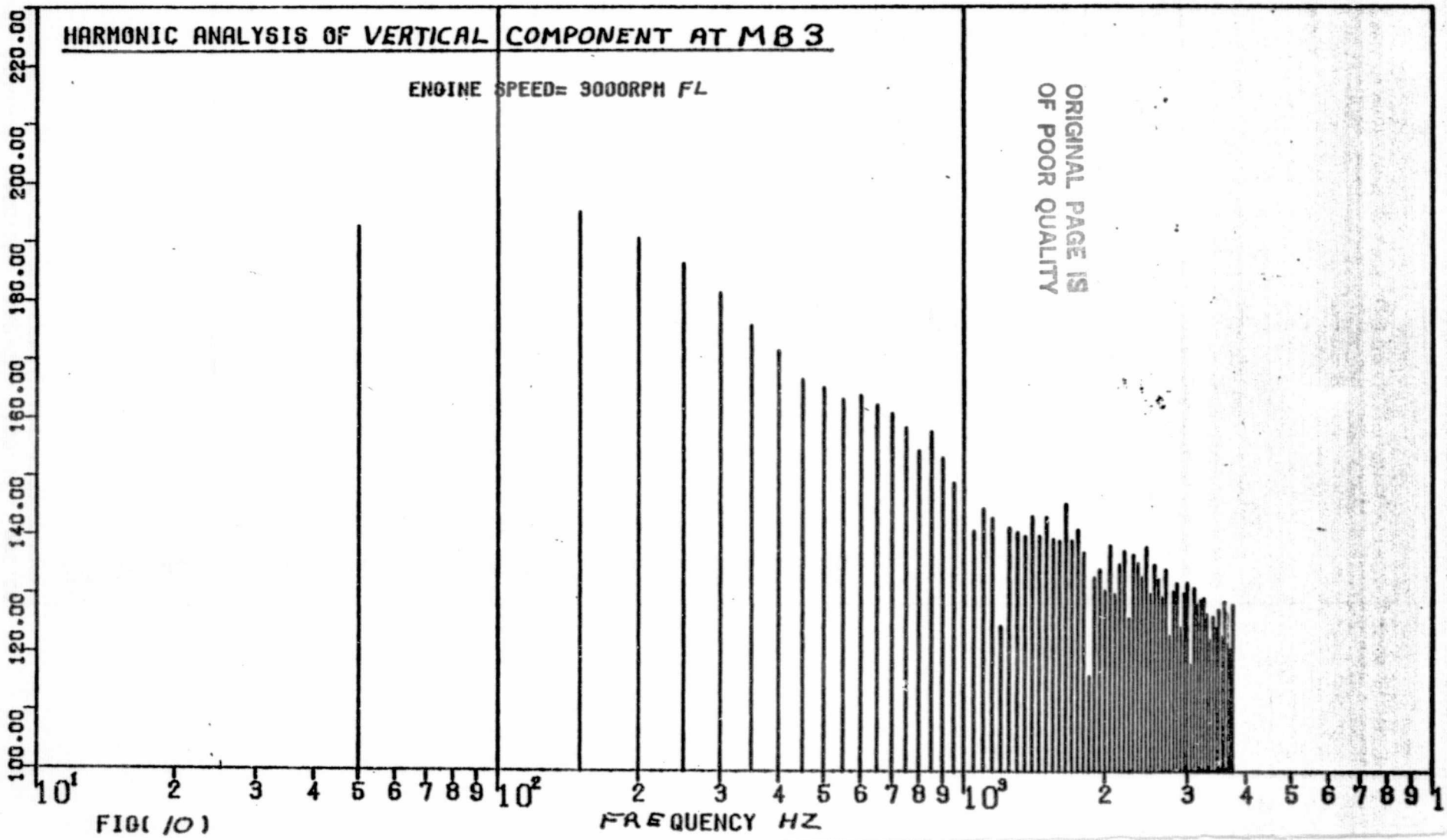
HARMONIC ANALYSIS OF VERTICAL COMPONENT AT MB3
ENGINE SPEED= 3000RPM FL
ORIGINAL PAGE IS
OF POOR QUALITY
DB [REF. 1E-6 N.]
100.00
120.00
140.00
160.00
180.00
200.00
220.00
10¹ 2 3 4 5 6 7 8 9 10² 2 3 4 5 6 7 8 9 10³ 2 3 4 5 6 7 8 9 10⁴
FREQUENCY HZ

FIG(10)

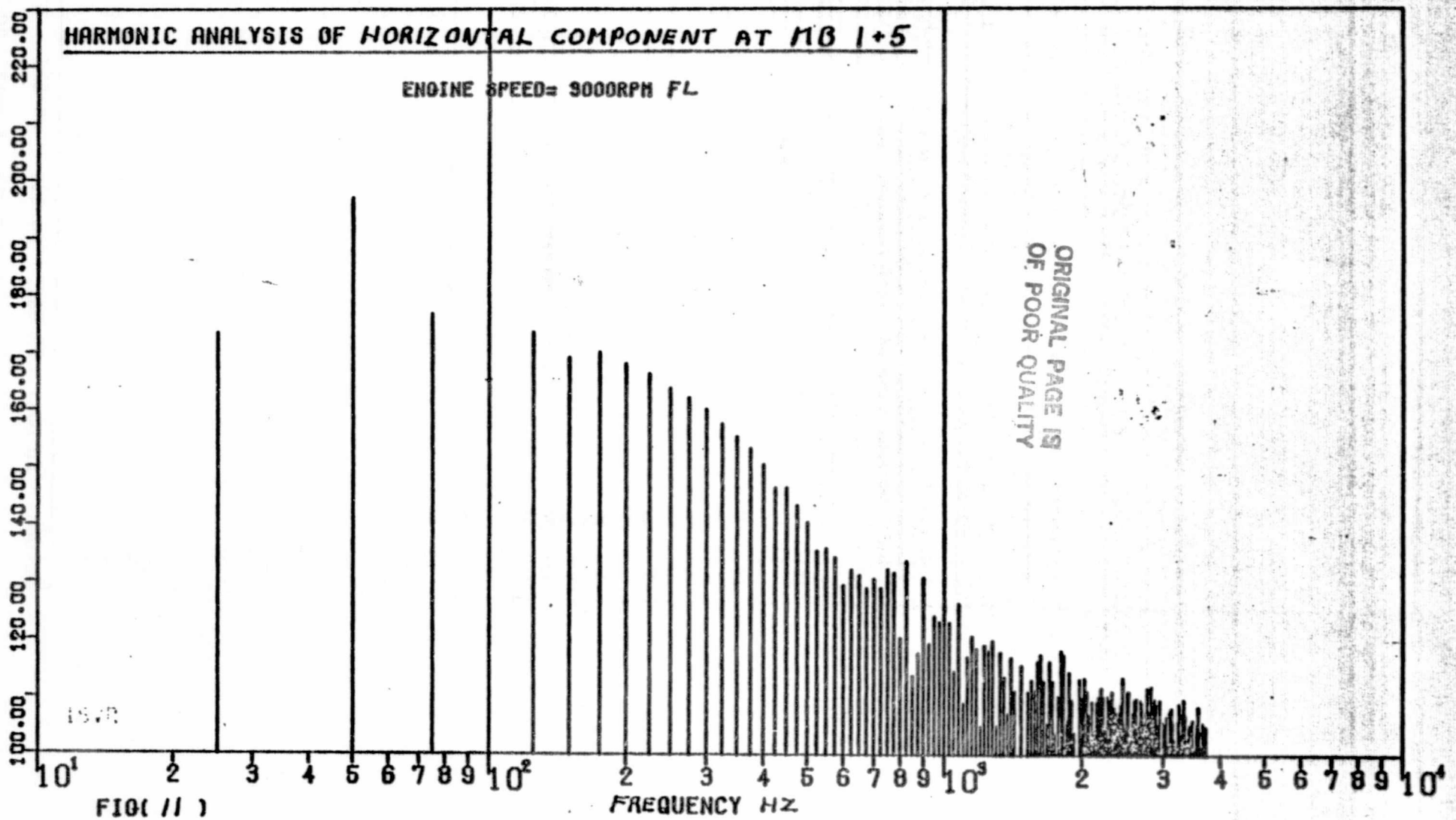

FIG(11)

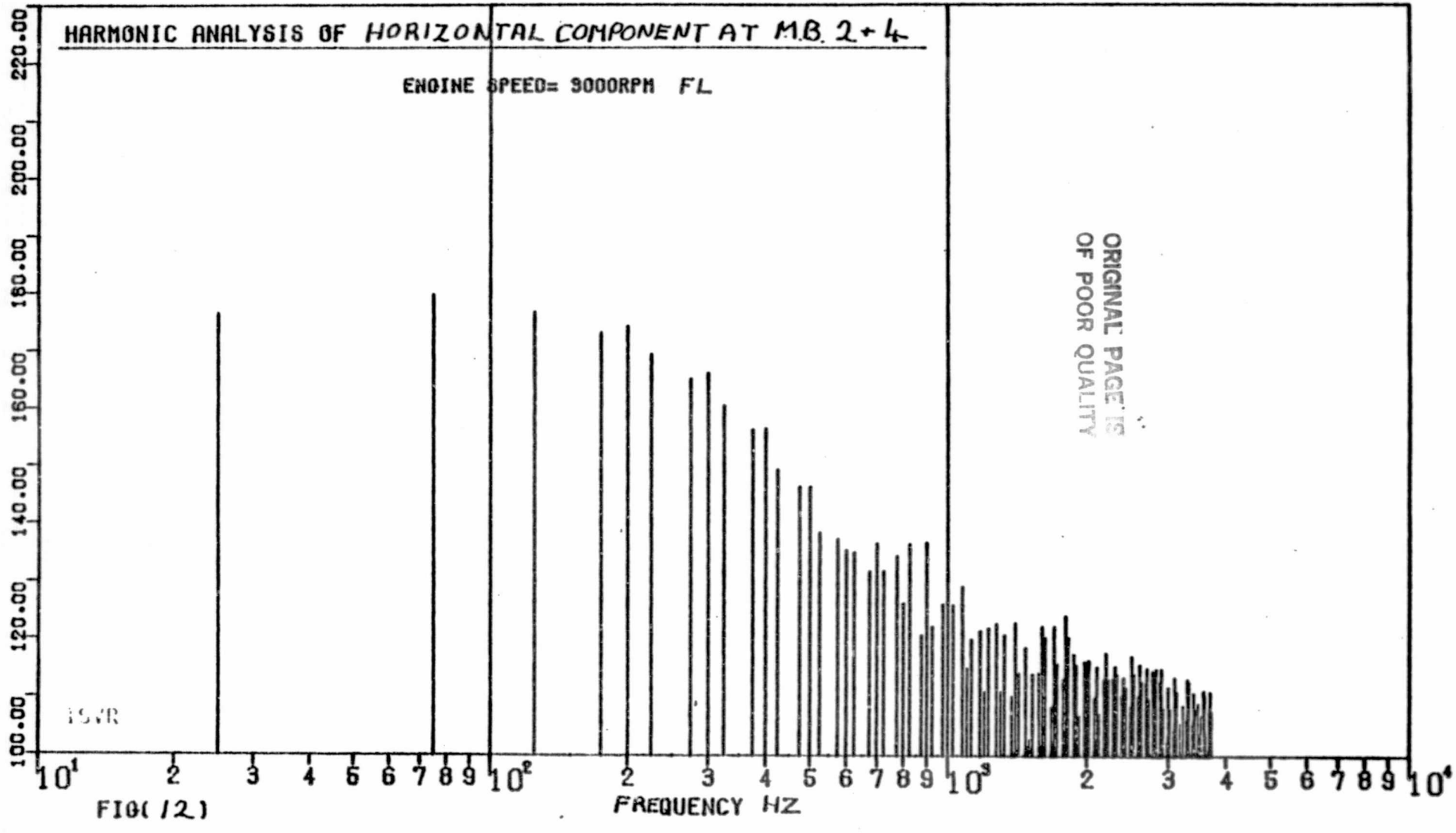

FIG(12)

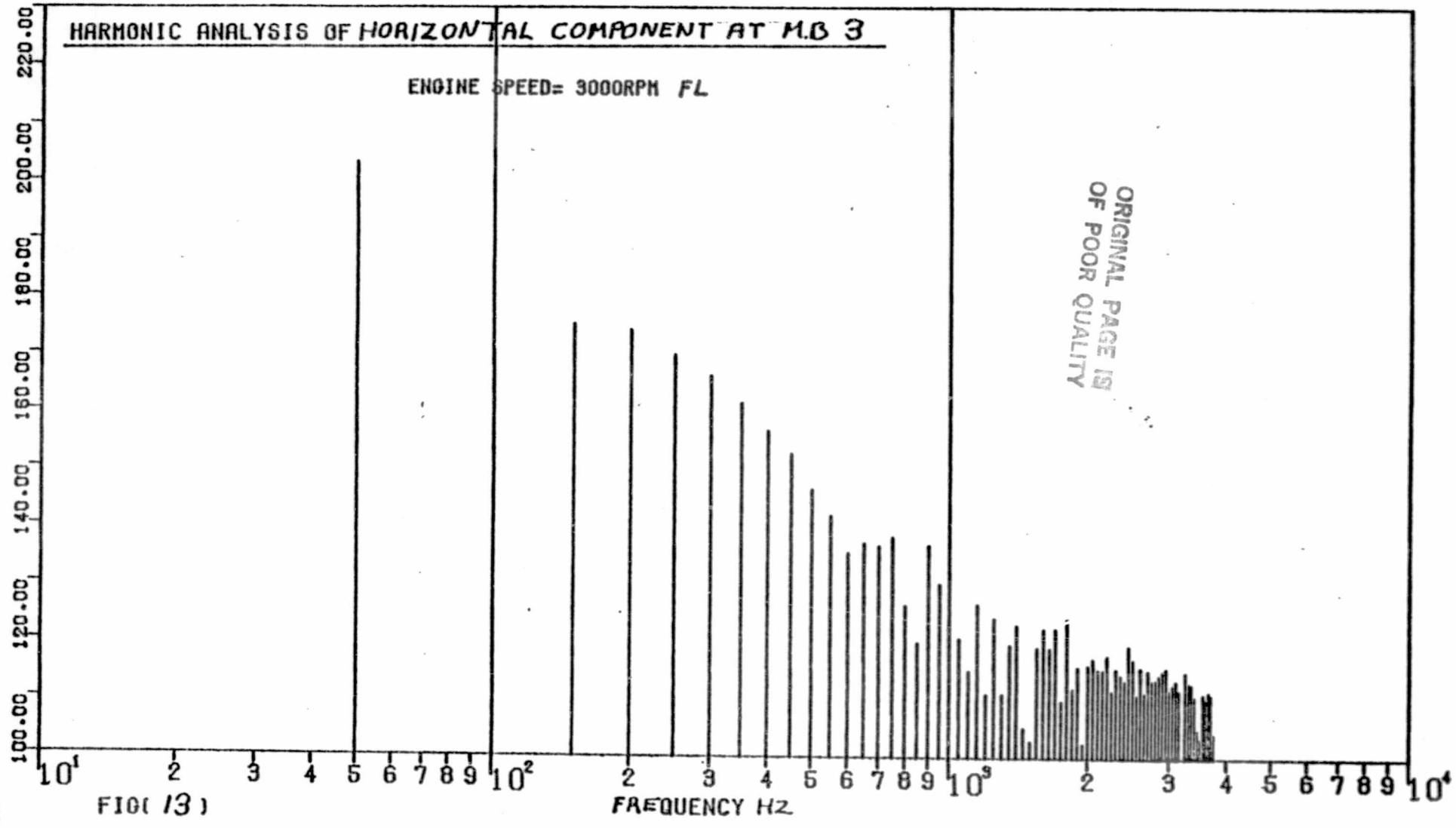

FIG(13)

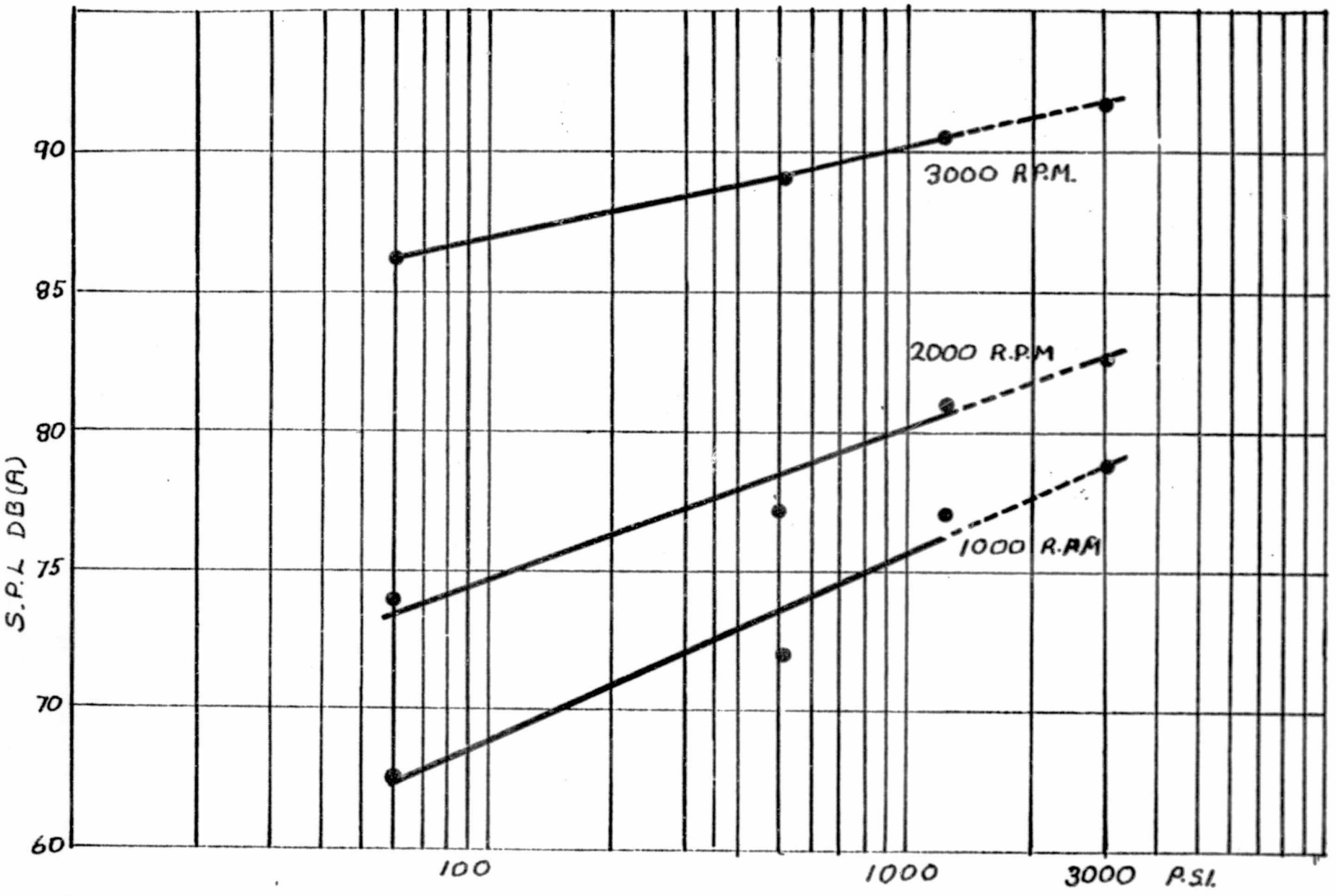

FIG. 11 - EFFECT OF [illegible]

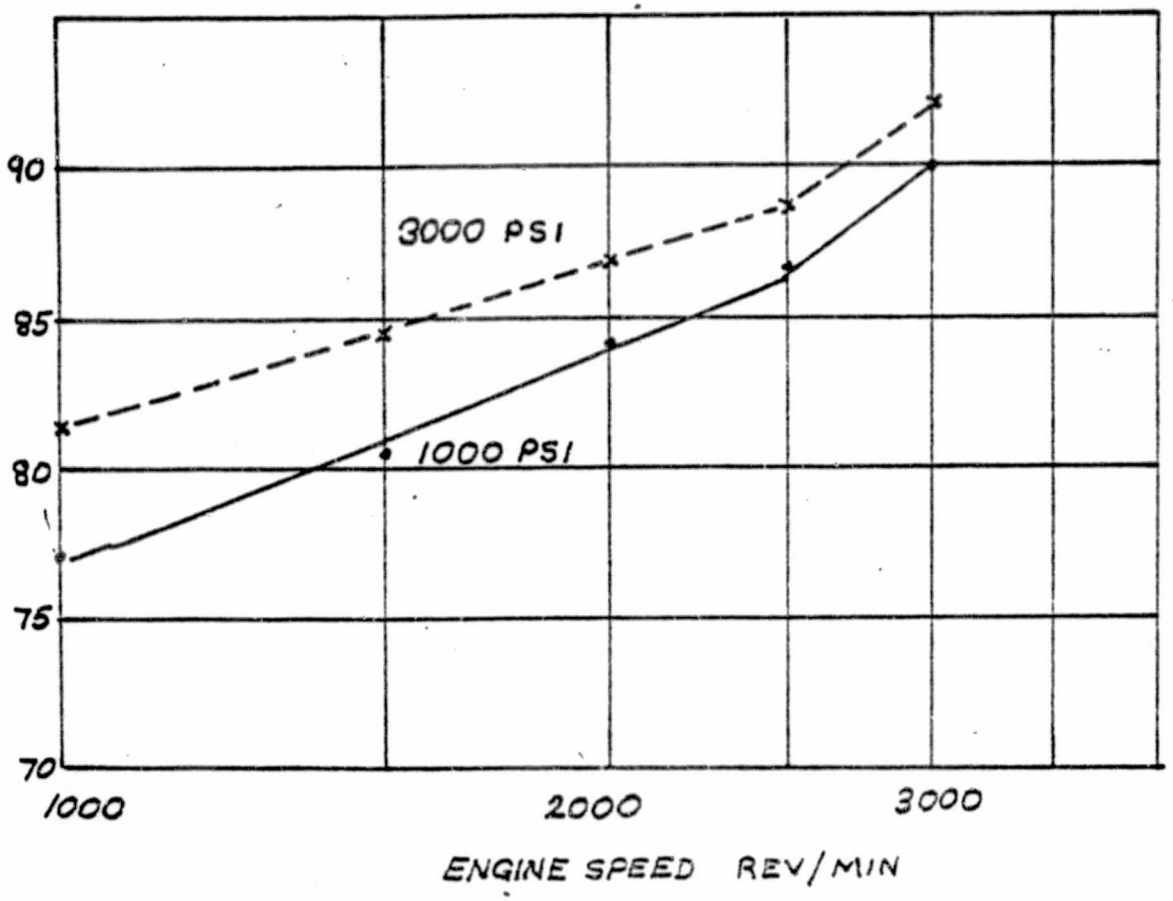

FIG 15 PREDICTED MOTORING NOISE

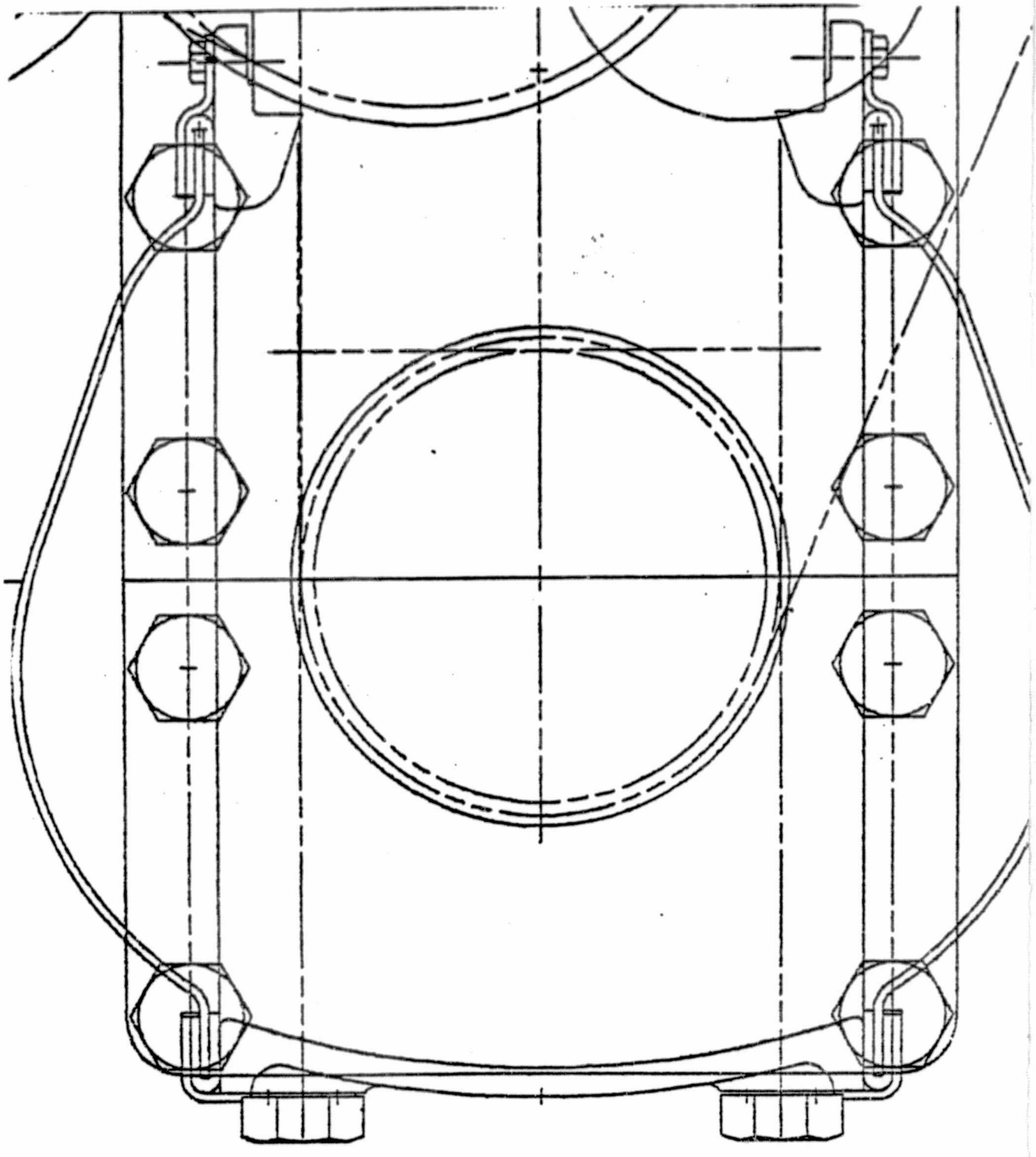

FIG 16 BEAM AND CRANK COVER DETAIL

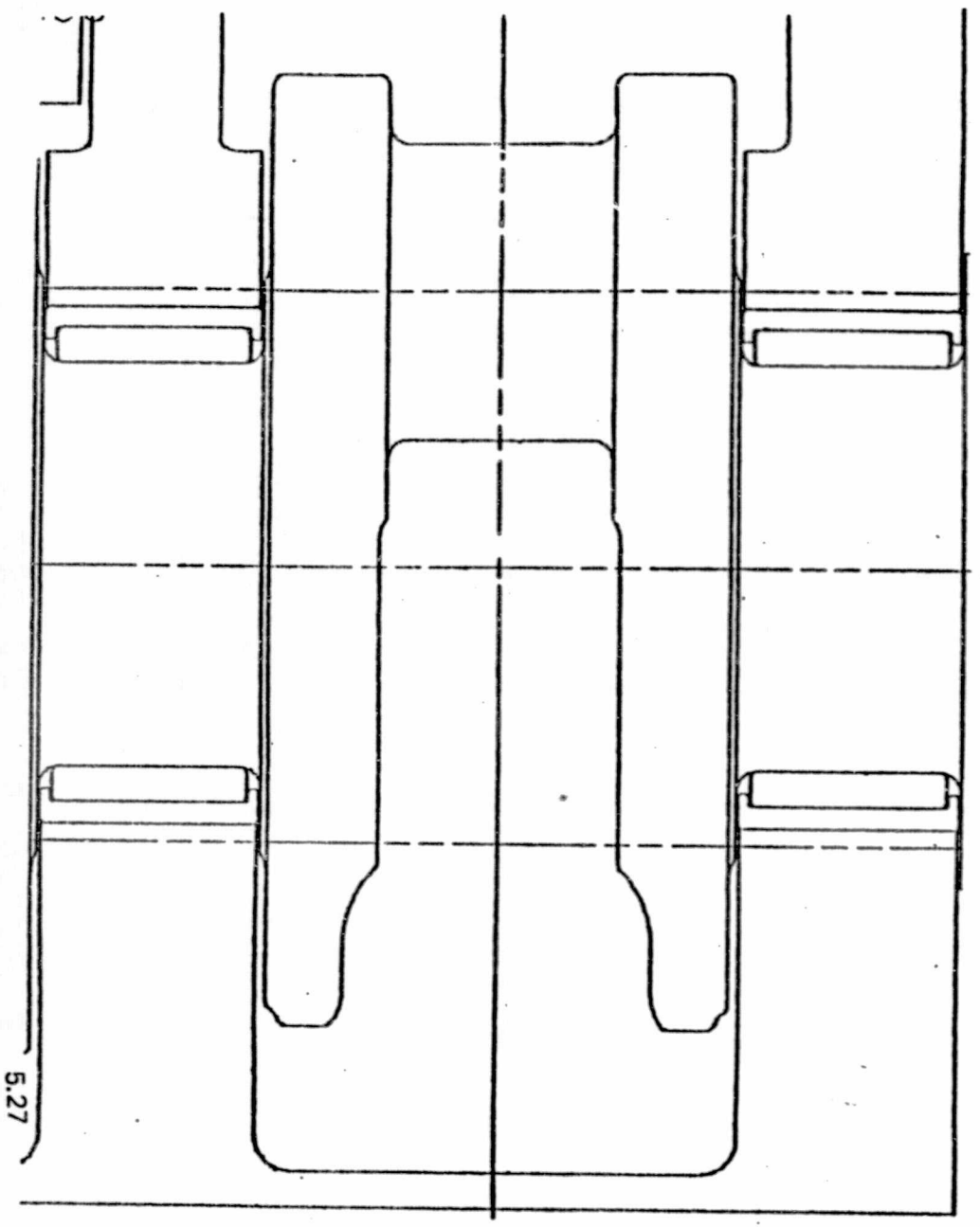

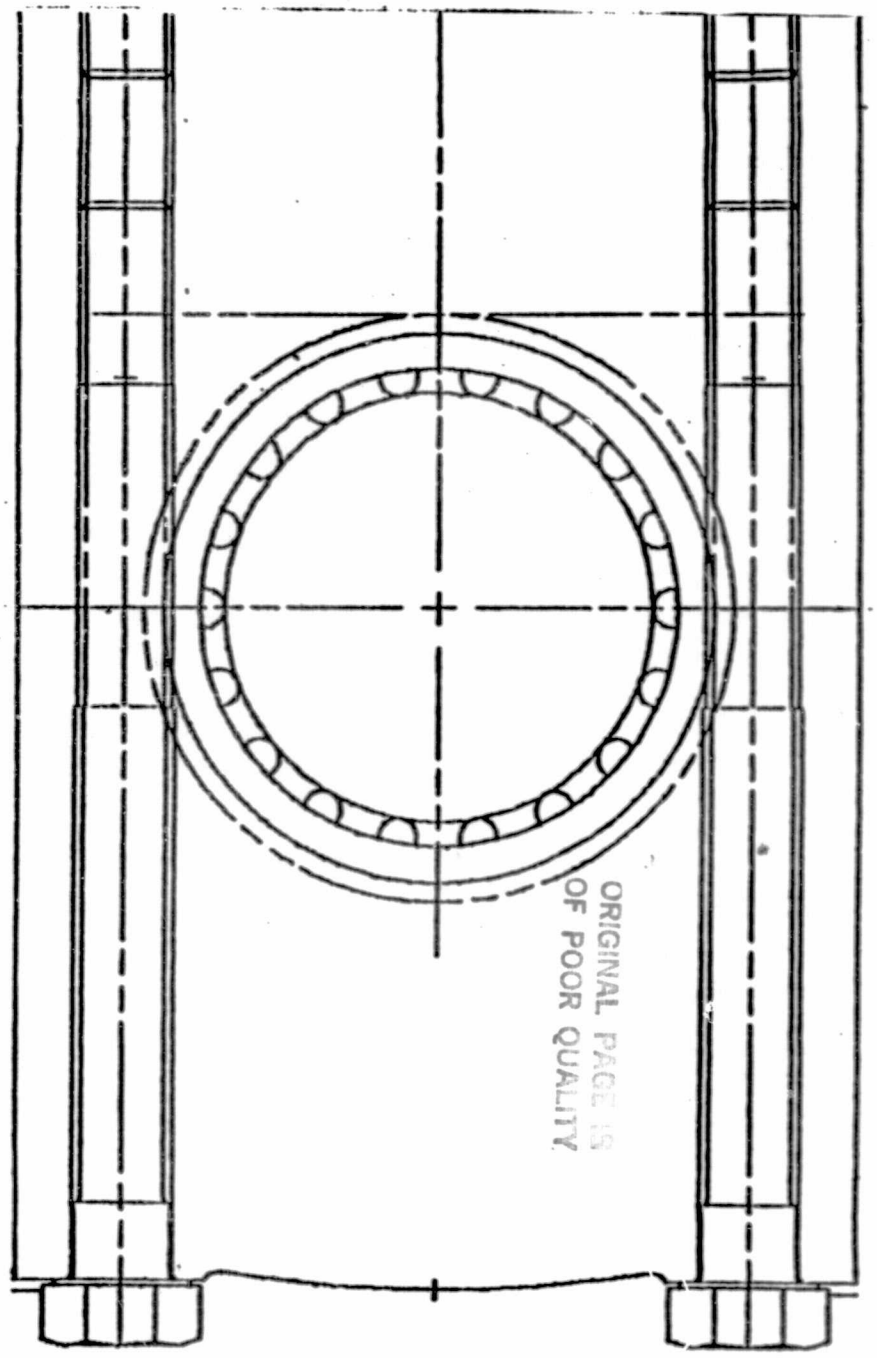

FIG 17 CRANK AND BEARING DETAIL

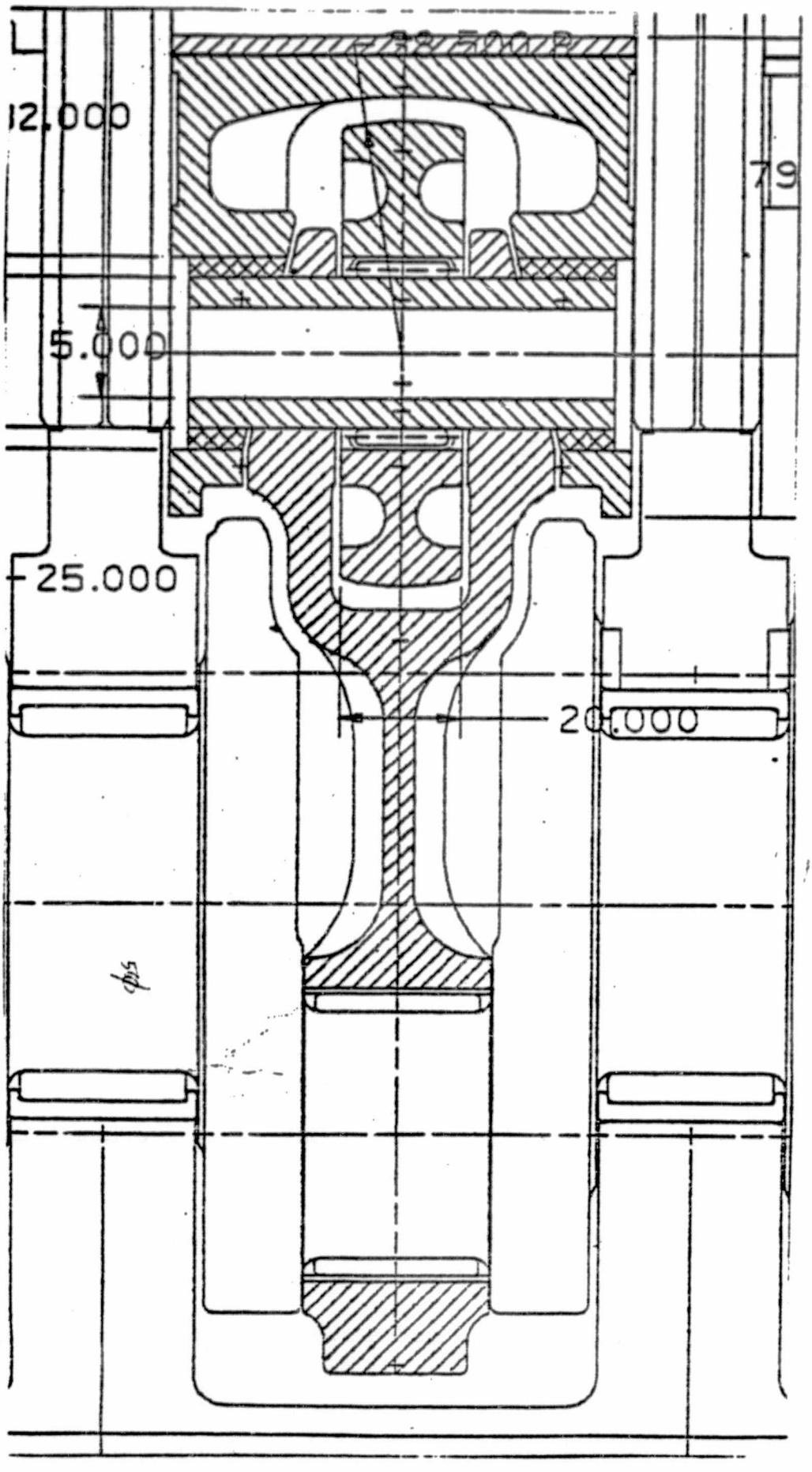

ORIGINAL PAGE IS
OF POOR QUALITY

FIG 18 PISTON AND ROD DETAIL

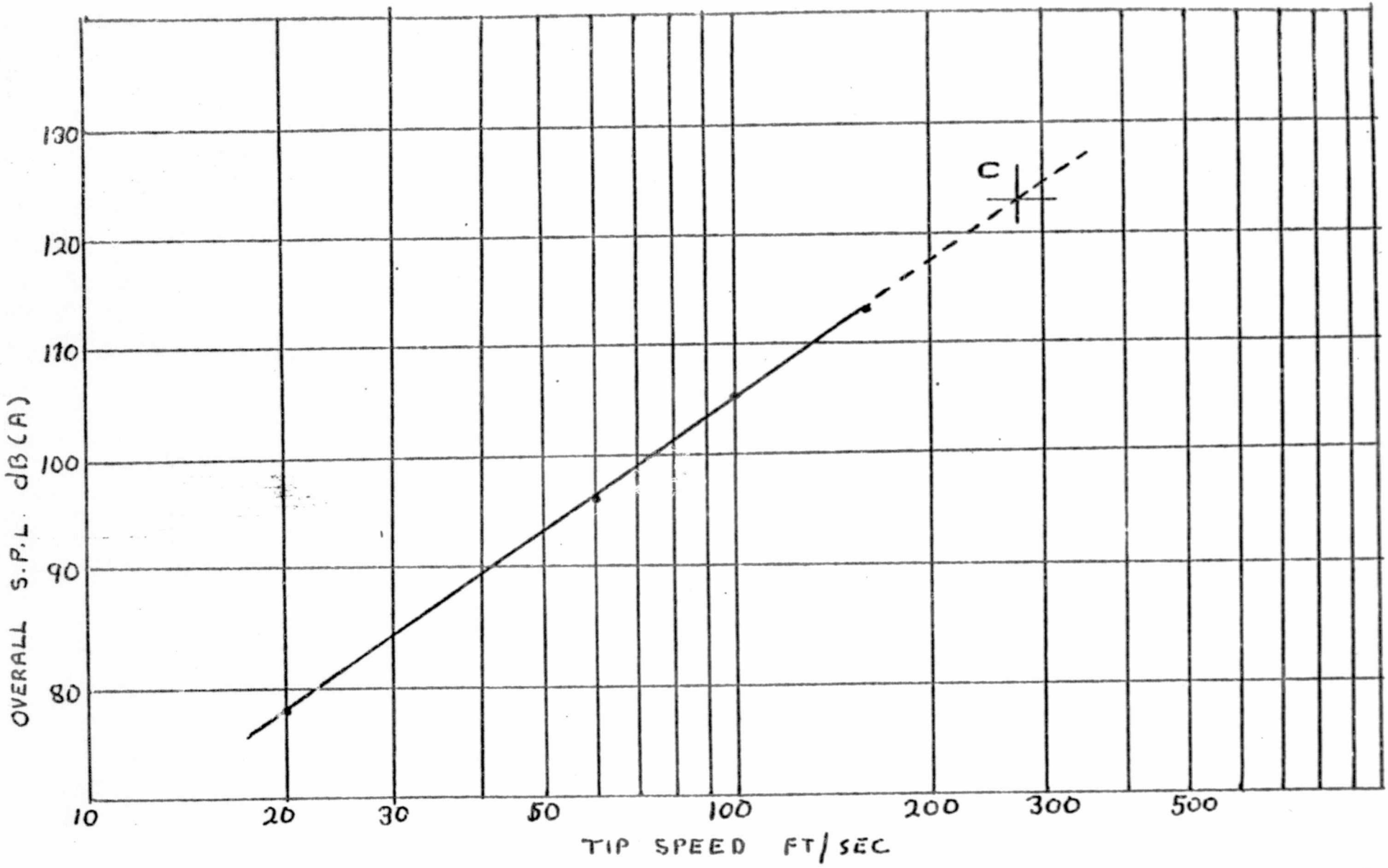

FIG. 19 ROTORY COMPRESSOR INLET NOISE AT 1 METRE

OMIT TO APPENDIX 7

APPENDIX 6

A.A.D. ENGINE LAYOUT DRAWINGS

CUMMINS ENGINE COMPANY
DESIGN STAFF

OUTLINE VIEW-FRONT END

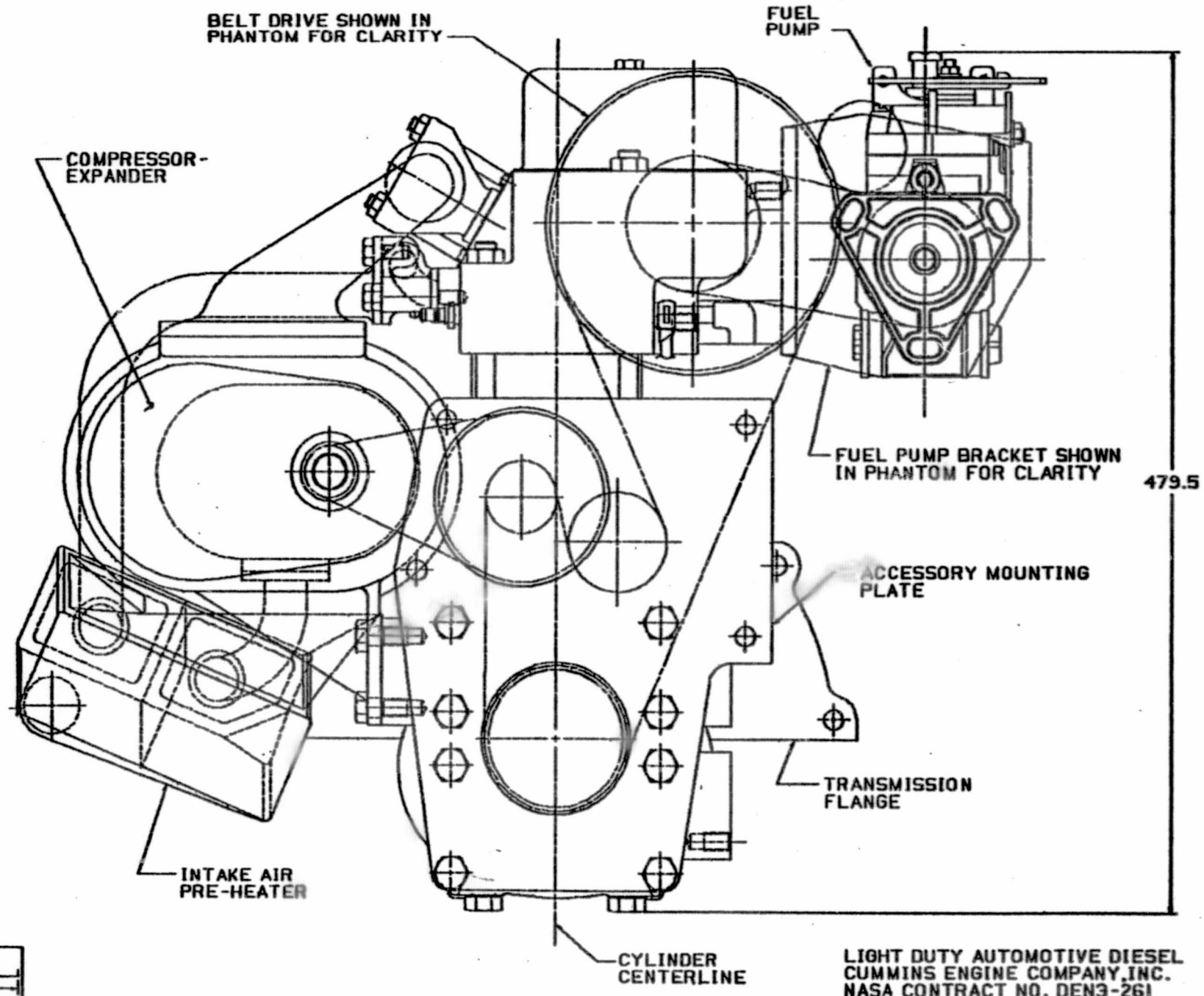

SCALE
100 MM

LIGHT DUTY AUTOMOTIVE DIESEL
CUMMINS ENGINE COMPANY,INC.
NASA CONTRACT NO. DEN3-261
6-21-83 -C.A.D.D.- FIGURE NO. 1.

EXPANDER SIDE OUTLINE VIEW

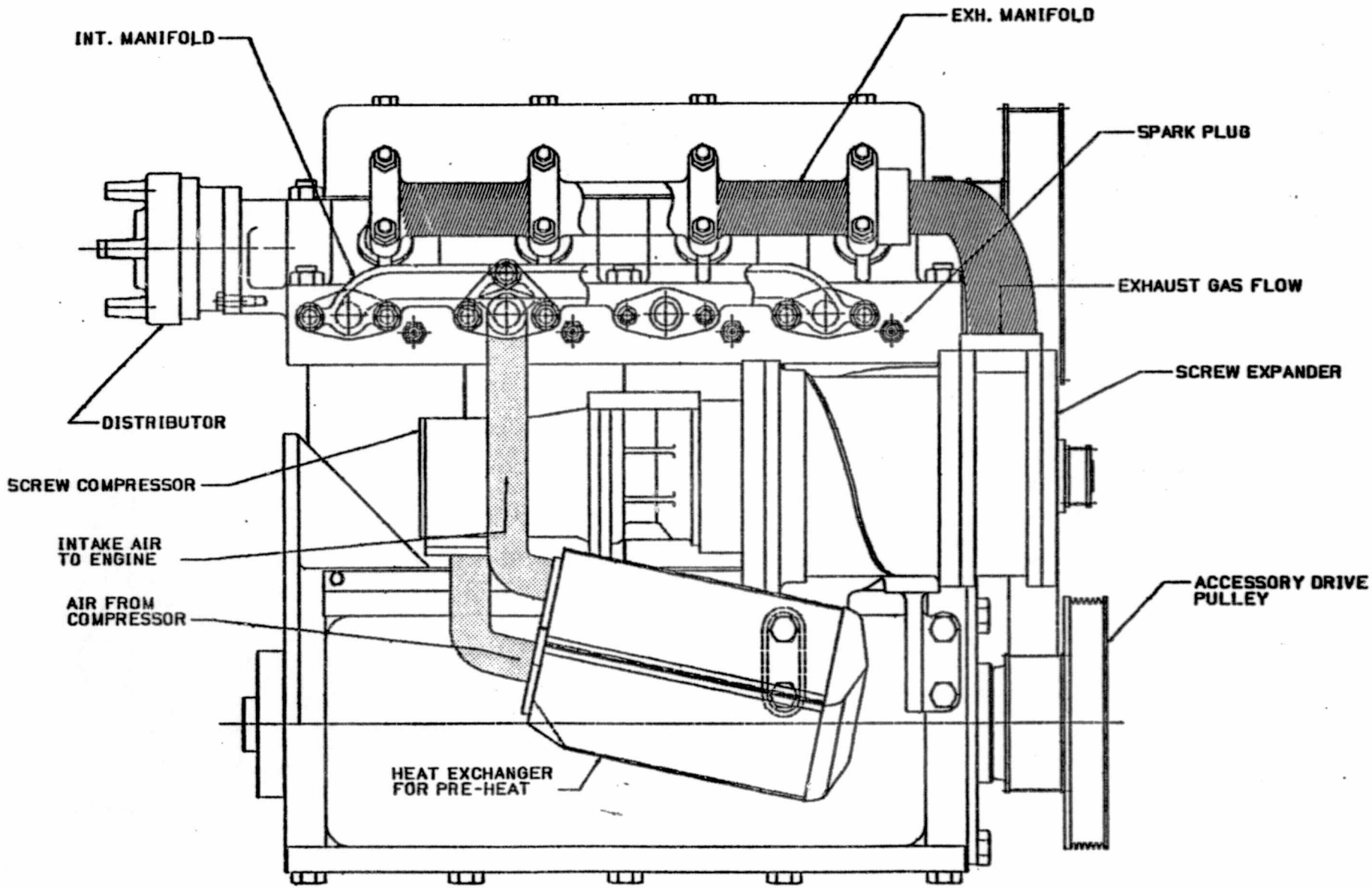

LIGHT DUTY AUTOMOTIVE DIESEL
CUMMINS ENGINE COMPANY,INC.
NASA CONTRACT NO. DEN3-261
6-17-83 -C.A.D.D.- FIGURE NO. 2.

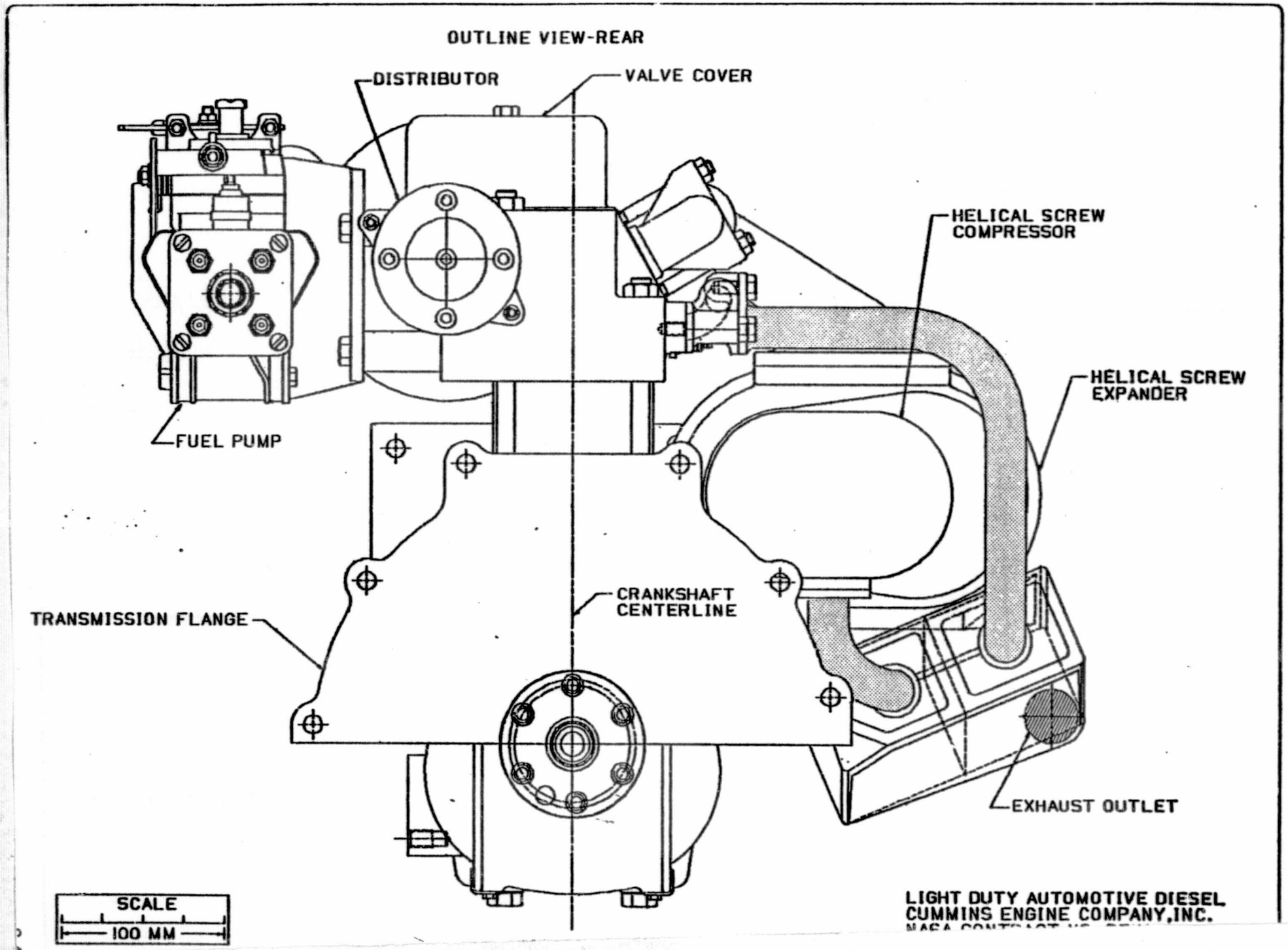
OUTLINE VIEW-REAR
DISTRIBUTOR
VALVE COVER
HELICAL SCREW COMPRESSOR
HELICAL SCREW EXPANDER
FUEL PUMP
CRANKSHAFT CENTERLINE
TRANSMISSION FLANGE
EXHAUST OUTLET
SCALE
100 MM
LIGHT DUTY AUTOMOTIVE DIESEL
CUMMINS ENGINE COMPANY, INC.

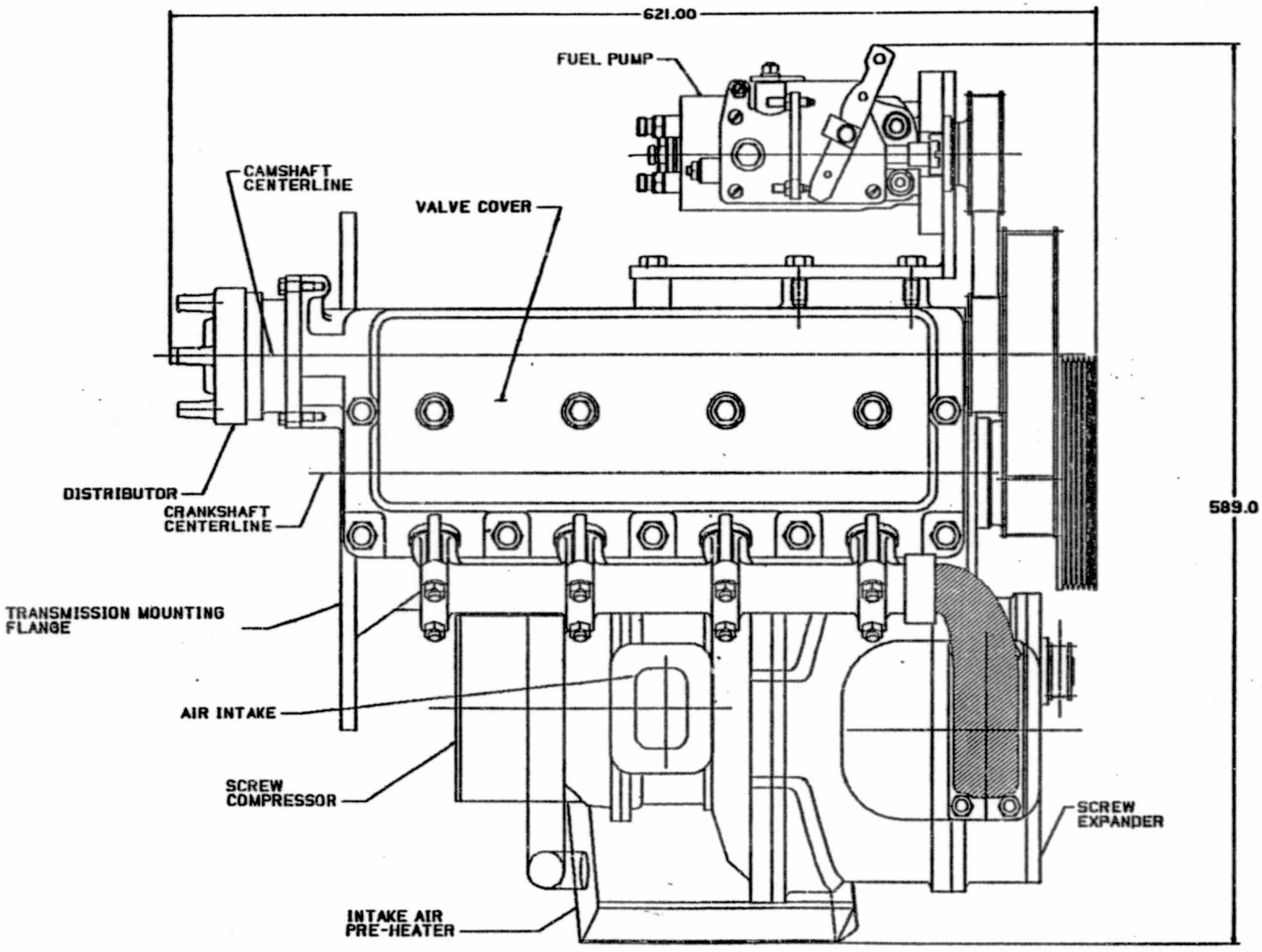

LIGHT DUTY AUTOMOTIVE DIESEL
CUMMINS ENGINE COMPANY, INC.
NASA CONTRACT NO. DEN3-261
6-21-83 -C.A.O.D.- FIGURE NO. 4.

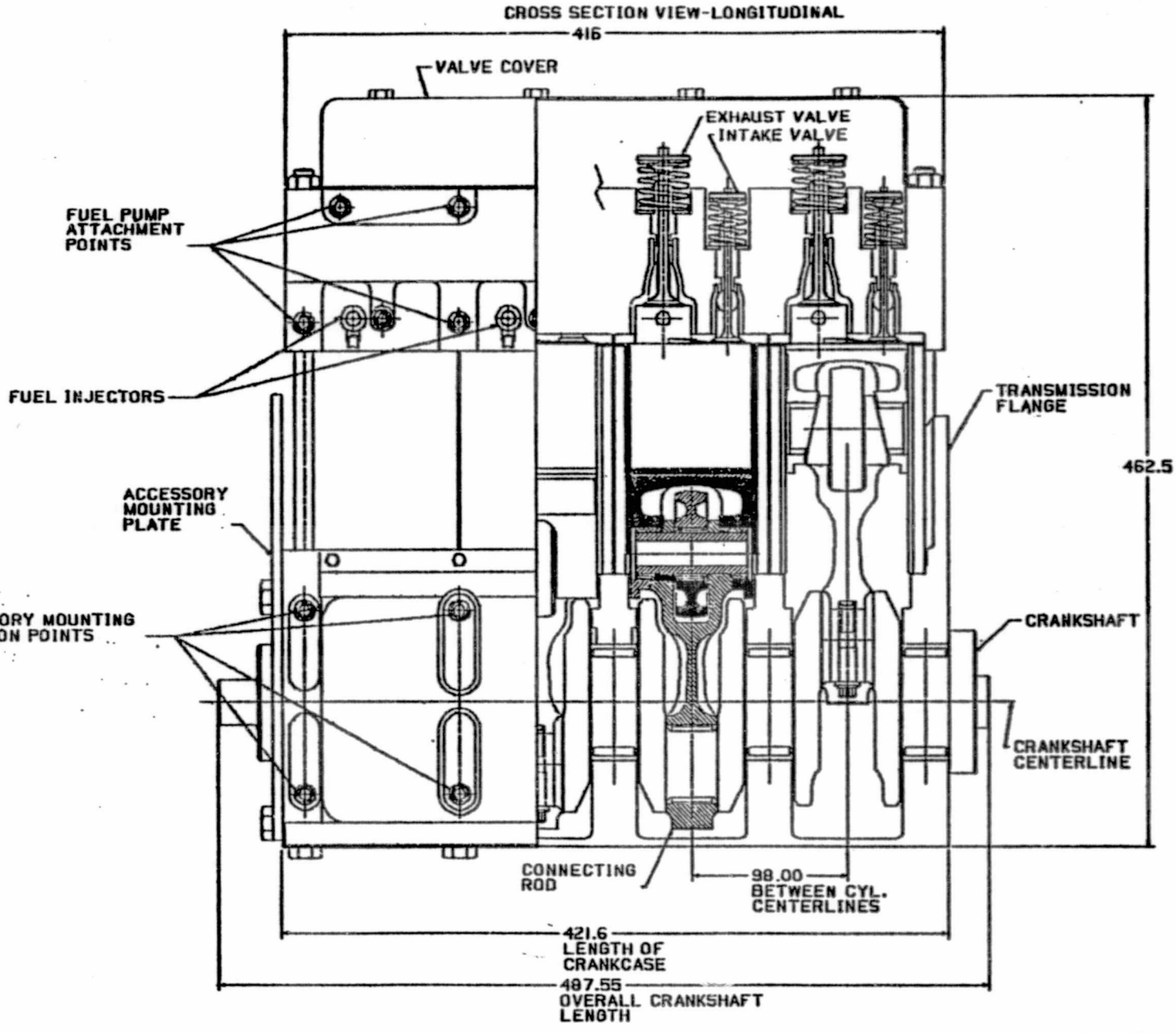

ORIGINAL PAGE IS
OF POOR QUALITY

LIGHT DUTY AUTOMOTIVE DIESEL
CUMMINS ENGINE COMPANY, INC.
NASA CONTRACT NO. DEN3-26

CROSS SECTION VIEW-TRANSVERSE
-EXHAUST VALVE
-CONNECTING ROD

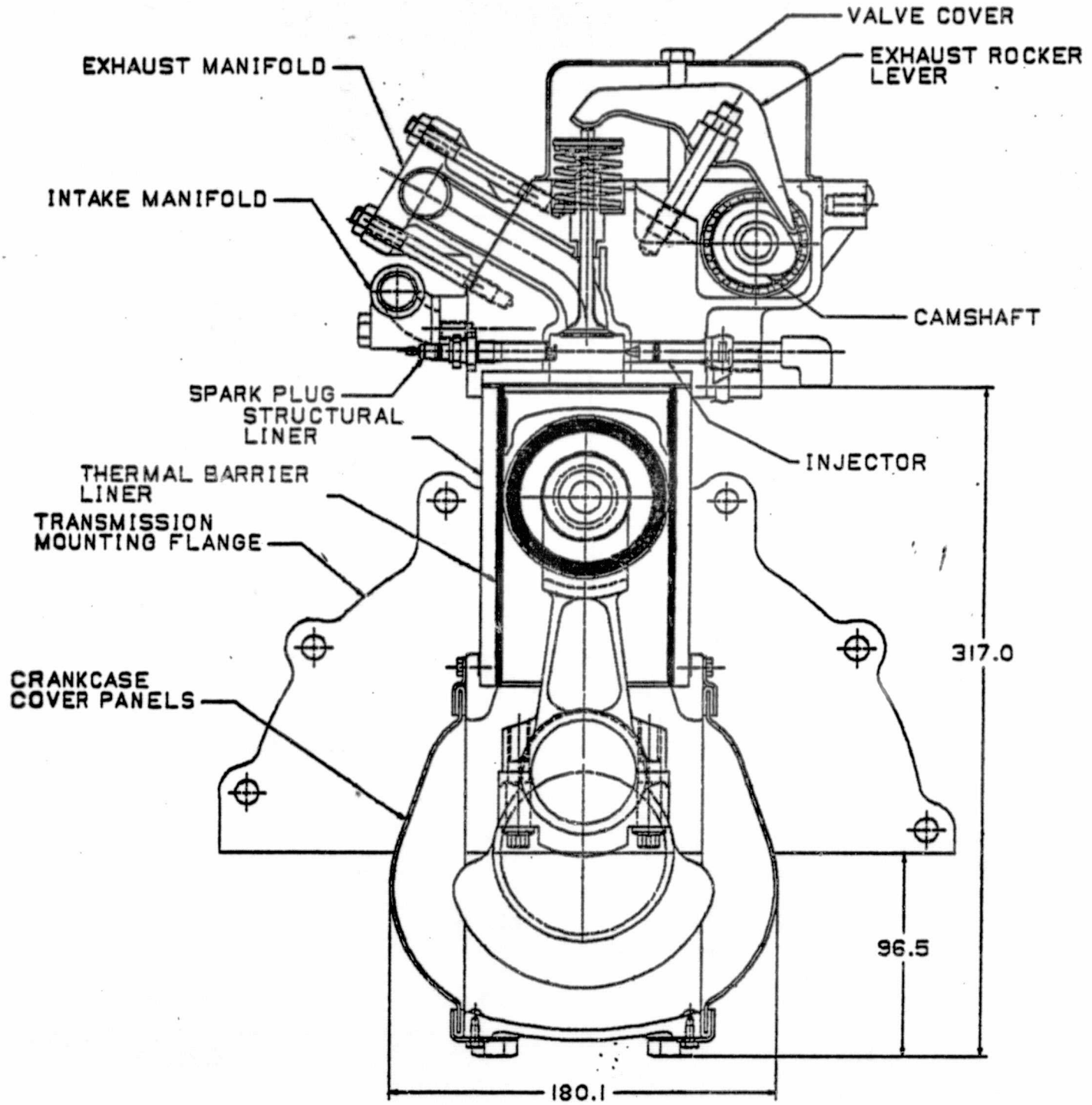

LIGHT DUTY AUTOMOTIVE DIESEL
CUMMINS ENGINE COMPANY,INC.
NASA CONTRACT NO. DEN3-261
6-24-83 -C.A.D.D.- FIGURE NO. 6.

CROSS SECTION VIEW-TRANSVERSE
-INTAKE VALVE
-MAIN BEARING

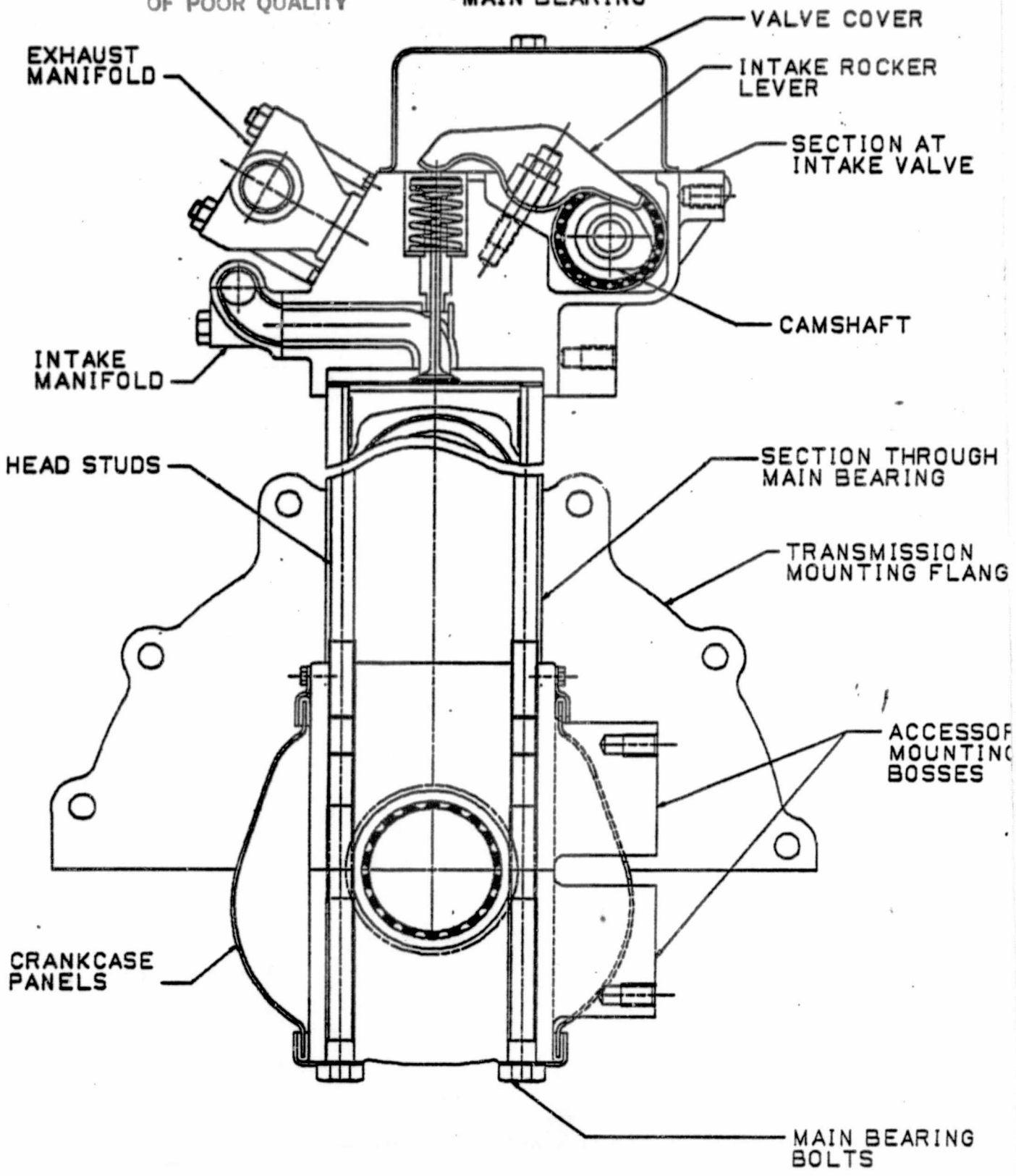

SCALE
100 MM

LIGHT DUTY AUTOMOTIVE DIESEL
CUMMINS ENGINE COMPANY,INC.
NASA CONTRACT NO. DEN3-261
6-27-83 -C.A.D.D.- FIGURE NO. 7

ENLARGED VIEW-
HEAD CROSS SECTION
AT INTAKE VALVE

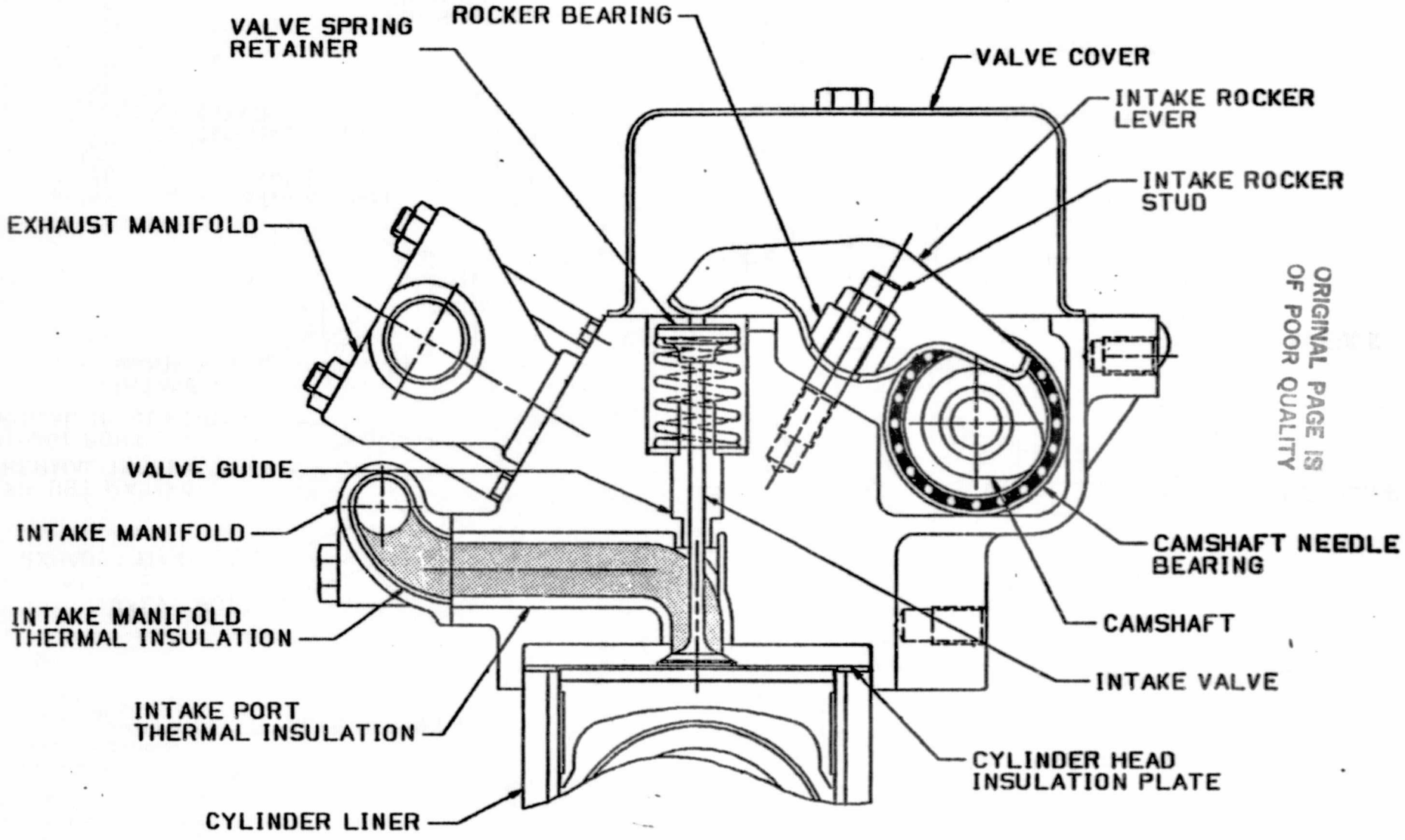

SCALE
100 MM

LIGHT DUTY AUTOMOTIVE DIESEL
CUMMINS ENGINE COMPANY,INC.
NASA CONTRACT NO. DEN3-261
6-27-83 -C.A.D.D.- FIGURE NO. 8.

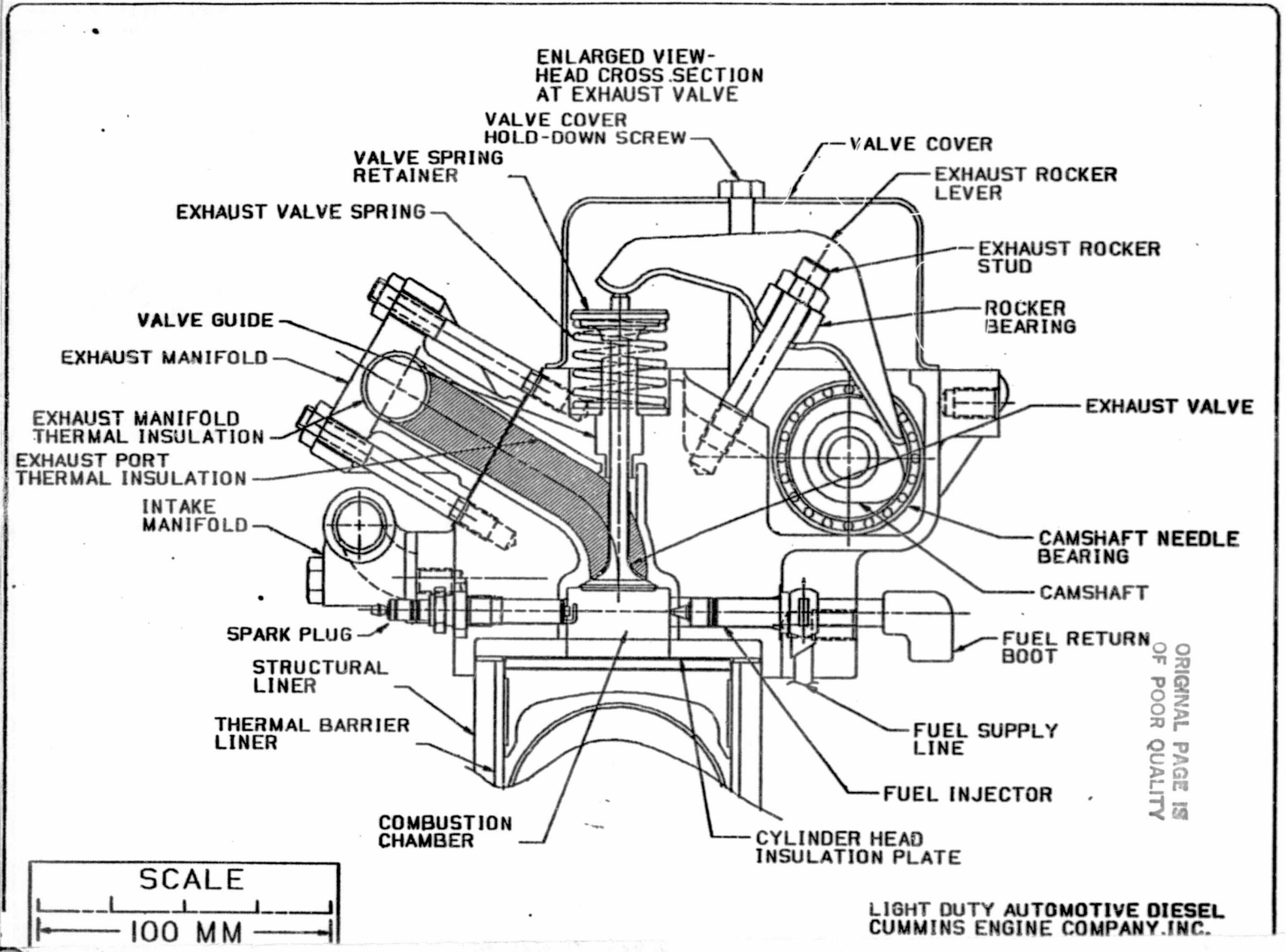

LAYOUT VIEW-TOP
HEAD CROSS SECTION

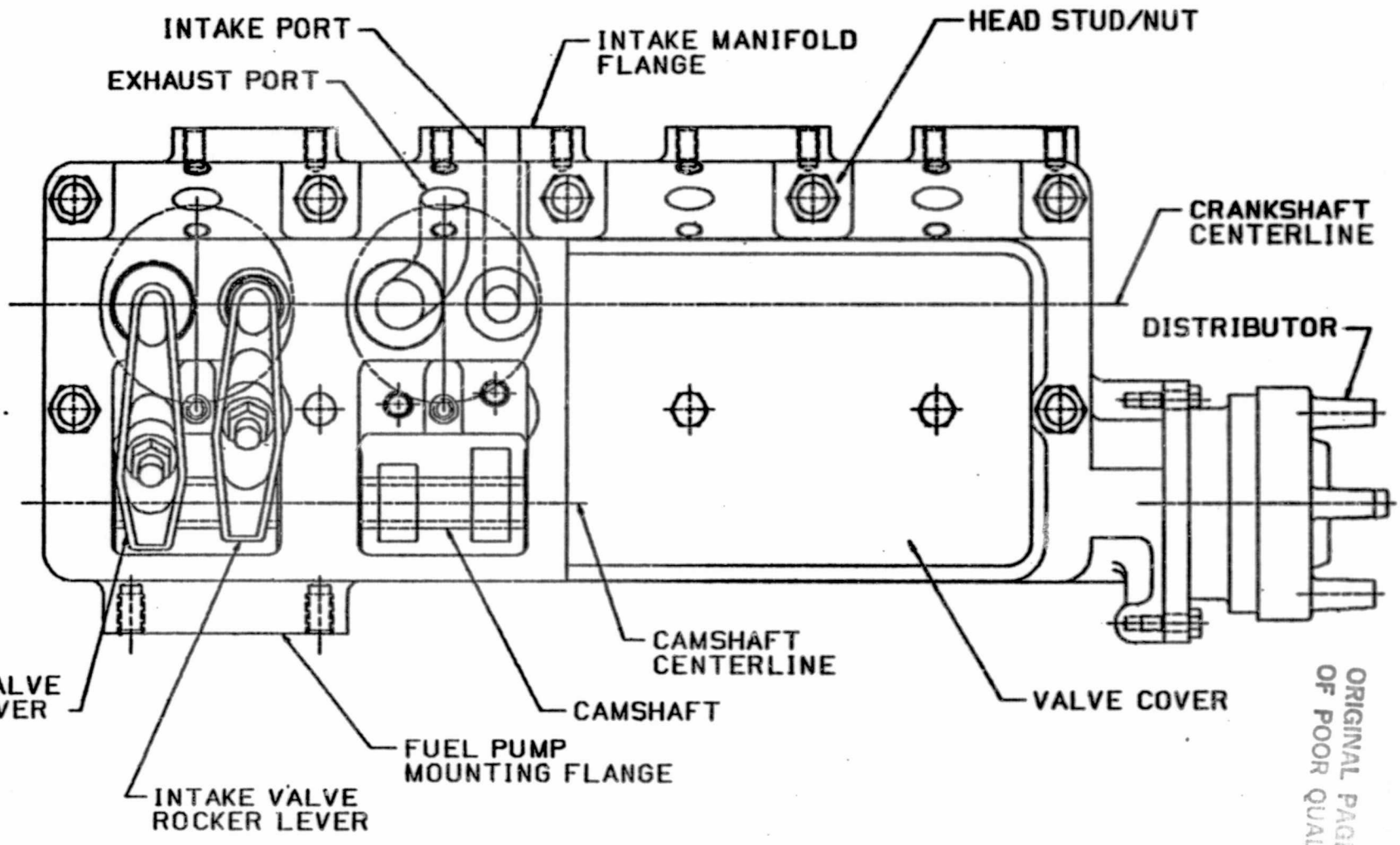

SCALE
100 MM

LIGHT DUTY AUTOMOTIVE DIESEL
CUMMINS ENGINE COMPANY,INC.
NASA CONTRACT NO. DEN3-261
6-27-83 -C.A.D.D.- FIGURE NO.10.

ENLARGED VIEW-TOP
HEAD CROSS SECTION

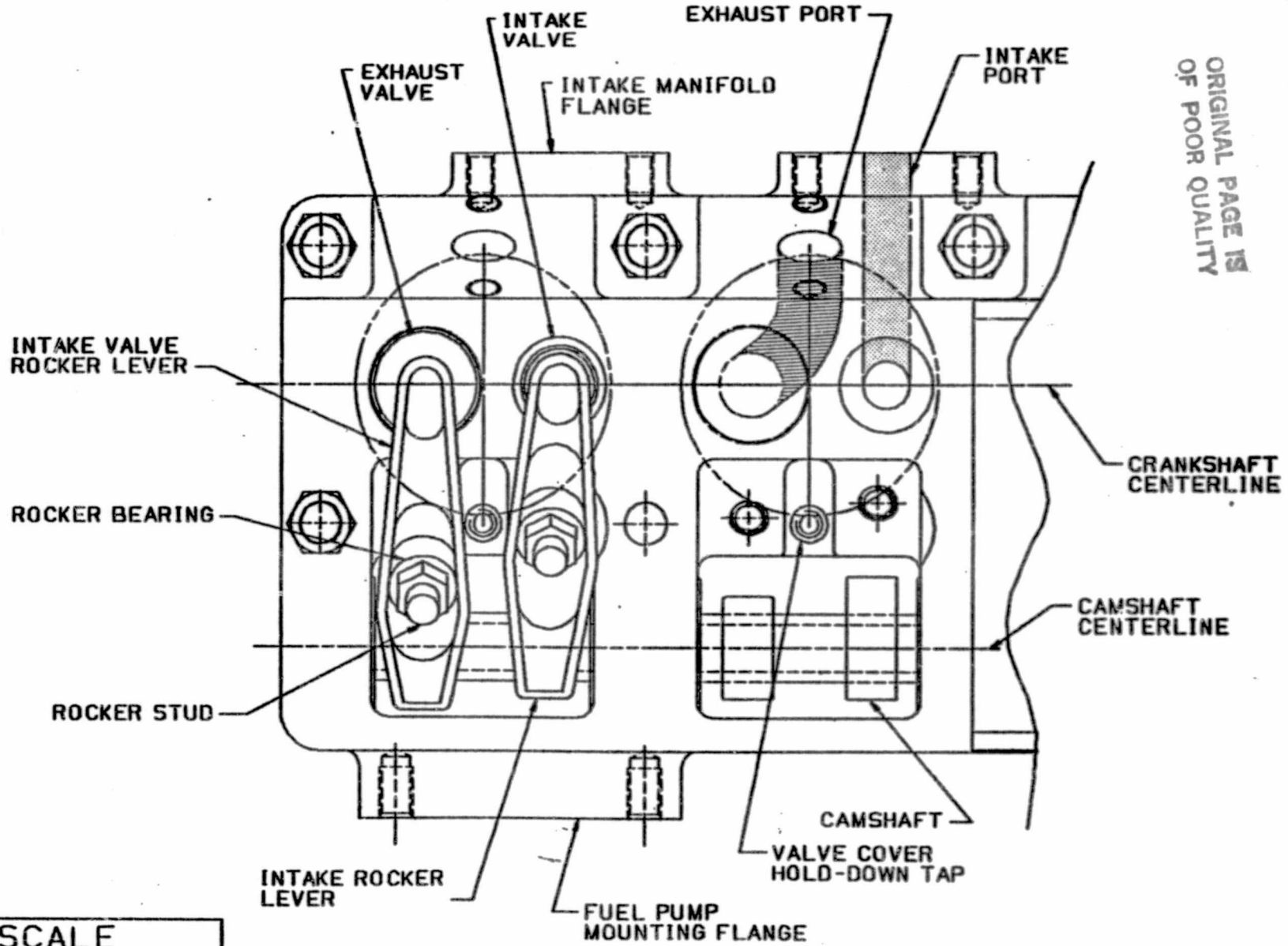

SCALE
100 MM

LIGHT DUTY AUTOMOTIVE DIESEL
CUMMINS ENGINE COMPANY, INC.

CONNECTING ROD
AND PISTON

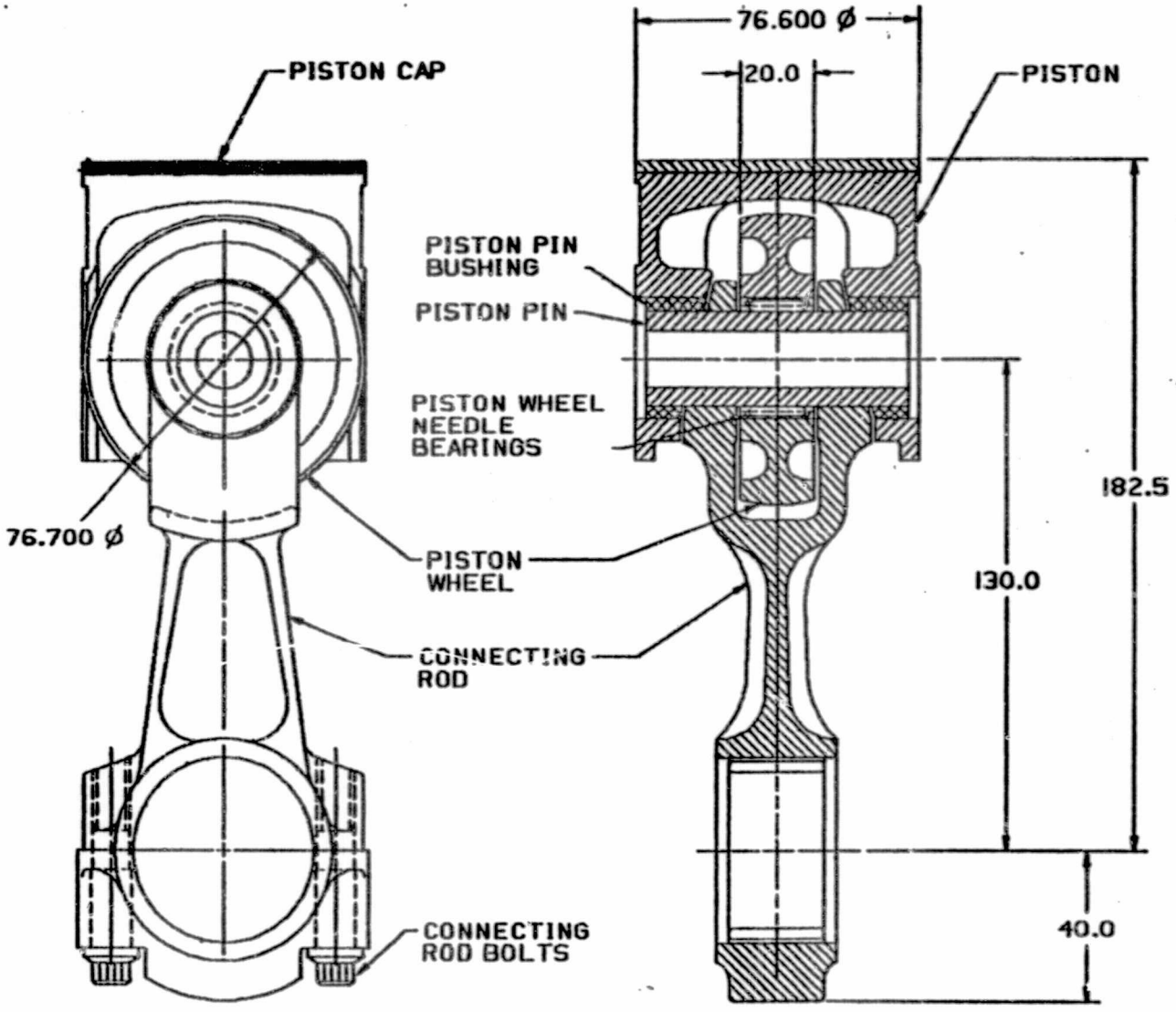

SCALE
100 MM

LIGHT DUTY AUTOMOTIVE DIESEL
CUMMINS ENGINE COMPANY, INC.
NASA CONTRACT NO. DEN3-261
6-29-83 -C.A.D.D.- FIGURE NO.12.

ENLARGED VIEW-SIDE
CRANKSHAFT AREA

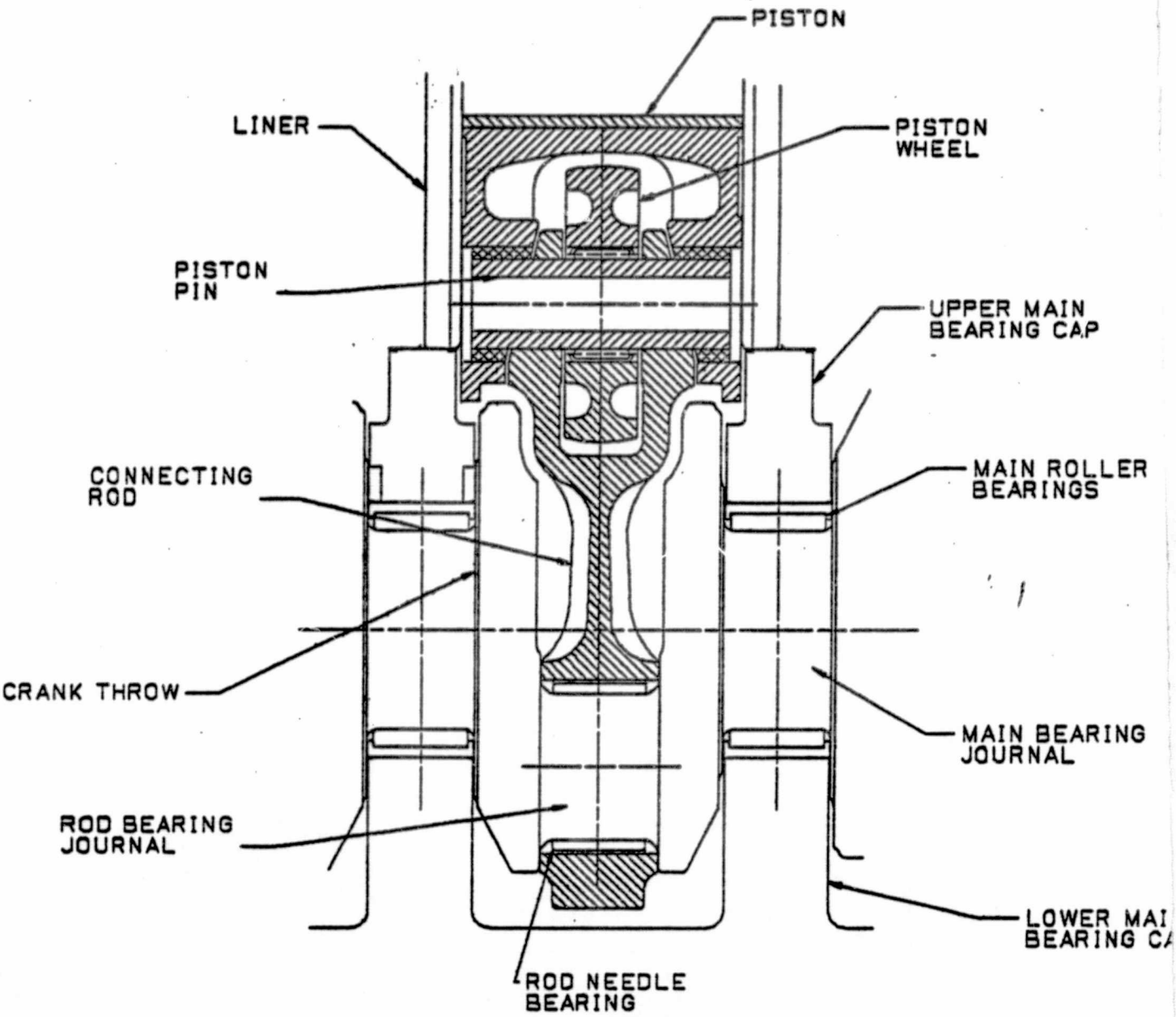

SCALE
100 MM

C-3

LIGHT DUTY AUTOMOTIVE DIESEL
CUMMINS ENGINE COMPANY, INC.
NASA CONTRACT NO. DEN3-261
6-29-83 -C.A.D.D.- FIGURE NO.13.

CRANKSHAFT

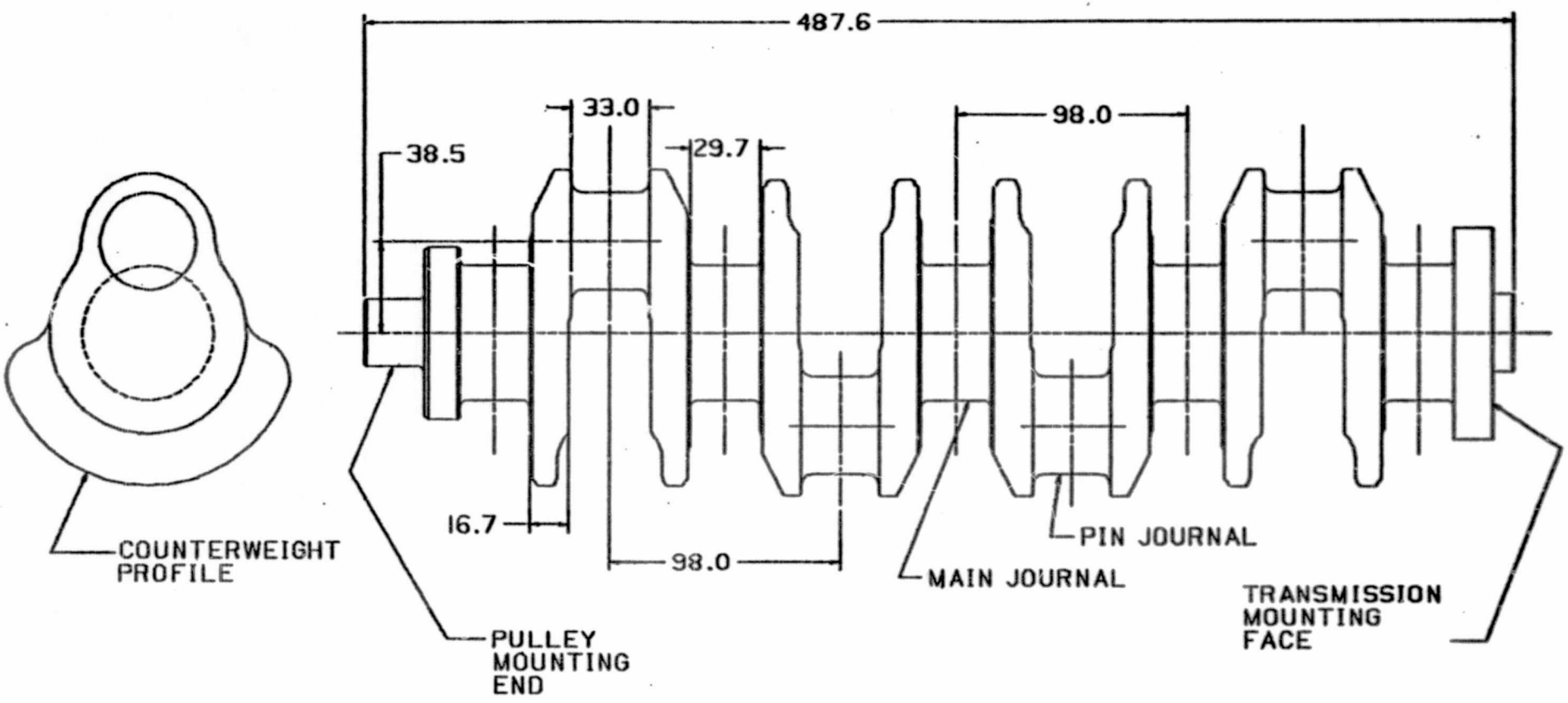

SCALE
100 MM

LIGHT DUTY AUTOMOTIVE DIESEL
CUMMINS ENGINE COMPANY, INC.
NASA CONTRACT NO. DEN3-261
6-29-83 -C.A.D.D.- FIGURE NO.14.

ALTERNATE CONNECTING
ROD AND PISTON

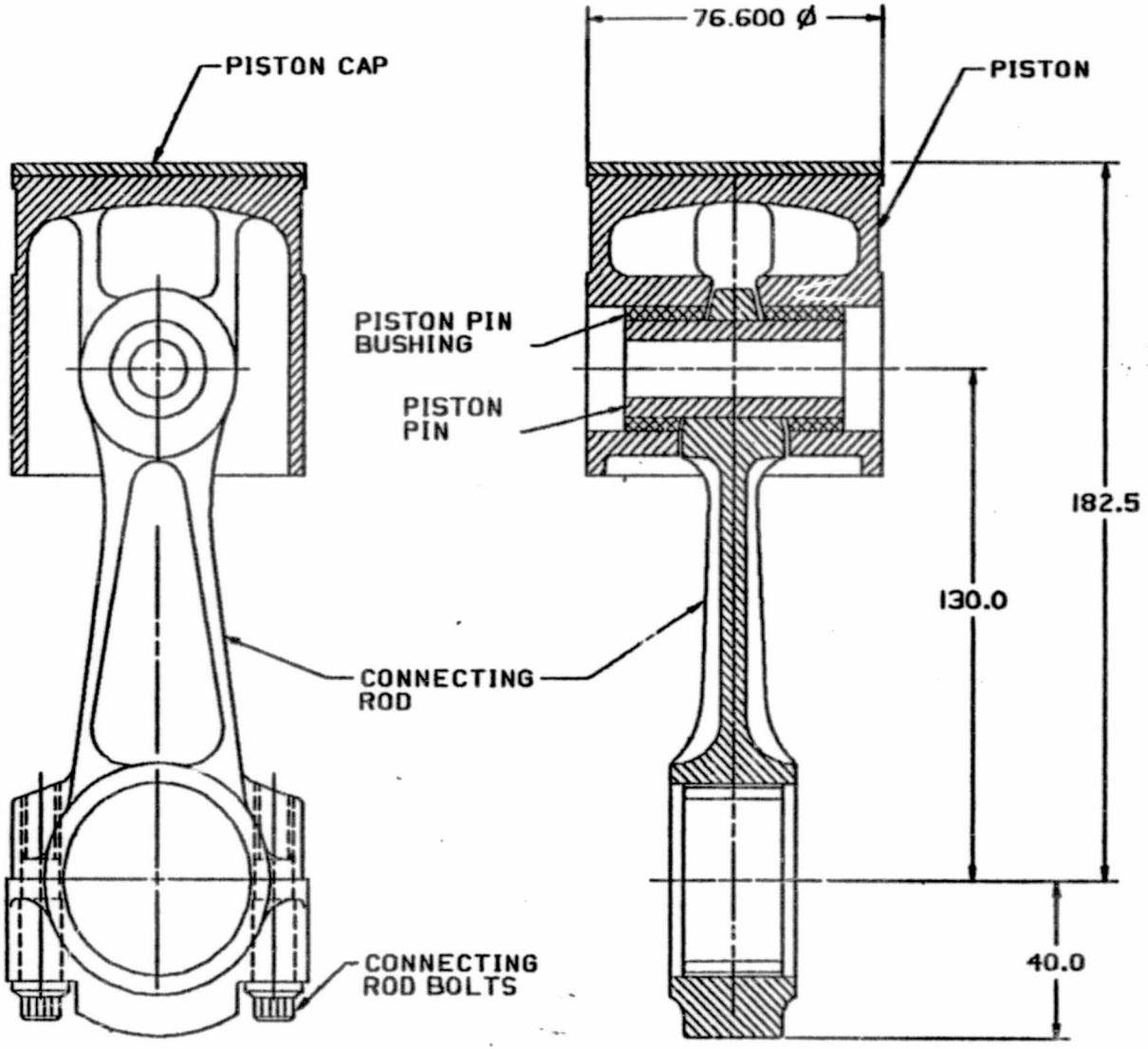

SCALE
100 MM

LIGHT DUTY AUTOMOTIVE DIESEL

LDAD ROD PATH GENERATION

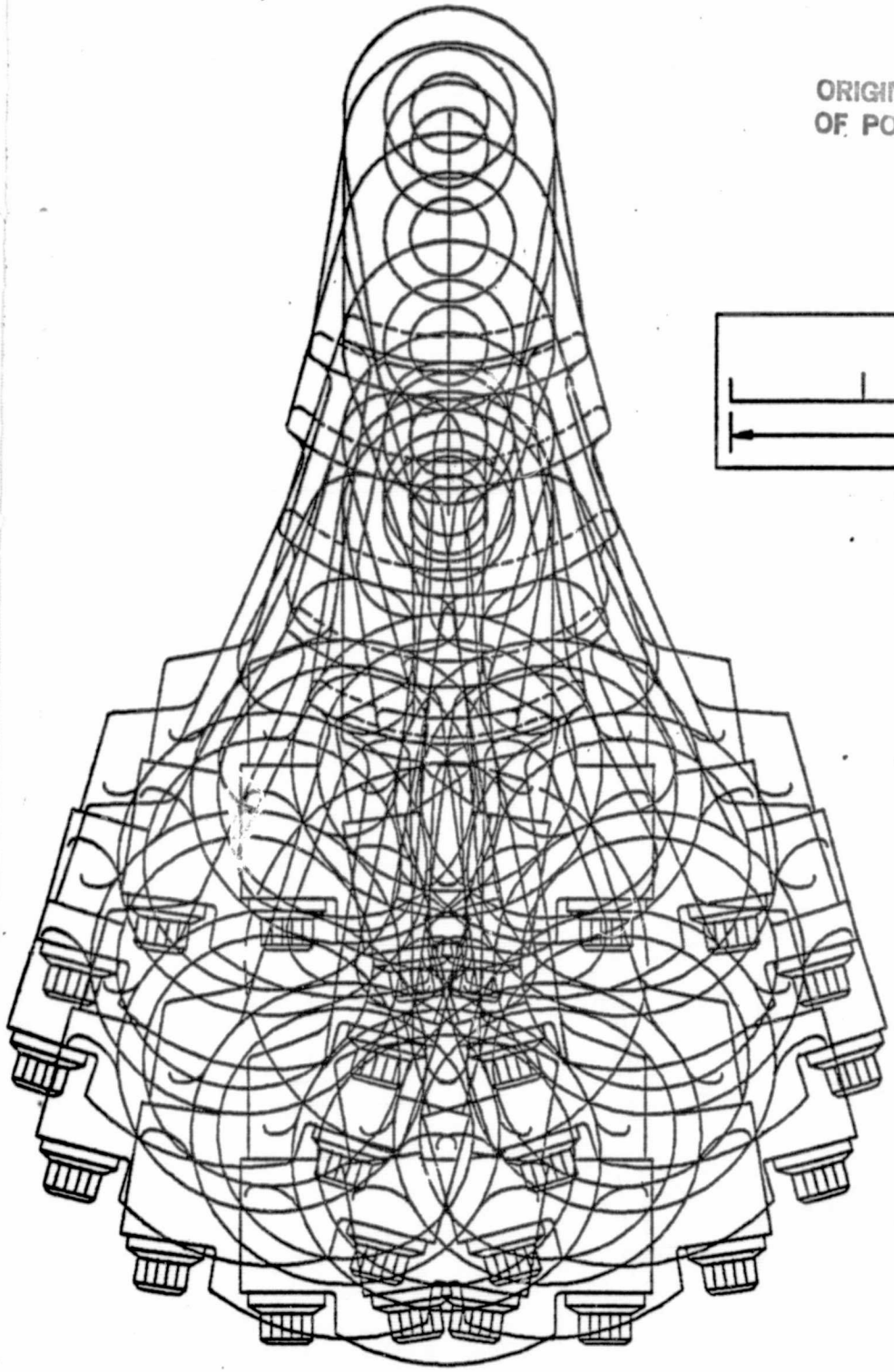

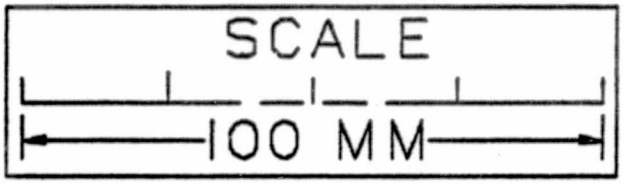

LIGHT DUTY AUTOMOTIVE DIESEL
CUMMINS ENGINE COMPANY,INC.
NASA CONTRACT NO. DEN3-261
6-30-83 -C.A.D.D.- FIGURE NO.16.

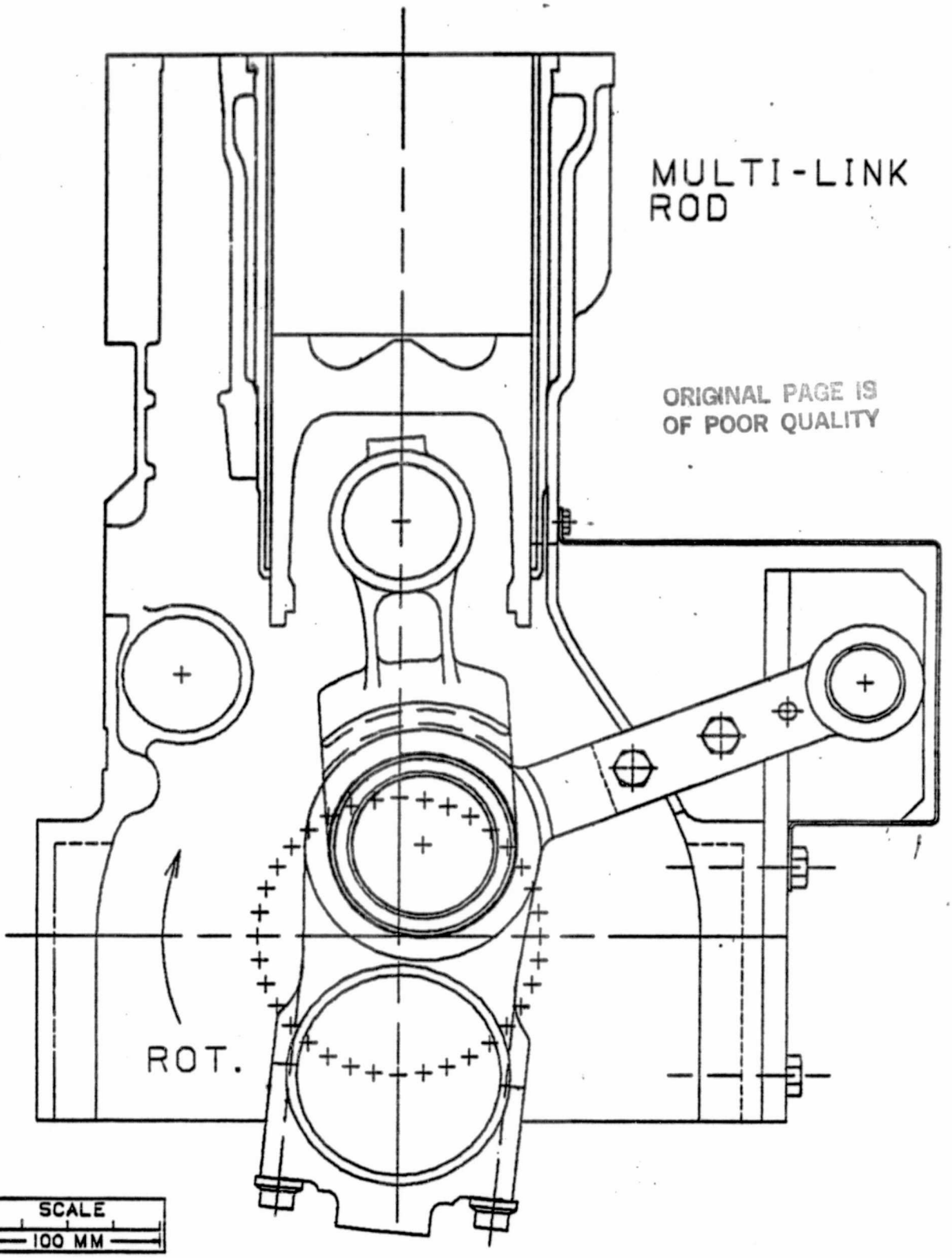

LIGHT DUTY AUTOMOTIVE DIESEL
CUMMINS ENGINE COMPANY, INC.
NASA CONTRACT NO. DEN3-261
6-30-83 -C.A.D.D.- FIGURE NO.17.

FRONT END BELT
DRIVE SYSTEM SCHEMATIC

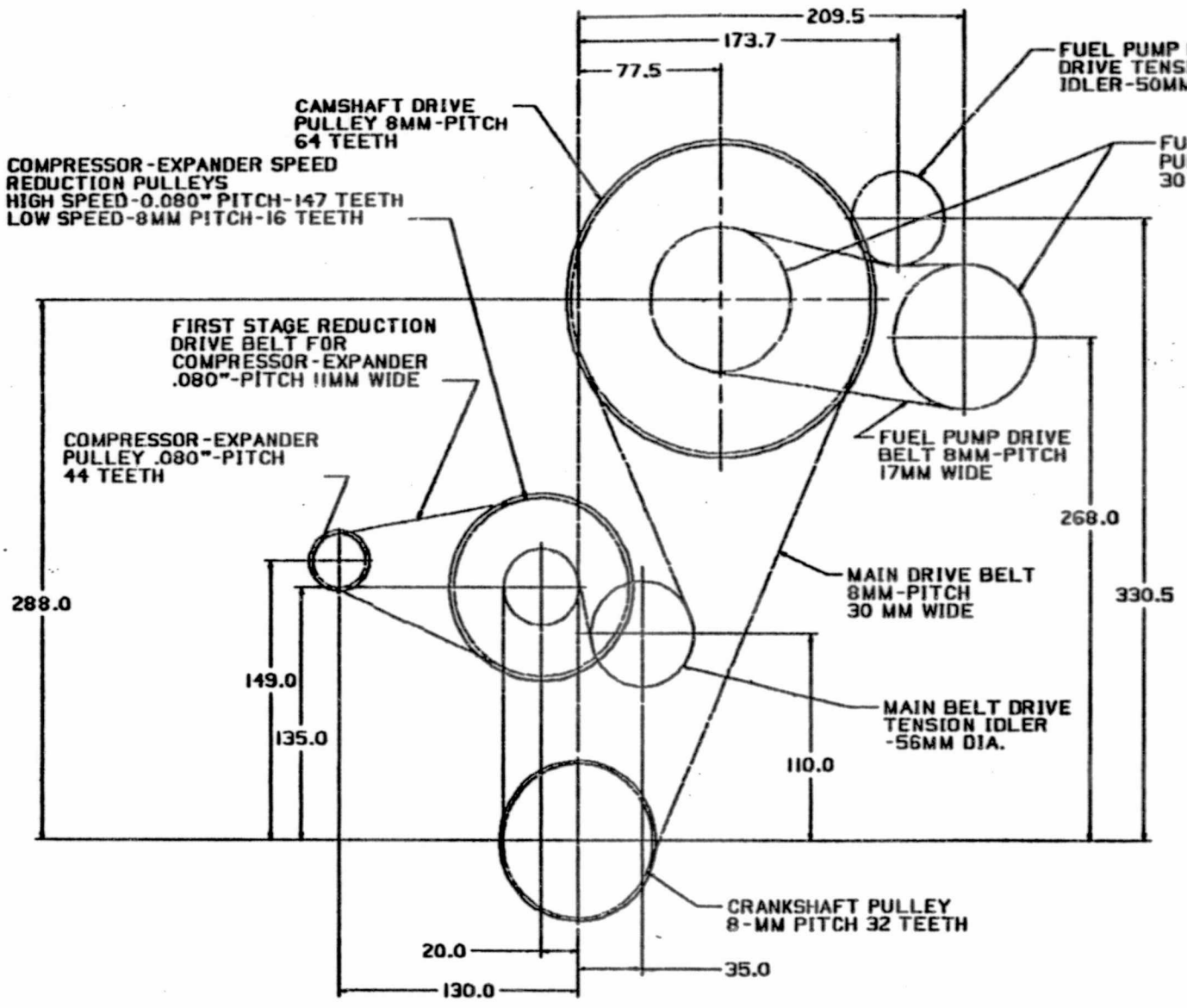

SCALE
100 MM

LIGHT DUTY AUTOMOTIVE DIESEL
CUMMINS ENGINE COMPANY, INC.
NASA CONTRACT NO. DEN3-261
6-30-83 -C.A.D.D.- FIGURE NO.18,

FUEL INJECTION NOZZLE

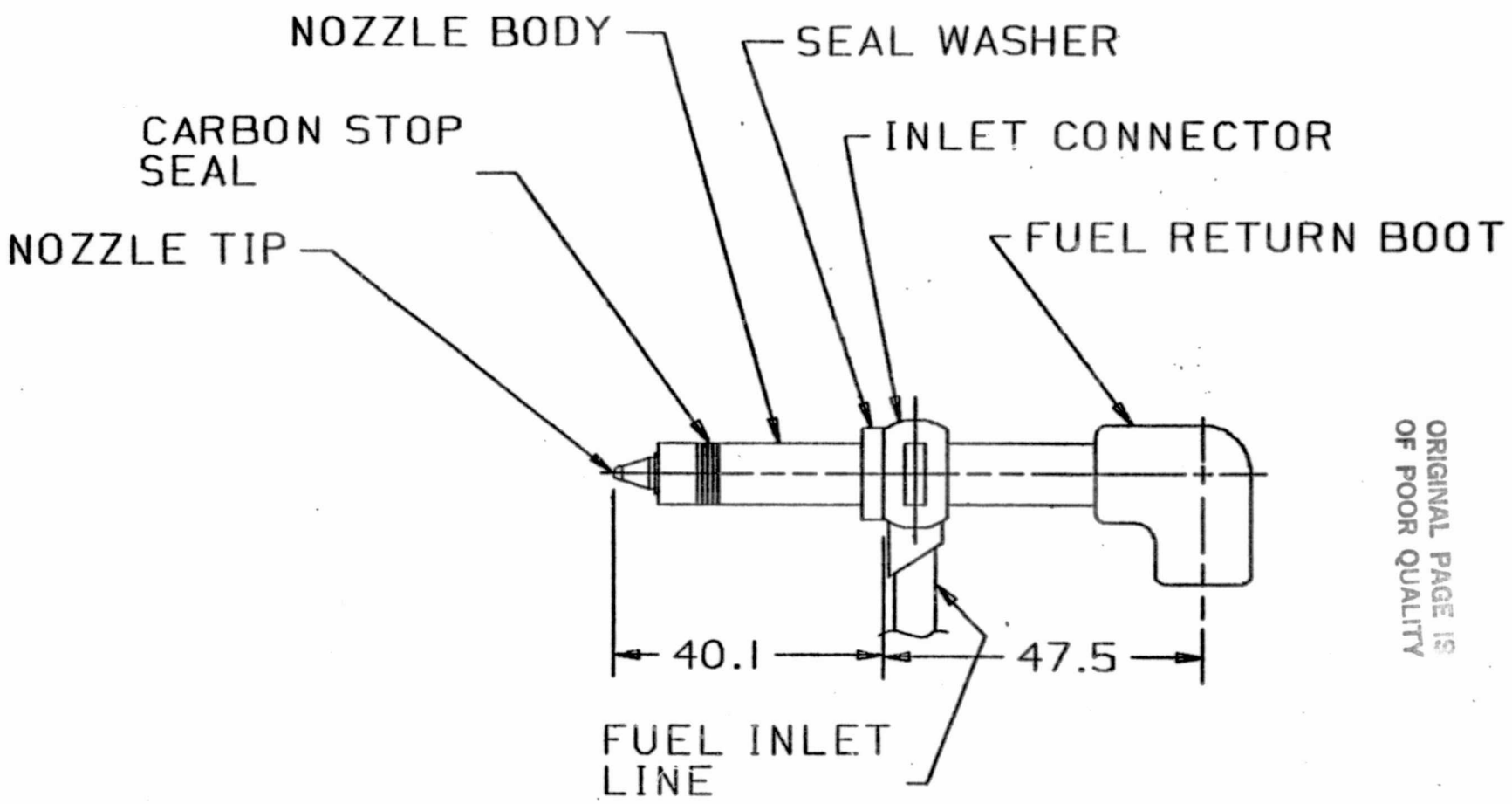

SCALE

100 MM

LIGHT DUTY AUTOMOTIVE DIESEL
CUMMINS ENGINE COMPANY, INC.
NASA CONTRACT NO. DEN3-261

APPENDIX 7

SCREW EXPANDER FOR LIGHT DUTY DIESEL ENGINES

INSTITUTE OF GAS TECHNOLOGY
ITT CENTER
CHICAGO, ILLINOIS 60616

TABLE OF CONTENTS

TABLE OF CONTENTS (Cont'd)

LIST OF FIGURES

LIST OF TABLES

EXECUTIVE SUMMARY

The work on this project consisted of preliminary selection and sizing of a positive displacement screw compressor-expander subsystem for a light-duty adiabatic diesel engine; development of a mathematical model to describe overall efficiencies for the screw compressor and expander; simulation of operation to establish overall efficiency for a range of design parameters and at given engine operating points; simulation to establish potential net power output at light-duty diesel operating points; analytical determination of mass moments of inertia for the rotors and inertia of the compressor-expander subsystem; and preparation of engineering layout drawings of the compressor and expander.

Our simulation of operation for the screw compressor and expander has shown efficiency maxima of 85% for the compressor and 88% for the expander. It has also shown acceptable net system power levels for the closer tolerance machines. Our assessment of the rotational inertia of the screw compressor and expander has indicated inertial levels that would only have a moderately negative effect on the transient performance of the system that can be easily compensated by an appropriate design of a flywheel.

As a result of this work, we have concluded that the screw compressor and expander designed for light-duty diesel engine applications are viable alternatives to turbo-compound systems, with acceptable efficiencies for both units, and only a moderate effect on the transient response.

Because of the preliminary nature of this work, we recommend that additional studies be performed to further quantify the effects of various parameters on performance, such as clearances, varying design pressure ratios, and dynamics of the expander inlet pressurization. We further recommend an assessment of the technological requirements in view of the desired clearances and tolerances.

INTRODUCTION AND OBJECTIVES

The technical objectives of this work are summarized as follows:

- Preliminary selection and sizing of a positive displacement compressor-expander subsystem that could be optimally combined with a light-duty diesel reciprocator to provide a mechanically-supercharged, positive-displacement, compound power system

- Development of mathematical models reflecting the functional relationships between overall efficiencies and design parameters and operating conditions for the screw compressor and expander

- Simulation to establish the potential efficiency of the screw compressor and expander (based on preliminary designs) for two sets of input data:

  1. The first set representing a range of design parameters based on selected nominal clearances

  2. The second set based on the light-duty diesel reciprocator operating characteristics

- Computer simulation to establish potential net power output characteristics (mapping) of the positive displacement expander-compressor subassembly

- Analytical determination of mass moments of inertia for the male and female rotors of the screw machine and numerical evaluation of inertia for the light-duty positive displacement compressor-expander subsystem

- Preparation of engineering layouts showing general arrangements of both compressor and expander.

The main emphasis of this work was on the development of analytical techniques that could predict the theoretical potential performances of screw machines. The effort was, therefore, a continuation of the developmental process described in the report "Expander-Compressor Design Study for Heavy Duty Compounded, Adiabatic Diesel Engine" in which the evaluation of potential efficiency characteristics for the screw expander was based on empirical data obtained from tests of existing machines. We believe that successful application of positive displacement power compounding must be based on a thorough understanding of all involved processes, conditions and parameters as well as the interactions between them.

ANALYSIS OF RECIPROCATOR (DIESEL ENGINE) PERFORMANCE DATA

Specification of the design parameters and subsequent sizing of the compressor/expander subsystem as well as simulation of its performance is dependent on the operating and performance characteristics of the light-duty diesel reciprocator. For this study the reciprocator characteristics were derived from simulation of a theoretical diesel cycle with partial exhaust after-supercharger heat regeneration, Table 1.

The power output and air mass flow rates of the reciprocator as a function of loading and operating speed characteristics are plotted in Figure 1.

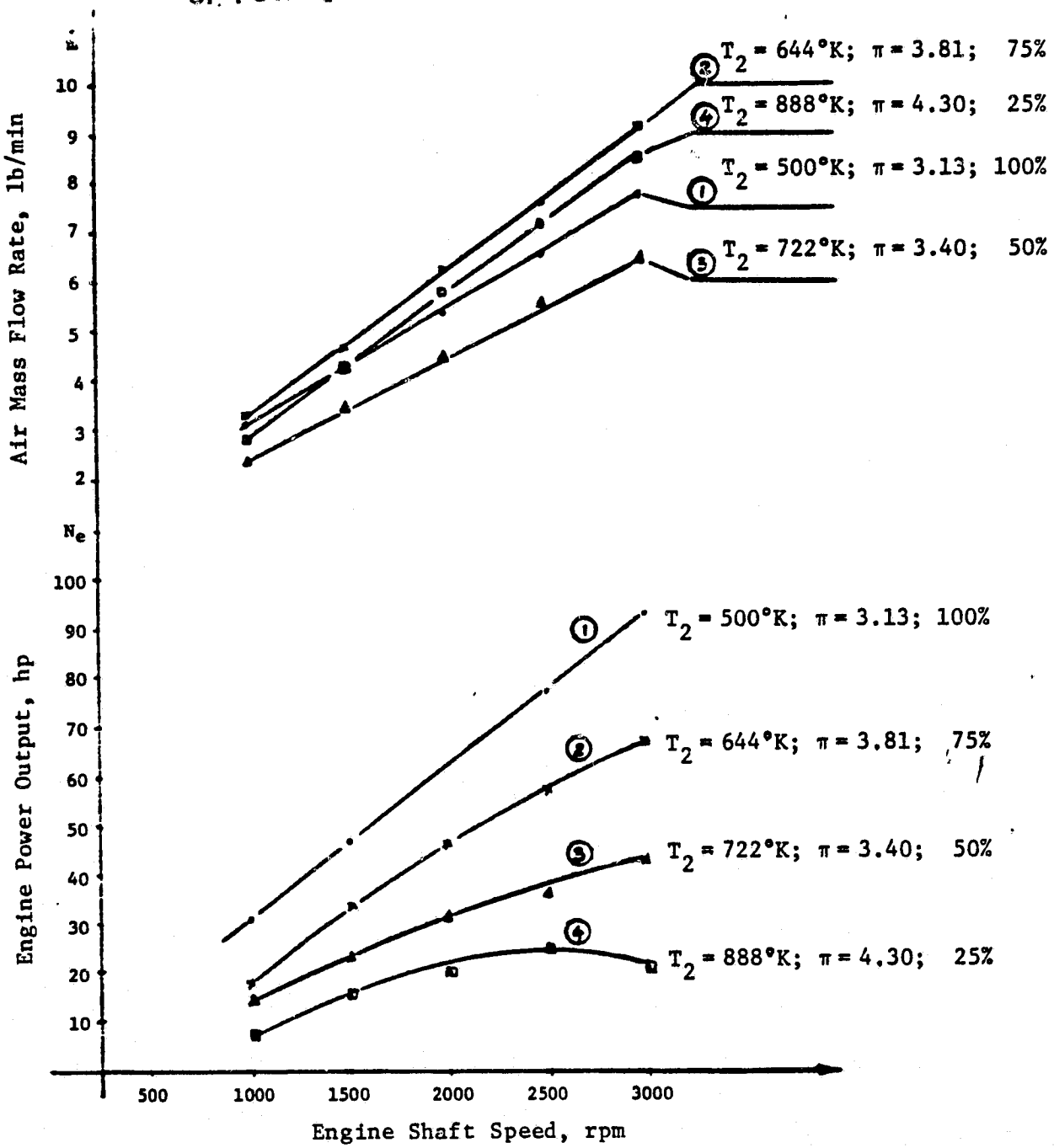

Figure 1. RECIPROCATOR (Diesel Engine) LOAD CHARACTERISTICS

LEGEND For each curve: intake temperature, T_2;
intake pressure ratio, π;
engine load factor, %

Table 1. RECIPROCATOR OPERATING AND PERFORMANCE DATA

(Reciprocator Displacement: V_{ss} = 1400 cm^3)

RPM	Load Factor, %	Power Output, HP	Intake Pressure (Absolute), kg/cm^2	Intake Temp., °K	Exhaust* Pressure (Absolute), kg/cm^2	Exhaust Temp., °K	Air Mass Flow, kg/min	Fuel Mass Flow, g/min
3000	100	93.0	3.13	499.6	3.59	1090	3.53	183.4
	75	66.5	3.81	644.0	4.23	1090	4.15	139.7
	50	43.0	3.40	721.8	2.99	1090	2.94	102.7
	25	21.0	4.30	888.5	3.92	1090	3.85	55.1
2500	100	77.5	3.13	499.6	3.65	1090	2.99	152.5
	75	56.0	3.81	644.0	4.20	1090	3.44	115.5
	50	36.0	3.40	721.8	3.09	1090	2.53	84.5
	25	25.0	4.30	888.5	3.98	1090	3.26	63.4
2000	100	62.6	3.13	499.6	3.72	1090	2.44	122.3
	75	45.8	3.81	644.0	4.35	1090	2.85	92.8
	50	31.0	3.40	721.8	3.10	1090	2.03	68.7
	25	20.0	4.30	888.5	4.00	1090	2.62	49.0
1500	100	47.0	3.13	499.6	3.95	1090	1.94	92.1
	75	34.0	3.81	644.0	4.34	1090	2.13	68.7
	50	23.0	3.40	721.8	3.22	1090	1.58	51.3
	25	15.0	4.30	888.5	3.95	1090	1.94	36.2
1000	100	31.0	3.13	499.6	4.26	1090	1.40	61.1
	75	18.0	3.81	644.0	4.55	1090	1.49	36.9
	50	15.6	3.40	721.8	3.30	1090	1.08	34.7
	25	7.5	4.30	888.5	3.85	1090	1.26	18.1

* Calculated as back-pressure based on assumed interaction of reciprocator and designed expander.

PRELIMINARY DESIGN SPECIFICATION OF THE SCREW COMPRESSOR

Rotor Sizing

To meet the boost requirements of the reciprocator, the supercharger should provide a flow capacity from 1.08 to 4.15 kg/min with the pressure ratio maintained between 3.13 and 4.30. The maximum mass flow capacity ($\dot{m}_{a(max)}$) and built-in pressure ratio (π_{cd}) of the screw compressor are the primary design parameters that need to be determined prior to sizing the rotors.

Maximum mass flow requirements are taken as the starting point of design. Using the equation for an ideal gas at ambient conditions, mass flow can be converted to volume flow:

$$\dot{V}_{a(max)} = \frac{\dot{m}_{a(max)} R T_0}{P_0} = 3.556 \text{ m}^3/\text{min} \qquad (1)$$

where:

$\dot{m}_{a(max)}$ = 4.15 kg/min

P_0 = 1 kg/cm^2

T_0 = 293°K

Assuming the volumetric efficiency (η_v) of the compressor to be 87%, the required maximum compressor volume flow rate is given by:

$$\dot{V}^*_{a(max)} = \frac{\dot{V}_{a(max)}}{\eta_v} = 4.087 \text{ m}^3/\text{min (standard)} \qquad (2)$$

Other design parameters set by the engine requirements are 1) maximum allowable speed of compressor shaft and 2) male rotor tip speed (u_{tm}). The maximum allowable speed of the compressor power shaft was 20,000 rpm as given by Cummins. To assure high volumetric-compression efficiency, the male rotor tip speed should be at least 100 m/sec.

The relationship among capacity (volume flow), male rotor tip speed and rotor diameter is shown in Figure 2 for an active area profile constant (C) of 0.5010, a wrap angle constant (C_{wa}) of 0.9688, and a rotor length to diameter ratio (L/D) of 1.5. The equation defining this relationship is:

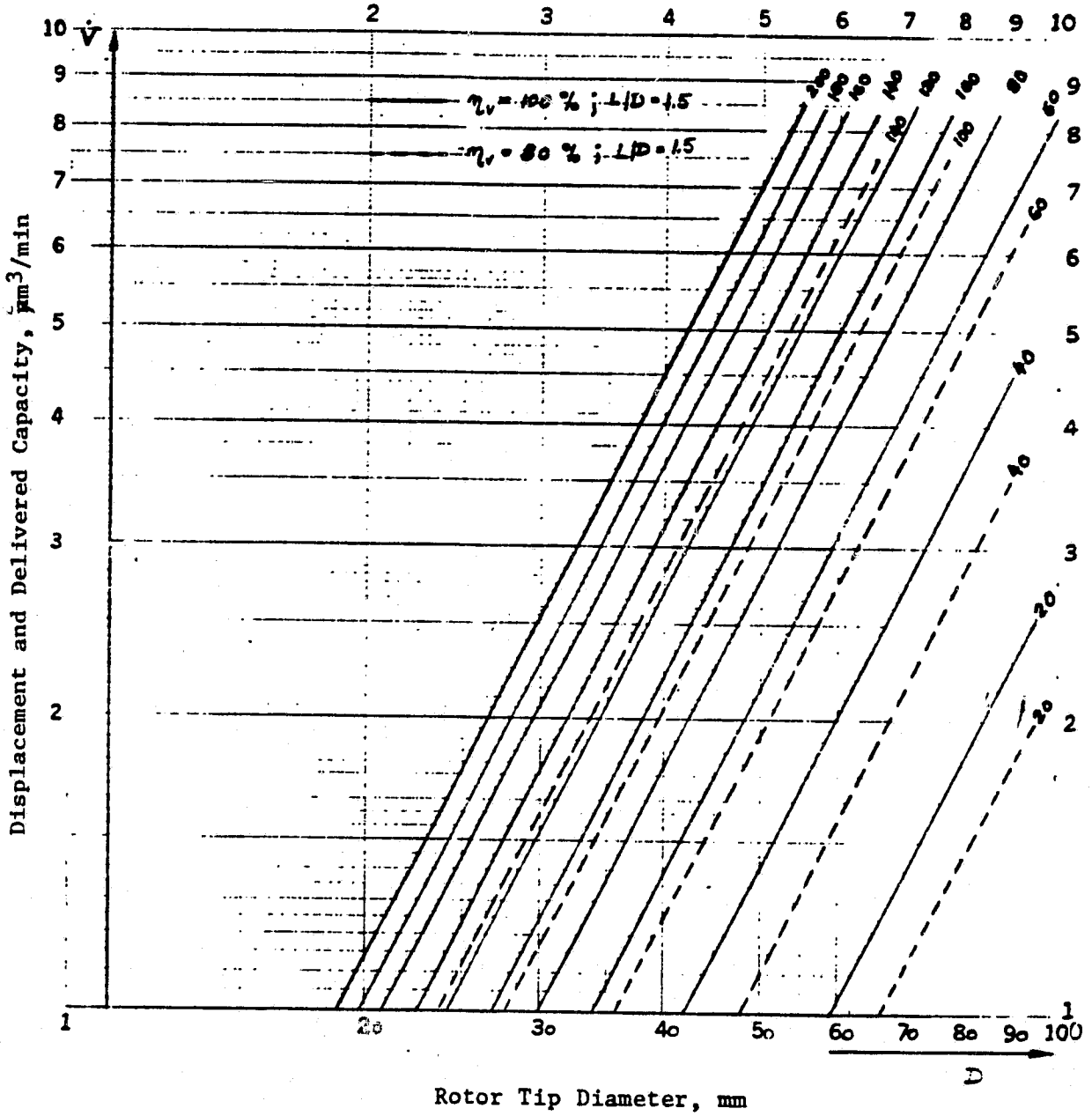

Figure 2. SCREW COMPRESSOR PERFORMANCE

$$\dot{V}_a = C\, C_{wa}\, D^3 \left(\frac{L}{D}\right) n_m \qquad (3)$$

where:

C = Active area profile constant

C_{wa} = Wrap angle constant

D = Rotor diameter

L = Rotor length

n_m = Male rotor speed

or

$$\dot{V}_a = \frac{60}{\pi}\, C\, C_{wa}\, D^2\, \frac{L}{D}\, u_{tm} \qquad (3a)$$

If small flow capacities are required, the rotor diameters also become small and the only way to increase tip speed is to increase the speed of the rotor. However, when the rotor speed is limited, the desired tip speed cannot be attained.

If the requirement of u_{tm} = 100 m/s at 20,000 rpm of male rotor were to be met, then the corresponding rotor diameter is given as:

$$D_m = \frac{60\, u_{tm}}{\pi\, n_m} = 9.54 \text{ cm} \qquad (4)$$

However, if D_m is 9.54 cm, the required capacity of the compressor cannot be met. Consequently, the only solution possible if the conditions of u_{tm} = 100 m/s and $\dot{V}^*_{a(max)}$ = 4.087 m^3/min are to be met is to apply the maximum speed requirement to the female rotor.

For a timing gear ratio (i_t) of 1.5, the male rotor rpm is:

$$n_{m(max)} = n_{f(max)}\, i_t = 30{,}000 \text{ rpm} \qquad (5)$$

From Equation 4: D_m = 6.2 cm; from Equation 3 for n_m = 30,000 rpm and $\dot{V}^*_{a(max)}$ = 4.087 m^3/min, L/D = 1.37, and L = 7.3 cm.

Basic Profile Dimensions

This section is presented as an example of basic profile dimensions. In sizing the machine, the geometric constant C represents an

asymmetrical profile such as that which most likely would be used in the final design. The same equations govern the overall geometry of symmetric and asymmetric profiles; however, additional relationships are needed to characterize the profile arcs. For this preliminary design, the profile type has no effect on the presented results. The set of equations below determine the basic dimensions characterizing a symmetrical, circular profile of both male and female rotors of above sized compressor.

$$L_c = r_m + r_f \tag{6}$$

$$r_f/r_m = 1.5 \tag{7}$$

$$2.5\, r_m = L_c \tag{8}$$

$$r_m = R_m - r_L \tag{9}$$

$$R_m = R_f \tag{10}$$

$$a = r_m - r_{mf} \tag{11}$$

$$r_{mf} = L_c - R_m \tag{12}$$

where:

R_f = Outside radius of female rotor

R_m = Outside radius of male rotor

r_{ff} = Root circle radius of female rotor

r_{mf} = Root circle radius of male rotor

r_f = Pitch radius of female rotor

r_m = Pitch radius of male rotor

L_c = Distance between axes of rotors

r_L = Lobe radius

a = Profile addendum.

All characteristic dimensions are shown in Figure 3.

Given a value of $R_m = R_f = 3.1$ cm, and assuming a practical value for the lobe radius of $0.3548\ R_m$, solution of equations set 6 to 12 gives:

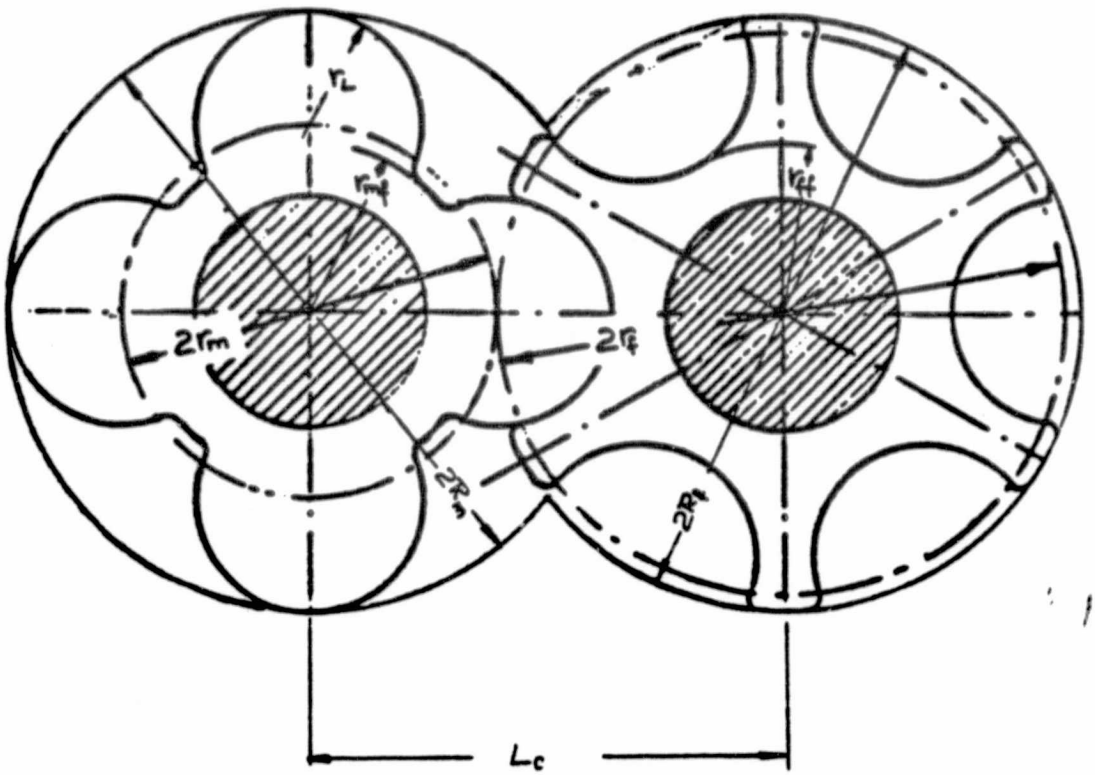

Figure 3. CHARACTERISTIC DIMENSIONS
OF SYMMETRIC PROFILE ROTORS

r_m = 2.0 cm; r_f = 3.0 cm; r_L = 1.1 cm; r_{mf} = r_{ff} = 1.9 cm; L_c = 5.0 cm, and a = 0.1 cm.

Built-In Pressure Ratio

As will be explained later, the built-in pressure ratio influences overall efficiency characteristics of the compressor and should be subject to optimization. However, optimization is beyond the scope of this effort. Consequently, the design pressure ratio π_{cd} was taken as 3.13 which is equal to the pressure ratio required at rated engine operating conditions.

Compressor Design Layout

The completed compressor layout can be seen in Figure 4. It should be noted that the design is based on the assumption that lubricated gears and vented bearings are used. In addition, the layout would be further simplified for a fully dry design.

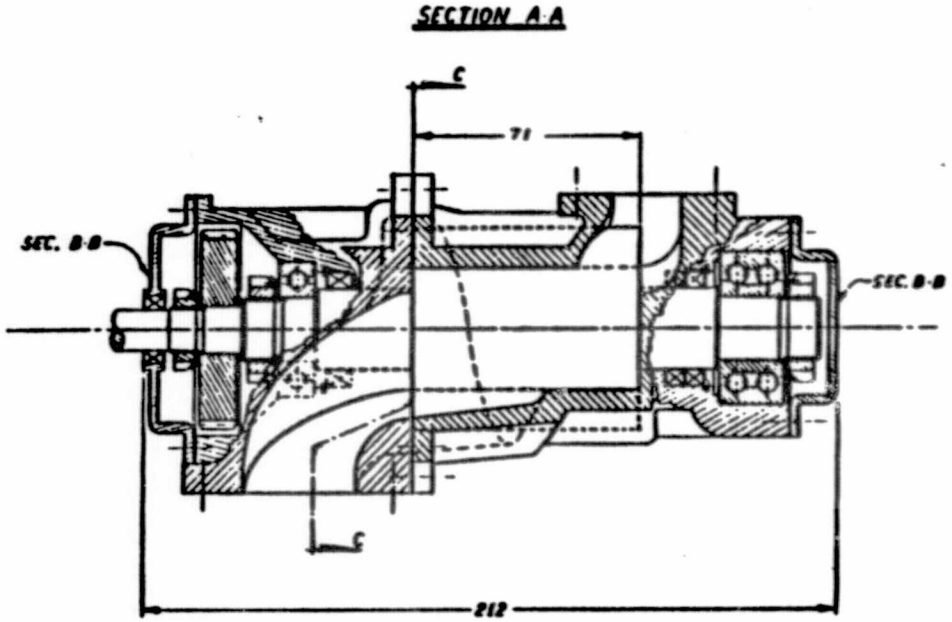

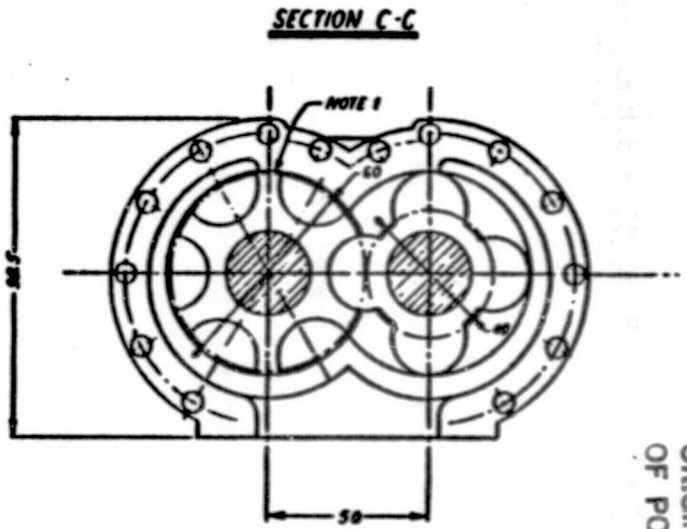

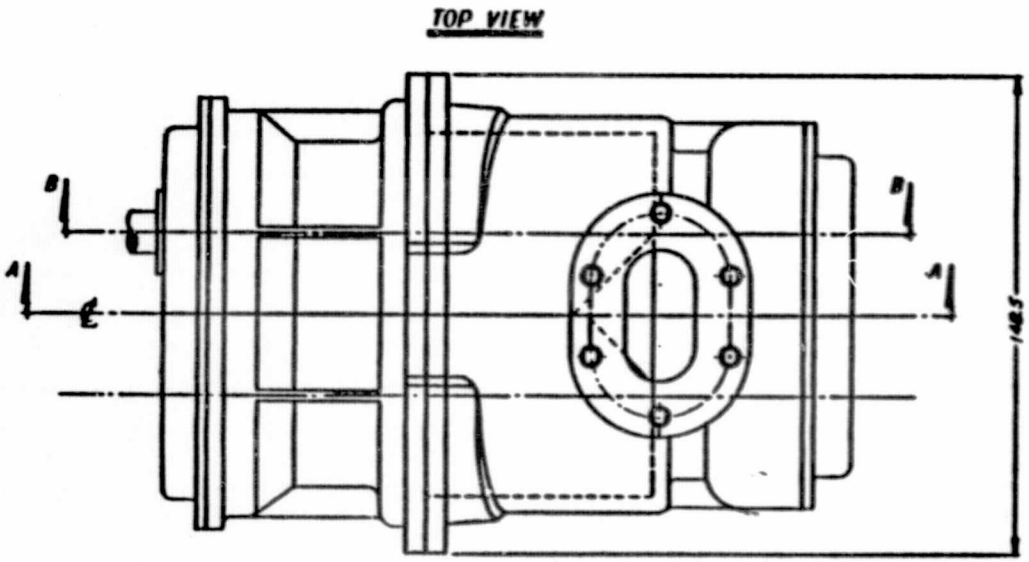

NOTE: Symmetric rotor profiles are shown for simplicity. Actual profiles will be asymmetric.

Figure 4. SCREW COMPRESSOR LAYOUT (62 mm diameter)

PRELIMINARY DESIGN SPECIFICATION FOR SCREW EXPANDER

Rotor Sizing

Sizing of an expander should be dictated by the required maximum exhaust back pressure as determined from conditions of optimal performance for the total compound system, and by the requirement of total pressure expansion from expander inlet conditions corresponding to this maximum back-pressure. The design point of the expander should be based on maximum rpm and maximum mass flow which, in this case, corresponds to engine operating point characteristics of 3000 rpm and 75% load. At these conditions, the expander should create a moderate back pressure exceeding the boost pressure by 0.4 kg/cm^2.

The first step in sizing the expander will be to determine the volume flow rate provided by the charging volume of the expander as it develops the required exhaust back pressure. The volume flow rate of the expander can be expressed by:

$$\dot{V}_{3d} = \frac{T_3}{T_2} \frac{p_2}{p_{3d}} \frac{n_r V_{ss}}{2} \tag{13}$$

where:

T_3 = Exhaust temperature at expander inlet

T_2 = Engine intake temperature

p_2 = Boosting pressure at engine entrance

p_{3d} = Design pressure in exhaust manifold for expander operation

n_r = Reciprocator speed

V_{ss} = Reciprocator displacement.

For design point: $T_3 = 1093°K$; $T_2 = 644°K$; $p_2 = 3.81\ kg/cm^2$; $p_{3d} = 4.21\ kg/cm^2$; $n_r = 3000$ rpm; $V_{SS} = 1.4 \times 10^3\ cm^3$ and $\dot{V}_{3d} = 3.21\ m^3/min$.

The volume flow rate to be provided by the expander design displacement by total adiabatic expansion of the working medium down to atmospheric pressure is given by:

$$\dot{V}_{4d} = \dot{V}_{3d} \left(\frac{p_{3d}}{p_0}\right)^{1/\kappa} = \dot{V}_{3d}\ \pi_{ed}^{1/\kappa} \tag{14}$$

For $\dot{V}_{3d}$ = 3.21 m^3/min, p_{3d} = 4.21 kg/cm^2, and p_0 = 1 kg/cm^2, $\dot{V}_{4d}$ = 8.89 m^3/min.

The rotor diameter is given by:

$$D_m = \frac{\dot{V}_{4d}}{C\, C_{wa}\, (\frac{L}{D})\, n_{m(max)}} \tag{15}$$

For $\dot{V}_{4d}$ = 8.89 m^3/min; C = 0.501; C_{wa} = 0.9688; (L/D) = 1.0; and $n_{m(max)}$ = 20,000 rpm (based on the same speed limitations for the expander as required for the compressor); D_m = 9.8 cm.

The rotor tip speed is given by:

$$u_{tm} = \frac{D_m\, n_{m(max)}}{\pi\, 60} \tag{16}$$

For D_m = 9.8 cm, $n_{m(max)}$ = 20,000 rpm, and π_{ed} = 4.21, u_{tm} = 102.6 m/sec. A tip speed of 102.6 m/sec is the accepted range which produces the expected efficiency.

Determination of Expander Inlet Pressure

The operating inlet pressure for the expander is determined by the method developed in the IGT report mentioned above.

The expander charging volume (volume of working medium taken in [before expansion] per male rotor rotation) is given by:

$$V_{ch} = \frac{\dot{V}_{3d}}{n_{m(max)}} = \frac{\dot{V}_{3d}}{i_d\, n_{r(max)}} \tag{17}$$

where:

$i_d = \frac{n_{m(max)}}{n_{r(max)}}$ = Drive ratio between power shaft of expander and reciprocator crankshaft.

For the design conditions of $n_{m(max)}$ = 20,000 rpm and $n_{r(max)}$ = 3000 rpm, i_d = 6.666.

Once the expander charging volume and drive ratio are fixed for a given design, the intake flow rate of the expander can be defined as a function of reciprocator speed:

$$\dot{V}_3 = V_{ch}\, n_r \tag{18}$$

Applying the ideal gas equation, the pressure at the entrance to the expander can be expressed as:

$$P_3 = \frac{\dot{m}_{ex}\, R\, T_3}{n_r\, V_{ch}} \tag{19}$$

where:

$\dot{m}_{ex}$ = Actual mass flow of exhaust gases

T_3 = Temperature of exhaust at expander inlet

n_r = Reciprocator rpm

V_{ch} = Expander charging volume.

Values of p_3 have been calculated for conditions corresponding to the reciprocator mapping data and are listed in Table 1 as "Exhaust Pressure."

Basic Profile Dimensions

For the design conditions of $R_m = R_f$, $D_m = 9.8$ cm, and $r_L \approx 0.3673\ r_m$, and using Equations 6 through 12, the characteristic dimensions of the symmetric profiles of the male and female rotors of the expander are: r_L = 1.8 cm, r_m = 3.1 cm, L_c = 7.75 cm, r_f = 4.65 cm, and $r_{mf} = r_{ff} \approx 2.85$ cm. It should be noted that the symmetric profile is used only as an example and that an asymmetric profile would be used in the final design.

Expander Design Layout

The completed expander layout can be seen in Figure 5. It should be noted that the design is based on the assumption that lubricated gears and vented bearings are used. In addition, the layout would be further simplified for a fully dry design.

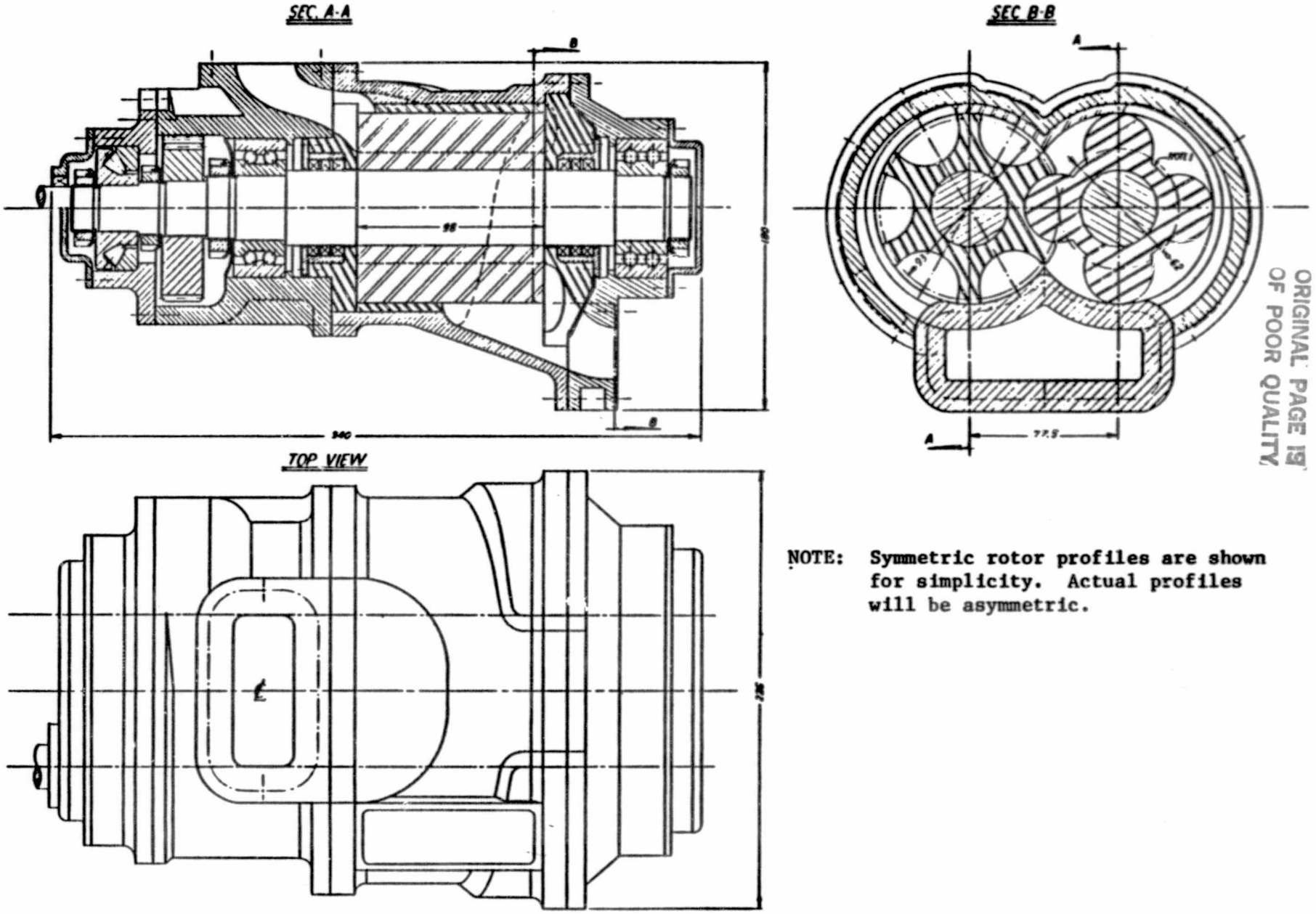

NOTE: Symmetric rotor profiles are shown for simplicity. Actual profiles will be asymmetric.

Figure 5. SCREW EXPANDER LAYOUT (98 mm diameter)

ANALYTICAL MODEL OF OVERALL ISENTROPIC EFFICIENCY FOR SCREW MACHINES

Because of the differences between compressor and expander operation of a screw machine, two separate mathematical models describing the relationships between design and operating parameters and predictable overall isentropic efficiencies of such machines have been established. Both models were then used as a basis for computer simulation to calculate the effects of changes in selected operating variables and design parameter efficiency. Input variables corresponding to the operating conditions of the given reciprocator were used to investigate the efficiency mapping for both expander and compressor when operating as subcomponents of a positive displacement supercharged-compound system.

Compressor Overall Efficiency Model

The overall efficiency of screw compressor can be, in general, expressed as:

$$\eta_o = \eta_{i(cor)} \times \eta_f \times \eta_m \tag{20}$$

where:

$\eta_{i(cor)}$ = Corrected ideal efficiency accounting for losses from the cycle related to adiabatic work produced by:

- Difference between actual operating external pressure ratio and internal, built-in pressure ratio of given machine (Figure 6 illustrates this operating feature)
- Pressure drops at intake and discharge of machine depending on inlet and discharge porting design and velocity of flows
- Mass inertia which is due to angular acceleration of charge.

η_f = Efficiency accounting for leakage losses related to theoretical displacement of change. These losses depend on: the radial clearance between the rotors and the housing walls, the axial clearance between the rotors and the end plates of the housing, the clearance between the rotors; tip speed of rotors, actual pressure ratio and finally dimensions of rotors.

η_m = Mechanical efficiency which is dependent predominantly on the design of machine and to a lesser extent on its operating conditions.

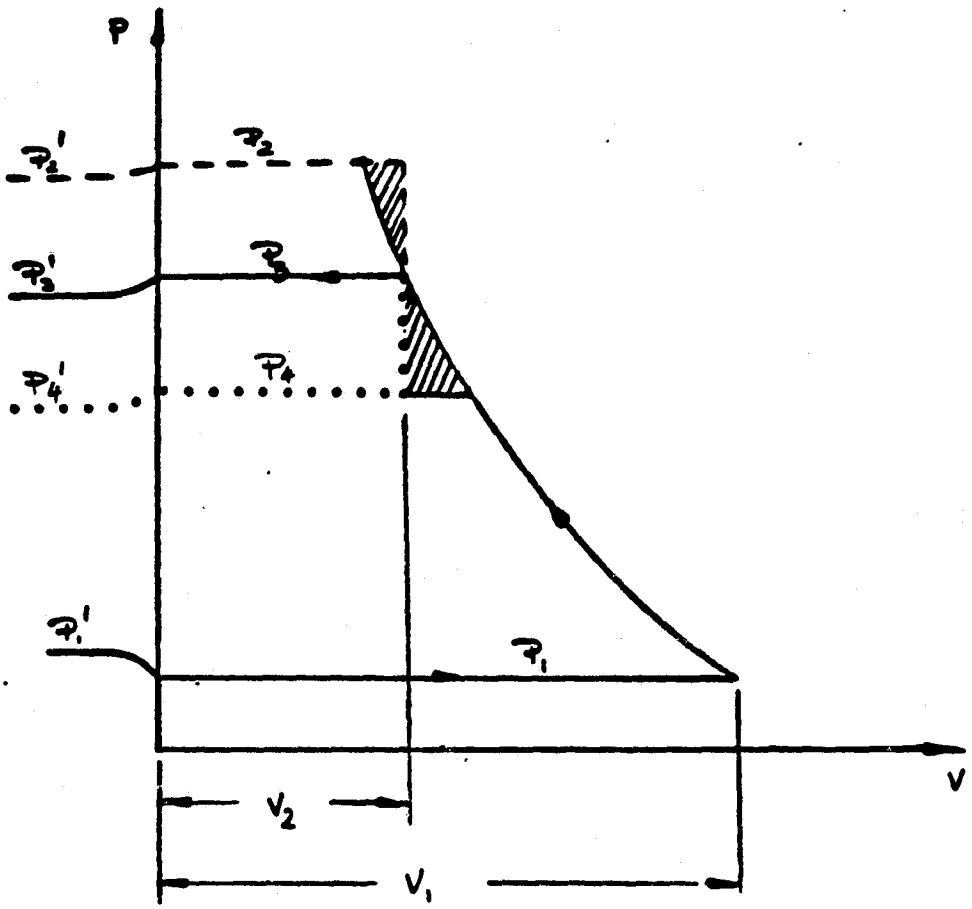

V_1 = Compressor displacement
V_2 = Compressor built-in compression volume
p_1 = Internal suction pressure
p_1' = External suction pressure
p_2; p_4 = Off-design internal discharge pressures
p_2'; p_4' = External discharge pressures corresponding to p_2 and p_4
p_3 = Design internal discharge pressure
p_3' = External discharge pressure corresponding to p_3

Figure 6. PRESSURE-VOLUME DIAGRAM OF SCREW COMPRESSOR

The terms of Equation 20 can be further represented in the following functional relationships:

Ideal Corrected Efficiency $\eta_{i(cor)}$

$$\eta_{i(cor)} = \frac{1}{\frac{1 + 2\frac{\kappa - 1}{\kappa + 1} M_u^2}{\eta_i} + \frac{2M_u^2}{9.81\left(\left[\frac{p_2}{p_1}\right]^{\frac{\kappa - 1}{\kappa}} - 1\right)}} \tag{21}$$

$$M_u = \frac{u_t}{u_s} = \frac{\pi D_m i_d n_r}{(60)(381)} \tag{21a}$$

$$\eta_i = \frac{\left(\frac{p_2}{p_1}\right)^{\frac{\kappa - 1}{\kappa}} - 1}{\frac{\varepsilon^{\kappa - 1}}{\kappa} - 1 + \frac{(\kappa - 1)}{\kappa} \frac{\frac{p_2}{p_1}}{\varepsilon \eta_{in} \eta_{out}}} \tag{21b}$$

$$\varepsilon = \frac{V_1}{V_2} = \left(\frac{p_3}{p_1}\right)^{1/\kappa} \tag{21c}$$

$$\eta_{in} = \left(1 - \frac{\kappa - 1}{\kappa + 1} [M_u \tan \alpha]^2\right)^{\frac{\kappa}{\kappa - 1}} \tag{21d}$$

$$\eta_{out} = \left(1 - \frac{\kappa - 1}{\kappa + 1} [M_u \tan \alpha]^2 \left[\frac{p_1}{p_2}\right]^{\frac{\kappa - 1}{\kappa}}\right)^{\frac{\kappa}{\kappa - 1}} \tag{21e}$$

where:

M_u = Tip speed Mach number

u_s = Speed of sound (381 m/sec at standard conditions)

p_1 = Internal suction pressure

p_2 = Internal discharge pressure

p_3 = Internal compression pressure

ε = Volume compression ratio

η_{in} = Inlet efficiency

η_{out} = Outlet efficiency

α = Rotor helix angle, angle between front plane and helix.

Flow Efficiency η_f

$$\eta_f = 1 - F_f \left(\frac{p_2}{p_1}\right)^{\frac{\kappa+1}{2\kappa}} \frac{K_1 \pi}{K_2 K_3 M_u} \tag{22}$$

F_f = Flow factor defined empirically as a function of (p_2/p_1) for screw machines. Predicted F_f for advanced rotor profiles is shown in Figure 7.

$$K_1 = \frac{A_{GAP}}{D_m^2} \tag{22a}$$

$$K_2 = \frac{A_e}{D_m^2} \tag{22b}$$

$$K_3 = \frac{L}{D_m} \tag{22c}$$

where:

K_1— Clearance Factor: For D_m = 1.2 — 4 in K_1 = 0.01

For D_m = 4 — 8 in K_1 = 0.0075

For D_m > 8 in K_1 = 0.005

K_2— Profile Factor: For profiles with full addendum K_2 = 0.568

Mechanical Efficiency η_m

Mechanical efficiency (η_m) in our model was taken as 0.97.

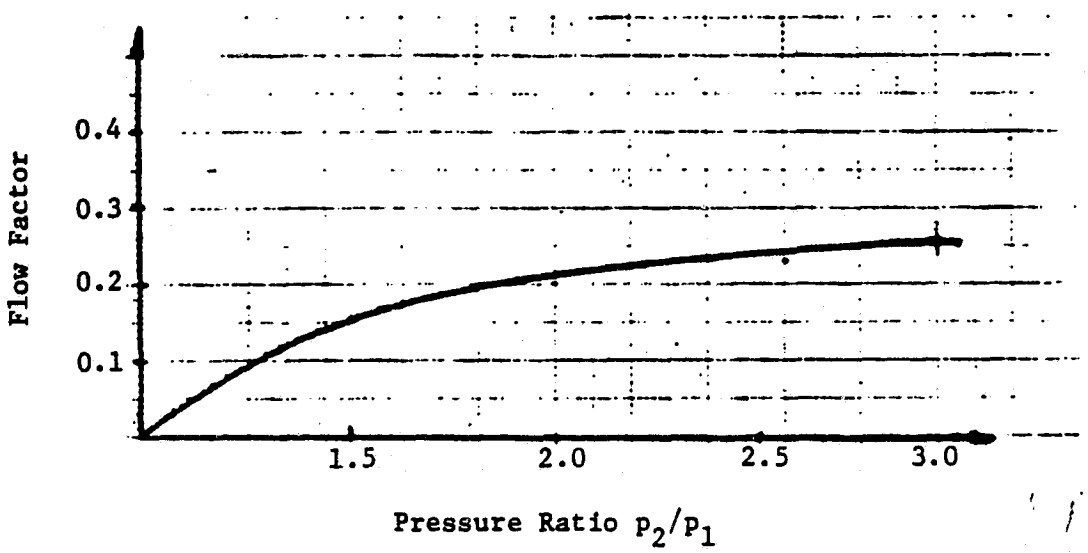

Figure 7. FLOW FACTOR VERSUS PRESSURE RATIO FOR ADVANCED ROTOR PROFILES FOR SCREW COMPRESSOR

Compressor Overall Efficiency Simulations

Compressor efficiency simulations have been carried out for design parameters specified previously. The influence of design changes on the overall efficiency of the compressor was considered by examining the sensitivity of efficiency to the clearance factor for K_1 = 0.01; 0.0075 and 0.0050.

The influence of operating conditions on overall efficiency was then analyzed in two different approaches. The first examined overall efficiency behaviour within pressure ratio range 1.5 to 5.0 for different fixed speeds of the compressor. Results of this part of analysis are enclosed in Appendix A. In the second approach, the expander was treated as a supercharger acting with a reciprocator. Overall efficiencies of the compressor-supercharger were correlated with four different speed characteristics specified by Cummins Diesel Co. corresponding approximately to 100%, 75%, 50%, and 25% of the reciprocator load. Results of this simulation are shown in Appendix B.

Expander Overall Efficiency Model

Figure 8 illustrates the expander operation for the screw machine. Our model of overall efficiency for the expander is based on the following assumptions:

- The expander is designed to meet the total expansion requirement; i.e., its displacement will assure total expansion of working medium from the highest expected expander feeding pressure
- The expander is equipped with an expansion ratio modulation system to prevent high overexpansion losses
- Venting losses represented in Figure 6 by the shaded area are a linear function of male rotor speed and flow through vent valve achieves critical value for reciprocator rpm, n_r = 3000
- The gas inertia losses are assumed to be 0. This is a realistic assumption because the acceleration losses are, to an extent, compensated for by the dynamic effect of expanded gases.

Given these assumptions, the expander overall efficiency is defined by:

$$\eta_o = \eta_{i(cor)}\ \eta_f\ \eta_m \qquad (23)$$

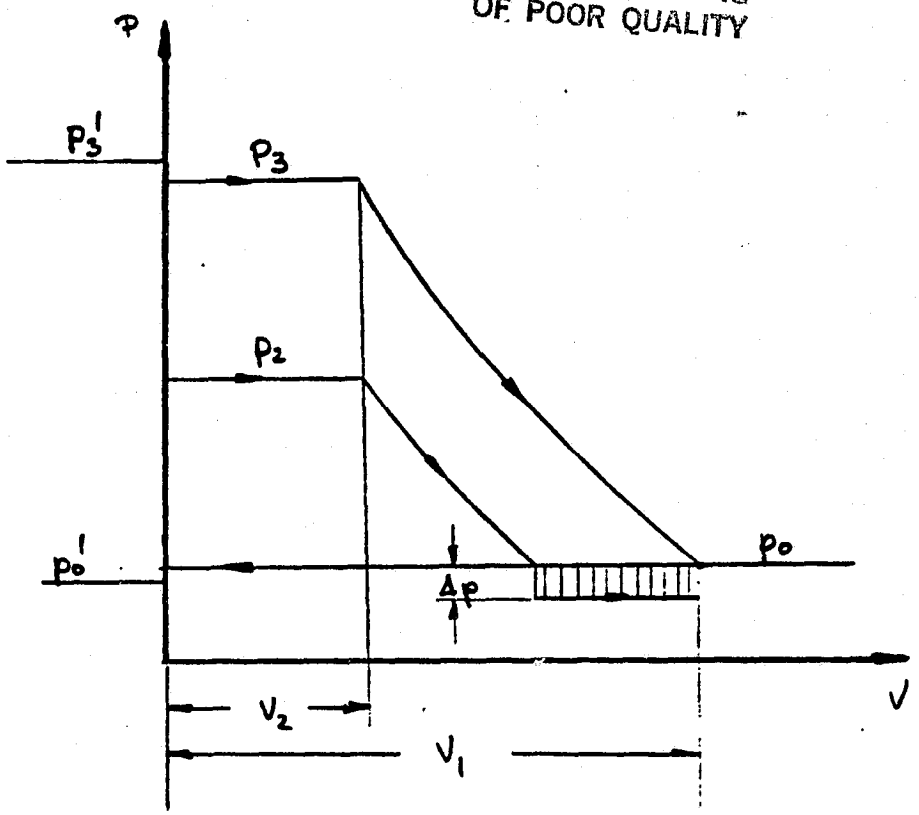

V_1 = Expander displacement
V_2 = Expander charging volume
Δp = Pressure drop corresponding to vent valve throttling
p_0 = Internal exhaust pressure
p_0' = External exhaust pressure
p_3 = Design point internal feeding pressure
p_3' = External pressure corresponding to p_3

Figure 8. PRESSURE-VOLUME DIAGRAM OF SCREW EXPANDER

Corrected Ideal Efficiency $\eta_{i(cor)}$

$$\eta_{i(cor)} = 1 - \frac{1 - \frac{1}{\varepsilon}\left(\frac{p_2}{p_0}\eta_{in}\,\eta_{out}\right)^{\frac{1}{\kappa}} 1.56 \times 10^{-4}\, n_r}{\frac{1}{\varepsilon} p_2 \frac{\kappa}{\kappa - 1}\left(1 - \left[\frac{p_0}{p_2}\right]^{\frac{\kappa - 1}{\kappa}}\right)} \qquad (24)$$

$\varepsilon = V_1/V_2 = (p_3/p_0)^{1/\kappa}$ (24a)

M_u = From Equation 21a (24b)

η_{in} = From Equations 21d (24c)

η_{out} = From Equations 21e (24d)

where:

p_2 = Actual expander feeding pressure

p_3 = Maximum expander feeding pressure

p_0 = Atmospheric pressure (or expander outlet pressure).

Flow Efficiency η_f

$$\eta_f = 1 - F_f \left(\frac{p_2}{p_0}\right)^{\frac{\kappa + 1}{2\kappa}} \frac{K_1}{K_2} \frac{\pi}{K_3 M_u} \qquad (25)$$

This formula is equivalent to Formula 22.

Mechanical Efficiency η_m

The expander mechanical efficiency, as in the case of the compressor, was assumed to be equal to 0.97.

Expander Overall Efficiency Simulations

The expander efficiency simulations were conducted for the fixed design parameters specified previously. The sensitivity of the efficiency of the expander to design changers was examined at clearance factor K_1 = 0.01, 0.0075 and 0.005.

The effect of operating conditions on overall efficiency was then analyzed in two different approaches. In the first we investigated the overall efficiency behaviour within a pressure ratio range of 1.5 to 6.0 for different fixed speeds of the expander. The overall efficiency values varied from negative 0.294 to positive 0.886 for engine speeds between 1000 to 3000 rpm and clearances factor (K1) between o.0050 and 0.010. In the second approach, the expander was treated as a component of a positive displacement compound system having clearance factor $K_1 = 0.0075$ and $K_1 = 0.005$, respectively. Pressure conditions at the expander inlet were those determined by Equation 19 and listed as "Exhaust Pressure" in Table 1. Temperature conditions at the expander inlet have been assumed as constant following the assumption made for the simulated reciprocator cucle. The expander overall efficiencies were correlated with reciprocator operating points specified by Cummins Diesel Co. corresponding approximately to 25%, 50%, 75% and 100% of the reciprocator load. The overall efficiency of the screw expander varied between 0.551 to 0.879 for engine speeds between 1000 to 3000 rpm.

SIMULATION OF POWER PERFORMANCE CHARACTERISTICS

After having determined the overall isentropic efficiencies for both compressor and expander, it was possible to conduct a numerical simulation of theoretical power required to drive the screw supercharger and theoretical power output to be expected from the screw expander.

The theoretical power input to the compressor at standard atmospheric conditions at the compressor inlet can be expressed as:

$$P_{com} = 6.706\ \dot{m}_a \frac{1}{\eta_{o\ com}} \left([\pi_c]^{\frac{\kappa - 1}{\kappa}} - 1\right) \qquad (26)$$

where:

P_{com} = Theoretical required power input, hp

$\dot{m}_a$ = Mass flow of supercharging air, kg/min

π_c = Compressor pressure ratio

$\eta_{o\ com}$ = Compressor overall isentropic efficiency.

The theoretical power output of the expander shaft at constant temperature conditions T_3 = 1090°K, as assumed by Cummins, can be expressed as:

$$P_{exp} = 23.985\ \dot{m}_a\ (1 + R_{f/a})\ \left(1 - \frac{1}{\pi_e}\right)^{\frac{\kappa - 1}{\kappa}}\ \eta_{o\ exp} \qquad (27)$$

where:

P_{exp} = Theoretical delivered power output, hp

$R_{f/a}$ = Fuel/air ratio of reciprocator

π_e = Expander expansion pressure ratio

$\eta_{o\ exp}$ = Expander overall isentropic efficiency.

Reciprocator shaft compounding power (excluding consideration of power train mechanical efficiency) can be defined as:

$$P_{comp} = P_{exp} - P_{com}$$

To obtain values of potential compressor power requirements, expander power delivery, and net system power delivery, the compressor and expander efficiencies were combined with the engine performance characteristics. This was done using clearance factors (K_1) of 0.0075 and 0.005. The results of this simulation for 25%, 50%, 75% and 100% of reciprocator full loading are between (a) 4.009 to 16.725 hp for the compressor power required, (b) 5.430 to 30.954 hp for the expander power delivered and (c) negative 0.970 to positive 15.097 net power delivered when varying the engine speed between 1000 to 3000 rpm.

DETERMINATION OF MASS MOMENTS OF INERTIA FOR SCREW MACHINE ROTORS

The evaluation of the contribution of the screw compressor-expander system to the overall inertia characteristics of a total compound system can be established when mass moments of inertia for rotors of both screw machines are known.

The following simplifying assumptions and design prerequisites are made for the derivation of analytical formulas describing mass moments of inertia of the rotors of both machines:

- Mass moments of inertia are determined for circular, symmetrical profiles
- Second area moments of actual shapes of male lobes and female voids are approximated by second area moments of semicircles with their centers located at pitch circles of male and female rotors respectively. This approximation introduces a negligible error of female rotor mass distribution, and the error for the male rotor can be easily corrected
- Actual component mass moment of root cylinder of the male rotor was replaced by mass moment of the relevant pitch cylinder, to correct for the mass distribution error introduced by the preceeding assumption
- Formulas for mass moments of inertia for both rotors are to account for rotor composite structure, i.e., steel core (shaft) and ceramic shell.

Figure 9 illustrates the above assumptions on the cross section of the profiles.

Mass Moment of Inertia for Female Rotor

Dividing the cross-sectional area of the female rotor into component areas shown in Figure 9 and then applying the parallel-axis theorem, the second moment of the female rotor cross-sectional area with respect to axis of rotation O_2 can be defined, in general, as:

$$I_{O_2,A_F} = I_{O_2,A_f} - 6(I_{O_2',A_L} + A_L r_f^2) + I_{O_2,A_c} \qquad (28)$$

where:

I_{O_2,A_F} = Second moment of cross-section area for female rotor with respect to axis O_2

I_{O_2,A_f} = Second moment of annular area for ceramic shell of female rotor with respect to axis O_2

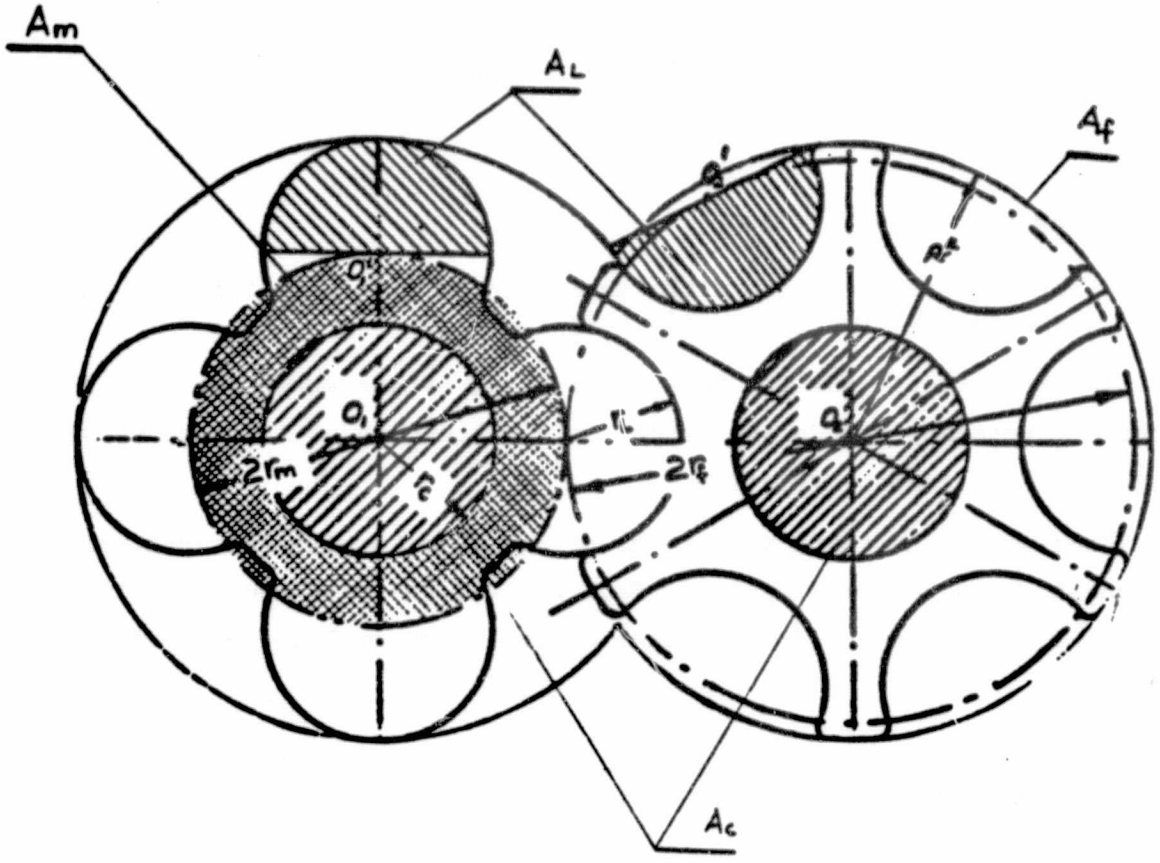

Figure 9. ROTOR CROSS SECTIONS CONSIDERED IN MASS MOMENT OF INERTIA ANALYSIS

I_{O_2',A_L} = Second moment of semicircular area for void in ceramic shell with respect to axis O_2' located at pitch radius r_f

I_{O_2,A_c} = Second moment of circular area for steel core of rotor with respect to axis O_2

A_L = Cross section area of void.

The second moment of area = the area moment of inertia.

The mass moment of inertia can then be expressed, in general, as:

$$I_{O,M} = \rho \int_{L_1}^{L_2} I_{O,A}(x)\, dx \qquad (29)$$

where:

ρ = Density of given mass

$I_{O,A}$ = Second moment of area with respect to axis of rotation as a function of section location along this axis.

For both the female and male rotors, all second moments of the component areas are constant and do not depend on the location of the section with respect to the axis or rotation.

Expressing the right side terms of Equation 28 with the appropriate component areas and then applying Equation 29, the mass moment of inertia in g cm^2 for the component female rotor of the screw machine takes the following form:

$$I_{O_2,MF} = \frac{\pi L}{2}\left(\rho_c\left[(R_F^4 - r_c^4) - 3r_L^2\,(r_L^2 + 2r_f^2)\right] + \rho_s\, r_c^4\right) \qquad (30)$$

where:

L = Length of rotor, cm

R_F = Outside radius of female rotor (without sealing strip), cm

r_c = Outside radius of steel core, cm

r_L = Void radius (same as lobe radius), cm

r_f = Pitch radius of female rotor, cm

ρ_c = Density of ceramics, g/cm^3

ρ_s = Density of steel, g/cm^3.

Equation 30 can be rewritten in units of kg ms^2:

$$I_{O_2,MF} = 5.1 \times 10^{-9}\ \pi L\ (\rho_c\ [R_F^4 - r_c^4] - 3r_L^2\ [r_L^2 + 2r_f^2]\ \rho_s\ r_c^4) \qquad (31)$$

Mass Moment of Inertia for Male Rotor

Dividing the cross section area of male rotor into component areas shown rotor cross-section with respect to axis of rotation O_1 can be defined as:

$$I_{O_1,A_M} = I_{O_1,A_m} + 4(I_{O_1',A_L} + A_L \times r_m^2) + I_{O_1,A_c} \qquad (32)$$

where:

I_{O_1,A_M} = Second moment of cross-section area for male rotor with respect to axis O_1

I_{O_1,A_m} = Second moment of annular area for ceramic shell of male rotor with respect to axis O_1

I_{O_1',A_L} = Second moment of semicircular area for lobe in ceramic shell with respect to axis O_1' located at pitch radius r_m

I_{O_1,A_c} = Second moment of circular area for steel core of rotor with respect to axis O_1

A_L = Cross section area of lobe (same as void area due to assumptions made).

Because Equation 29 is also valid for the male rotor, the equation for mass moment of inertia for composite male rotor reads in units of g cm^2 is:

$$I_{O_1,MM} = \frac{\pi L}{2}\ (\rho_c\ [r_m^4 - r_c^4] + 2r_L^2\ [r_L^2 + 2r_m^2] + \rho_s\ r_c^4) \qquad (33)$$

where:

L = Length of rotor, cm

r_m = Pitch radius of male rotor, cm

r_c = Outside radius of steel core, cm

r_L = Lobe radius (same as void radius), cm

ρ_c = Density of ceramics, g/cm^3

ρ_s = Density of steel, g/cm^3

Equation 33, restated in units of kg ms^2, is:

$$I_{O_1,MM} = 5.1 \times 10^{-9} \pi L \left(\rho_c \left[(r_m^4 - r_c^4) + 2r_L^2 (r_L^2 + 2r_m^2)\right] + \rho_s r_c^4\right) \quad (34)$$

Evaluation of Mass Moments of Inertia for Light-Duty Compressor-Expander System

Equations 32 and 35 have been used in determining numerical values of mass moments of inertia for rotors of both compressor and expander preliminarily designed previously. The specifications used and results obtained are listed below:

Compressor

$\rho_c = 3.2$ g/cm^3

$\rho_s = 7.6$ g/cm^3

Male Rotor

$L = 7.1$ cm

$r_c = 1.0$ cm

$r_m = 2.0$ cm

$r_L = 1.1$ cm

$I_{O_1,MM} = 1.44 \times 10^{-5}$ kg ms^2

Female Rotor

$R_F = 3.1$ cm

$r_f = 3.0$ cm

$I_{O_2,MF} = 8.73 \times 10^{-6}$ kg ms^2

Expander

$\rho_c = 3.2$ g/cm^3

$\rho_s = 7.6$ g/cm^3

Male Rotor

$L = 9.8$ cm

$r_c = 1.0$ cm

$r_m = 3.1$ cm

$r_L = 1.8$ cm

$I_{O_1,MM} = 1.20 \times 10^{-4}$ kg ms^2

Female Rotor

$R_F = 4.9$ cm

$F_f = 4.65$ cm

$I_{O_2,MF} = 6.33 \times 10^{-5}$ kg ms^2

SUMMARY OF RESULTS AND RECOMMENDATIONS

In summary, we have preliminarily designed a screw compressor and expander for use in a light-duty, positive displacement, compounded diesel system. We have also assessed the potential efficiency characteristics of these machines across a range of operating conditions, with maxima of 85% for the compressor and 88% for the expander, and estimated the compressor, expander, and acceptable net system power levels for various operating points of a light duty diesel engine. In addition, we have assessed the rotational inertia of the compressor and expander and estimated their effect on the system.

The analysis described in this report is of a preliminary nature and pursuit of this promising concept would require additional study to further quantify the effects of various parameters on performance, such as clearances, varying design pressure ratios, and expander inlet pressurization (ramming). Because of this, we have to recommend that more extensive and detailed analytical work be carried out to improve understanding of the above effects and their influence on design parameters of both machines and to assess the technological requirements in view of the desired clearances and tolerances.

CONCLUSIONS

As a result of our work, we have concluded that:

- The screw compressor and expander designed for light-duty Diesel engine applications are viable alternatives to turbo-compound systems, producing acceptable efficiencies for both units

- The rotational inertia of the screw compressor and expander will only have a moderately negative effect on the transient performance of the system, which can be easily compensated by an appropriate design of the flywheel.

BIBLIOGRAPHY

Abbott, M. M. and Van Ness, H. C., Thermodynamics. New York: McGraw-Hill Book Co., 1972.

Adkins, R. W. and Larson, C. S., "Basic Geometric Methods in Helical Lobe Compressor Design." Paper 70-WA/FE-23, presented at the ASME Winter Annual Meeting, New York, November 29-December 3, 1970.

Beer, F. P. and Johnston, Jr, E. R., Vector Mechanics for Engineers: Statics and Dynamics. New York: McGraw-Hill Book Co., 1972.

Chlumsky, V., Reciprocating and Rotary Compressors. Prague, Czechoslovakia: SNTL-Publishers of Technical Literature, 1965.

Fischer, W. C., "Production Design of a Modern, Axial-Flow Positive-Displacement Rotary Compressor." Paper No. 59-OGP-3 presented at the Oil and Gas Power Conference and Exhibit of the American Society of Mechanical Engineers, Houston, April 19-23, 1959.

Hodge, J., "Some Aspects of Screw Compressors." Paper 16, Proc. Institution Mech. Engrs., 1969-70, V. 184, p. 153-158.

O'Neill, P. and Beatts, W., "The Oil-Free Screw Compressor." Paper 19, Proc. Institution Mech. Engrs., 1969-70, V. 184, p. 175-182.

Scheel, L. F., "A Technology for Rotary Compressors," Journal of Engineering for Power, p. 207-16 (1970) July.

Schibbey, H., "Present Status of the Screw Compressor and Its Noise Problems." Gas Warme International, 22 (11), p. 431-4 (1973) November.

Trulsson, I., "A New Development in Rotary Screw Compressor Design." Paper 14, Proc. Institution Mech. Engrs., 1969-70, V. 184, p. 137-143.

Wichert, K. W., "Characteristics of Helical, Rotary, Positive Displacement Compressors." Paper No. 61-HYD-18 presented at the joint ASME-EIC Hydraulic Conference, Montreal, May 7-10, 1961.

NOMENCLATURE

Nomenclature used in Analysis of Reciprocator Performance Data, Preliminary Design Specification of the Screw Compressor, and Preliminary Design of the Screw Expander sections.

a	= Profile addendum
C	= Active area profile constant for rotor
C_{wa}	= Wrap angle constant for rotor
D	= Outside diameter of rotor
D_m	= Outside diameter of male rotor
i_d	= Drive ratio between power shaft of expander and reciprocator crankshaft
i_t	= Timing gear ratio of compressor
L	= Length of rotor
L_c	= Distance between axes of rotors in screw machine
$\dot{m}_{a(max)}$	= Maximum mass flow rate of compressor
$\dot{m}_{ex}$	= Mass flow of exhaust gases
n_f	= Female rotor rotational speed
n_m	= Male rotor rotational speed
n_r	= Reciprocator speed
p_0	= Atmospheric pressure
p_2	= Boosting pressure at engine intake
p_{3d}	= Design pressure in exhaust manifold for expander operation
R_f	= Outside radius of female rotor
R_m	= Outside radius of male rotor
r_f	= Pitch radius of female rotor
r_m	= Pitch radius of male rotor
r_{ff}	= Root circle radius of female rotor
r_{mf}	= Root circle radius of male rotor

r_L = Lobe radius

T_0 = Ambient temperature

T_2 = Engine intake temperature

T_3 = Exhaust temperature of reciprocator
= Inlet temperature of expander

u_{tm} = Male rotor tip speed

$\dot{V}_a$ = Volume flow rate of compressor

$\dot{V}_{a(max)}$ = Maximum ideal volume flow rate of compressor

$\dot{V}^*_{a(max)}$ = Maximum actual volume flow rate

V_{ch} = Expander charging volume

V_{ss} = Engine displacement

$\dot{V}_{3d}$ = Volumetric flow rate at exhaust conditions
= Volumetric flow rate of expander

$\dot{V}_{4d}$ = Volumetric flow rate at expander outlet

π_{cd} = Design pressure ratio of compressor

π_{ed} = Expander design pressure ratio

η_v = Volumetric efficiency

Nomenclature used in the Analytical Model of Overall Isentropic Efficiency for Screw Machines and Simulation of Power Performance Characteristics sections.

A_e = Area factor for leakage between rotors, related to profile type

A_{GAP} = Area factor for leakages around rotors, related to clearance

D_m = Male rotor outer diameter

F_f = Flow factor for calculation of flow efficiency

i_d = Compressor to engine crankshaft drive ratio

K_1 = Clearance factor

K_2 = Profile factor

K_3 = Ratio of rotor length to male diameter

L	= Length of rotor
M_u	= Tip speed Mach numbers (tip speed/speed of sound)
$\dot{m}_a$	= Mass flow rate of supercharging air
n_r	= Engine speed
P_0	= Internal exhaust pressure of expander
P_1	= suction pressure of compressor
P_2	= Discharge pressure of compressor
P_3	= Design discharge pressure of compressor
P_3	= expander feeding (inlet) pressure
Δp	= Pressure drop due to vent valve throttling
P_{com}	= Theoretical power requirement of compressor
P_{comp}	= Theoretical power delivered by positive displacement compound system to engine
P_{exp}	= Theoretical power delivered by expander
$R_{f/a}$	= Ratio of fuel to air for reciprocator
u_s	= Speed of sound
u_t	= Rotor tip speed
V_1	= Compressor displacement
V_2	= Compressor built-in compression volume
V_1	= Expander displacement
V_2	= Expander charging volume
α	= Rotor helix angle, angle between front plane of rotor and helix
ϵ	= Design volume compression ratio
η_f	= Efficiency accounting for leakage and flow losses
η_i	= Adiabatic efficiency
$\eta_{i(cor)}$	= Corrected ideal efficiency of compressor or expander
η_{in}	= Inlet efficiency of the compressor
η_m	= Mechanical efficiency

η_o = Overall efficiency of screw compressor or expander

η_{out} = Outlet efficiency of the compressor

$\eta_{o\ com}$ = Overall isentropic efficiency of compressor

$\eta_{c\ exp}$ = Overall isentropic efficiency of expander

π_c = Compressor pressure ratio

π_e = Expander pressure ratio

Nomenclature used in the Determination of Mass Moments of Inertia for Screw Machine Rotors section.

A_L = Cross-section area of void in rotor/cross-section area of rotor lobe

I_{O_1,A_M} = Second moment of cross-section area for male rotor with respect to axis O_1

I_{O_1,A_m} = Second moment of annular area for ceramic shell of male rotor with respect to axis O_1

I_{O_1',A_L} = Second moment of semicircular area for lobe in ceramic shell with respect to axis O_1' located at pitch radius r_m

I_{O_1,A_c} = Second moment of circular area for steel core of rotor with respect to axis O_1

$I_{O_1,MM}$ = Mass moment of inertia of male rotor

I_{O_2,A_F} = Second moment of cross-section area for female rotor with respect to axis O_2

I_{O_2,A_f} = Second moment of annular area for ceramic shell of female rotor

I_{O_2',A_L} = Second moment of semicircular area for void in ceramic shell with respect to axis O_2' located at pitch radius r_f

I_{O_2,A_c} = Second moment of circular area for steel core of rotor with respect to axis O_2

$I_{O_2,MF}$ = Mass moment of inertia for female rotor

L = Length of rotor

R_F = Outside radius of female rotor

r_c = Outside radius of steel core

r_f = Pitch radius of female rotor

r_L = Void radius (same as lobe radius)

r_m = Pitch radius of the male rotor

ρ_c = Density of ceramic

ρ_s = Density of steel

D8

N85 13243

APPENDIX 8

THERMAL AND MECHANICAL ANALYSIS OF MAJOR COMPONENTS FOR THE ADVANCED ADIABATIC DIESEL ENGINE

CUMMINS TECHNOLOGY STAFF

ADVANCED ADIABATIC DIESEL CYLINDER HEAD

PROPOSED HEAD DESIGN

The proposed design for the Light Duty Diesel is an in-line four cylinder spark assisted diesel engine mounted transversely in the front of the vehicle. The engine has a one piece cylinder head, with one intake valve and one exhaust valve per cylinder. A flat topped piston is used with a cylindrical combustion chamber recessed into the cylinder head directly under the exhaust valve. A single ceramic insert is cast into the cylinder head to insulate both the combustion chamber and the exhaust port. A similar ceramic insert is cast into the head to insulate the intake port. A ceramic faceplate is pressed into the combustion face of the head to insulate the face of the head from hot combustion gas. The valve seats are machined directly into the ceramic faceplate for the intake valve and into the ceramic exhaust port insert for the exhaust valve. Additional ceramic applications in the head are the use of ceramic valve guides and ceramic insulated valves. The ceramic valve guides are press fit into the head and are used for increased wear resistance. The ceramic insulated valves are conventional valves with the valve faces plasma spray coated with ceramic for insulation.

FINITE ELEMENT THERMAL ANALYSIS

The prime focus of the finite element thermal analysis was the development of a model to predict temperatures in the ceramic and iron head during rated engine operating conditions. With no water cooling in the head, the potential for quite high metal temperatures exists. If sufficient insulation is not obtained around the combustion chamber, high cylinder head temperatures could make the uncooled head design impossible to use.

To predict head temperatures, a three-dimensional thermal finite element model was built using the ANSYS general purpose finite element program. The full thermal model contains approximately 1140 3-D solid elements, and is shown in Figures 1-3. Figure 1 shows a top view of the full model, while Figure 2 shows the model with the top layers removed to reveal the exhaust and intake ducts. Figure 3 shows the model looking up at the combustion face. If one considers the two interior cylinders of the head, due to the repeating symmetry of the design both side faces of the model should produce the same temperature profile. Special convection links were inserted between the two cut faces of the model with a high convection coefficient to force the two cut faces to the same temperature.

The finite element model is thermally loaded by convection with combustion gas across the faceplate and combustion chamber, exhaust gas inside the exhaust port, intake air inside the intake port, and outside ambient air on the exterior surfaces. Convection coefficient and gas temperature for the combustion process was taken from the cycle simulation performed by Luigi Tozzi using DCS. Temperatures for intake and exhaust gases were also taken from DCS. Convection coefficients were calculated using fully developed pipe flow theory and the mass flow rate for intake and exhaust gases. Outside convection coefficient and ambient temperature were based on past experience with thermal modeling of exhaust manifolds for NH and K engines. On these engines the exterior surface of the exhaust manifold sees the same free convection environment as the cylinder head. All convection coefficients and gas temperatures used with the model are included in Table 1. Material properties used for the iron and ceramic materials are listed in Table 2.

Figures 4-8 show the predicted temperature contours for the baseline set of convection boundary conditions. Figure 4 shows temperature contours on the surface of the ceramic faceplate, with a maximum temperature of 1680 deg. F occuring at the edge of the combustion chamber. Figure 5 shows temperature contours on the plane parallel to the combustion face just above the ceramic plate. This section just above the iron/ceramic interface is where the maximum iron temperatures of 1300 deg. F occur. Figures 6 and 7 are planes normal to the crank axis taken through the center of the exhaust valve/combustion chamber and intake valve respectively. Figure 8 shows temperature contours on the plan parallel to the crank axis passing through center of both valves and combustion chamber. As shown by Figures 6-8, the bulk of the cast iron head runs between 1000 and 1200 deg. F, with the exterior surface of the head running just over 1000 deg. F. These high exterior surface temperatures could pose installation problems requiring some type of insulation on the underside of the vehicle's hood.

The baseline combustion gas convection coefficient predicted by DCS assumes that uniform heat transfer exists across the head face. Since the combustion process will be primarily contained in the combustion chamber, higher heat transfer would be expected to occur in the combustion chamber than across the head face. It was assumed the convection coefficient across the face, and that the total heat flux (convection coefficient times the area that it acts over) would be the same as the DCS baseline convection coefficient. New convention coefficients calculated are also included in Table 1. Temperatures predicted using the 2:1 split in combustion convection coefficient are shown in Figures 9-13.

With the locally higher heat transfer in the combustion chamber, the maximum temperature seen at the ceramic surface does increase. However, the region of ceramic in excess of 1600 deg. F is smaller because it is contained locally to the region just around the combustion chamber. The maximum iron temperature that occurs just above the ceramic faceplate, (the area running above 1200 deg. F) is smaller. Overall, the difference in temperatures is small, and the assumption of uniform convection coefficient across the head face and combustion chamber is quite adequate.

To determine the effect of exterior cooling, the outside convection coefficient was doubled and the predicted temperatures are shown in Figures 14-18. The increased exterior cooling has a significant effect on the maximum iron temperature, with the maximum temperature just above the ceramic faceplate at 1125 deg. F as seen in Figure 15. The exterior surface of the head also shows a significant reduction in temperature to approximately 800-820 deg. F. Even with this 200 deg. F reduction in exterior head temperature, the engine compartment of the automobile may still need to be heavily insulated.

Examining the temperatures in the three previous cases shows the tendency of the intake port to cool the air. When intake air is heated under part load operation the insulation of the ceramic intake port will help maintain intake gas temperature when the head is cool. With the high metal temperatures being predicted, the increased cooling benefit of eliminating the ceramic intake insert might reduce heat temperatures and improve durability of the head. To determine the benefit of eliminating the ceramic intake insert the ceramic elements were replaced with iron in the cylinder model. Figure 19 shows temperatures along the plane through the intake. When compared to Figure 17, the elimination of the ceramic intake insert provides only minimal cooling for the head.

FINITE ELEMENT THERMAL STRESS ANALYSIS

To determine what thermal stresses could be expected in the proposed cylinder head, the thermal finite element model was modified to predict thermal stresses. In order to reduce computer time, just the lower part of the thermal model was used to determine thermal stresses in the ceramic faceplate and adjoining iron. Since the main thermal gradient runs through the thickness of the ceramic faceplate, the primary thermal expansion is expected in the plane of the combustion face. Experience with modeling the combustion face of the K cylinder head has shown that modeling just the lower portion of the head gives reasonable thermal stress results.

Thermal stresses in the lower portion of the model, under loading and with baseline temperatures, are shown in Figures 20 and 21.

Figure 20 shows the maximum compressive principal stress on the five cutting planes and Figure 21 shows the maximum tensile principal stress. The ceramic faceplate goes into compression and the surrounding iron goes into tension because the ceramic is hotter and is trying to grow more than the surrounding head. Maximum compressive stress in the ceramic is -59 ksi and occurs at the surface of the ceramic faceplate at the edge of the combustion chamber. Maximum tensile stress predicted in the iron is approximately 30 ksi and occurs just above the ceramic faceplate between the combustion chamber and the intake port.

The maximum tensile stress of 30 ksi in the iron is much too high for a typical cast iron operating at 1000+ deg. F. To achieve higher material strength at the elevated temperatures observed in the proposed head, an alloyed ferritic ductile cast iron, similar to that used for exhaust manifold castings, could be used. Since the finite element model assumes the faceplate to be rigidly attached to the surrounding iron, the tensile stresses predicted by the model are probably higher than those in the actual head. Even with a ferritic ductile iron and realizing the assumptions built into the model, the predicted tensile stresses in the iron are still high and methods to further cool the head should be explored.

CONCLUSIONS

Based upon temperatures predicted with a thermal finite element model, the proposed cylinder head will run quite warm, with exterior surface temperatures running around 800-1000 deg. F. The high exterior surface temperature of the head could pose a problem with installation of the engine, requiring additional insulation in the engine compartment. Maximum temperatures in the ceramic faceplate and combustion chamber insert are around 1680-1700 deg. F, with maximum temperatures in the surrounding iron running 1300 deg. F. Thermal stresses in the head are compressive in the ceramic faceplate and tensile in the iron around the faceplate. The potential for large tensile stresses in the ceramic intake insert at rated temperatures does exist, and should be recognized as a potential problem. Removing the ceramic insert from the intake duct would help cool the head, but only marginally.

With temperatures in the iron just above the faceplate running 1200-1300 Def. F, an alloyed ferritic ductile cast iron similar to CMS 41,081 should be used instead of gray iron to provide better high temperature material properties.

Only minimal press fit is needed on the ceramic faceplate to hold it in place during operation. The ceramic faceplate runs much hotter than the surrounding iron and has a similar coefficient of thermal

expansion, consequently the fit of the ceramic plate will tighten as the head heats up. The amount of press needed to secure the faceplate during machining of the valve seats will be the limiting factor as to how little press fit can be used.

TABLE 1
THERMAL BOUNDARY CONDITIONS

	h (Btu/(hr-sq.in-deg F)	T (deg F)
Baseline Case:		
Combustion Face	0.812	1828
Combustion Chamber	0.812	1828.
Inside Intake Port	0.598	440.
Inside Exhaust Port	0.387	1062.
Exterior Surface	0.054	100.
Lip Around Liner	0.065	1300.
2:1 Combustion Split:		
Combustion Face	0.612	1828.
Combustion Chamber	1.224	1828.
Twice Exterior Cooling:		
Exterior Surface	0.108	100.

TABLE 2
MATERIAL PROPERTIES

Cast Iron:

Thermal Conductivity, k	2 50 Btu/(hr-in-deg F)
Modulus of Elasticity, E	12,000,000 psi
Poisson's Ratio, ν	0.29
Coef. of Thermal Expansion, α	7.50 micro in./(in.-deg F)

Ceramic - NGK Z-37 Y2O3 Stabilized Zirconia:

Thermal Conductivity, k	0.117 Btu/(hr-in-deg F)
Modulus of Elasticity, E	29,000,000 psi
Poisson's Ratio, ν	0.31
Coef. of Thermal Expansion, α	5.72 micro in./(in.-deg F)

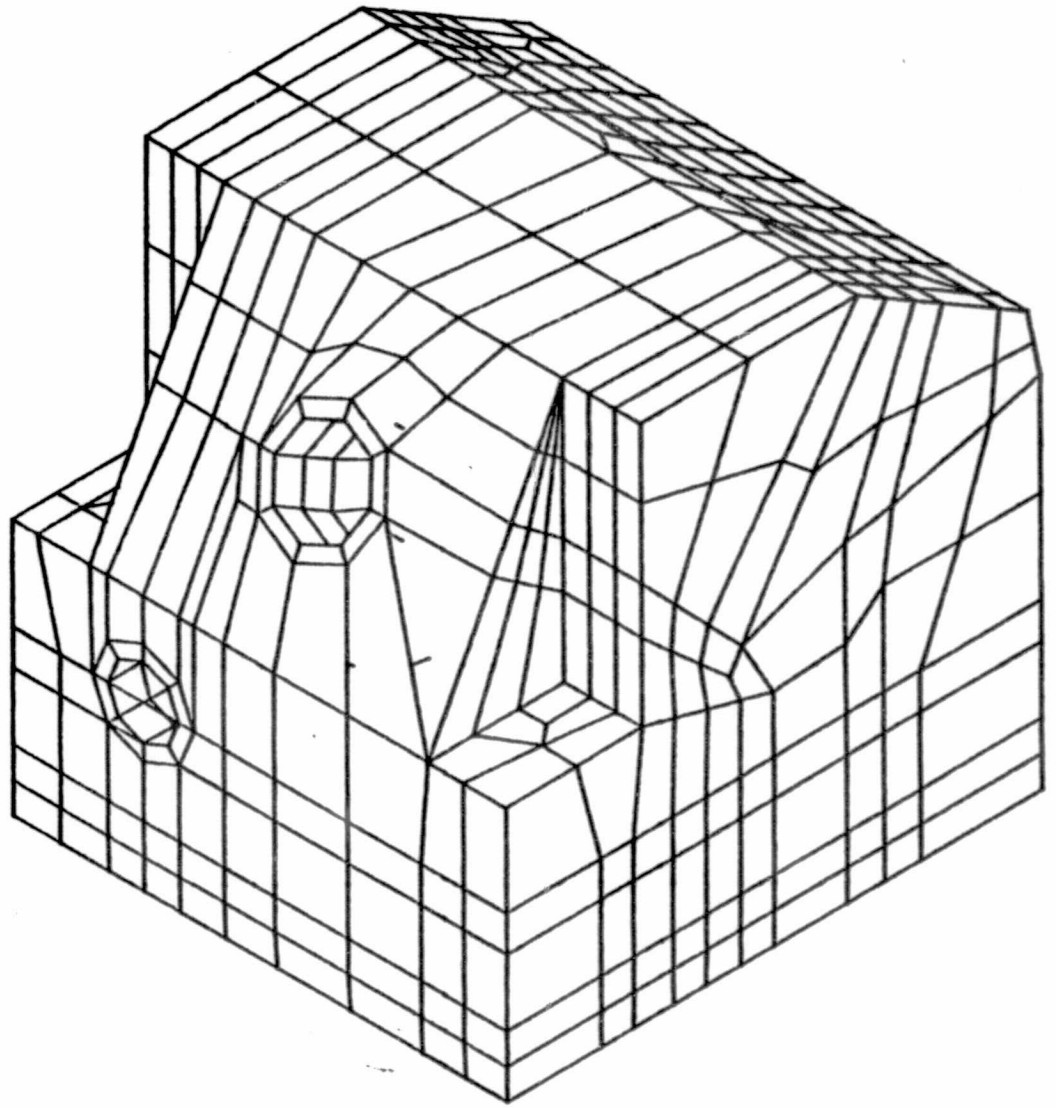

ORIGINAL PAGE IS
OF POOR QUALITY

Figure 1. THERMAL MODEL OF NASA LIGHT DUTY DIESEL CYLINDER HEAD HIDDEN ANSYS 1

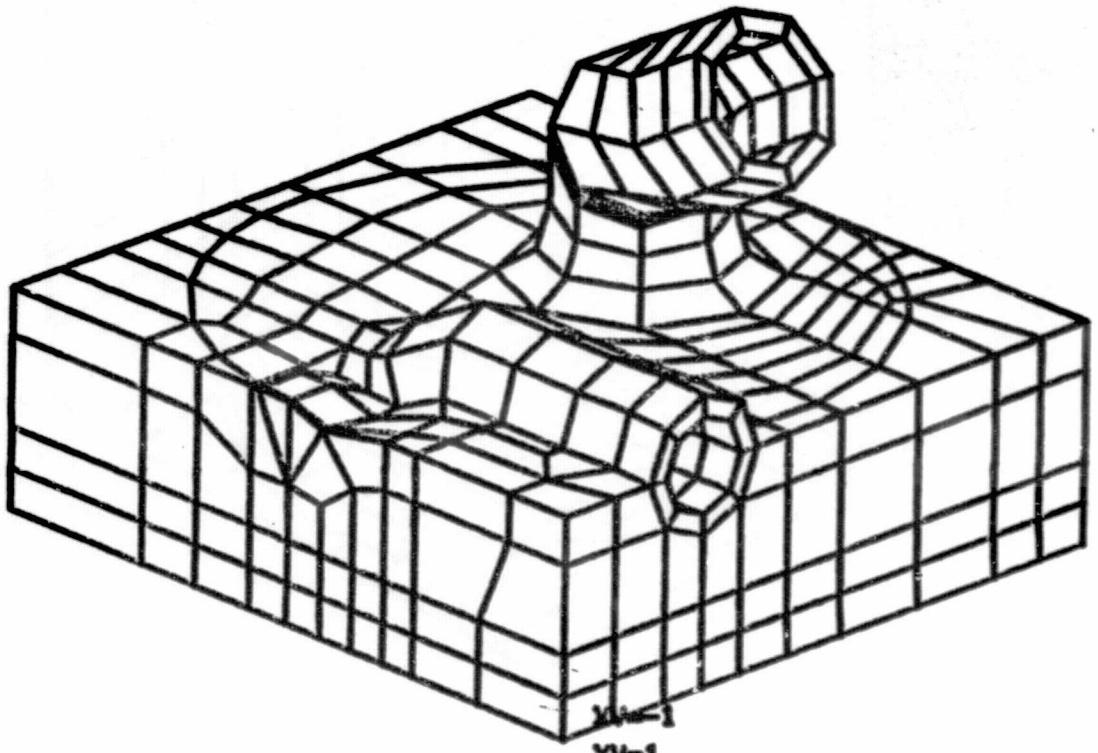

Figure 2. LIGHT DUTY DIESEL CYLINDER HEAD MODEL

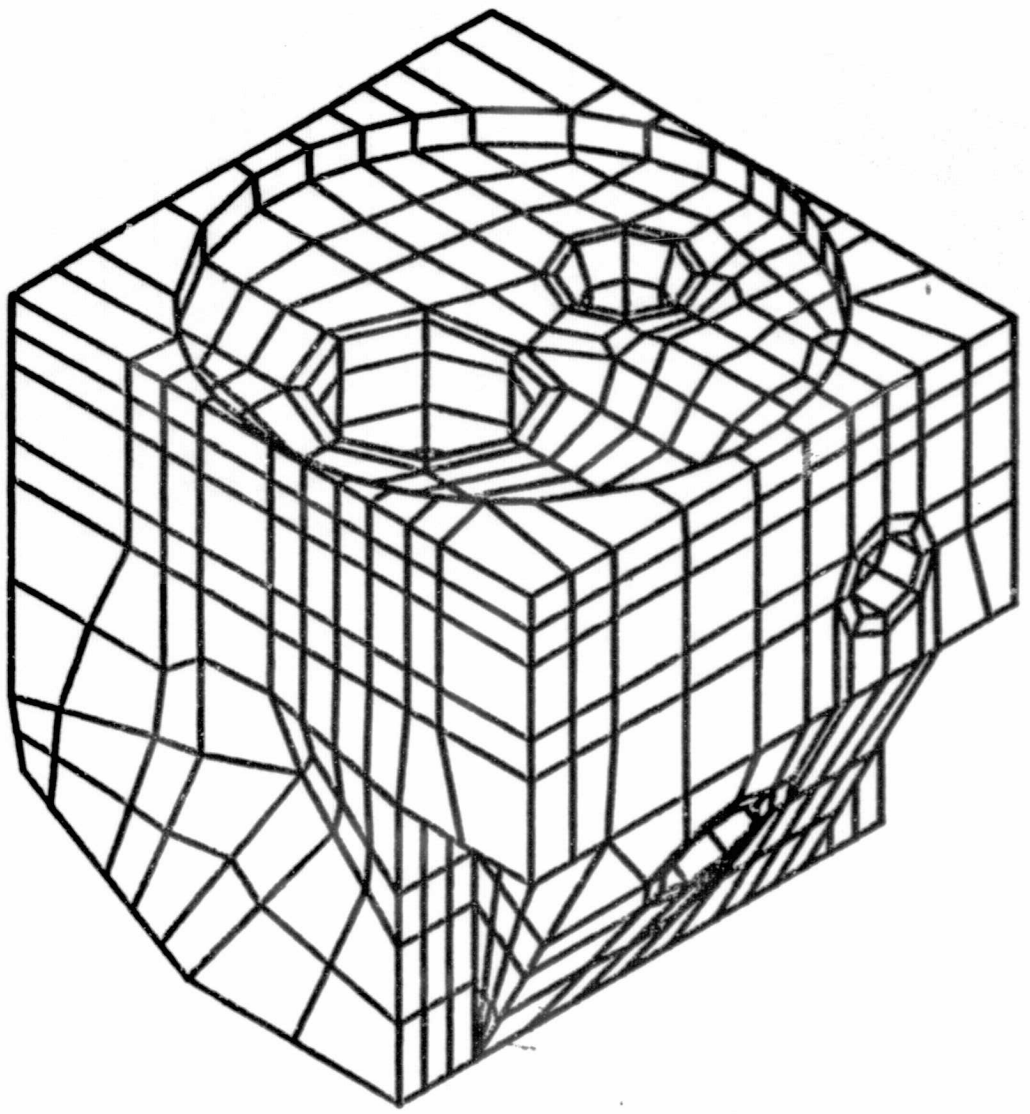

Figure 3. LIGHT DUTY DIESEL CYLINDER HEAD MODEL

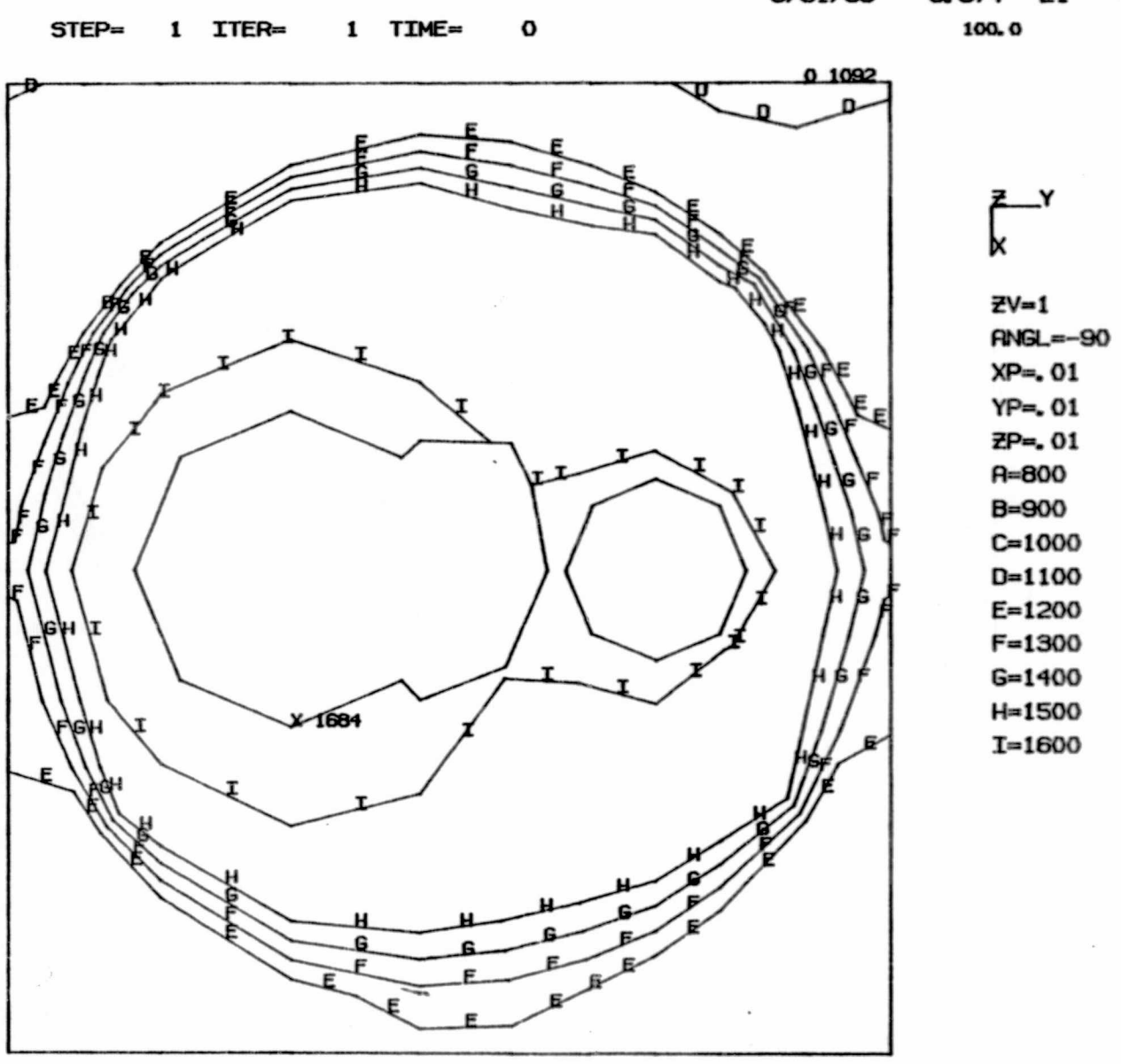

Figure 4. LIGHT DUTY DIESEL WITH BASELINE BOUNDARY CONDITIONS TEMP ANSYS 5

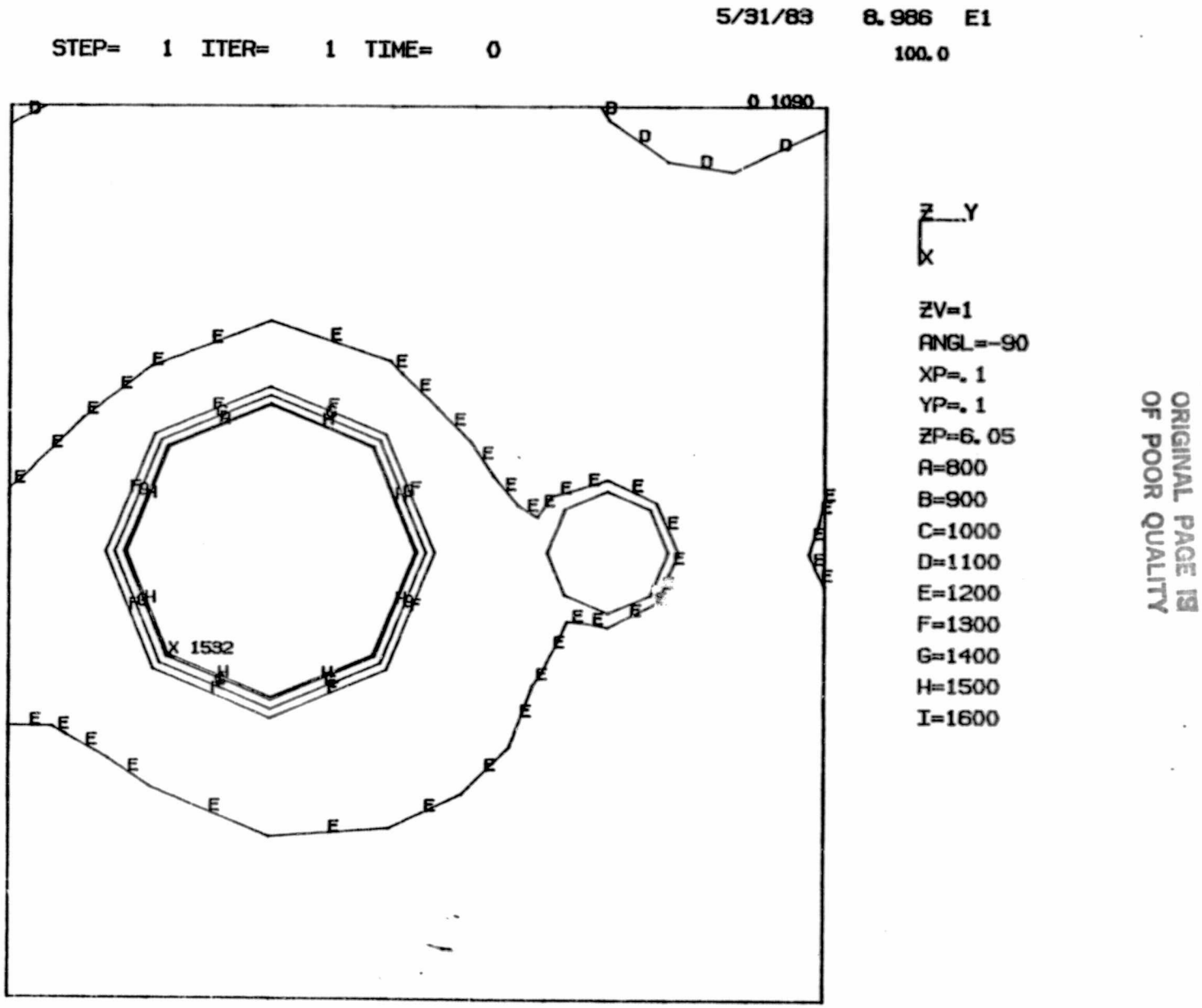

Figure 5. LIGHT DUTY DIESEL WITH BASELINE BOUNDARY CONDITIONS

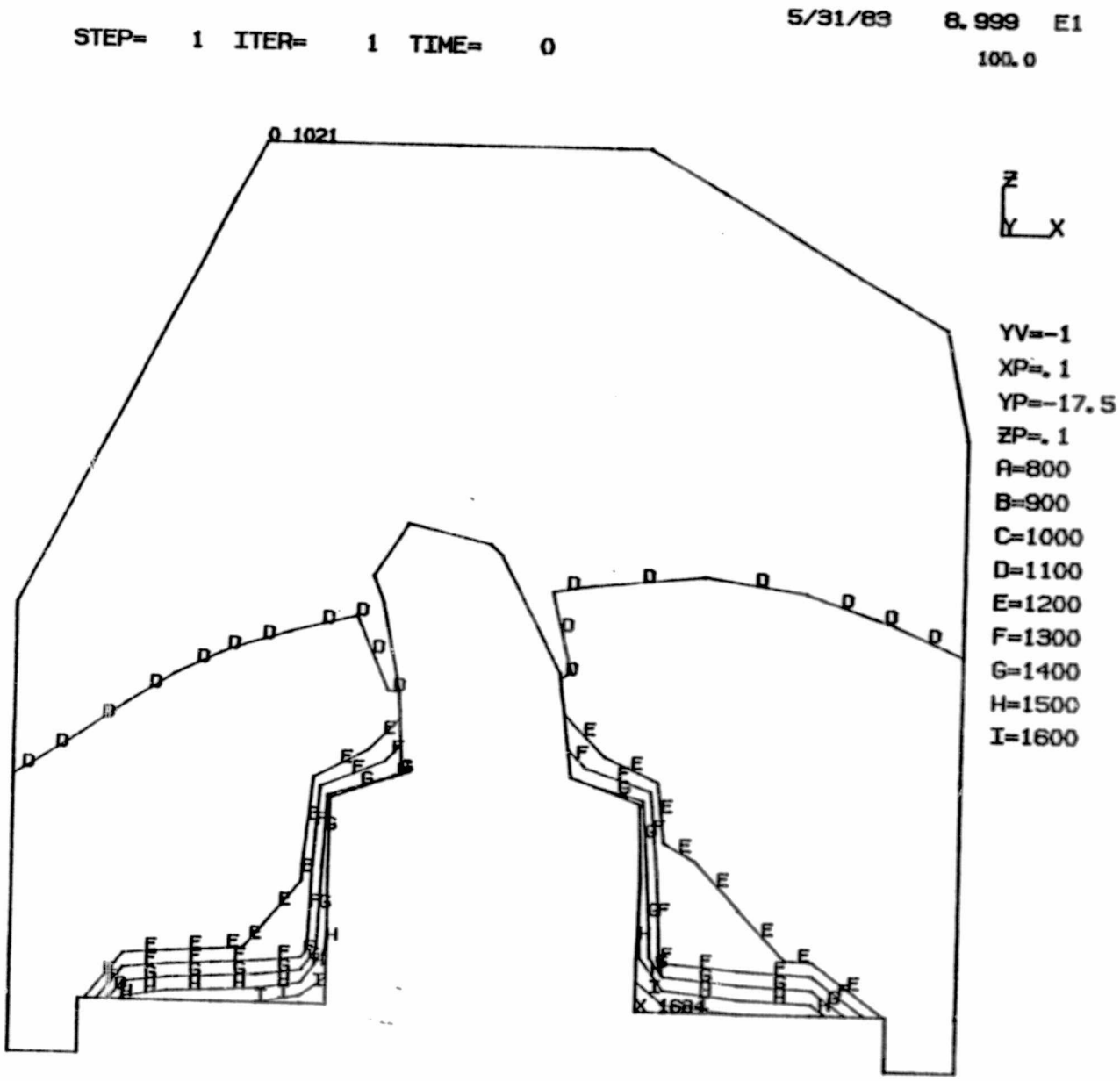

Figure 6. LIGHT DUTY DIESEL WITH BASELINE BOUNDARY CONDITIONS

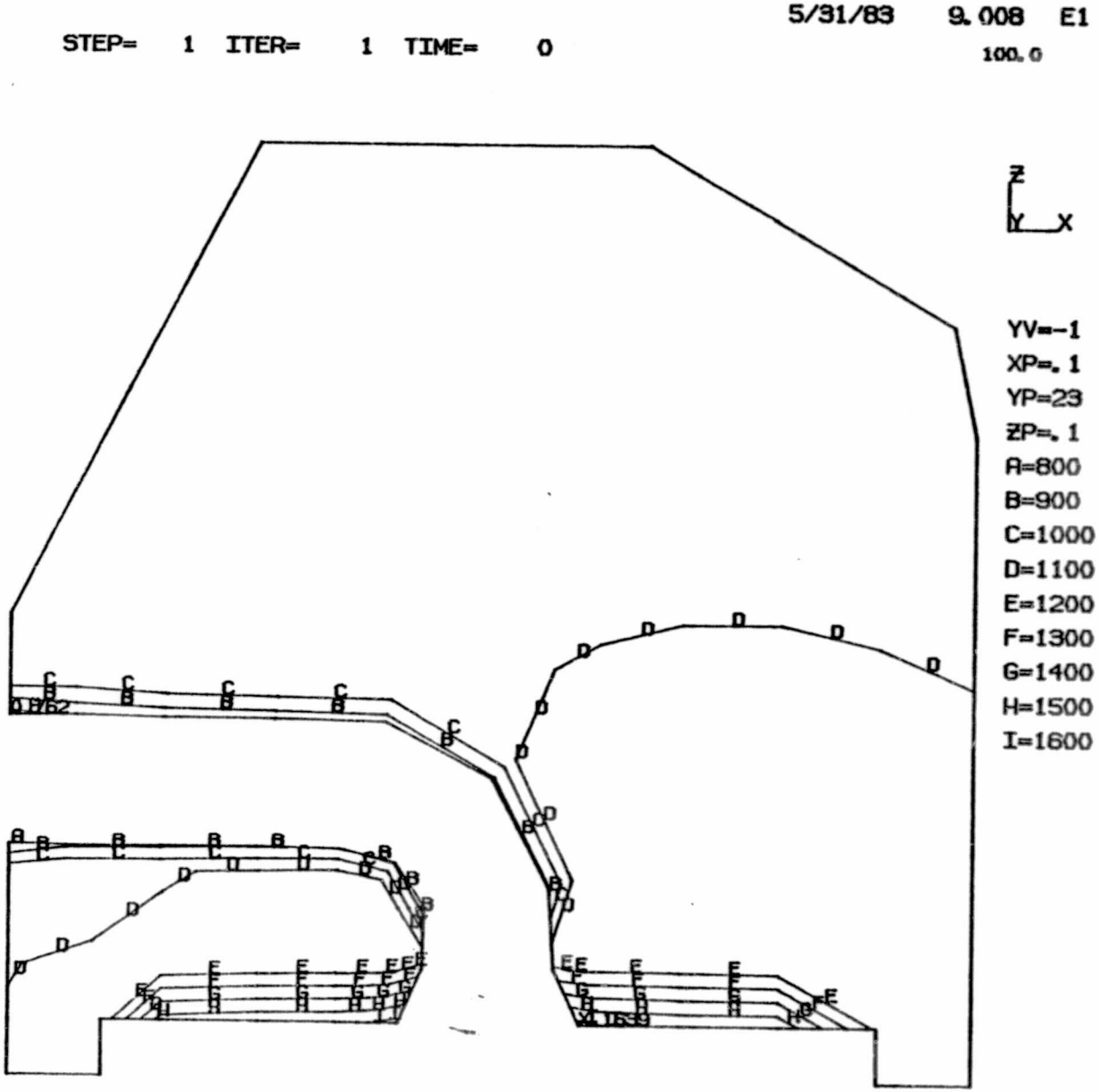

Figure 7. LIGHT DUTY DIESEL WITH BASELINE BOUNDARY CONDITIONS

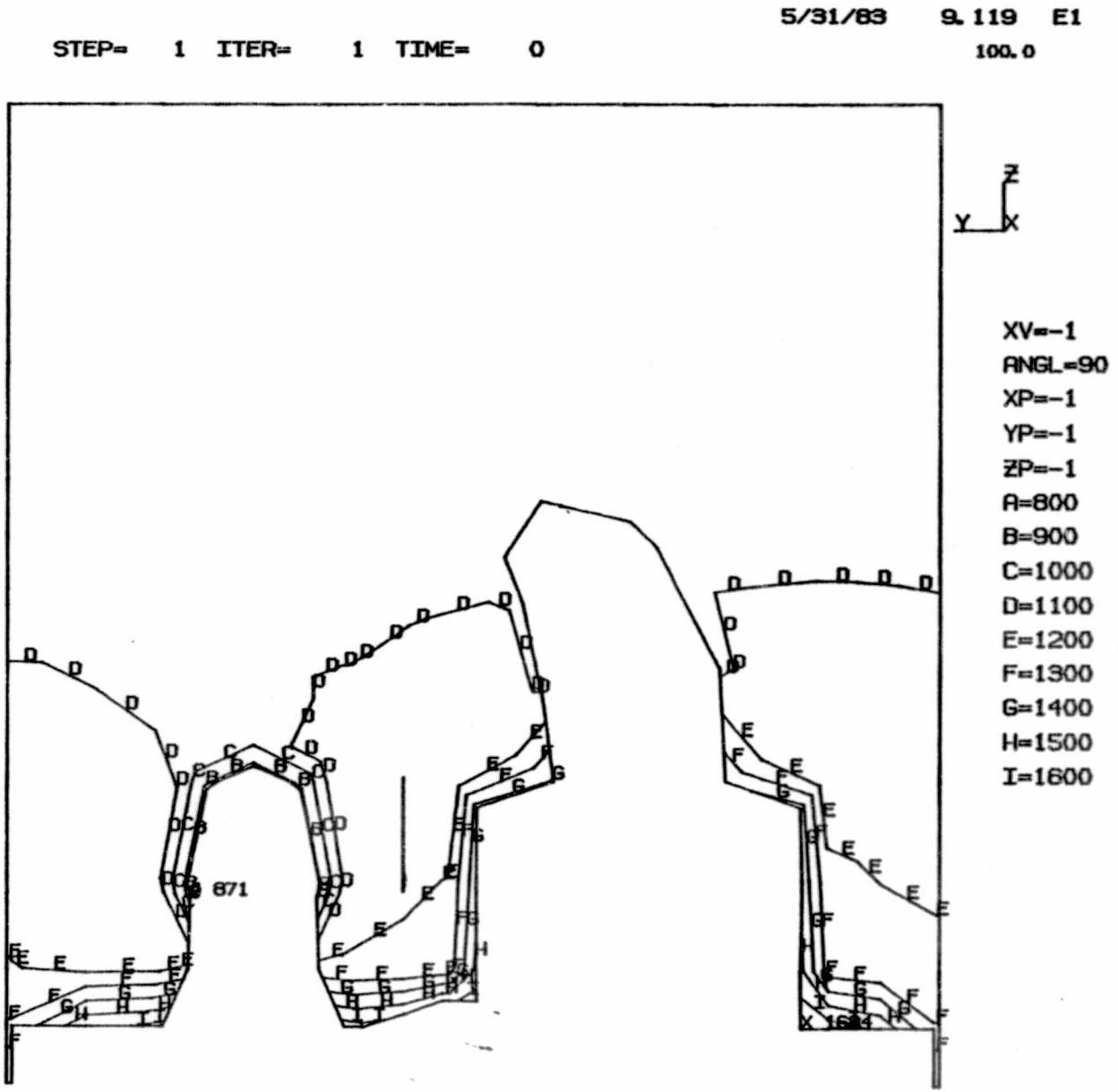

Figure 8. LIGHT DUTY DIESEL WITH BASELINE BOUNDARY CONDITIONS

TEMP ANSYS 15

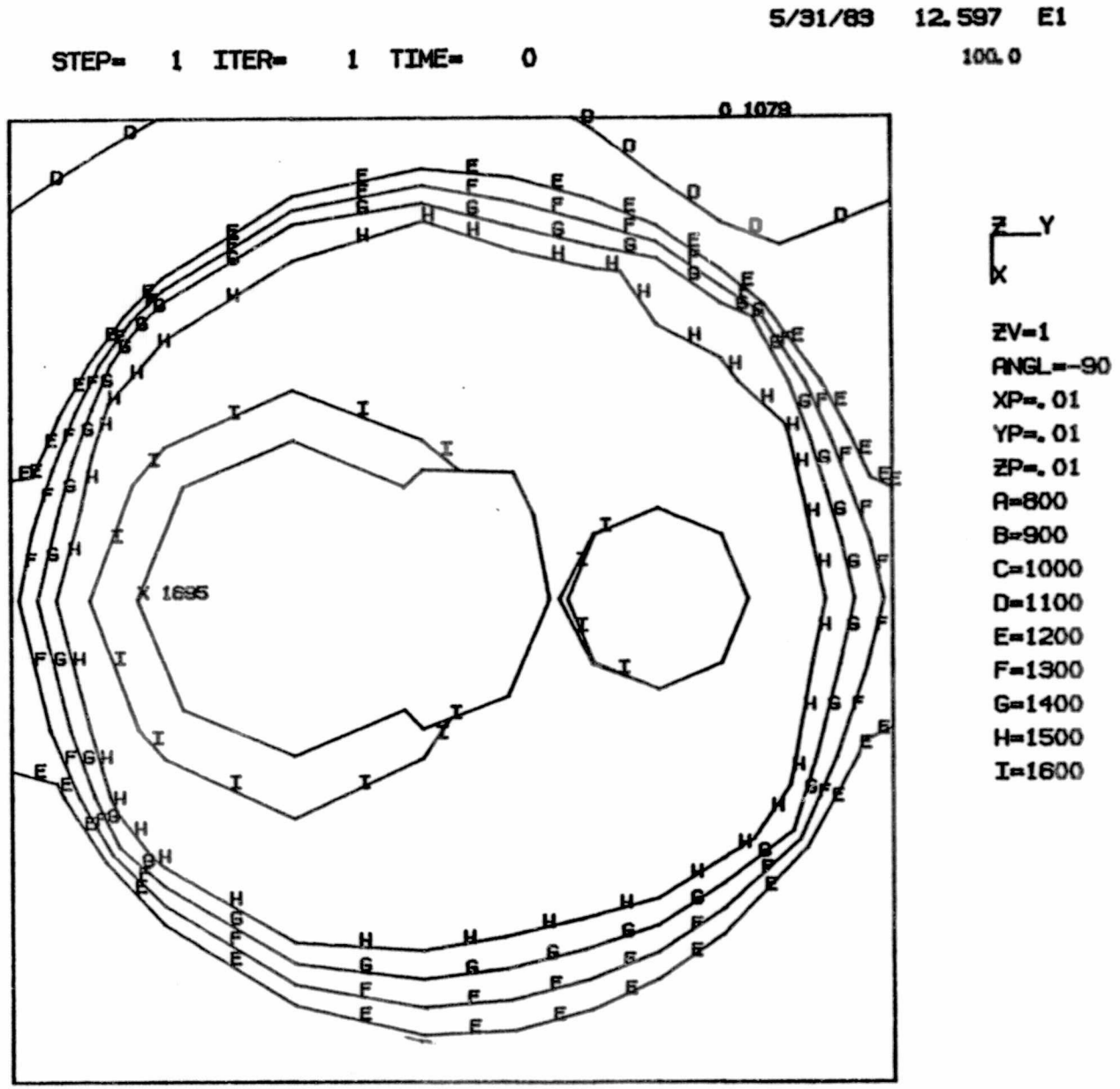

Figure 9. LIGHT DUTY DIESEL HEAD WITH 2-1 H SPLIT IN COMBUSTION TEMP ANSYS 9

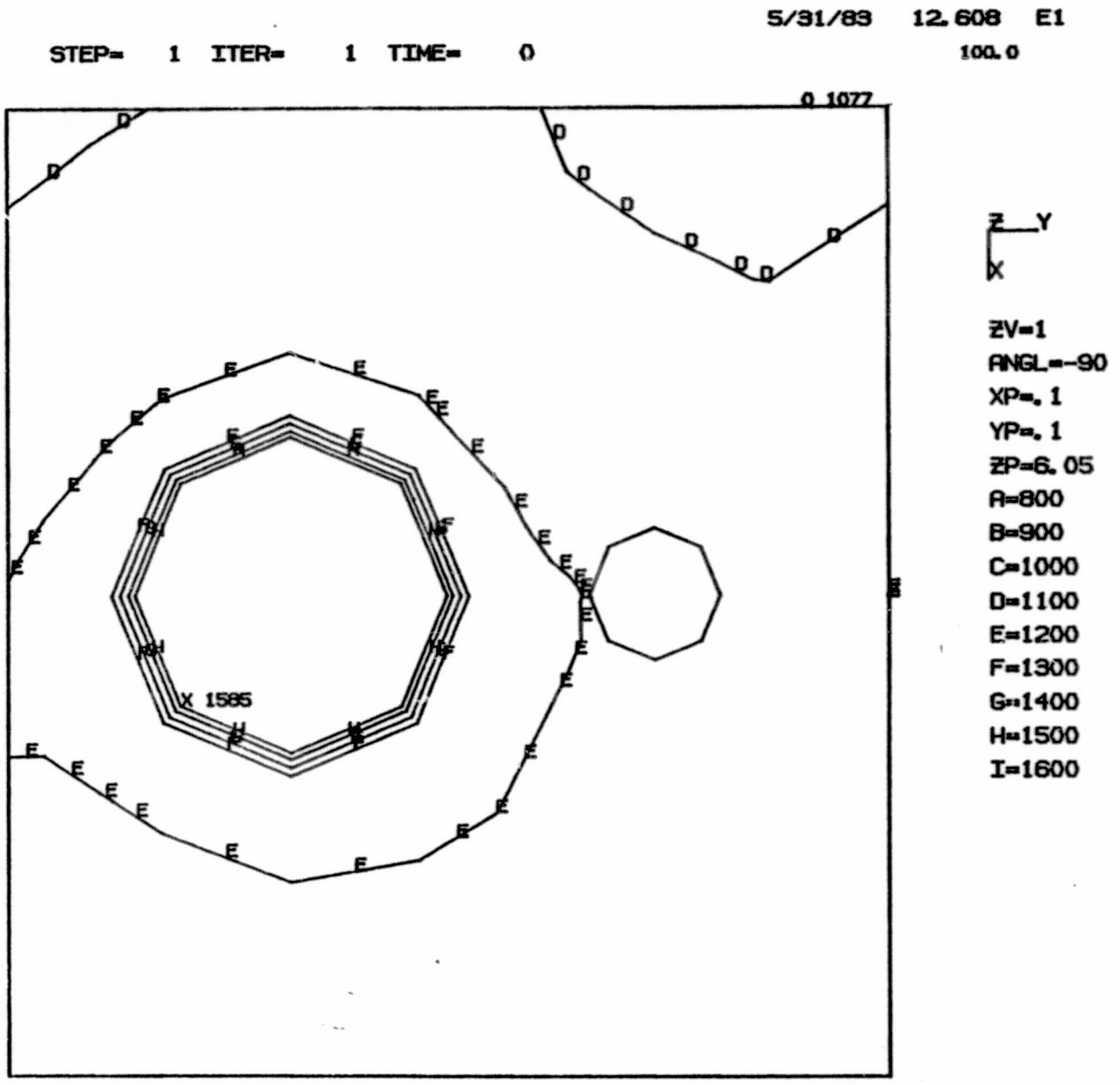

Figure 10. LIGHT DUTY DIESEL HEAD WITH 2-1 H SPLIT IN COMBUSTION TEMP ANSYS 10

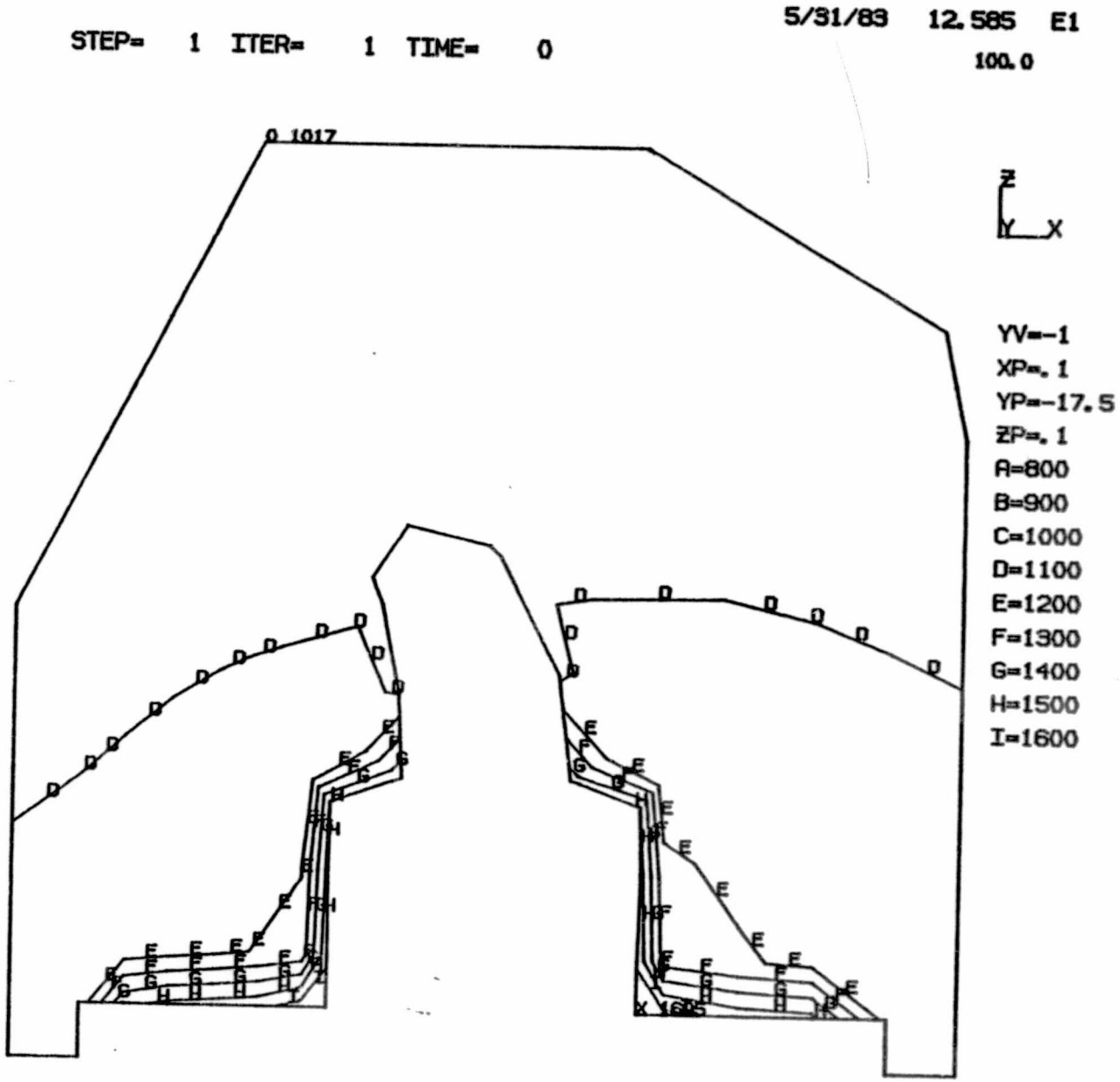

Figure 11 LIGHT DUTY DIESEL HEAD WITH 2-1 H SPLIT IN COMBUSTION

TEMP ANSYS 8

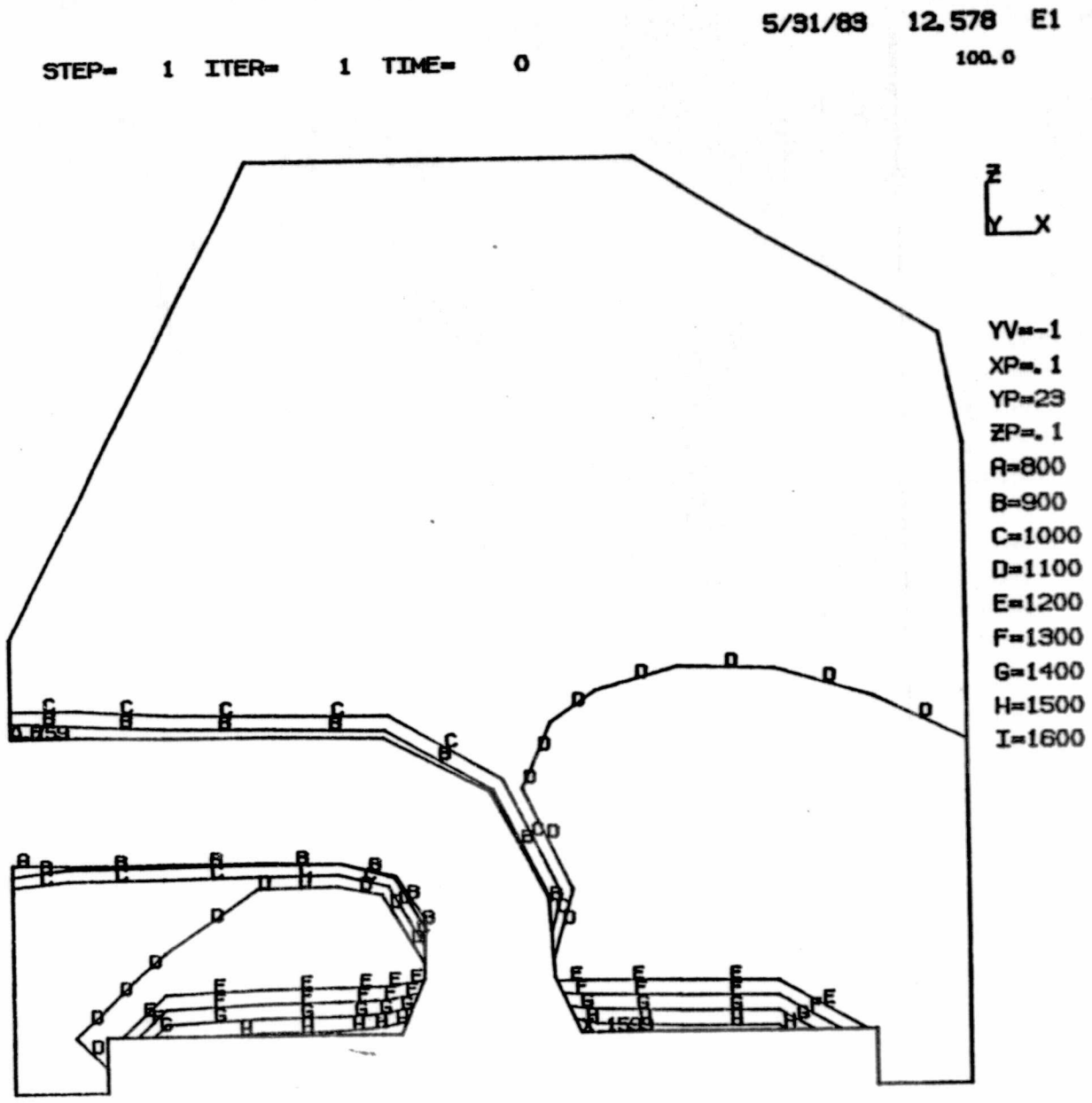

Figure 12. LIGHT DUTY DIESEL HEAD WITH 2-1 H SPLIT IN COMBUSTION

TEMP ANSYS 7

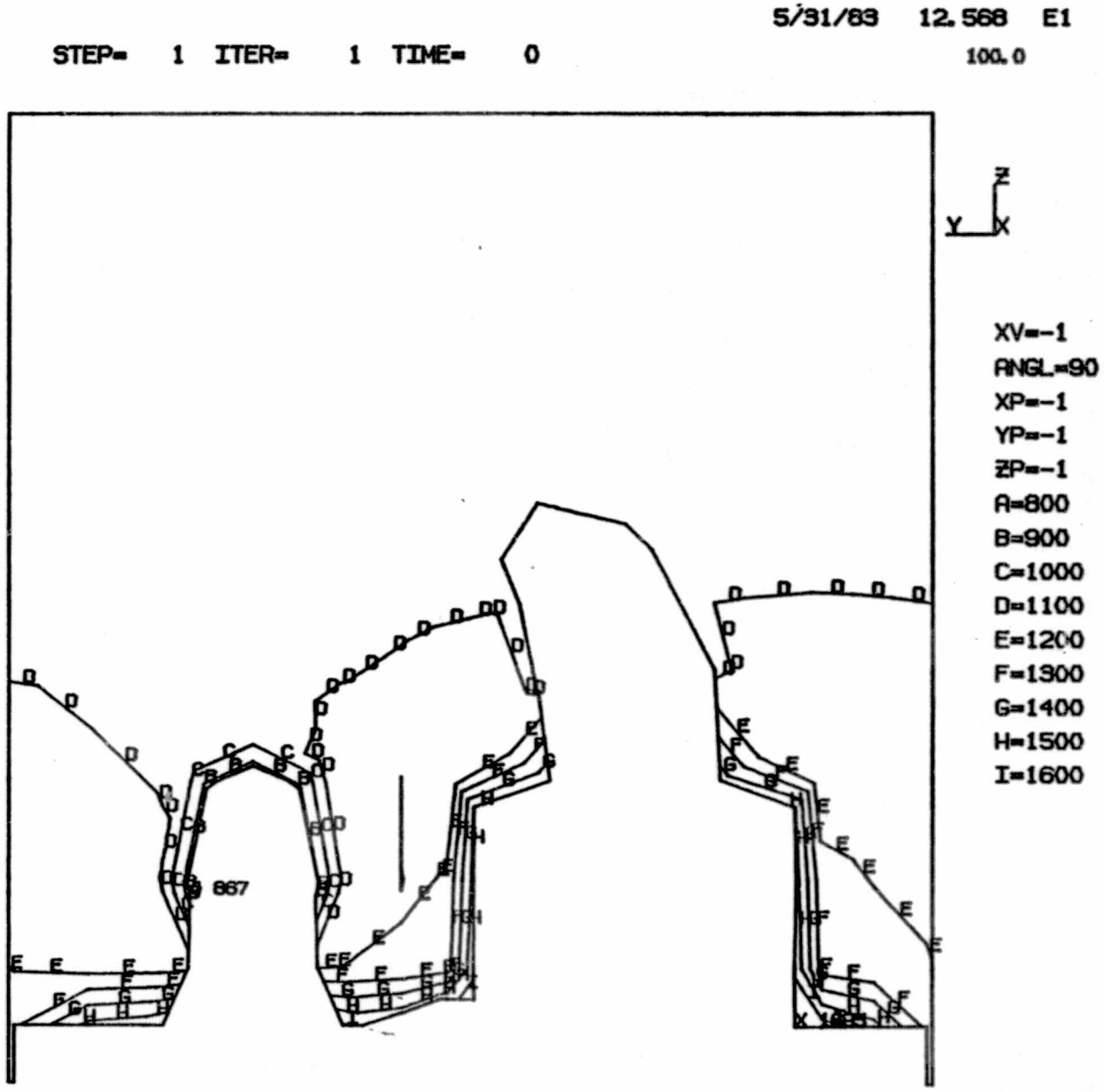

Figure 13. LIGHT DUTY DIESEL HEAD WITH 2-1 H SPLIT IN COMBUSTION TEMP ANSYS 6

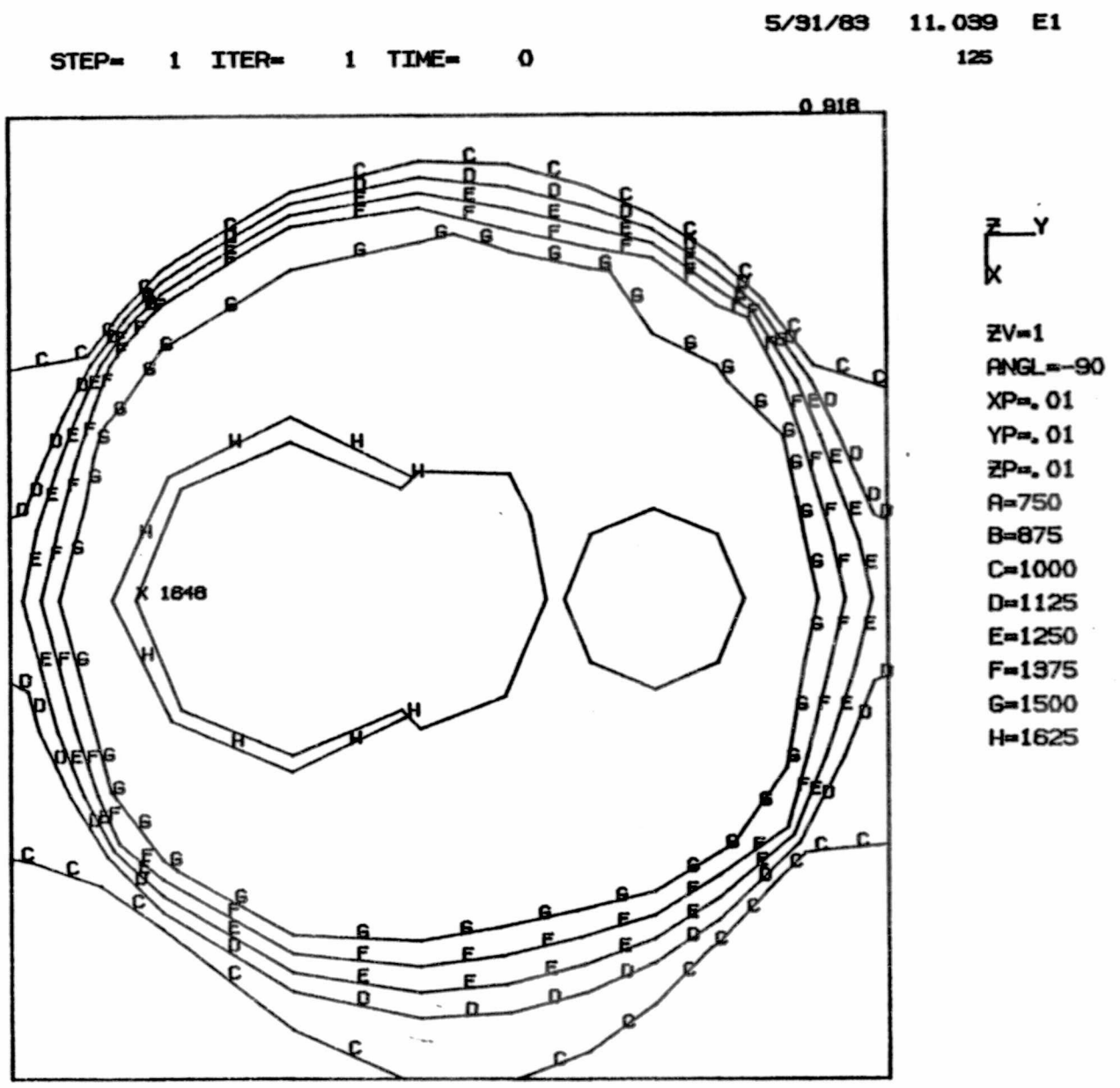

Figure 14. LIGHT DUTY DIESEL WITH TWICE BASELINE EXTERIOR COOLING TEMP ANSYS 9

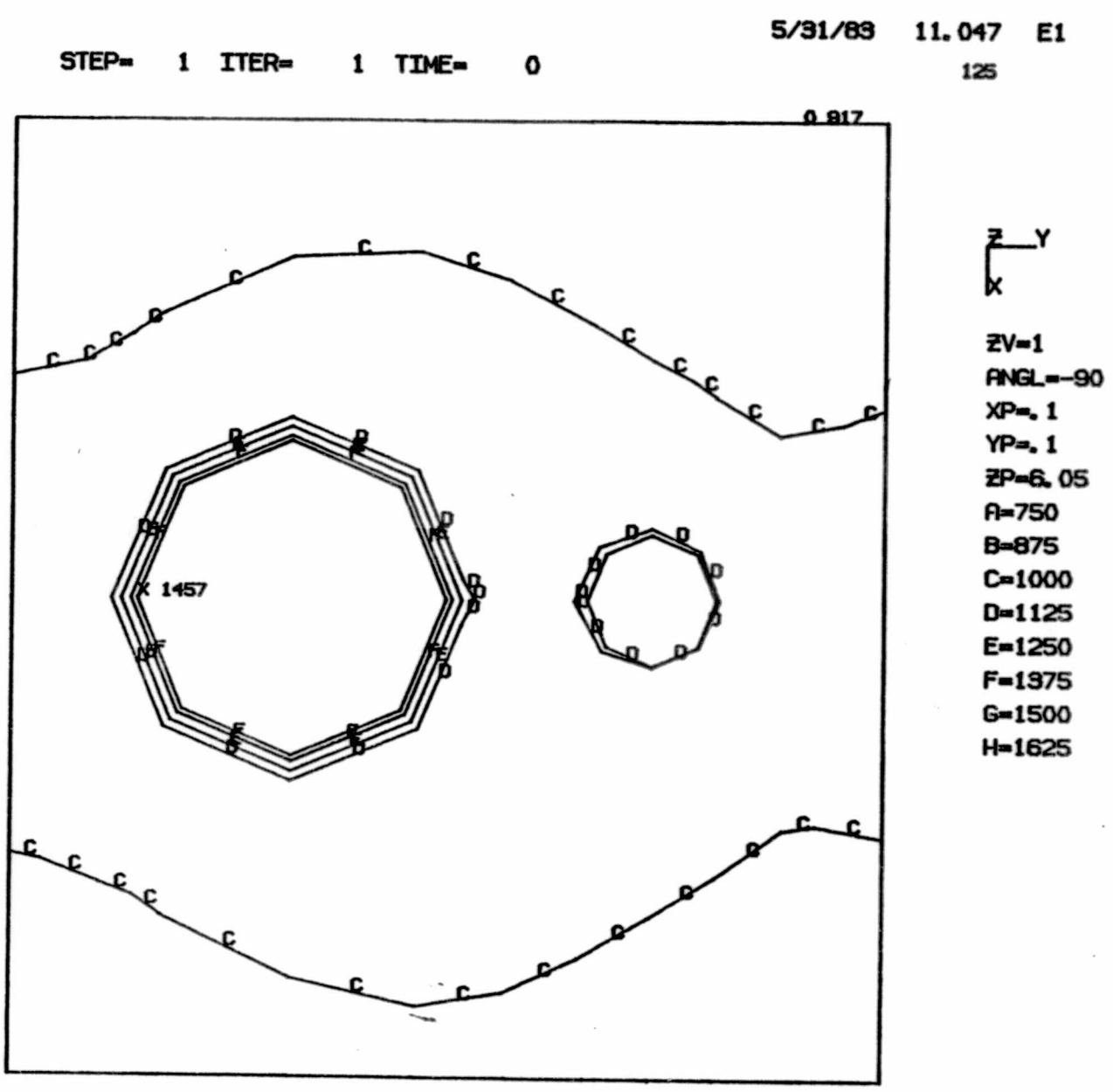

Figure 15. LIGHT DUTY DIESEL WITH TWICE BASELINE EXTERIOR COOLING

TEMP ANSYS 4

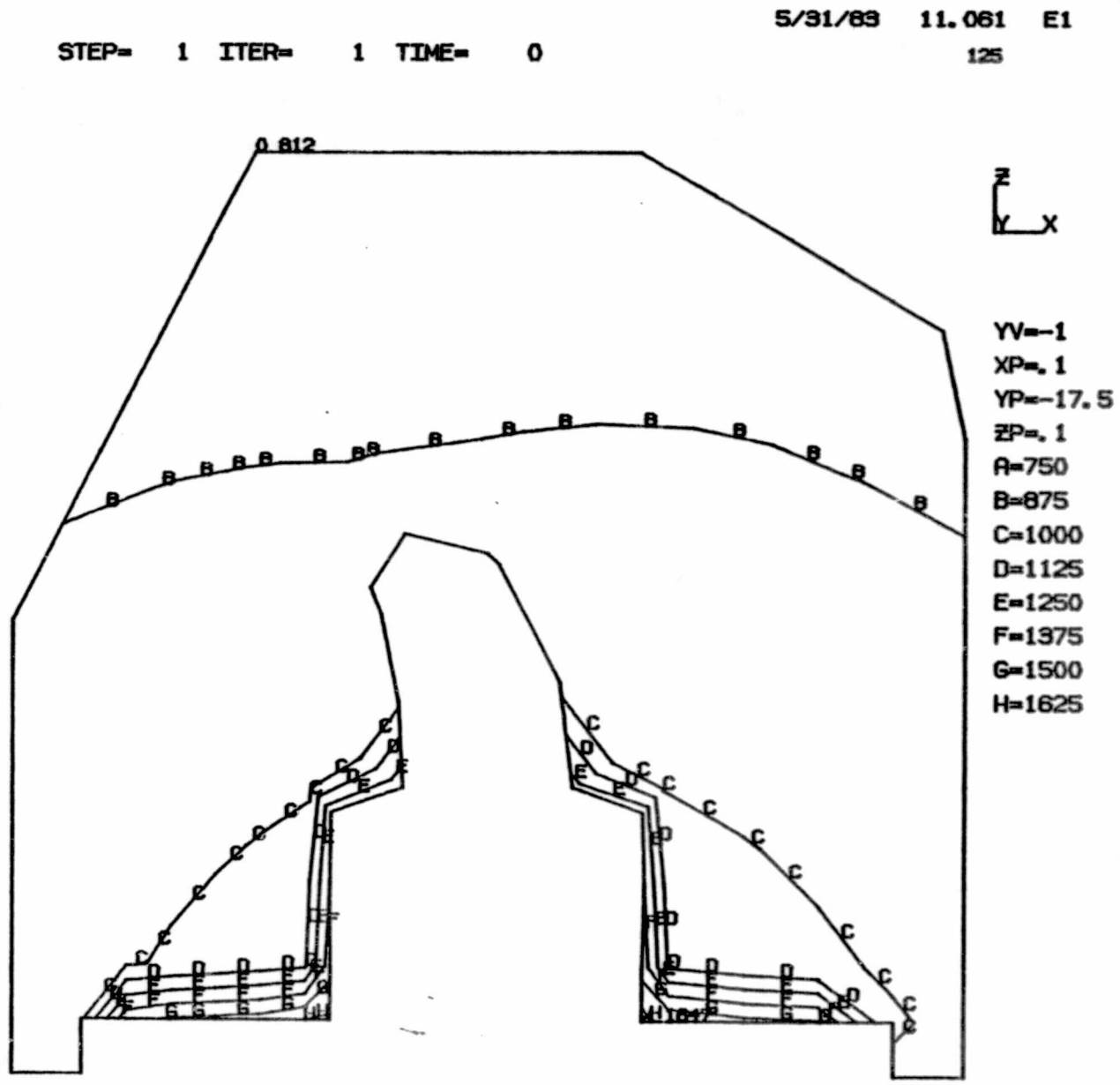

Figure 16. LIGHT DUTY DIESEL WITH TWICE BASELINE EXTERIOR COOLING

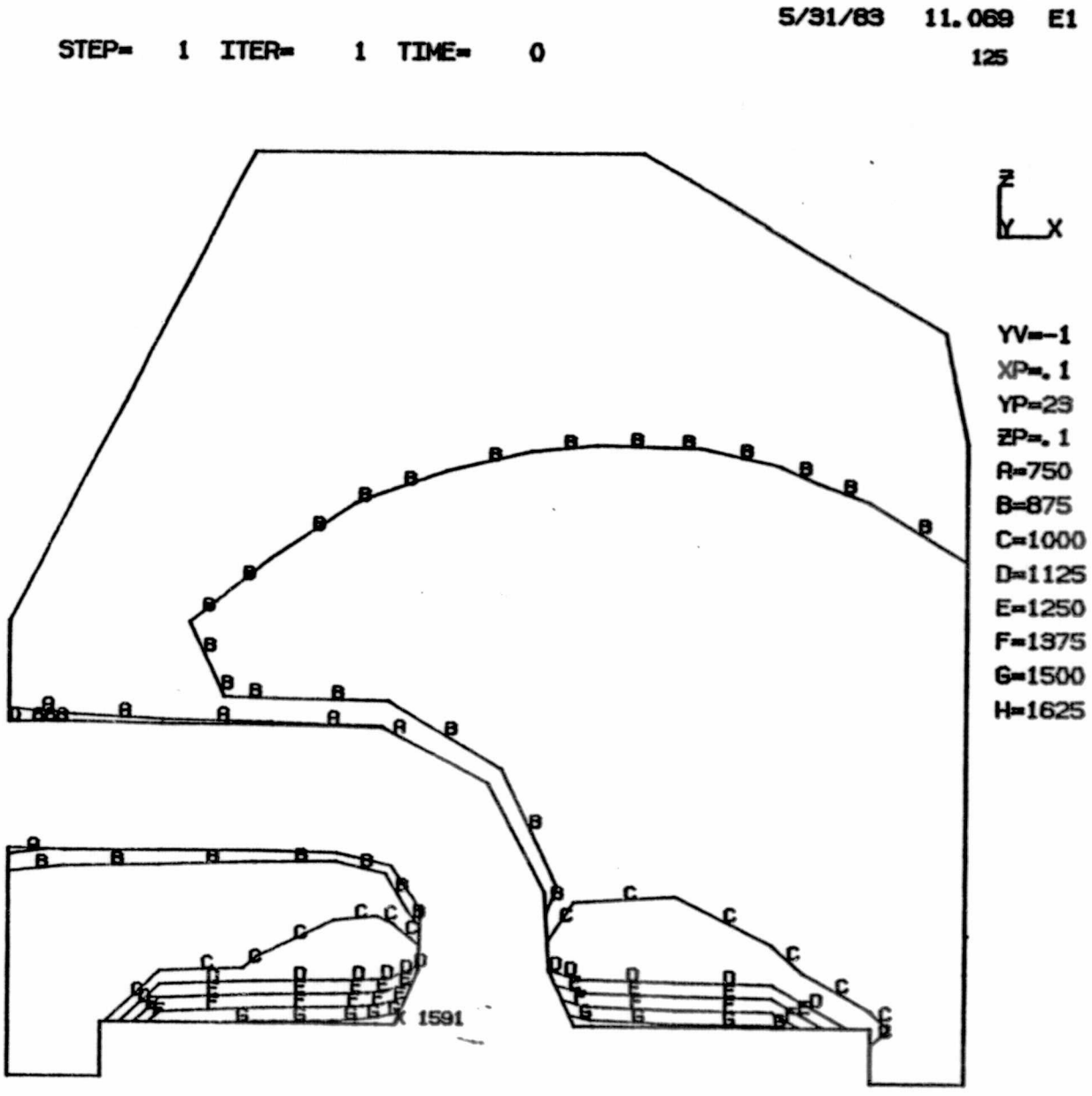

Figure 17. LIGHT DUTY DIESEL WITH TWICE BASELINE EXTERIOR COOLING

TEMP ANSYS 6

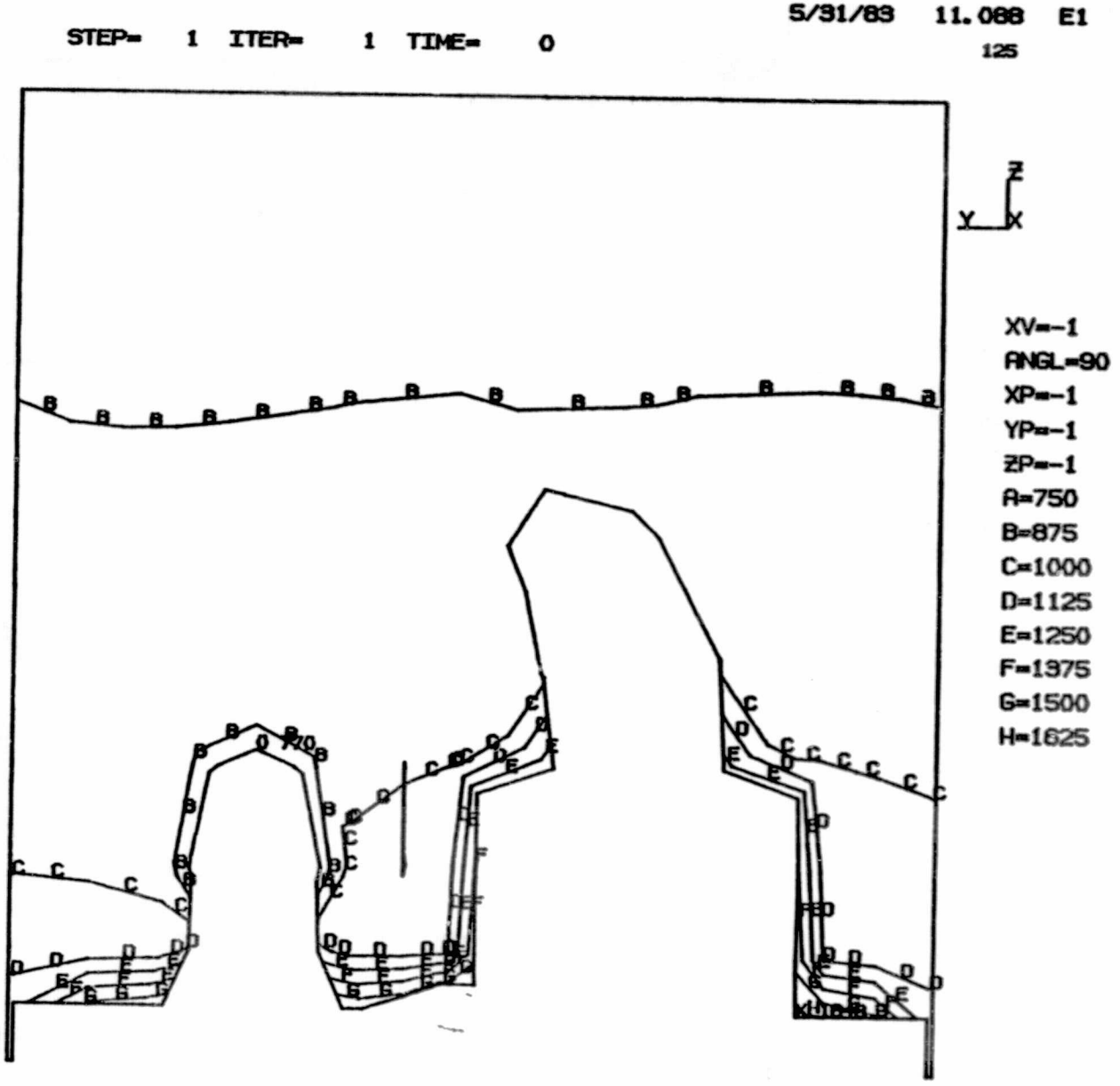

Figure 18. LIGHT DUTY DIESEL WITH TWICE BASELINE EXTERIOR COOLING

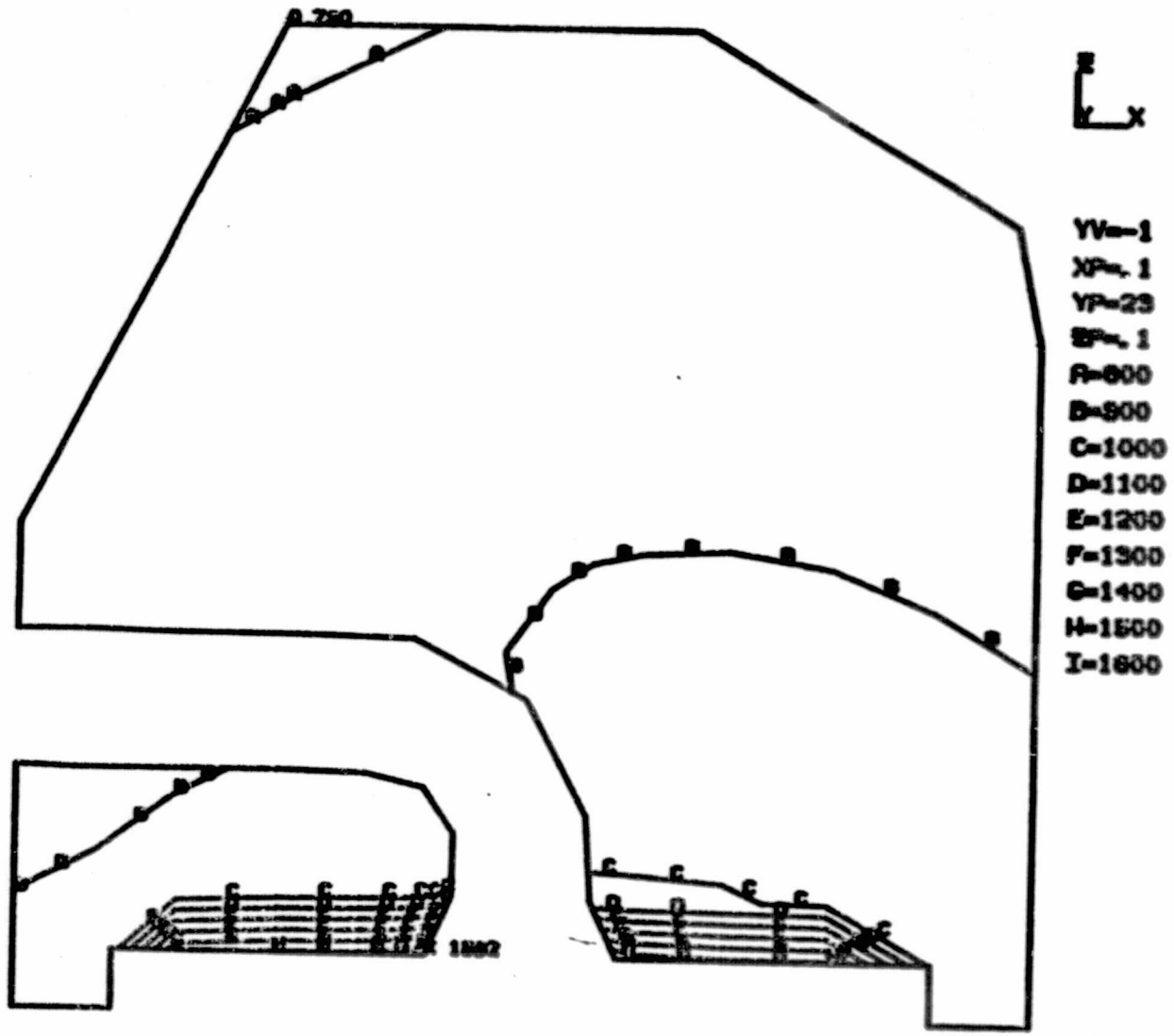

NASA HERO - HOD 3 BC 8 WITH NO CERAMIC INTAKE DUCT TEMP ANSYS 8

Figure 19

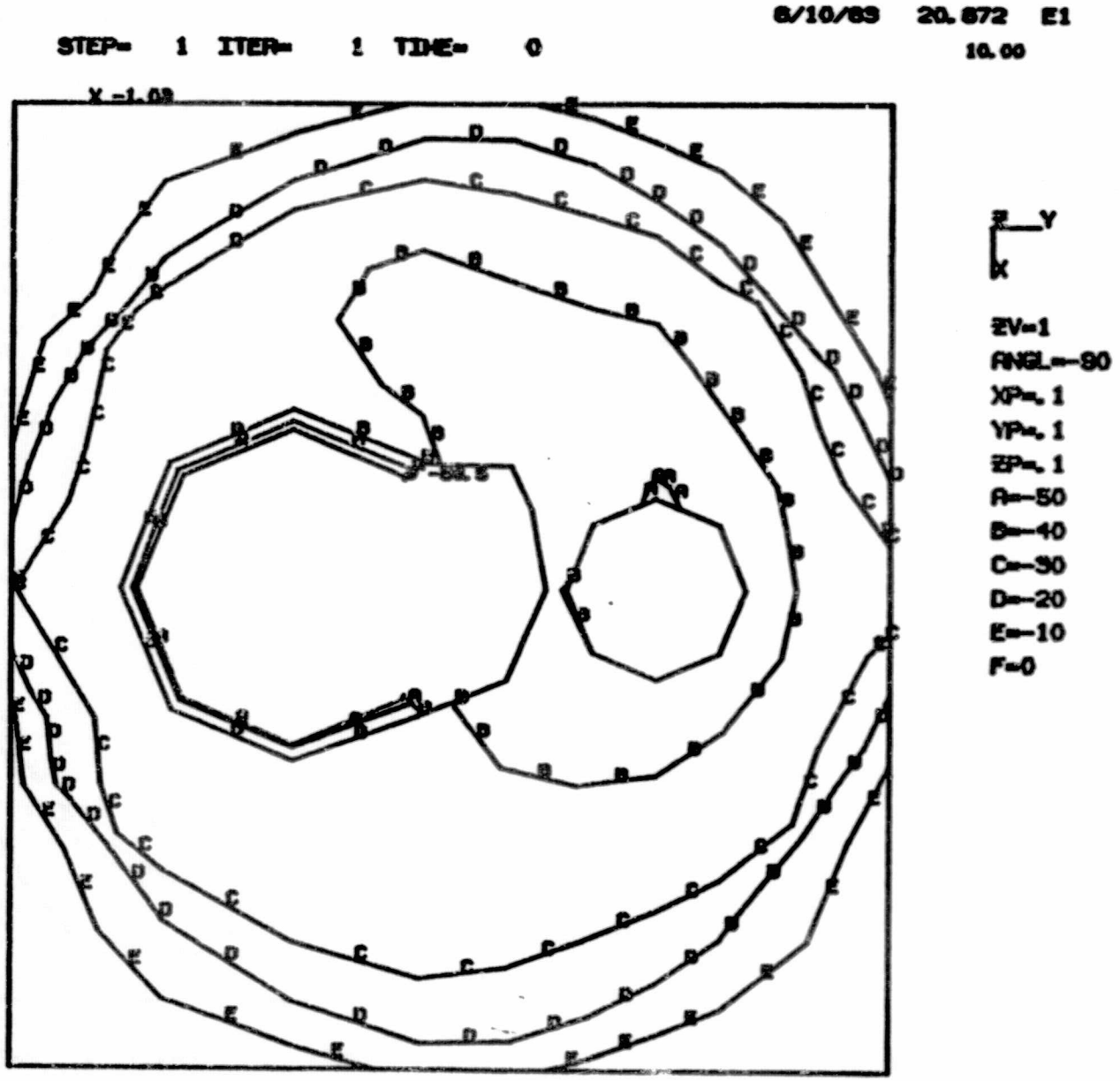

Figure 20.

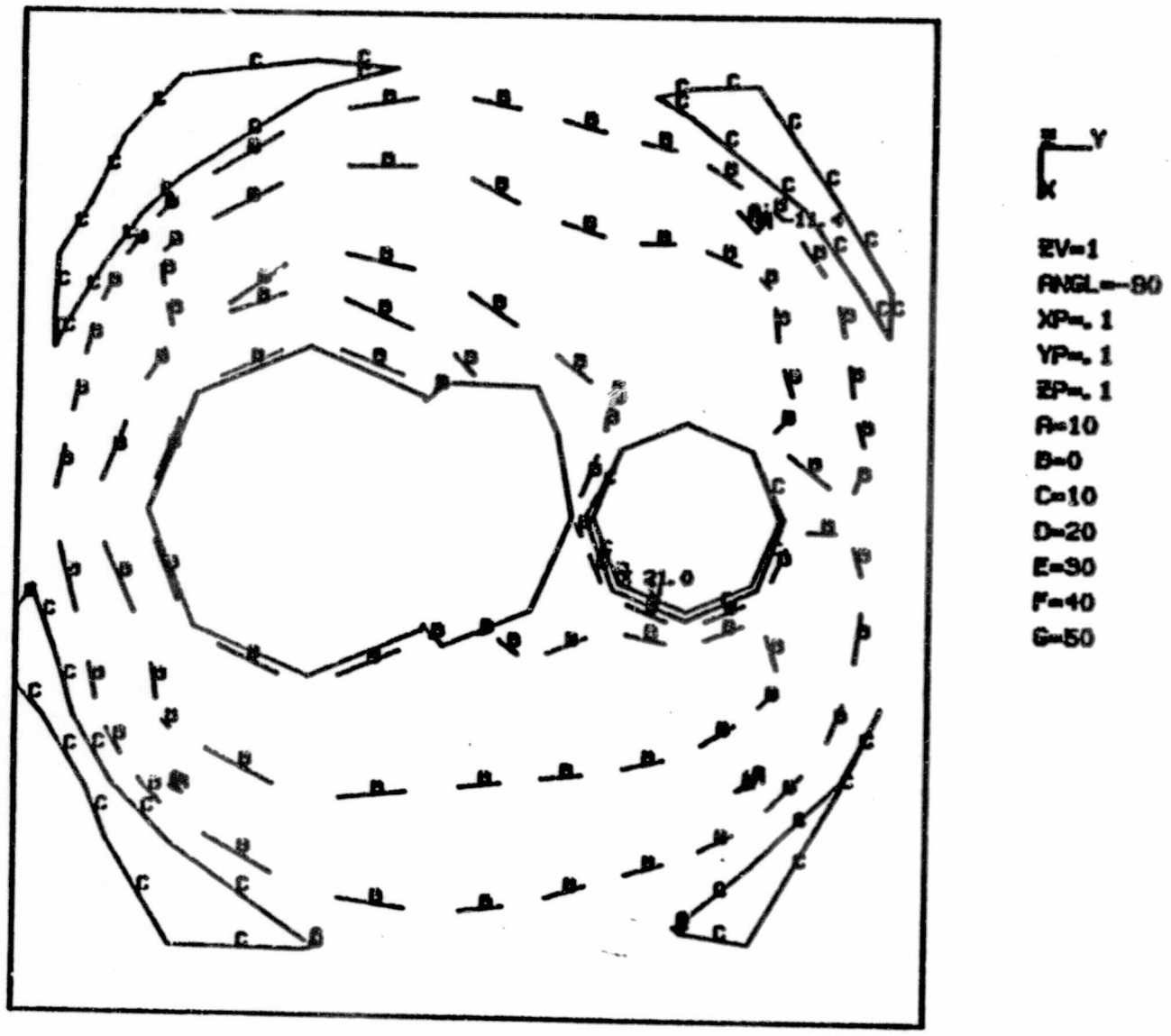

LIGHT DUTY DIESEL THERMAL STRESS FOR BASELINE BOUNDARY CONDITIONS SIG1 ANSYS 2

ADVANCED ADIABATIC DIESEL ENGINE PISTON AND LINER

FINITE ELEMENT MODEL - PISTON

A finite element model of the piston was construed using the ANSYS Finite Element Program. The model consisted of 984 8-noded, 3-D brick elements and was used for all three analyses. Two planes of symmetry exist in the piston, therefore, it was only necessary to model one-fourth of the piston by fixing the XZ plane in the Y direction and the YX plane in the X direction. The model was fixed in the Z direction through the top of the pin bore (Figures 1 to 4).

The piston was modeled as one monolithic piece with the top layer of elements (3 mm) given ceramic material properties, and the remainder of the elements given iron material properties (Tables 1 and 2).

The ceramic material on the side of the piston (.02 mm) was not included in the model because it would only have minimal effect on the thermal or stress analysis.

FINITE ELEMENT THERMAL ANALYSIS - PISTON

Thermal boundary conditions were added to the model as shown in Fig. 1. At the top of the piston (the combustion face) the temperature (T) was assumed to be 2590 degree R and the heat convection coefficient (h_c) was assumed to be .5052 BTU/(in^2 °R x Hr.). Along the outside of the piston the temperature ranged from a peak value of 1560 degree R at the top to 960 degree R at the bottom. The h_c value was assumed to be .1 BTU/(in^2 x °R x Hr). On the underside of the piston cap the temperature and heat convection boundary conditions were assumed to be 660 degree R and .2 BTU/(in^2 x °R x Hr) respectively. (The low temperature on the underside of the piston is expected due to crankcase air flow.) These values were arrived at by using the Diesel Cycle Simulation computer program and using information gathered from measured data on other diesel engines.

There is a very high temperature gradient through the ceramic insulation. The maximum ceramic temperature is 1894 degree R (1434 degree F) and the minimum is 1600 degree R (1140 degree F). The maximum iron temperatures is 1600. The minimum iron temperature is 1080 degree R (620 degree F) and it occurs at the base of the piston.

The isotherms of various piston cross sections are given in Figures 5 to 12. Figure 5 is a plot of the piston combustion face surface temperatures (.001 of an inch below the surface). Figures 6 and 7 are plots of the temperatures at the ceramic-iron interface. In

Figure 8 a section is cut through the bottom of the piston cap where the maximum temperature is 1558 degree R (1098 degree F). Figure 9 is a section through the center of the piston, perpendicular to the pin bore axis. This section clearly illustrates the high temperature gradient through the ceramic layer. Figure 10 is a section perpendicular to the pin bore, 1.15 inches from the center. Figure 11 is a section through the center of the pin bore axis. The section in Figure 12 is parallel to the pin bore axis and .72 inches from the piston centerline.

FINITE ELEMENT THERMAL STRESS ANALYSIS - PISTON

Output generated during the thermal analysis was used as input for the ANSYS thermal stress analysis. This analysis uses the same model within as the thermal analysis, except that the element type is switched from thermal (STIF 70) to stress (STIF 45).

The high stress at the ceramic-iron interface is due to the difference in the coefficient of thermal expansion of the two materials. At high temperatures the iron has a higher coefficient than the ceramic material. Thus, the iron will try to expand more than the ceramic material. This causes high compressive stresses in the iron and high tensile stresses in the ceramic materials. This situation can possibly be alleviated if the ceramic cap can be brazed onto the piston at a temperature close to the anticipated operating temperature. The iron will be expanded more than the ceramic material during this brazing operation and will contract more during cool down. This will put a residual compressive stress in the ceramic material and a residual tensile stress in the iron.

Figure 13 is a plot of the thermal stresses in the piston, and Figure 14 is a plot of the piston displacements due to the thermal stresses.

MECHANICAL STRESS ANALYSIS - PISTON

The peak cylinder pressure during engine operation is 3000 psi. This load was applied to the top surface of elements on the finite element model. For ease of modeling, the fillet radii between the stiffener and the cap, and the wall and the pinbore, were zero. (The actual piston has very generous radii in these areas). This caused very high stress concentrations in these regions. Since the model was not truly representative of the piston in these areas we will only consider the stresses in the center of the cap. Stresses in other areas are expected to be lower than the stresses in the cap.

The peak equivalent stress in the cap due to the 3000 psi cylinder pressure was 34 Ksi (Fig. 15 to 25) and it occured on the

underside of the cap in the iron (Fig. 23). The unnotched endurance limit for the iron is approximately 40 Ksi.

The deflection of the piston due to the maximum cylinder pressure is shown in Figures 26 to 29. Comparing the deflected shape of piston due to the pressure load, Figures 26 to 29, with the deflected shape of the piston due to the thermal load Figures 21 to 24, reveals the deflections are in opposite directions for the cap. This indicates that the stresses due to the thermal load tend to reduce the stresses due to the pressure load. The stresses due to the inertia load, though small, also tend to reduce the stresses due to the pressure load.

ALTERNATE PISTON DESIGN - PISTON

An alternate piston without a ceramic wheel was modeled as a backup for the piston with the wheel (Figure 30). A thermal analysis was done for this piston and compared to the piston with the wheel. The results show that the temperature distribution is very similar for both pistons. This would indicate that the stress distribution in the cap due to the thermal loads would also be similar. However, the stress distribution due to the cylinder pressure should be different because of cap support. There is more support for the cap in the piston without the wheel, because no opening is needed in the side of the piston for the wheel.

FINITE ELEMENT THERMAL ANALYSIS - LINER

A two dimensional axisymmetric finite element model of the liner was constructed. The model contained 450 quadrilateral elements. The two inside columns of elements (3 mm) had ceramic material properties and the three outside column elements (7 mm) had iron material properties (Figure 31).

The maximum ceramic temperature for the liner was 1075 degree F and the maximum iron temperature was 1040 degree F. There does not appear to be any problem with liner temperatures.

CONCLUSIONS

The finite element analysis of the piston with the wheel indicated the piston cap is a highly stressed area due to the alternating thermal load and the alternating pressure load. The analysis also indicated that the stress from one load tends to offset the stress from the other load. Two areas of major concern in the cap are the ceramic plate and the bond at the ceramic-iron interface. Although we have determined the value of the alternating stresses in these areas, we do not yet have reliable fatigue data to compare these

stresses to. We only know the compressive and tensile strengths of the ceramic material and that the compressive strength is considerably higher than the tensile strength.

Reliable fatigue data on the ceramic material and on the ceramic-iron bond should be developed in the second phase of the project.

The thermal analysis of the piston without the wheel yielded results similar to the thermal analysis of the piston with the wheel.

The liner thermal analysis revealed that the temperature of the ceramic material and the iron were both tolerable.

ACTIONS

The temperature of the iron in the piston needs to be reduced by using a thicker ceramic cap and/or increasing cooling to the underside of the piston. More stiffening should be added to the piston underside. Also, a ferritic or high temperature alloy such as Cummins Material Specification (CMS) 41,081 should be used, which has a minimum tensile strength of 80 Ksi and a minimum yield strength of 65 Ksi.

Figures

Tables

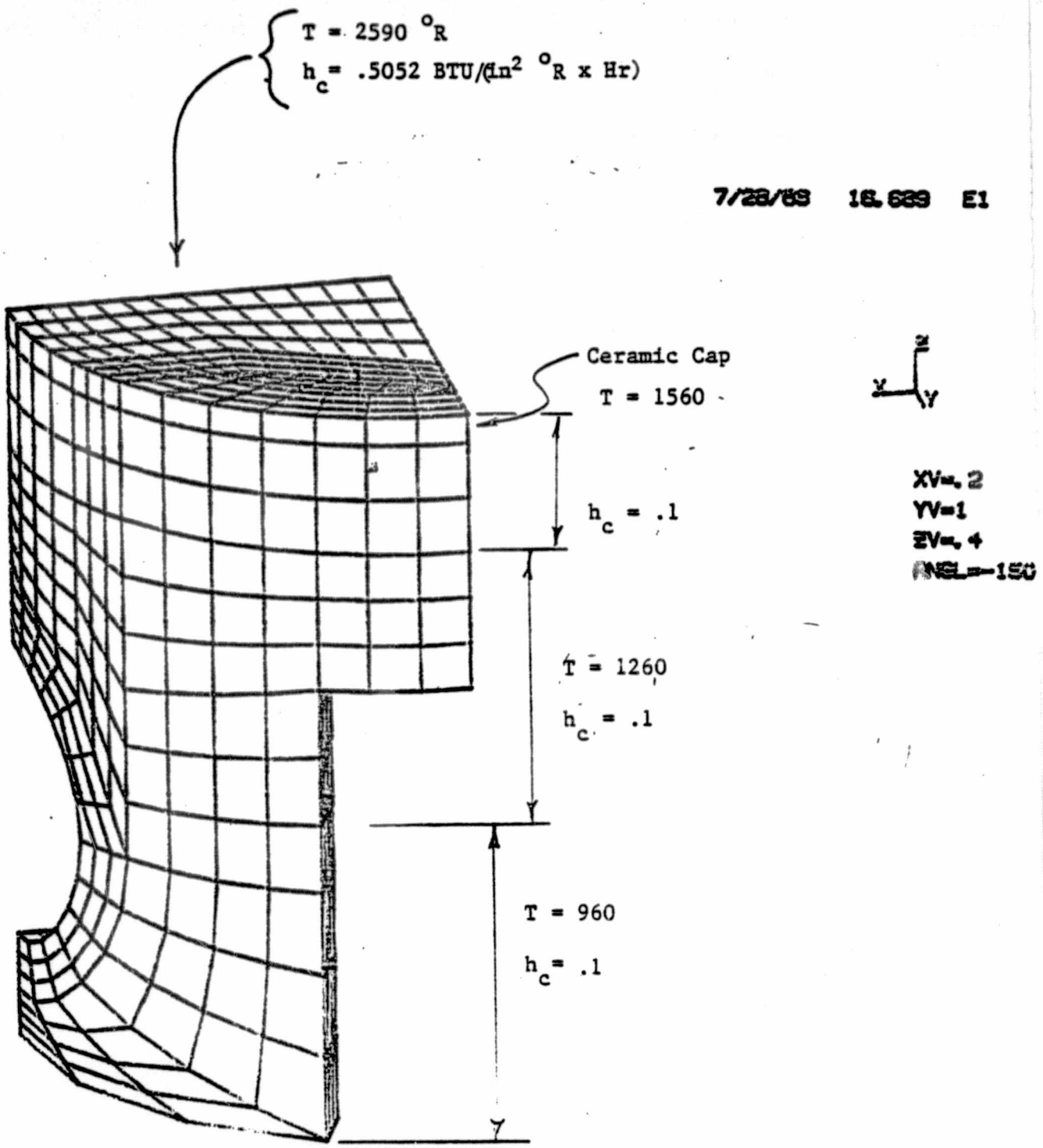

Figure 1

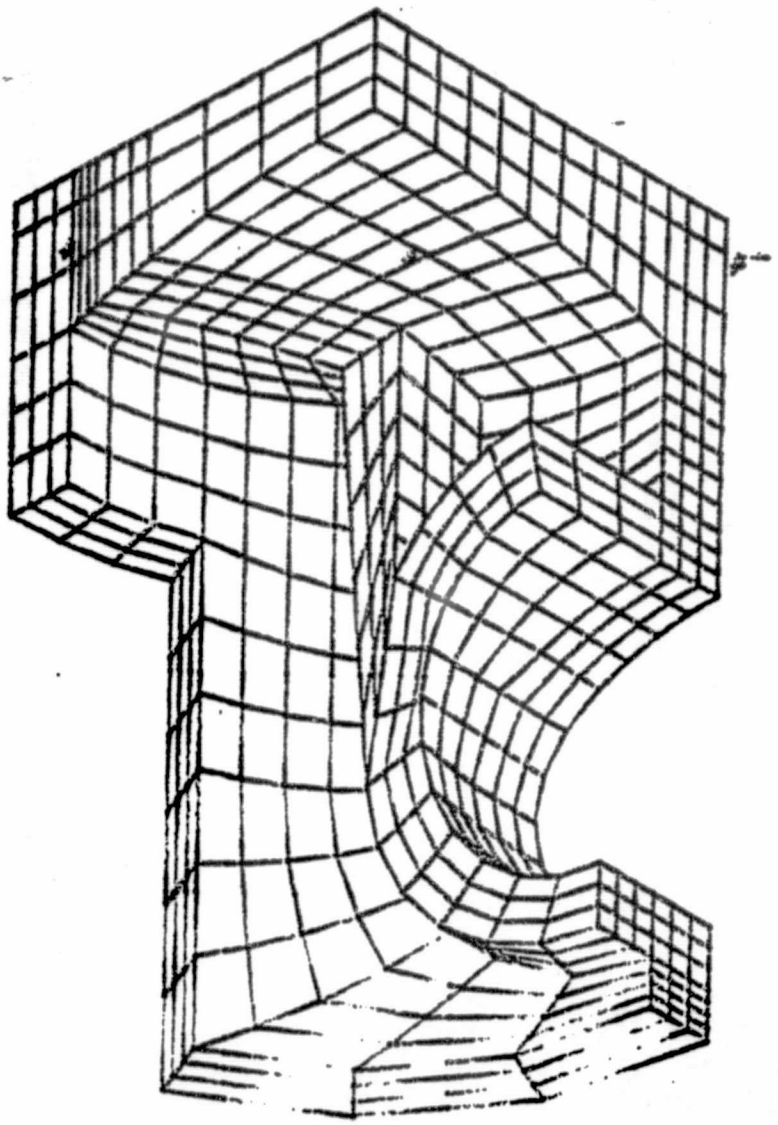

Figure 2

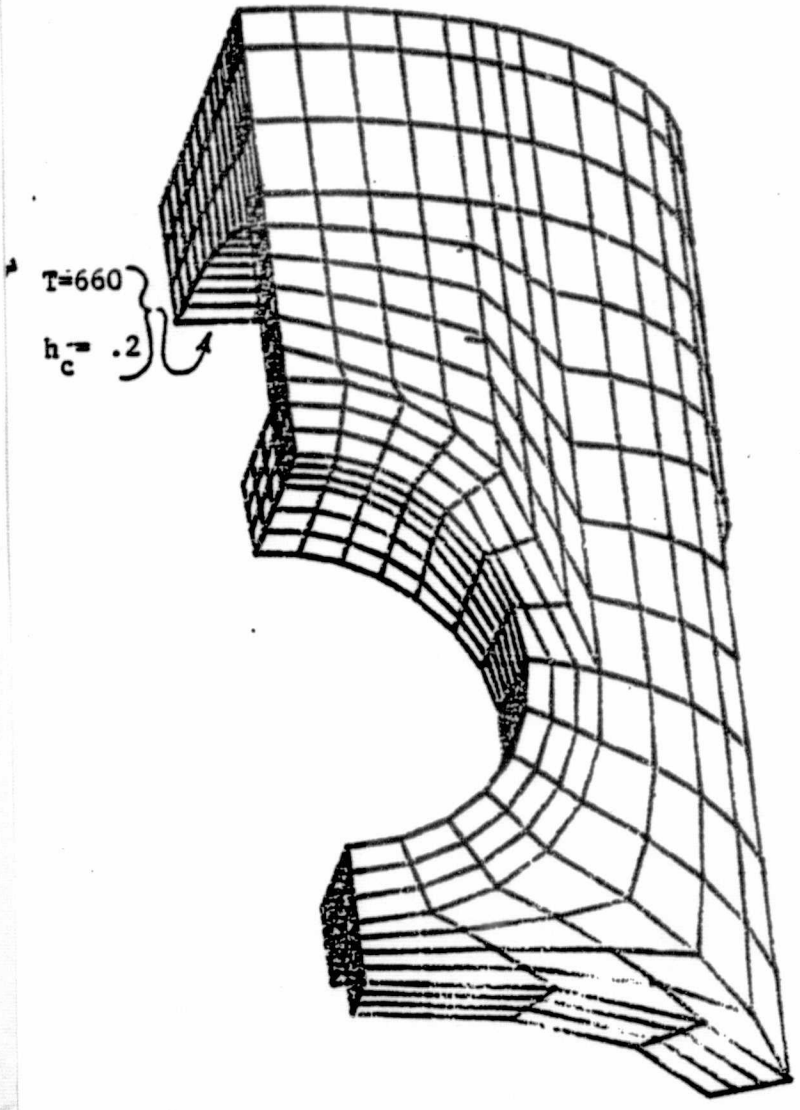

Figure 3

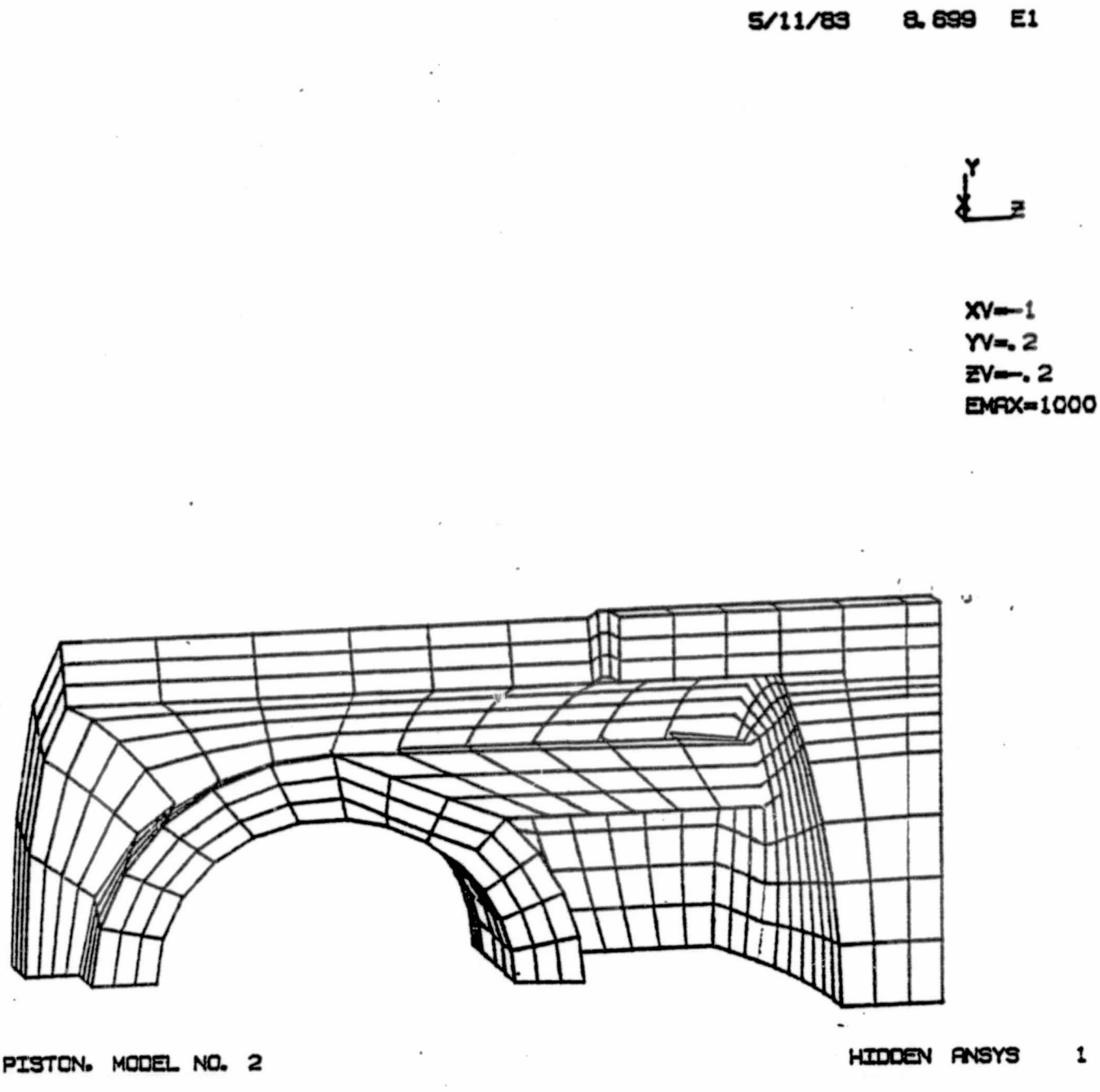

Figure 4. Hidden Line Plot of Piston

ORIGINAL PAGE IS
OF POOR QUALITY

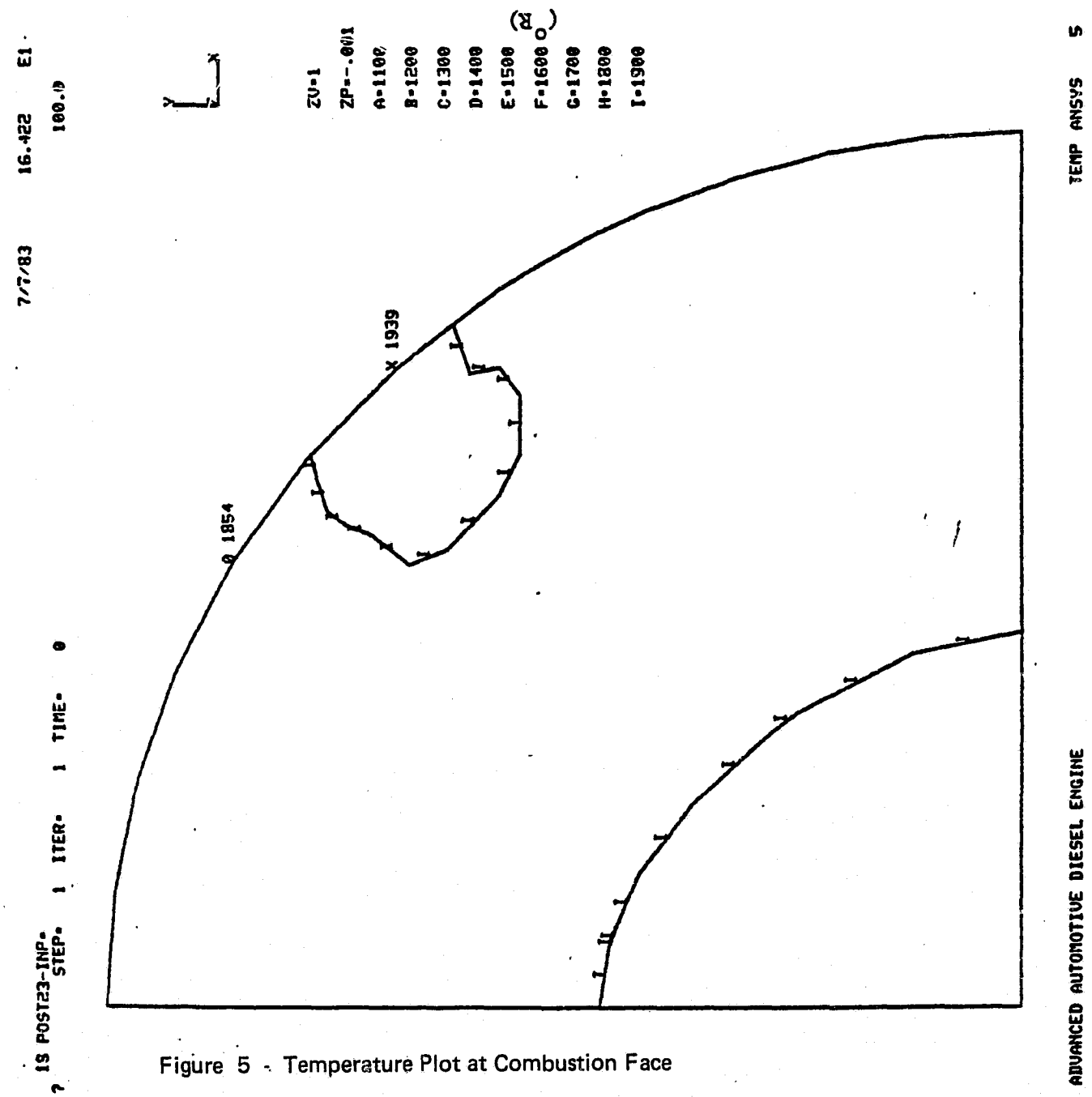

Figure 5 - Temperature Plot at Combustion Face

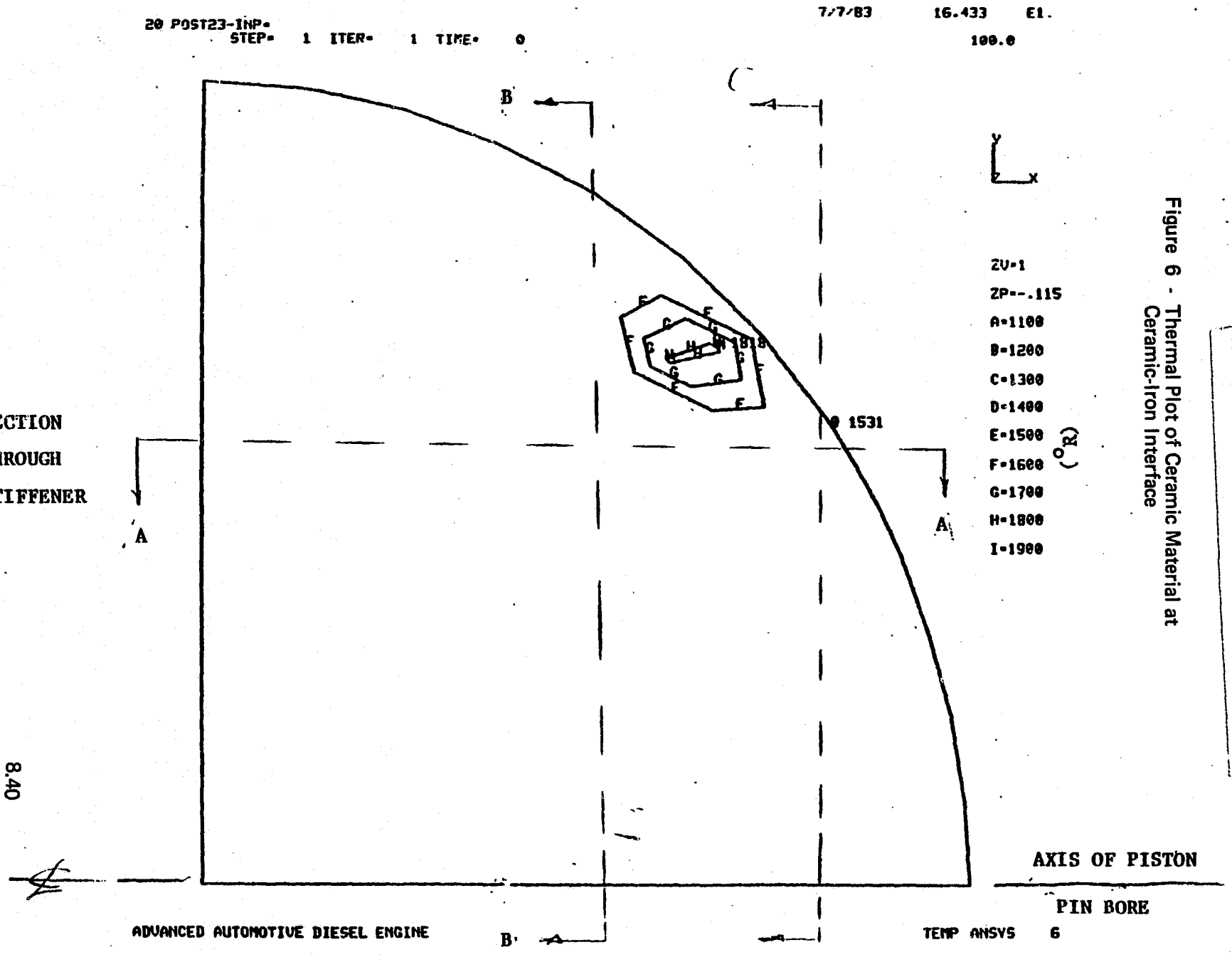

Figure 6 - Thermal Plot of Ceramic Material at Ceramic-Iron Interface

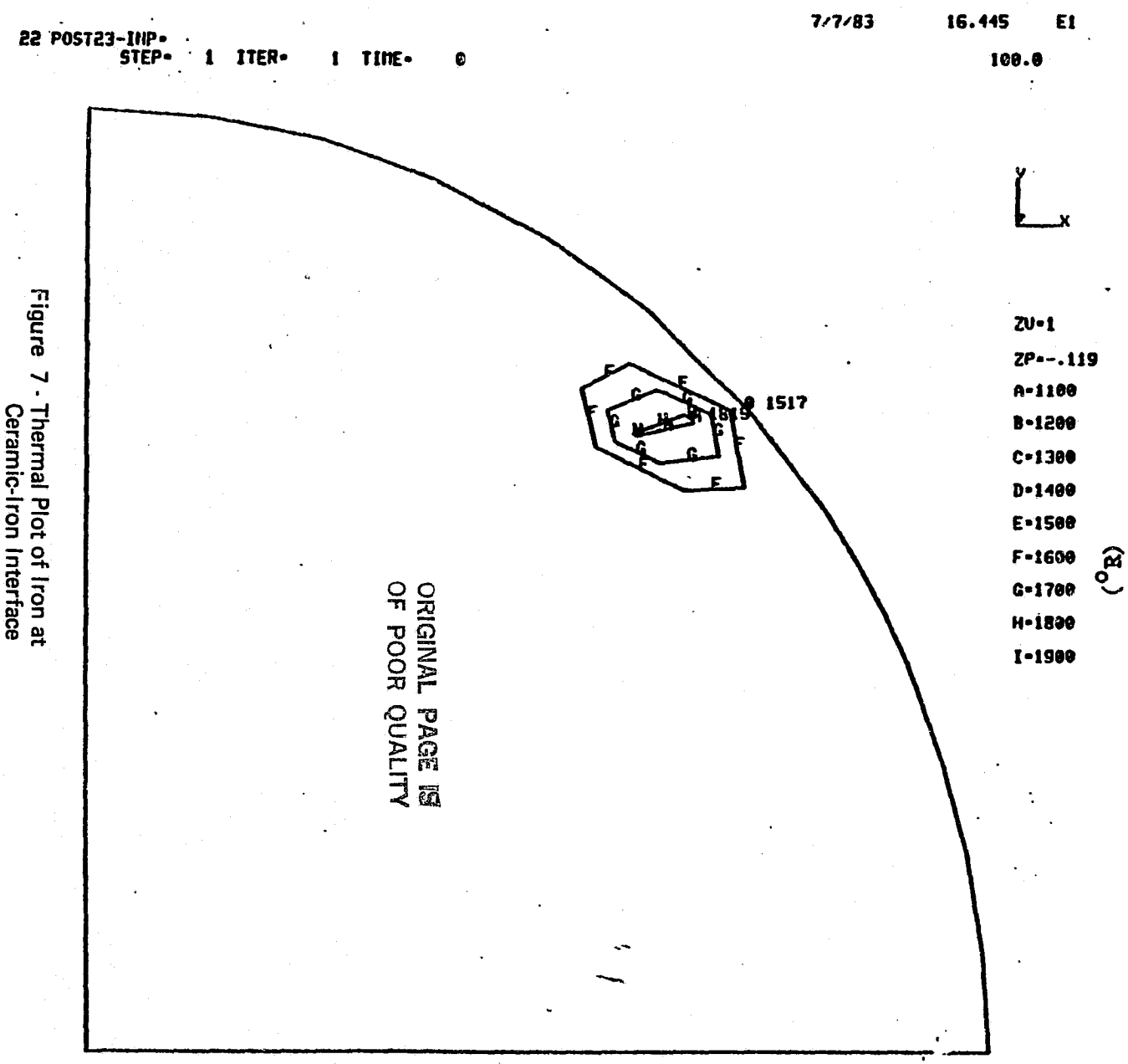

Figure 7 - Thermal Plot of Iron at Ceramic-Iron Interface

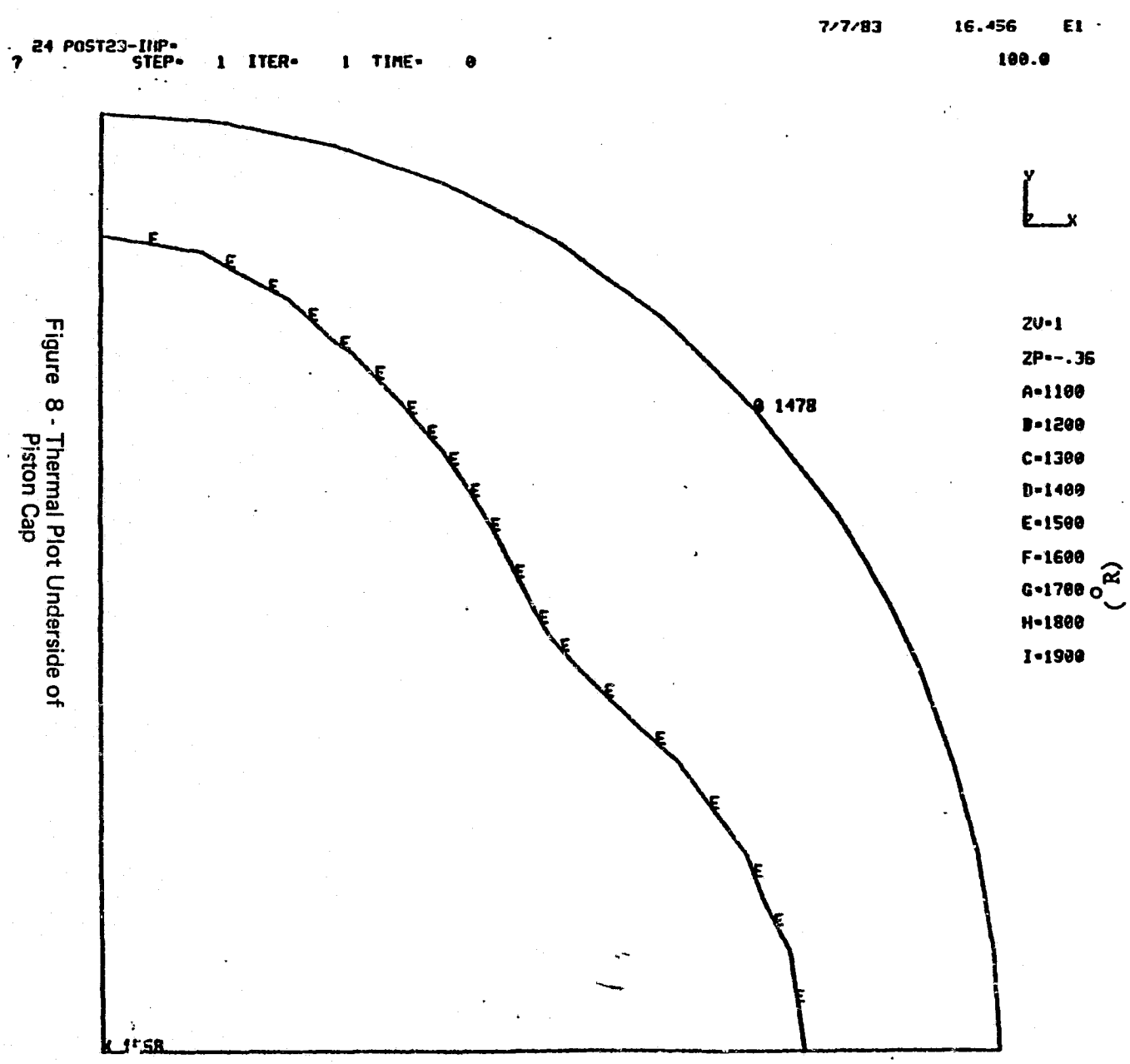

Figure 8 - Thermal Plot Underside of Piston Cap

8 POST23-INP•
STEP• 1 ITER• 1 TIME• 0

7/7/83 . 16.363 E1 .
100.0

XV=1
XP=.001
A=1100
B=1200
C=1300
D=1400
E=1500
F=1600
G=1700
H=1800
I=1900

(°R)

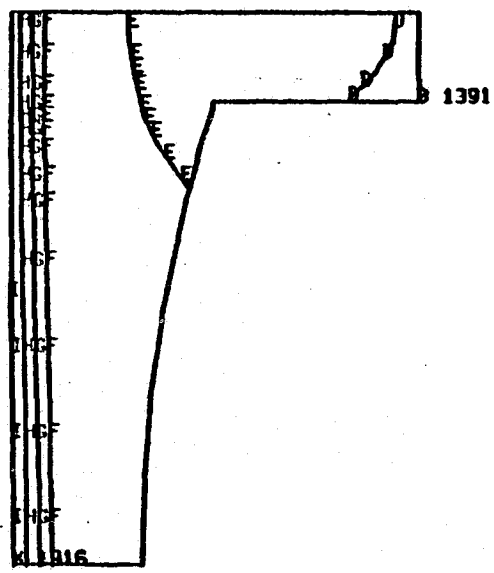

Figure 9 - Thermal Plot, Section Through the Center of the Piston, YZ Plane

C-4

Figure 10 - Thermal Plot - Section A

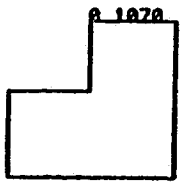

YU=1
YP=.001
A=1100
B=1200
C=1300
D=1400
E=1500
F=1600
G=1700
H=1800
I=1900

($^{\circ}$R)

Figure 11 - Thermal Plot XZ Plane Through the Center of the Piston

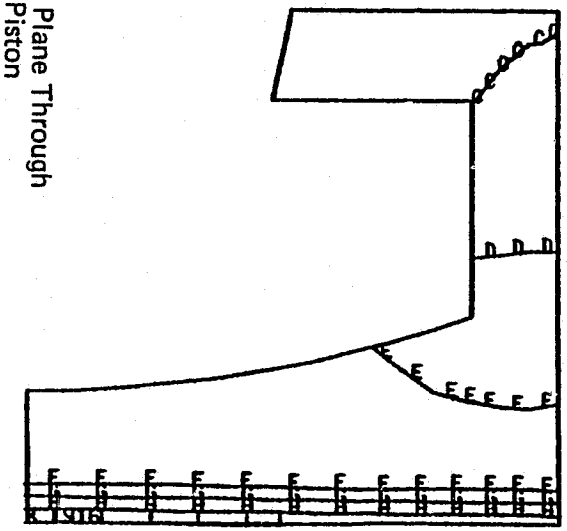

15 PO. 123-INP-
STEP= 1 ITER= 1 TIME= 0

7/7/83 16.408 E1

100.0

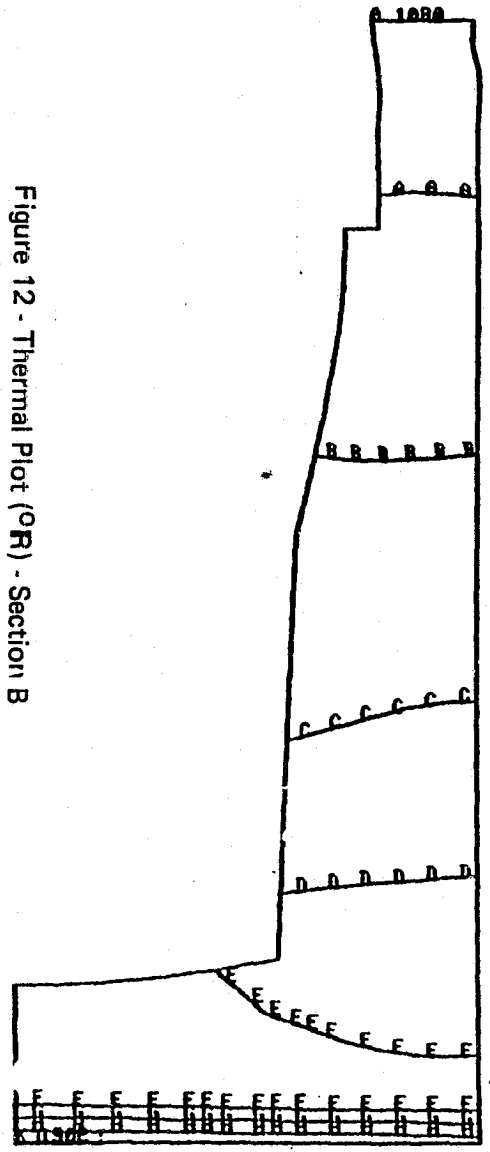

VU=1
VP=.72
A=1100
B=1200
C=1300
D=1400
E=1500
F=1600
G=1700
H=1800
I=1900

Figure 12 - Thermal Plot (°R) - Section B

ADVANCED AUTOMOTIVE DIESEL ENGINE

TEMP ANSYS 4

29 POST23-INP•
STEP• 1 ITER• 1 TIME• 9

7/7/83 13.955 E1.
4000

XU=1
XP=1.15
A=4000
B=8000
C=12000
D=16000
E=20000
F=24000
G=28000
H=32000

(PSI)

Figure 13 - Thermal Stress Plot
Equivalent Stress
Section A

ADVANCED AUTOMOTIVE DIESEL ENGINE

SIGE ANSYS 15

34 POST23-INP•
- STEP• 1 ITER• 1 TIME• 0

7/7/83 14.079 E1
.0203

XV=1
XP=1.15

Figure 14 - Deflection Due to Thermal Load - Section A

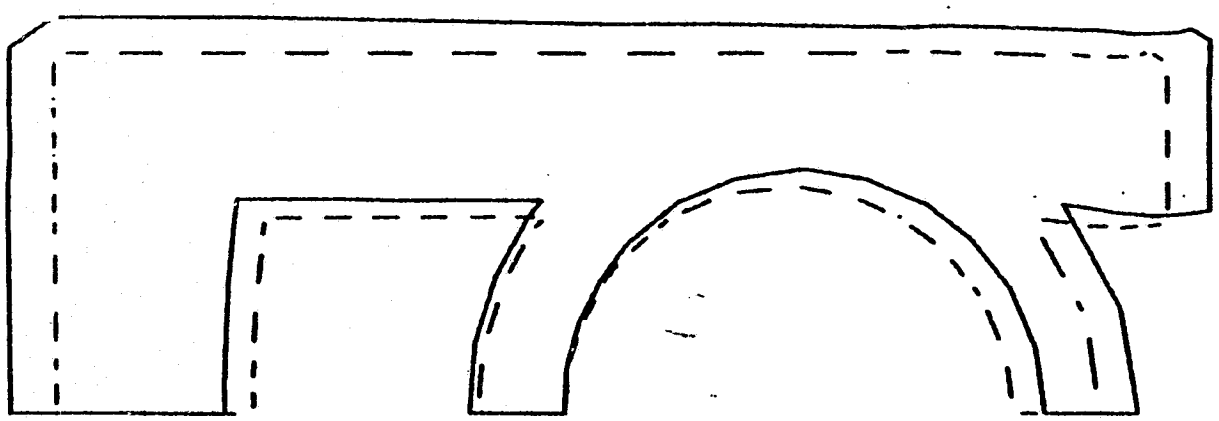

ADVANCED AUTOMOTIVE DIESEL ENGINE

DISP ANSYS 20

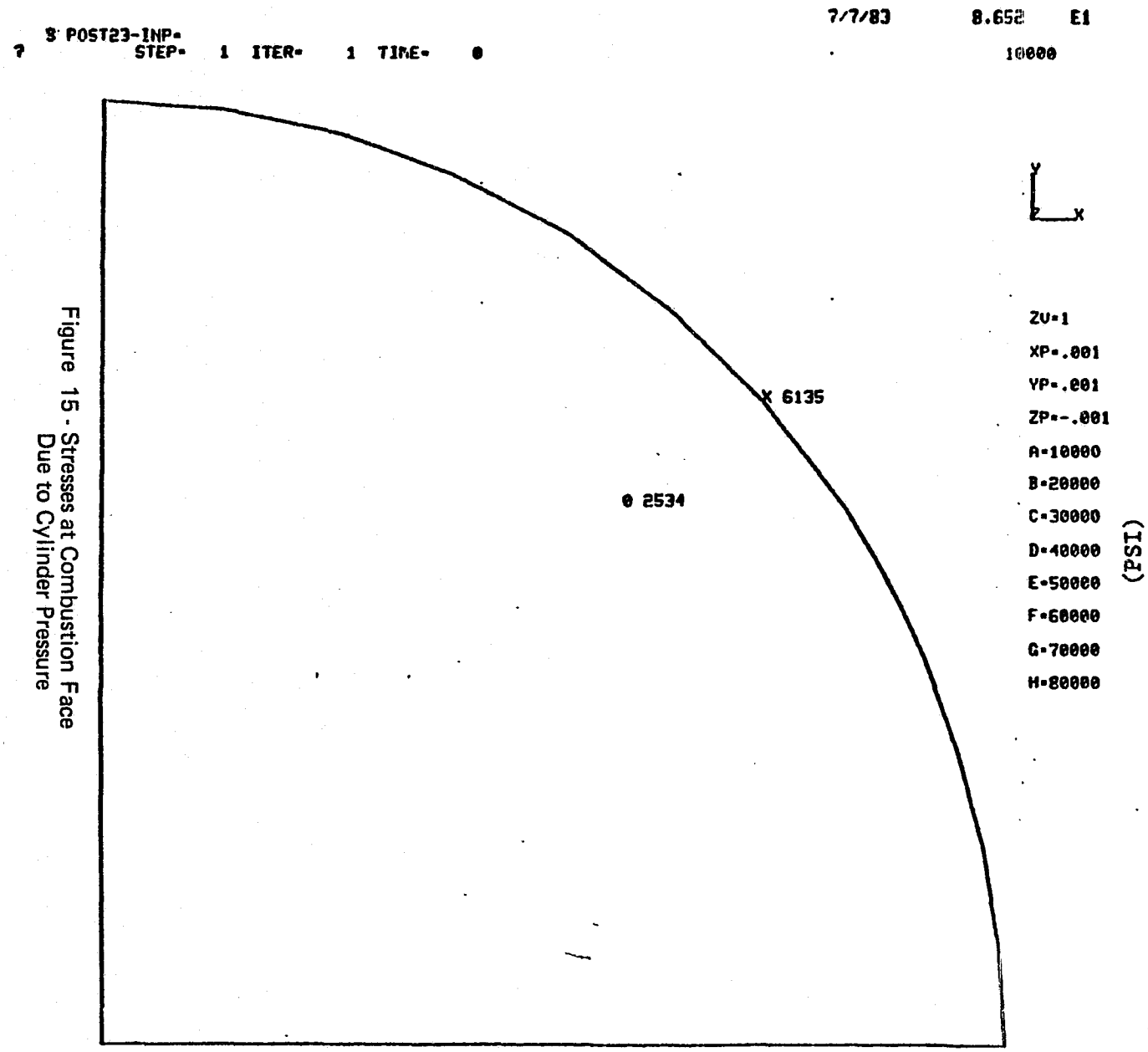

Figure 15 - Stresses at Combustion Face Due to Cylinder Pressure

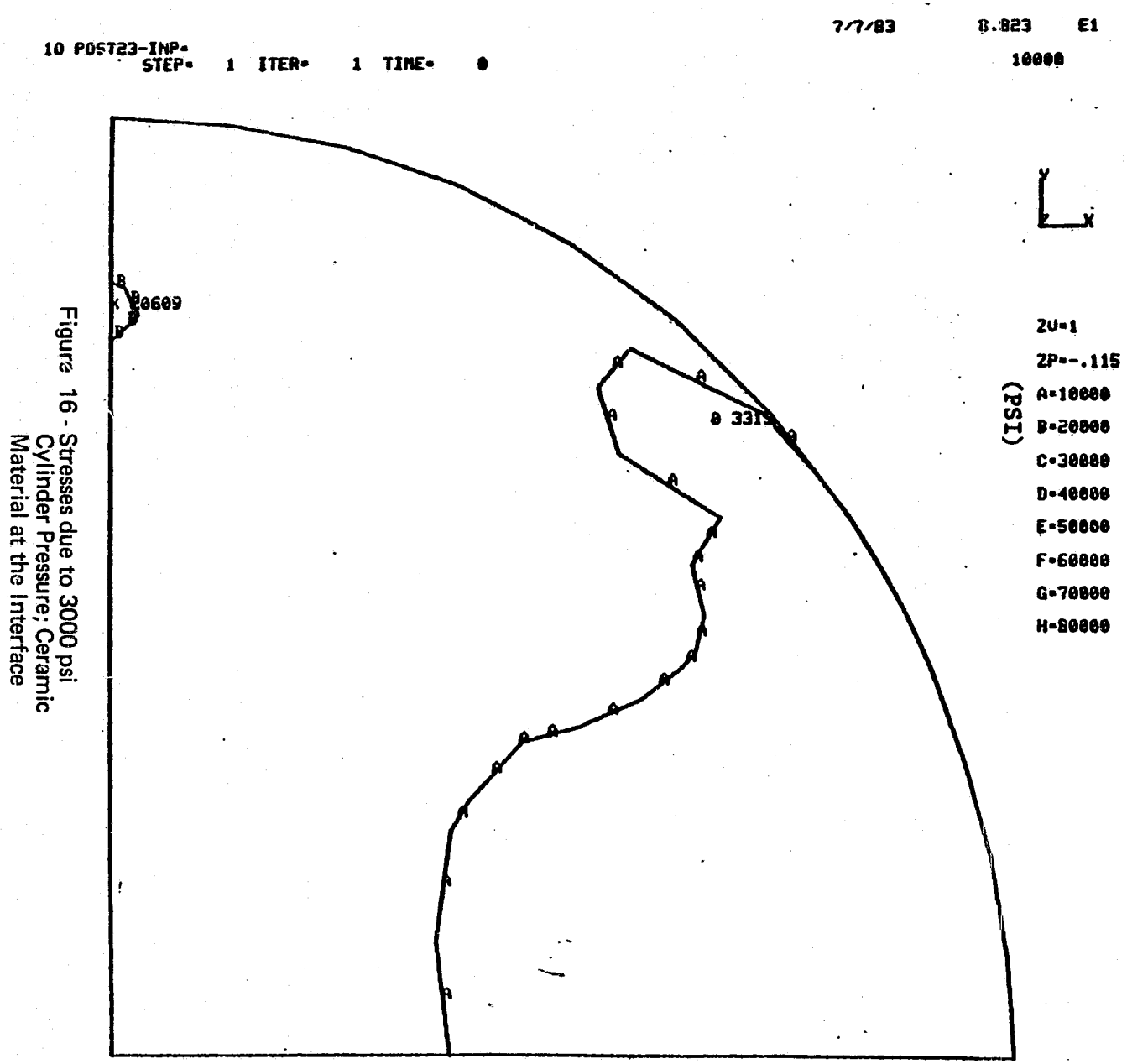

Figure 16 - Stresses due to 3000 psi Cylinder Pressure; Ceramic Material at the Interface

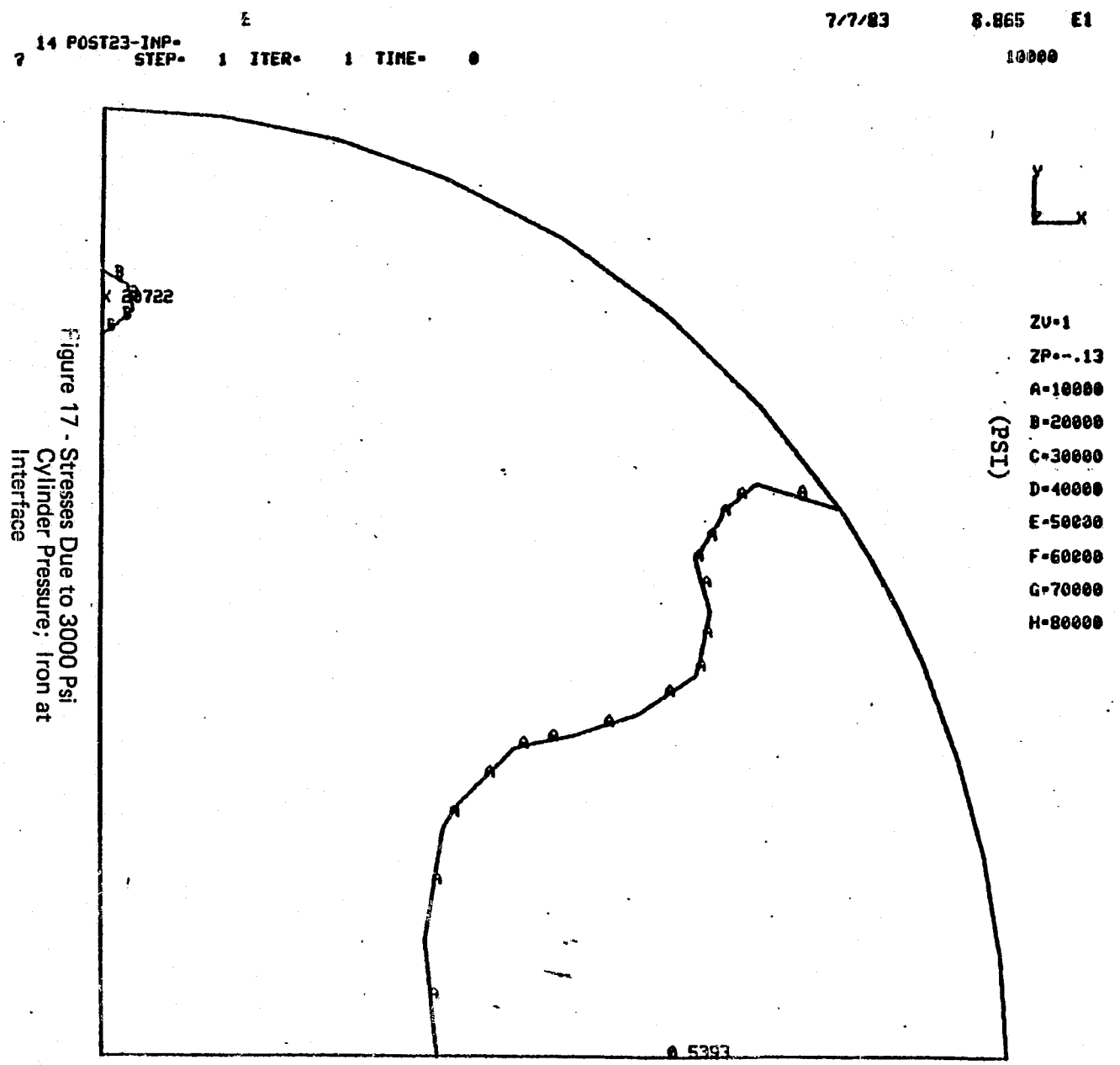

Figure 17 - Stresses Due to 3000 Psi Cylinder Pressure; Iron at Interface

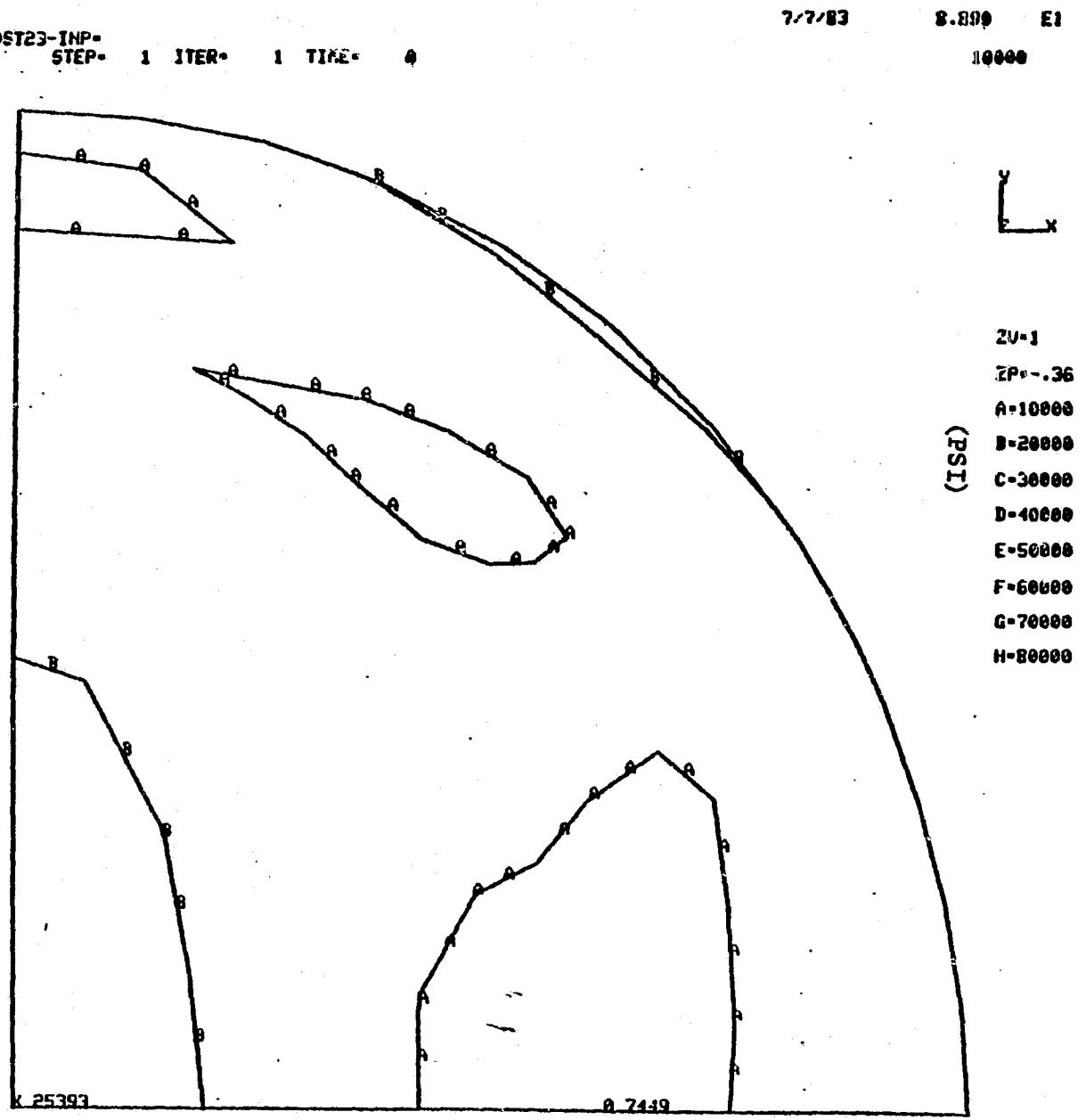

Figure 18 - Stresses Due to 3000 psi Cylinder Pressure - Section thru Underside of Piston Cap

ADVANCED AUTOMOTIVE DIESEL ENGINE

SIGE ANSYS 5

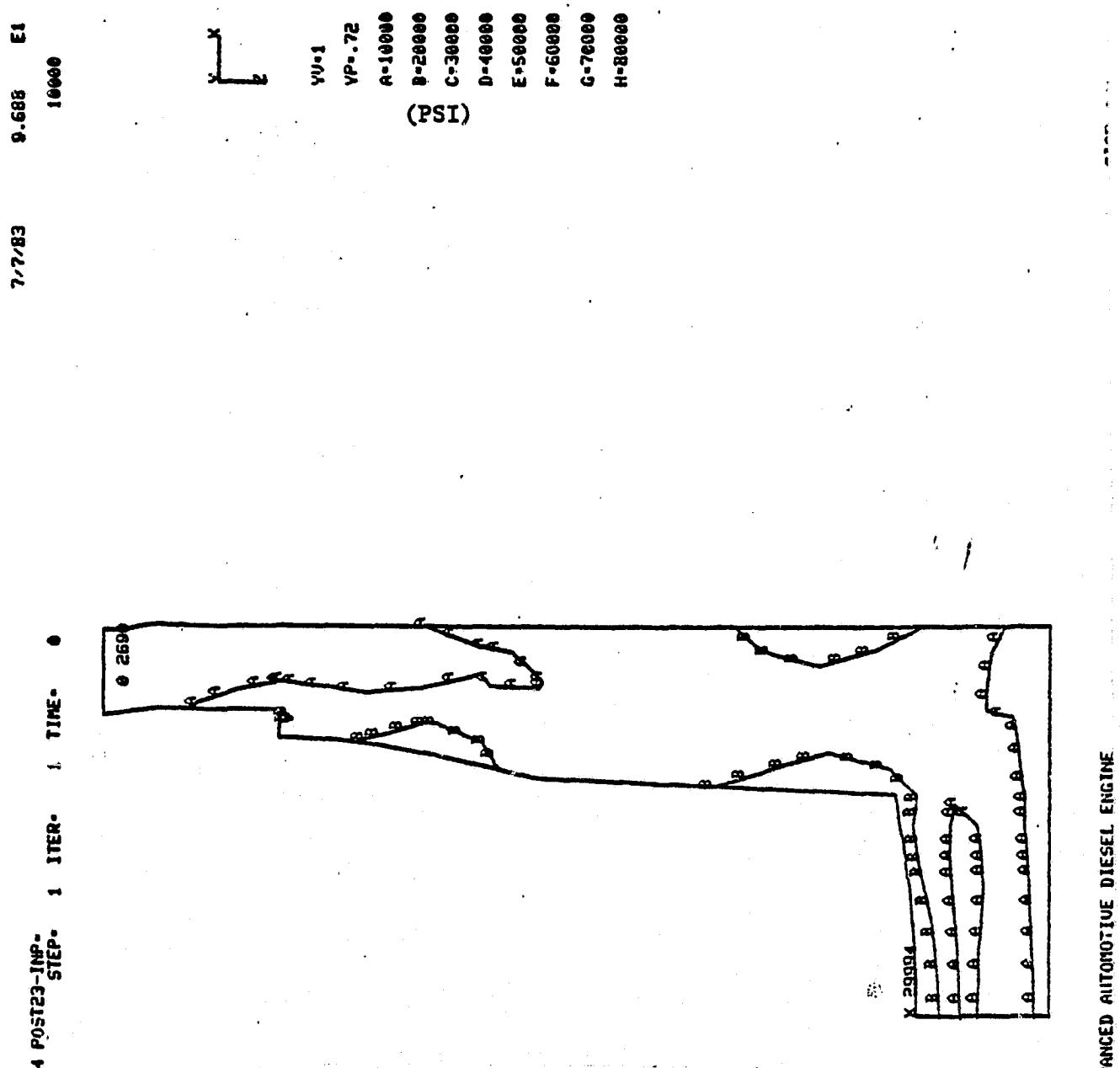

Figure 19 - Equivalent Stress - Section B
3000 psi Cylinder Load

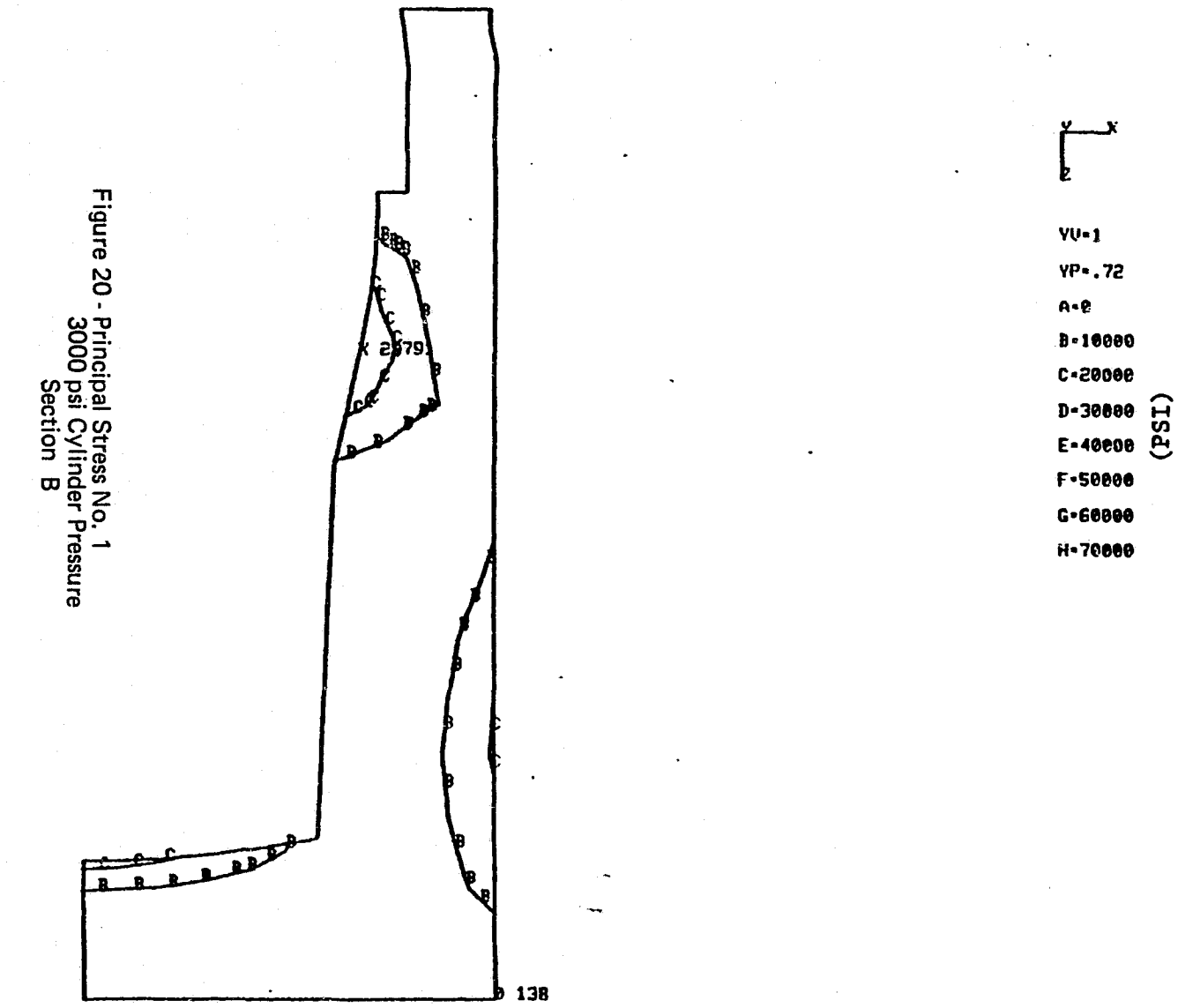

Figure 20 - Principal Stress No. 1
3000 psi Cylinder Pressure
Section B

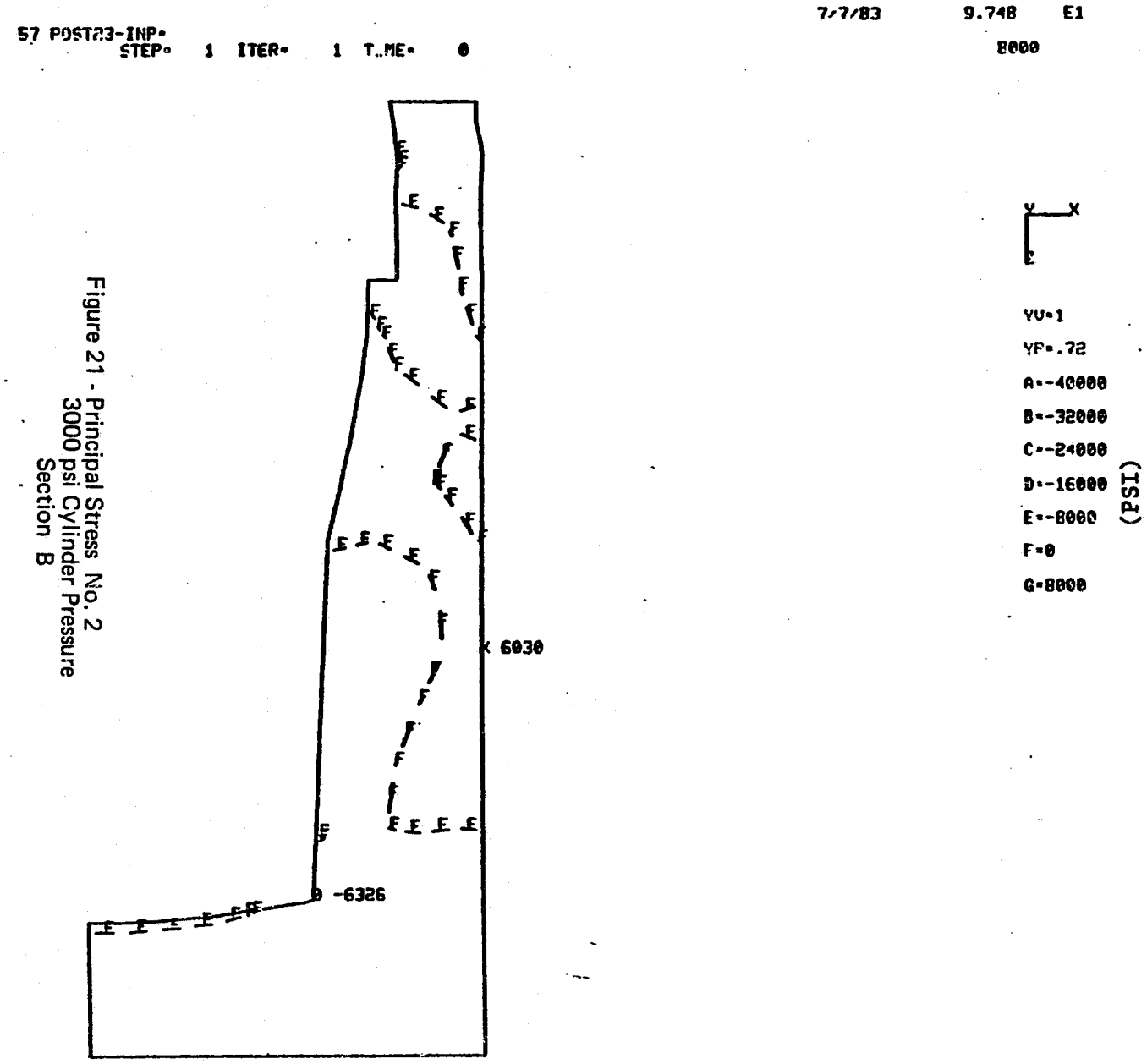

Figure 21 - Principal Stress No. 2
3000 psi Cylinder Pressure
Section B

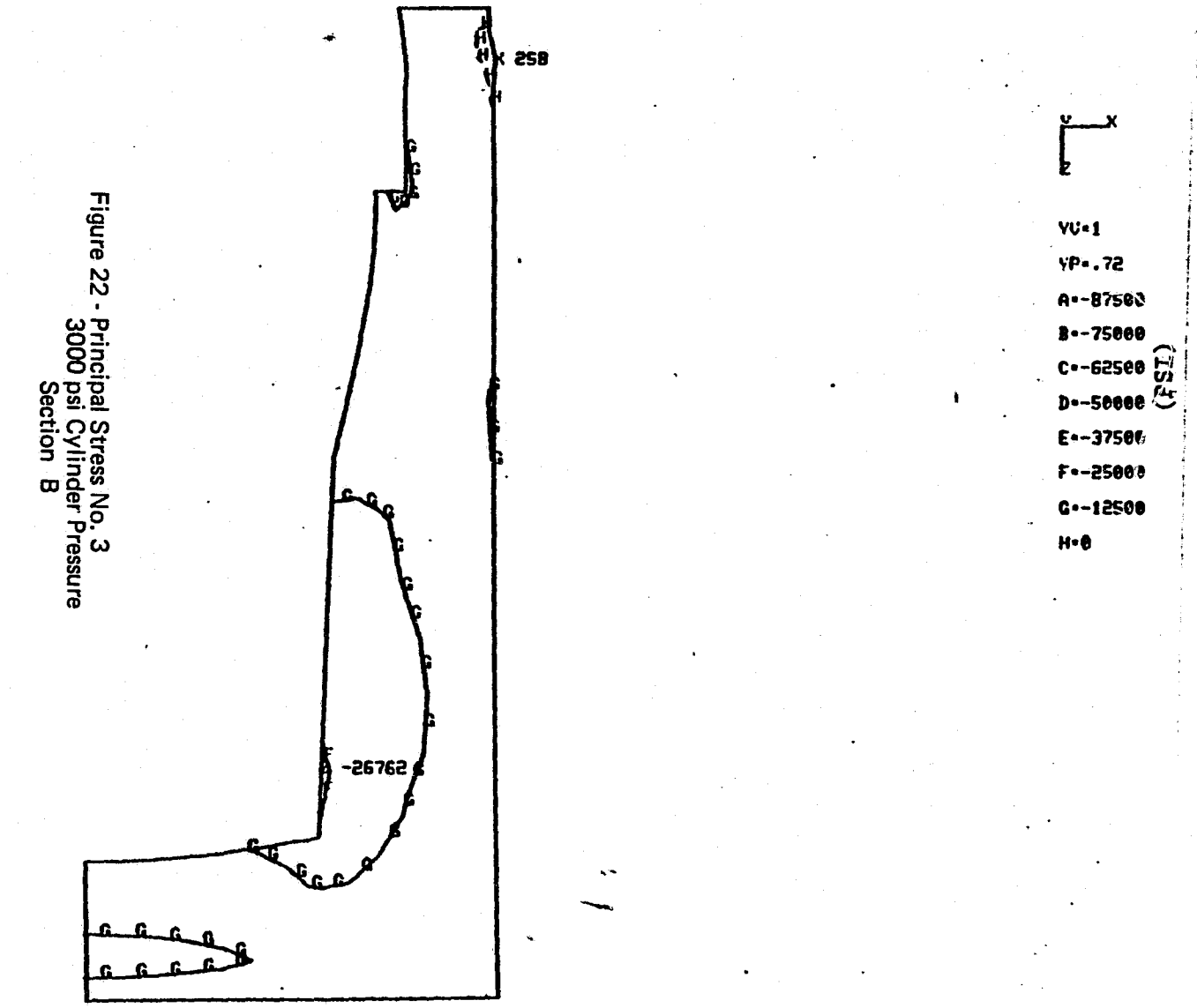

Figure 22 - Principal Stress No. 3
3000 psi Cylinder Pressure
Section B

Figure 23 - Equivalent Stress; 3000 psi Cylinder Pressure - Section C

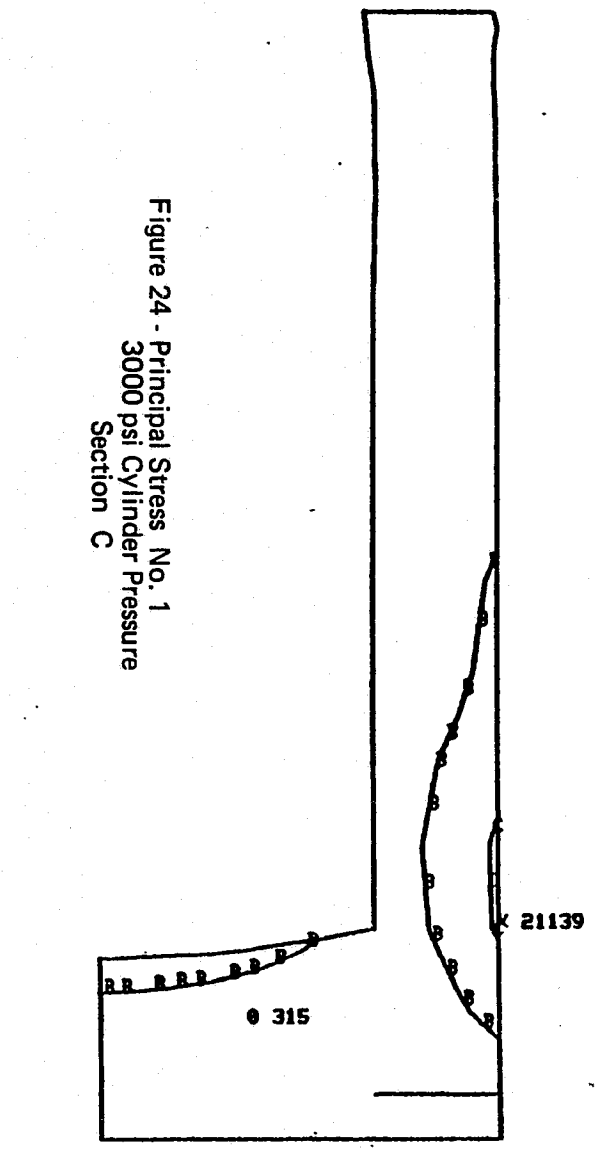

Figure 24 - Principal Stress No. 1
3000 psi Cylinder Pressure
Section C

Figure 25 - Principal Stress No. 3
3000 psi Cylinder Pressure
Section C

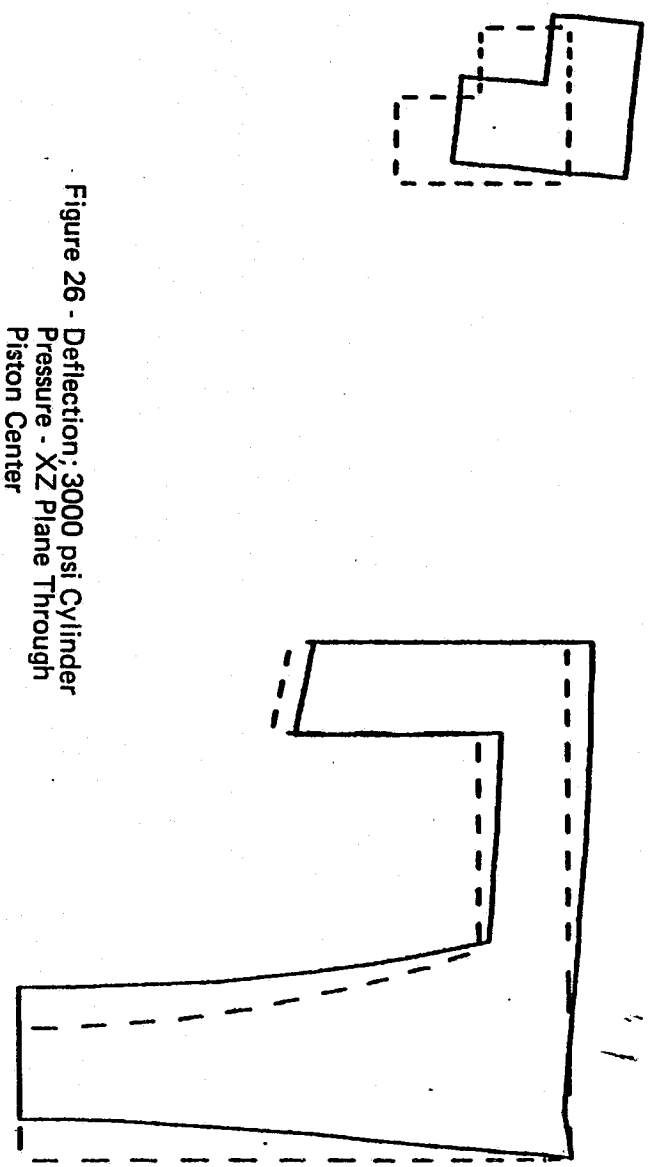

Figure 26 - Deflection; 3000 psi Cylinder Pressure - XZ Plane Through Piston Center

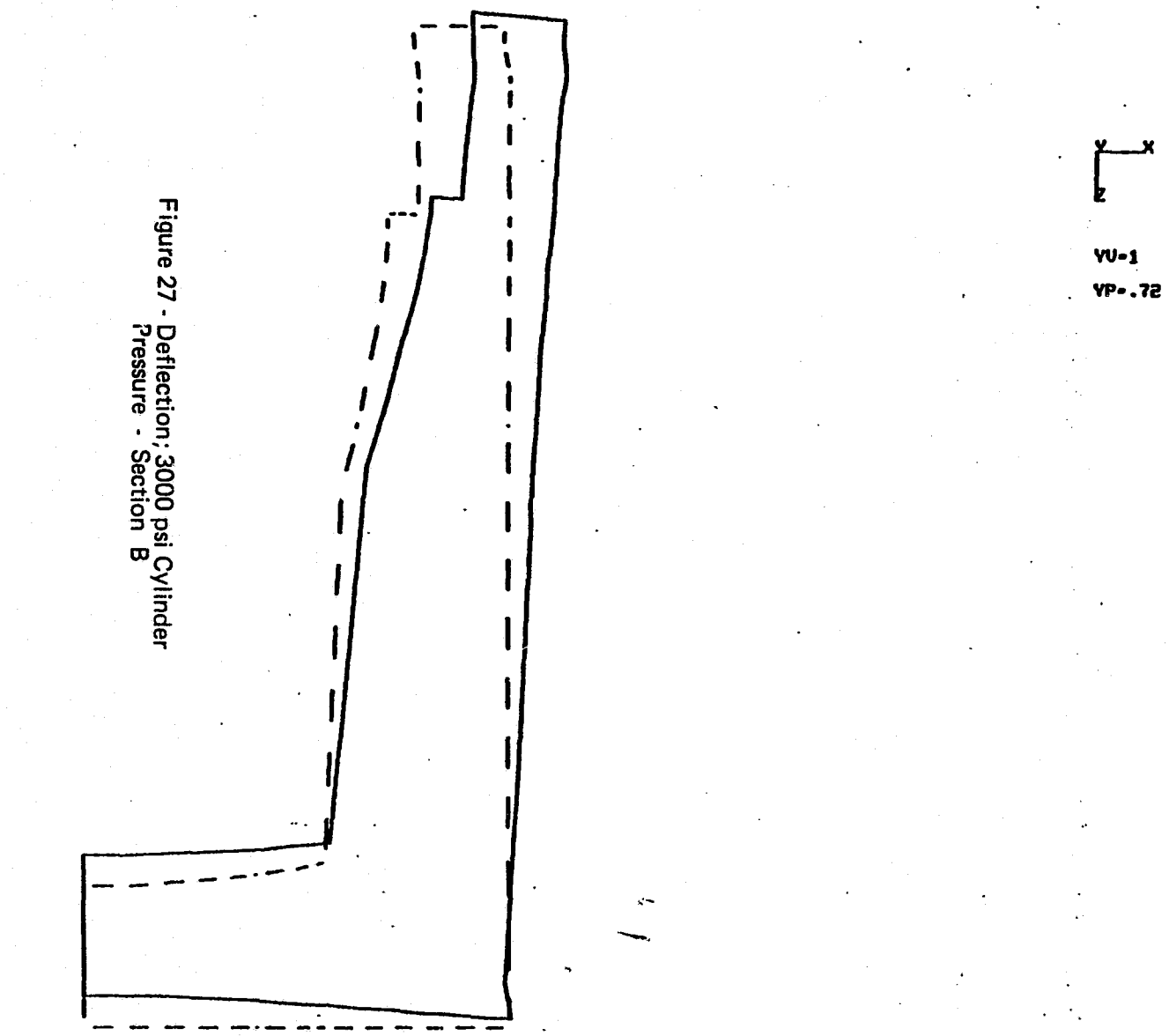

Figure 27 - Deflection; 3000 psi Cylinder Pressure - Section B

XV=1
XP=1.15

Figure 28 - Deflection
3000 psi Cylinder Pressure
Section A

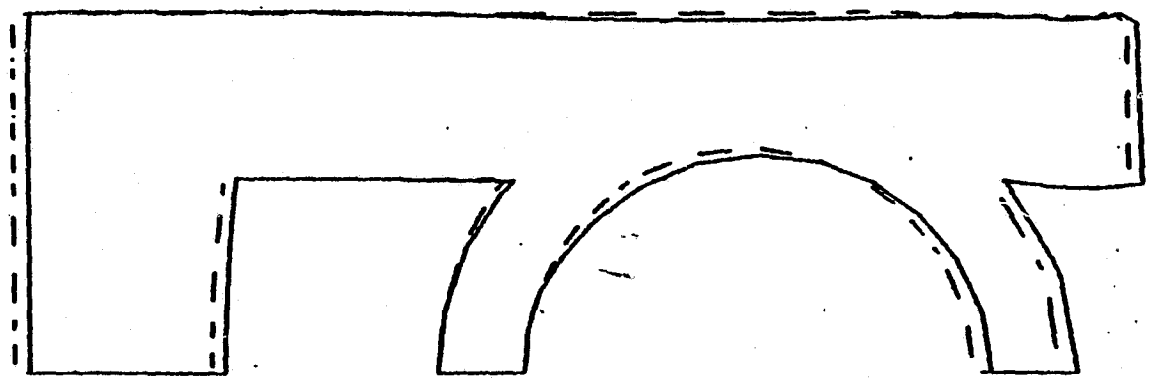

25 POST23-INP•
STEP• 1 ITER• 1 TIME• 0

7/7/83 14.528 E1

.01000

XU=1

XP=.001

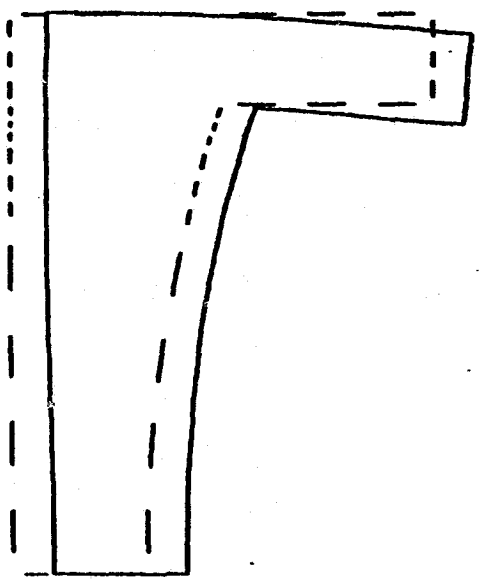

Figure 29 - Deflection; 3000 psi Cylinder Pressure - YZ Plane Through Piston Center

ADVANCED AUTOMOTIVE DIESEL ENGINE

DISP ANSYS

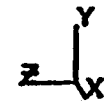

XV=1
YV=.9
ZV=.2

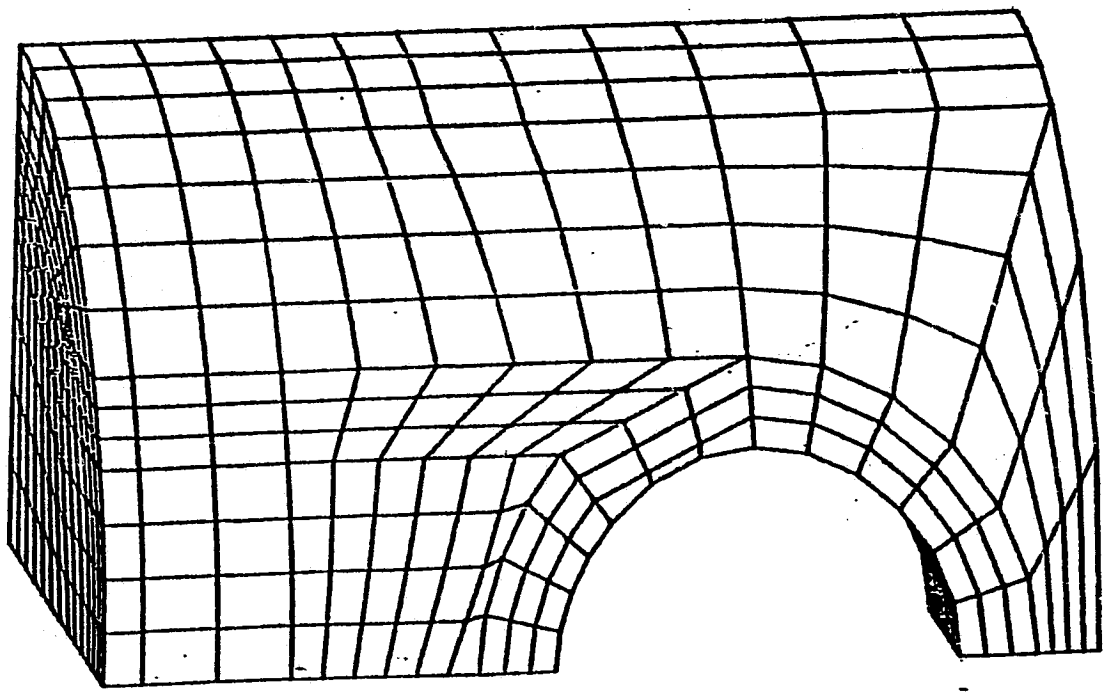

ADVANCED AUTOMOTIVE DIESEL ENGINE

HIDDEN ANSYS 1

Figure 30 - Alternate Piston (No Wheel)

Figure 31 - Liner Finite Element Model

ORIGINAL PAGE IS
OF POOR QUALITY

OMIT TO APPENDIX 10

APPENDIX 9

A.A.D. MARKET DESCRIPTION (ASSUMPTIONS AND HIGHLIGHTS)

PLANNING STAFF - CUMMINS AND
MARKETING STAFF - FORD

NORTH AMERICAN AUTO MARKET
PRODUCT SEGMENTS

GENERAL ASSUMPTIONS

- CONSIDER DOMESTIC MANUFACTURE AND MARKETS ONLY.
- MUCH DOWNSIZING ALREADY DONE: WILL BE ESSENTIALLY COMPLETE BY 1988.
- SIZE STABILIZATION BETWEEN 88/93 WITH EMPHASIS ON AERODYNAMICS AND DRIVETRAIN IMPROVEMENTS.
- SEGMENT SIZES REMAIN STABLE OVER TIME.
- PERFORMANCE STANDARDS (ACCELERATION) NO WORSE THAN TODAY'S WITH PRESSURE TO IMPROVE DIESEL PERFORMANCE ("ADEQUACY" CONCEPT).

	0-60 TIME (SEC)*	
	TODAY	1993
GAS	11-14	11-13
DIESEL	14-20	13-16

*NOT INCLUDING PERFORMANCE MODELS (7-10 SEC)

ORIGINAL PAGE IS
OF POOR QUALITY

NORTH AMERICAN AUTO MARKET

PRODUCT SEGMENTS

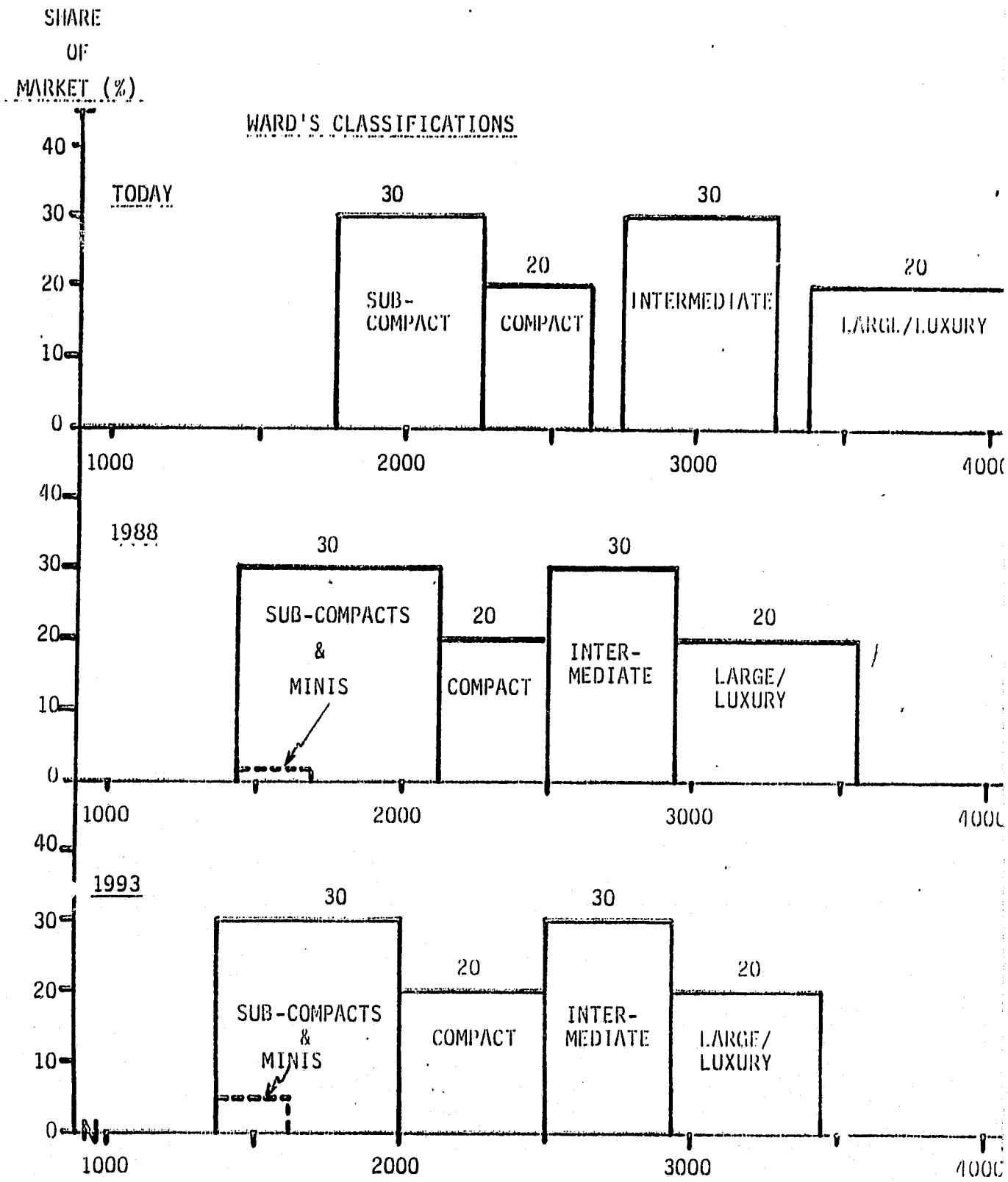

NORTH AMERICAN AUTO MARKET

GASOLINE ECONOMY PROGRESSION

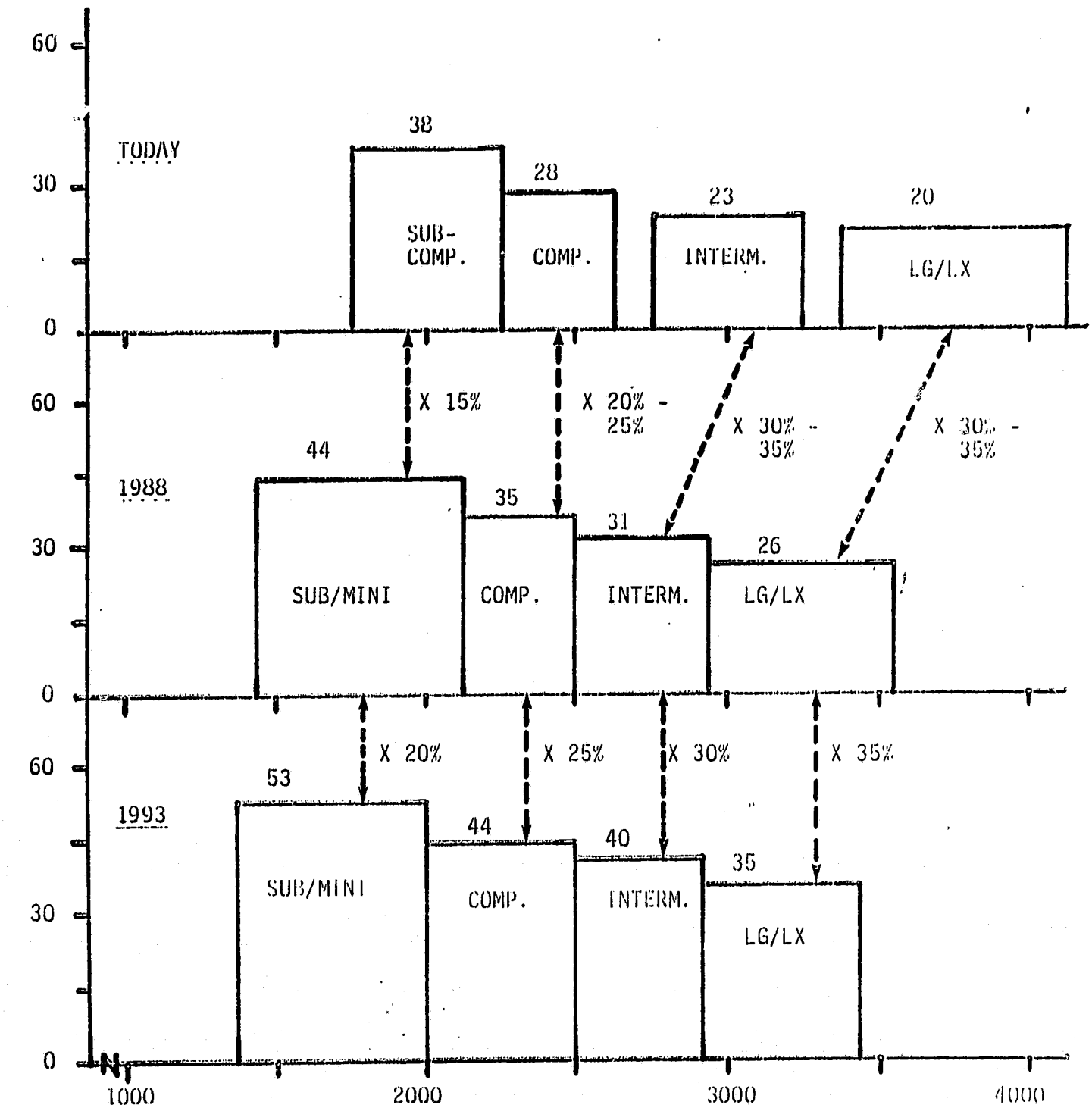

NORTH AMERICAN AUTO MARKET
GASOLINE ECONOMY PROGRESSION

ASSUMPTIONS

- MINIS ARE A SMALL PART (2/30 IN 88, 5/30 IN 93) AND, THUS, HAVE SMALL INFLUENCE ON THE OVERALL CLASS MPG.

- FAST BURN ENGINE DESIGN EXPECTED TO PROVIDE 10-15% MPG IMPROVEMENT ON 4-CYLINDER AND SMALL V-6 ENGINES, 5-10% ON LARGE V6 AND V8 ENGINES.

- DOWNSIZING, AERODYNAMICS, AND TRANSMISSION IMPROVEMENTS ACCOUNT FOR THE BALANCE OF 83-88 MPG INCREASE.

- ADDITIONAL ENGINE IMPROVEMENTS (MULTIPOINT EFI, HIGHER COMPRESSION RATIO, VARIABLE VALVE EVENTS, TURBOCHARGING) GIVE ADDITIONAL 8-10% MPG BY 93.

- GREAT EMPHASIS ON AERODYNAMICS, TRANSMISSIONS (CVT, 5/6 SPEED) PROVIDE ADDITIONAL IMPROVEMENTS BY 93. LARGER CLASSES ARE ESPECIALLY RESPONSIVE TO AERODYNAMIC CHANGES.

NORTH AMERICAN AUTO MARKET

FUEL ECONOMY PROGRESSION

EVOLUTIONARY TECHNOLOGY

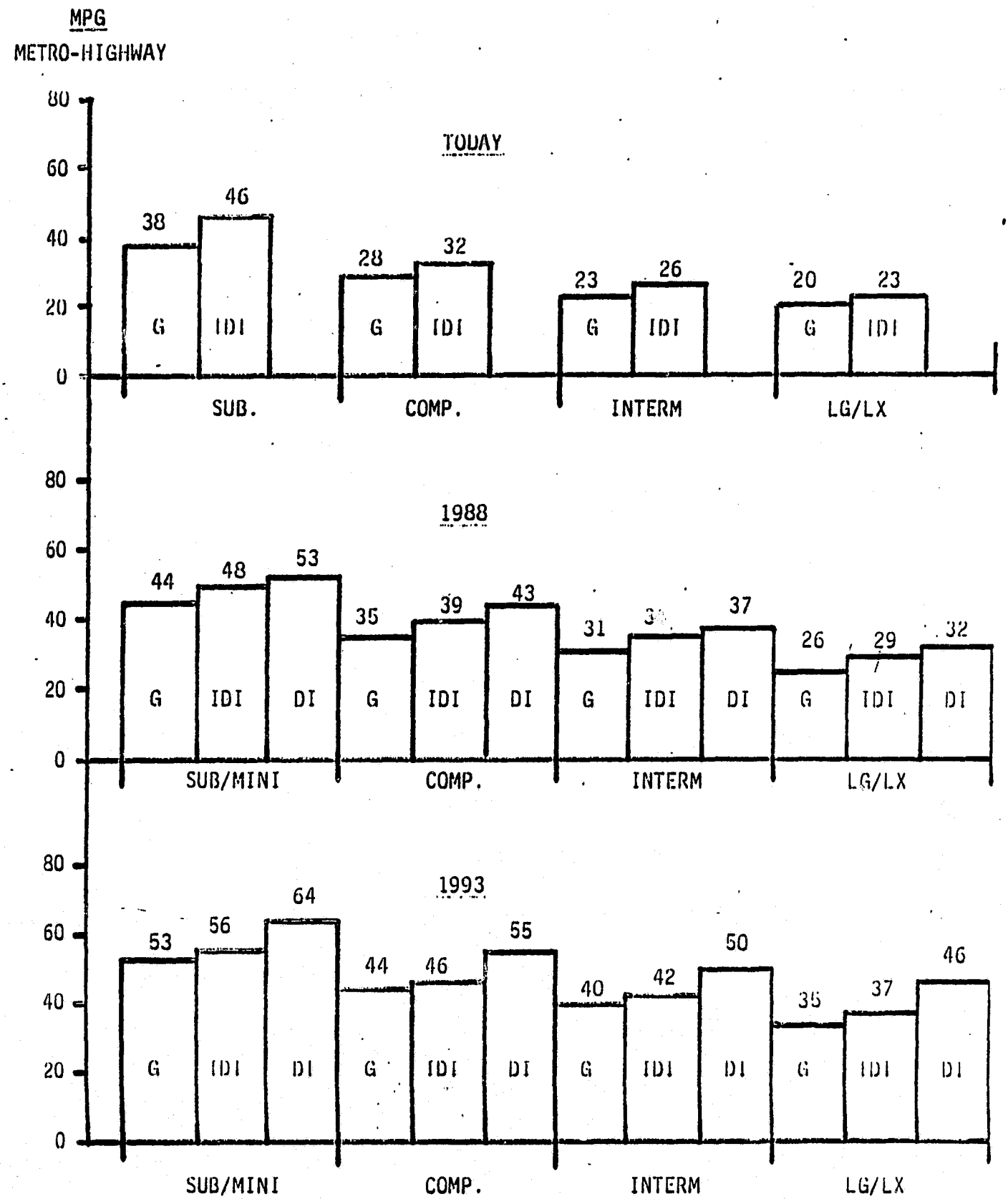

NORTH AMERICAN AUTO MARKET

FUEL ECONOMY PROGRESSION

1993 LIGHT ENGINE TARGETS

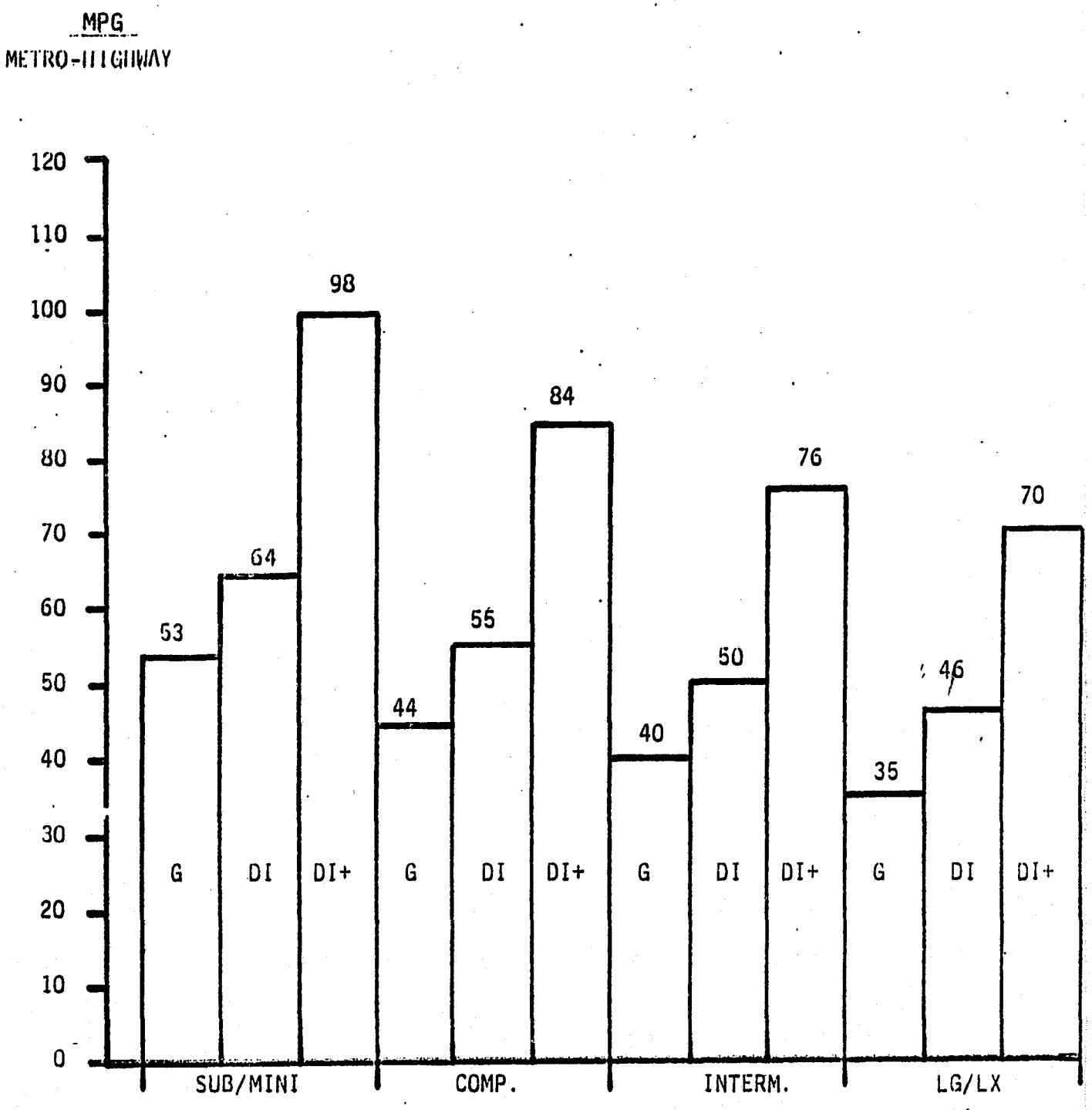

NORTH AMERICAN AUTO MARKET

FUEL ECONOMY PROGRESSION*

CLASS	COMMENT	GAS MPG	IMPR %	COMMENT	IDI MPG	IMPR %	COMMENT	DI MPG	IMPR %	COMMENT	DI+ MPG
TODAY											
Sub		38	20	Low HP,	46						
Compact		28	15	BTU,	32						
Interm		23	15	efficiency	26						
Lg/Lx		20	12.5		23						
1988											
Sub/Mini	Downsize	44	10	Resource	48	10	Demonstrated	53			
Compact	aero, trans,	35	10	emphasis on	39	10	DI IDI	43			
Interm	+10% gas	31	10	DI, gas	34	10		37			
Lg/Lx		26	10		29	10		32			
1993											
Sub/Mini	Aero, trans,	53	5	Resource	56	15**	Improved	64			
Compact	+10% gas	44	5	emphasis on	46	20	turbo, fuel	55			
Interm		40	5	DI, gas,	42	20	systems, high	50			
Lg/Lx		35	5	driveability	37	25	temp. technol	46			
1993/DI+											
Sub/Mini		53					Using Lg/Lx (70 MPG)			Adiabatic,	98
Compact		44					as base, keep same			oilless, impr.	84
Interm		40					ratio as 93 DI,			fuel system, impr.	76
Lg/Lx		35					ex. (50/46)·70 =			combustion, cpd.	70
							76			air chg.	

*Metro-highway

**DI will receive development emphasis. Larger displacement/higher power DI will show best improvement. Larger cars will benefit more from aerodynamic and transmission development.

NORTH AMERICAN AUTO MARKET
CAFE SCENARIOS

ASSUMPTION

MANUFACTURERS WILL NOT BE ABLE TO ADJUST THE GAS/DIESEL MIX TO MEET CAFE BUT WILL HAVE TO RESPOND TO CUSTOMER DESIRES. ANTICIPATED DIESEL RATE RANGE IS 5-15%.

QUESTIONS

- WHAT IS CAFE EXPECTATION POST-85?

LAW		POSSIBLE EXTENSION
83	26	
84	27	(ADD 0.5 MPG/YR)
85	27.5	
		86 28
		87 28.5
		88 29
		89 29.5
		90 30
		91 30.5
		92 31
		93 31.5

- WILL MODEL MIX, FUEL ECONOMY, AND DIESEL RATE ASSUMPTIONS TO THIS POINT MEET CAFE?

NORTH AMERICAN AUTO MARKET

CAFE SCENARIOS

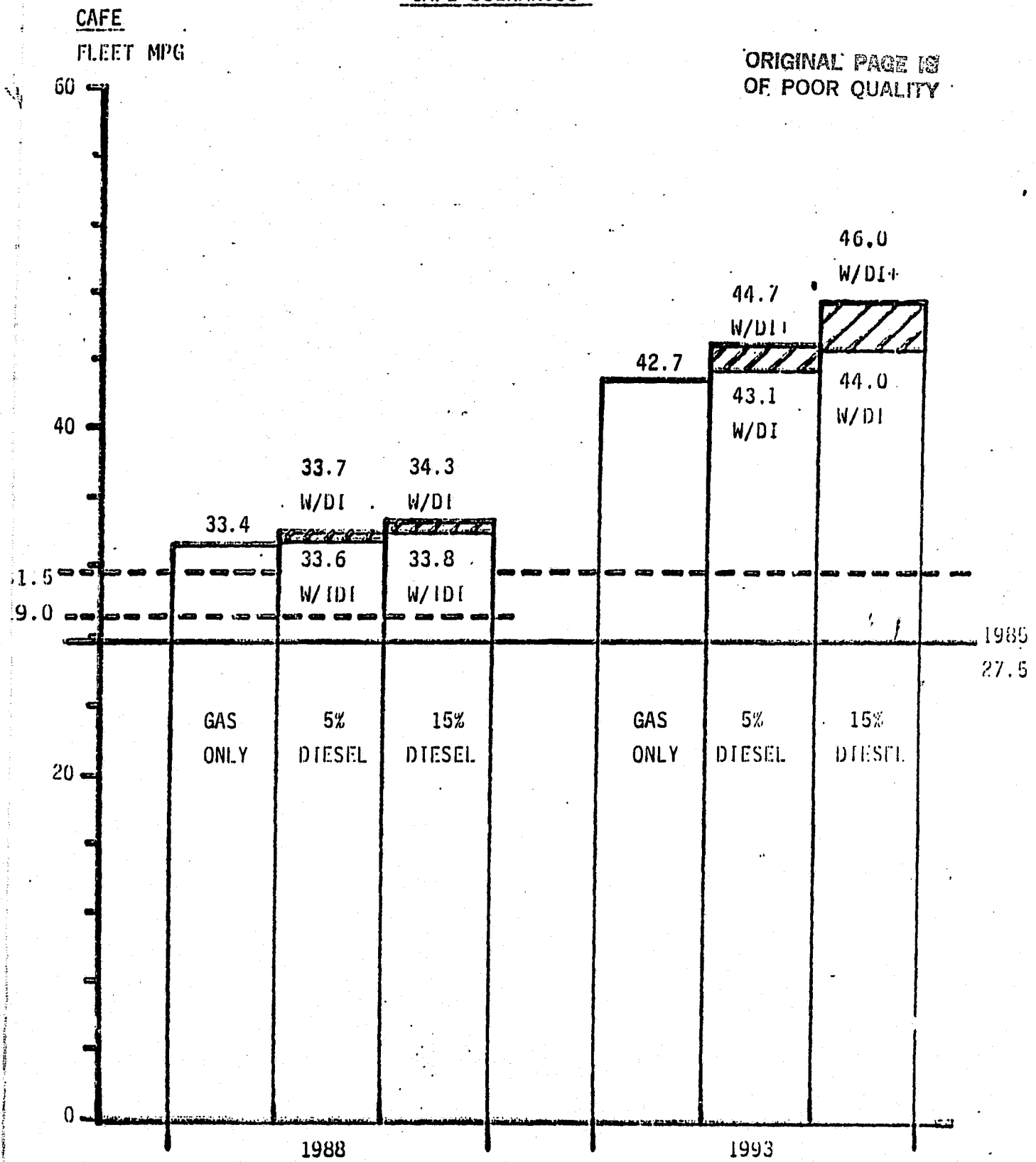

NORTH AMERICAN AUTO MARKET

CAFE SCENARIOS

CALCULATIONS

1988 CLASS	GAS WI	GAS MPG	IDI WI	IDI MPG	DI WI	DI MPG
SUB/MINI	30	44	30	48	30	53
COMPACT	20	35	20	39	20	43
INTERMEDIATE	30	31	30	34	30	37
LARGE/LUXURY	20	26	20	29	20	32
M-H MPG		33.4		36.9		40.5
M-H W/5% DIESEL			G+IDI:	33.6	G+DI:	33.7
M-H W/15% DIESEL			G+IDI:	33.9	G+DI:	34.3

1993 CLASS	GAS WI	GAS MPG	DI WI	DI MPG	DI+ WI	DI+ MPG
SUB/MINI	30	53	30	64	30	98
COMPACT	20	44	20	55	20	84
INTERMEDIATE	30	40	30	50	30	76
LARGE/LUXURY	20	35	20	46	20	70
M-H MPG		42.7		53.6		81.7
M-H W/5% DIESEL			G+DI:	43.1	G+DI+:	44.7
M-H W/15% DIESEL			G+DI:	44.0	G+DI+:	46.0

FORMULA

$$\frac{1}{\frac{S/M\ \%}{MPG} + \frac{C\%}{MPG} + \frac{I\%}{MPG} + \frac{L/L\%}{MPG}}$$

AND

$$\frac{1}{\frac{GAS\ \%}{GAS\ MPG} + \frac{DIESEL\ \%}{DIESEL\ MPG}}$$

NORTH AMERICAN AUTO MARKET

AVERAGE ANNUAL MILES

SEGMENT	AVG. ANNUAL MILES*
SUB/MINI	12,000
COMPACT	12,000
INTERMEDIATE	12,000
LARGE/LUXURY	12,000

*BASED ON INDUSTRY NEW CAR BUYERS DATA: AVERAGE RANGE 11,600-12,800

NORTH AMERICAN AUTO MARKET

FUEL PRICE SCENARIOS

1993 ASSUMPTIONS

PUMP PRICE* ($/GAL)	LOW	BASE	HIGH
SELF SERVICE GAS	$2.30	$2.60	$3.10
SELF SERVICE DIESEL	$2.39	$2.70	$3.22

*INDIANA PRICES WITH ALL STATE AND FEDERAL TAXES

NORTH AMERICAN AUTO MARKET

FUEL COST SCENARIOS - 1993

ORIGINAL PAGE IS
OF POOR QUALITY

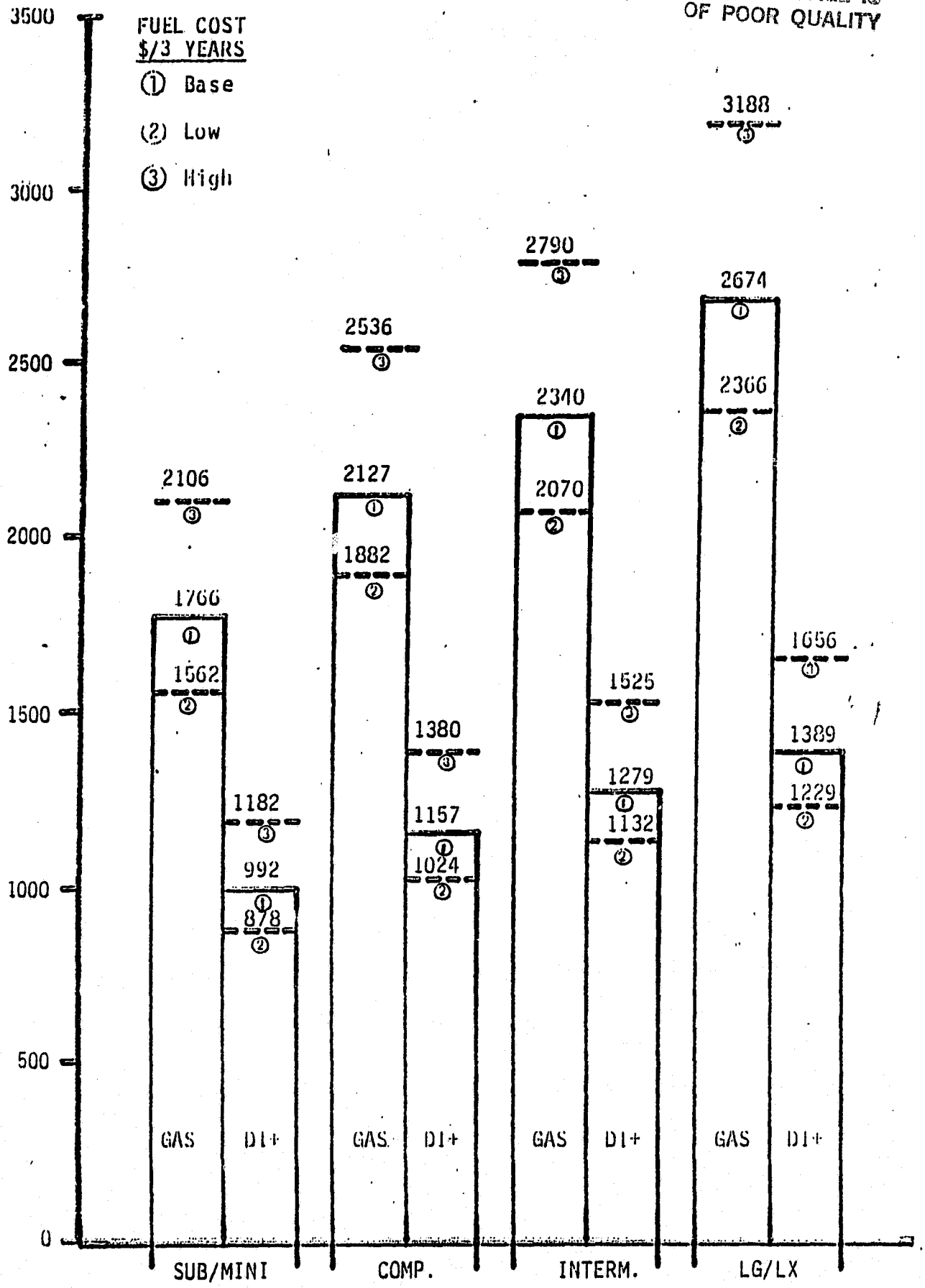

NORTH AMERICAN AUTO MARKET

FUEL COST SCENARIOS

ASSUMPTIONS

- 1993 SEGMENT MPG AS DERIVED.
- 1993 FUEL COST AS DESCRIBED. HELD CONSTANT.
- 1993 ANNUAL MILEAGE AS DESCRIBED.
- ANTICIPATES THREE YEAR PAYBACK PERIOD (BASED ON TYPICAL FINANCING PERIOD).

NORTH AMERICAN AUTO MARKET

FUEL COST SCENARIOS - 1993

CALCULATIONS

CLASS	ANNUAL MILES	GAS MPG	GAS* COST	DI+ MPG	DI+* COST	GAS > * DI+
			①		①	
SUB/MINI	12,000	53	1766	98	992	774
COMPACT	12,000	44	2127	84	1157	970
INTERMEDIATE	12,000	40	2340	76	1279	1061
LARGE/LUXURY	12,000	35	2674	70	1389	1285
			②		②	
SUB/MINI			1562		878	684
COMPACT			1882		1024	858
INTERMEDIATE			2070		1132	938
LARGE/LUXURY			2366		1229	1137
			③		③	
SUB/MINI			2106		1182	924
COMPACT			2536		1380	1156
INTERMEDIATE			2790		1525	1265
LARGE/LUXURY			3188		1656	1532

* IN 3 YEARS

① BASE CASE

② LOW CASE

③ HIGH CASE

NORTH AMERICAN AUTO MARKET

POTENTIAL DIESEL PRICE PREMIUM - 1993

PAYBACK ANALYSIS

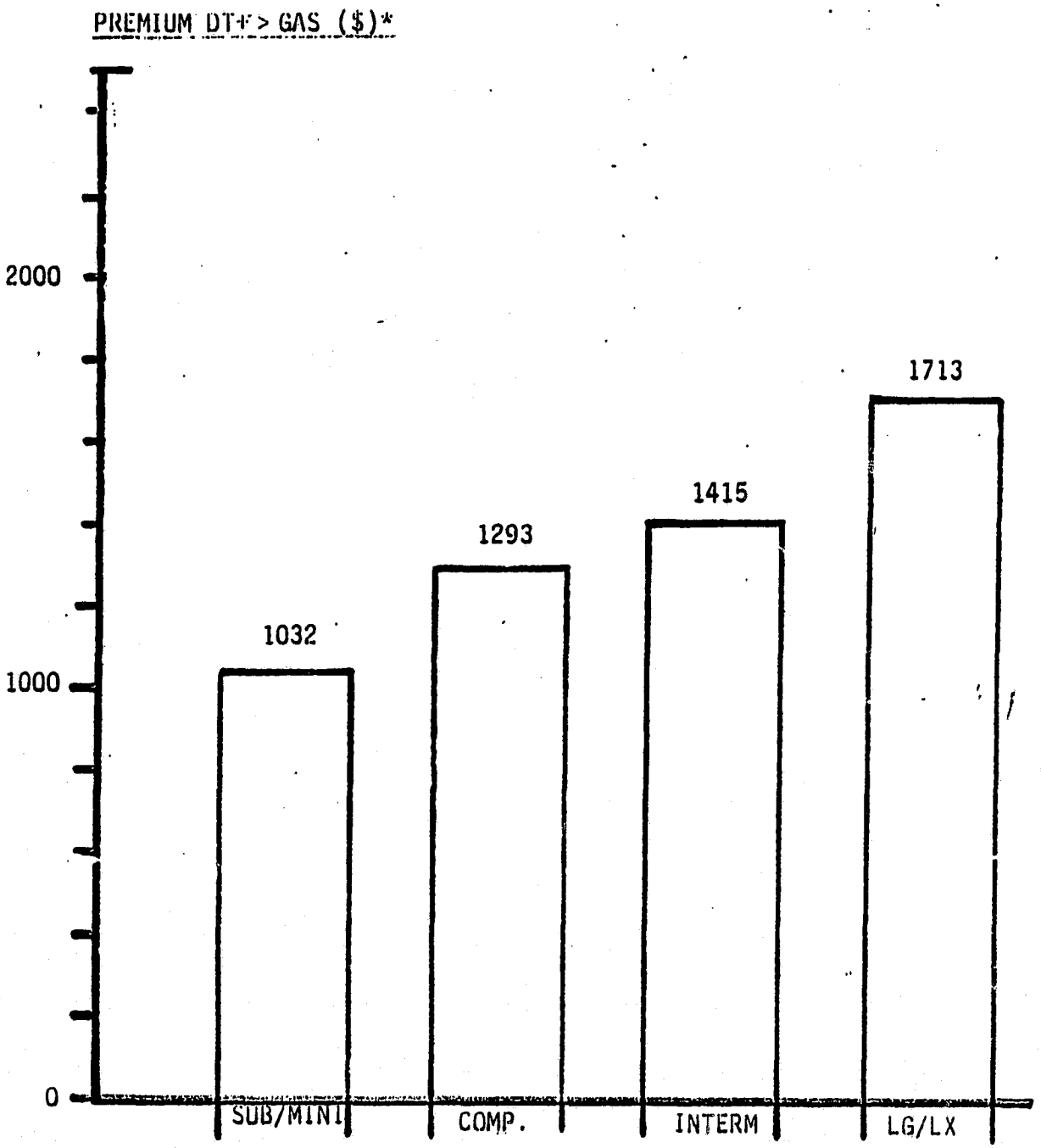

* AT BASE CASE FUEL COST

NORTH AMERICAN AUTO MARKET
PAYBACK SCENARIOS

ASSUMPTIONS

- FUEL COST AS CALCULATED
- THREE YEAR PAYBACK
- DRIVER NEITHER EXPLICITLY NOR IMPLICITLY RECOGNIZES NPV CONCEPT BUT, RATHER, COMPARES TOTAL FUEL COST SAVINGS TO ENGINE PREMIUM.
- DIESEL RESALE VALUE (RETURN OF PREMIUM) IS SET AT 25%* TO BE CONSERVATIVE ($\leq$0 TODAY FOR SOME MODELS. ESTIMATED BY FORD TO BE 25-75% BASED ON MILEAGE IN 1993)
- PREMIUM = FUEL SAVINGS + RETURN OF PREMIUM

$$P = \frac{S}{1-\%}$$

- DIFFERENCES IN SCHEDULED MAINTENANCE HAVE NOT BEEN CONSIDERED
  - COMPARING OILLESS/UNCOOLED DI+ TO TREND TO EXTENDED MAINTENANCE ON GAS CARS. THIS APPEARS LEGITIMATE

*STRAIGHT LINE DEPRECIATION AT 25%/YEAR FOR THREE YEARS

NORTH AMERICAN AUTO MARKET

PAYBACK SCENARIOS

CALCULATIONS

CLASS	TOTAL MILES	FUEL* SAVINGS	PREMIUM RETD	POSSIBLE** PREMIUM
SUB/MINI	36,000	774	25%	1032
COMPACT	36,000	970	25%	1293
INTERMEDIATE	36,000	1061	25%	1415
LARGE/LUXURY	36,000	1285	25%	1713

*BASE CASE FUEL COST

**ECONOMICALLY DETERMINED DI+ OPTION PRICE

NORTH AMERICAN AUTO MARKET
VOLUME POTENTIAL - 1993

ASSUMPTIONS

- 12,000,000 RETAIL SALES IS A REPRESENTATIVE FORECAST
  - 75% DOMESTIC
  - NO INVENTORY ADJUSTMENT
- PRODUCT SEGMENTATION AS DISCUSSED
- USE DIESELIZATION RANGE OF 5-15% AS MOST LIKELY
  - MANUFACTURERS LIKELY WILL NOT HAVE TO "PUSH" DIESELS TO MEET CAFE
  - DIESEL PENETRATION IS DIFFICULT TO SYSTEMATICALLY FORECAST AS CUSTOMERS RESPOND TO MORE THAN PURELY ECONOMIC STIMULI. OTHER FACTORS INCLUDE OPTION PRICE, MID-EAST POLITICS, DIESEL ODOR/NOISE, TANK MILEAGE, PRODUCT HISTORY (NEW/OLD, POSITIVE/NEGATIVE), VEHICLE FEATURES, "FASHION".

NORTH AMERICAN AUTO MARKET
VOLUME POTENTIAL - 1993

TOTAL MARKET	DOMESTIC	SEGMENT	%	% D	DIESELS
12,000,000	75%	SUB/MINI	30	5	135,000
				15	405,000
		COMPACT	20	5	90,000
				15	270,000
		INTERMEDIATE	30	5	135,000
				15	405,000
		LARGE/LUXURY	20	5	90,000
				15	270,000

NORTH AMERICAN AUTO MARKET
VOLUME POTENTIAL - 1993

ISSUE

- INSPECTION OF THE AUTO NUMBERS INDICATES SOMEWHAT LOW POTENTIAL DEMAND FOR DI+ WHEN COMPARED TO ECONOMIC PLANT SIZE CONSIDERATIONS (500,000/YEAR) ESPECIALLY WHEN SPLIT AMONG MANUFACTURERS.

PRINCIPAL CANDIDATE	DIESEL VOLUME RANGE
LARGE/LUXURY	90,000-270,000
SECONDARY CANDIDATES*	
INTERMEDIATE	135,000-405,000
COMPACT	90,000-270,000
TOTAL	315,000-945,000

*FOR SMALLER/DERATED DI+

- ADDITIONAL MARKET DEMAND SHOULD BE IDENTIFIED.
  - COMPACT TRUCKS APPEAR TO BE GOOD CANDIDATES

NORTH AMERICAN AUTO MARKET
LIGHT TRUCK VOLUMES - 1993

ASSUMPTIONS

- COMPACT LIGHT TRUCKS HAVE A SIGNIFICANT PERSONAL USE MISSION AND ROUGHLY THE SAME CURB WEIGHT AS FUTURE LARGE/LUXURY CARS.

- ON OCCASIONS WHEN COMPACT TRUCKS ARE LOADED, THE HORSEPOWER AND TORQUE CHARACTERISTICS OF DI+ AS NOW DEFINED ARE VERY ATTRACTIVE.

- IT IS ANTICIPATED THAT THE BULK OF COMPACT TRUCKS WILL REMAIN REAR WHEEL DRIVE THUS REQUIRING MINOR RE-ENGINEERING OF DI+ TO FIT LONGITUDINAL INSTALLATIONS. THIS ASSUMPTION MIGHT BE MODIFIED SOMEWHAT DEPENDING ON THE DIRECTION COMPACT VANS TAKE RE FWD VERSUS RWD.

- 3,500,000 RETAIL SALES IS A REPRESENTATIVE FORECAST

    - 75% DOMESTIC MANUFACTURE
    - 50-70% COMPACTS (50-30% FULL SIZE)
    - 5 TO 15% DIESEL

- PAYBACK ANALYSIS IDENTICAL WITH LARGE/LUXURY CARS.

NORTH AMERICAN AUTO MARKET
LIGHT TRUCK VOLUMES - 1993

TOTAL MARKET	DOMESTIC	COMPACTS	% D	DIESELS
3,500,000	75%	50%	5	65,600
			15	196,800
		70%	5	91,900
			15	275,700

NORTH AMERICAN AUTO MARKET
TOTAL DI+ DEMAND - 1993

TOTAL DEMAND POTENTIAL

PRINCIPAL CANDIDATES	DIESEL VOLUME RANGE	PER DAY @ 240
LARGE/LUXURY	90,000- 270,000	375-1125
COMPACT LT	66,000- 276,000	275-1150
SUB TOTAL PRINCIPAL	156,000- 546,000	650-2275
SECONDARY* CANDIDATES		
INTERMEDIATE	135,000- 405,000	565-1690
COMPACT	90,000- 270,000	375-1125
SUB TOTAL SECONDARY	225,000- 675,000	940-2815
GRAND TOTAL	381,000-1,221,000	1590-5090

*FOR SMALLER/DERATED DI+

NORTH AMERICAN AUTO MARKET

SUMMARY

- POTENTIAL EXISTS FOR SUBSTANTIAL FUEL ECONOMY INCREASE VIA EXPECTED TECHNOLOGY PROGRESSION (DOWNSIZING, EVOLUTIONARY ENGINE/TRANSMISSION/ AERODYNAMICS).

- DI+ OFFERS A QUANTUM JUMP IN ECONOMY.

- OWING TO THE SUCCESS OF EXPECTED TECHNOLOGY, MANUFACTURERS WILL LIKELY <u>NOT</u> BE FORCED TO MAKE STRATEGIC SEGMENT MIX OR DIESEL PROMOTIONAL CHANGES TO MEET "REASONABLE" FORESEEABLE CAFE LEGISLATION.

NORTH AMERICAN AUTO MARKET

CONCLUSIONS

- DI+ VIABILITY WILL DEPEND ON ITS ABILITY TO OFFER SUBSTANTIAL ECONOMY IMPROVEMENT AT AN ACCEPTABLE PRICE PREMIUM ALL IN THE CONTEXT OF "ADEQUATE" PERFORMANCE VERSUS GASOLINE ENGINES.

- ECONOMICS SUGGEST LARGE/LUXURY CARS AND COMPACT LT ARE THE MOST ATTRACTIVE CANDIDATES FOR DI+. IT IS LIKELY THAT THESE PLATFORMS ARE ALSO BEST FROM AN ENGINEERING (ENGINE BAY ENVELOPE) AND MARKETING (RETAIL PRICE SENSITIVITY) PERSPECTIVE.

- CALCULATED DEMAND VOLUMES FOR PRINCIPAL CANDIDATES APPEAR TO NEED DETAILED REVIEW IN TERMS OF ECONOMIC PLANT SIZE: IF RULE OF THUMB MINIMUM (500,000/YEAR, 2100/DAY) IS TRUE, VOLUMES APPEAR MARGINAL WHEN SPLIT AMONG COMPETING OEMS. THIS SUGGESTS PROGRAMS TO INCREASE DIESELIZATION RATE IN THE PRINCIPAL CANDIDATE SEGMENTS (STRATEGIC PRICING?), OR USE OF DI+ OR COMPONENTS THEREOF IN THE SECONDARY CANDIDATE SEGMENTS, OR THE ESTABLISHMENT OF AN INDEPENDENT ENGINE MANUFACTURER CAPABLE OF BUILDING DI+ FOR ALL VEHICLE MANUFACTURERS, OR, FINALLY, A JOINT VENTURE AMONG INTERESTED DI+ USERS.

NORTH AMERICAN AUTO MARKET
PRICE/COST

OPTION PRICE

- PAYBACK ANALYSIS SUGGESTS THAT A DI+ OPTION PRICE IN THE $1500-1800 RANGE WOULD BE ACCEPTABLE TO THE RATIONAL BUYER.

- AS SUGGESTED EARLIER, HOWEVER, A LARGE NUMBER OF BUYERS ARE NOT "RATIONAL". IN VIEW OF THE FACT THAT DI+ WILL BE A NEW AND UNUSUAL PRODUCT AND UNDERSTANDING THE ROLE OF "STICKER SHOCK" AS A BUYING DETERRENT, AN INTUITIVELY SET PRICING TARGET OF $1000 IS SUGGESTED.

- THIS TARGET MAY BE ADJUSTED OVER TIME AS WE IMPROVE OUR UNDERSTANDING OF THE 1993 DIESEL MARKET.

NORTH AMERICAN AUTO MARKET
PRICE/COST

MANUFACTURING COST

- INSTALLATION COSTS FOR DI+ ARE LIKELY TO BE ABOUT THE SAME AS FOR A COMPETITIVE GASOLINE OR OTHER CONVENTIONAL DIESEL ENGINE. VEHICLE COOLING SYSTEM SAVINGS WILL BE APPROXIMATELY OFFSET BY PASSENGER COMPARTMENT HEATING SYSTEMS. IT IS ASSUMED THAT DI+ ELECTRONICS ARE COMPATIBLE WITH THE VEHICLE ELECTRONICS, THAT DI+ IS COMPATIBLE WITH EXISTING DRIVETRAIN COMPONENTS, AND THAT THE VEHICLE MANUFACTURERS WILL NOT DEVELOP A SPECIAL CHASSIS/BODY FOR DI+.

- WHILE VEHICLE MANUFACTURERS MIGHT BE WILLING TO SELL DI+ AT A LOSS FOR A SHORT TIME IN ORDER TO ESTABLISH THE MARKET, THE LONG TERM SOLUTION IS TO CONTROL DI+ COST TO MAKE THE PRICING TARGET SUSTAINABLE IN A BUSINESS SENSE.

- THIS SUGGESTS THAT THE INSTALLED COST PREMIUM FOR DI+ OVER THE BASE GASOLINE ENGINE BE IN THE RANGE OF $500 TO A MAXIMUM OF $1000.

NORTH AMERICAN AUTO MARKETS
DI TIMING

1993 MODEL YEAR LAUNCH

- GIVEN A LAUNCH DATE FOR THE 1993 MODEL YEAR, THE KEY DATES SUGGEST AN AGGRESSIVE PROGRAM BEGINNING NOW (SEE FOLLOWING CHART).
- BEGIN COMPONENT/ENGINE DESIGN/DEVELOPMENT NOW.
- DEMONSTRATE ENGINE CONCEPT FEASIBILITY BY END OF 1985 - DEVELOPMENT CONTINUES, OF COURSE, INTO FUTURE.
- PRODUCE AND SHIP 20 ENGINES PER VEHICLE MANUFACTURER BY MID-1987.
- VEHICLE MANUFACTURERS DEMONSTRATE COMPLETE POWER TRAIN FEASIBILITY MID-1987 TO MID-1988.
- BEGIN ENGINE AND VEHICLE SYSTEMS PRODUCTION ENGINEERING LATE 1988.
- RECEIVE ENGINE AND VEHICLE MANUFACTURING EQUIPMENT AND TOOLING QUOTES LATE 1989.
- ORDER LONGLEAD TOOLING EARLY 1990.
- INSTALL AND RUNOFF EQUIPMENT FIRST Qr 1992.
- BEGIN SERIES PRODUCTION AT MODEL CHANGEOVER MID-1992.

ADVANCED AUTOMOBILE DIESEL

TIME/PHASE TO 1993 MY LAUNCH

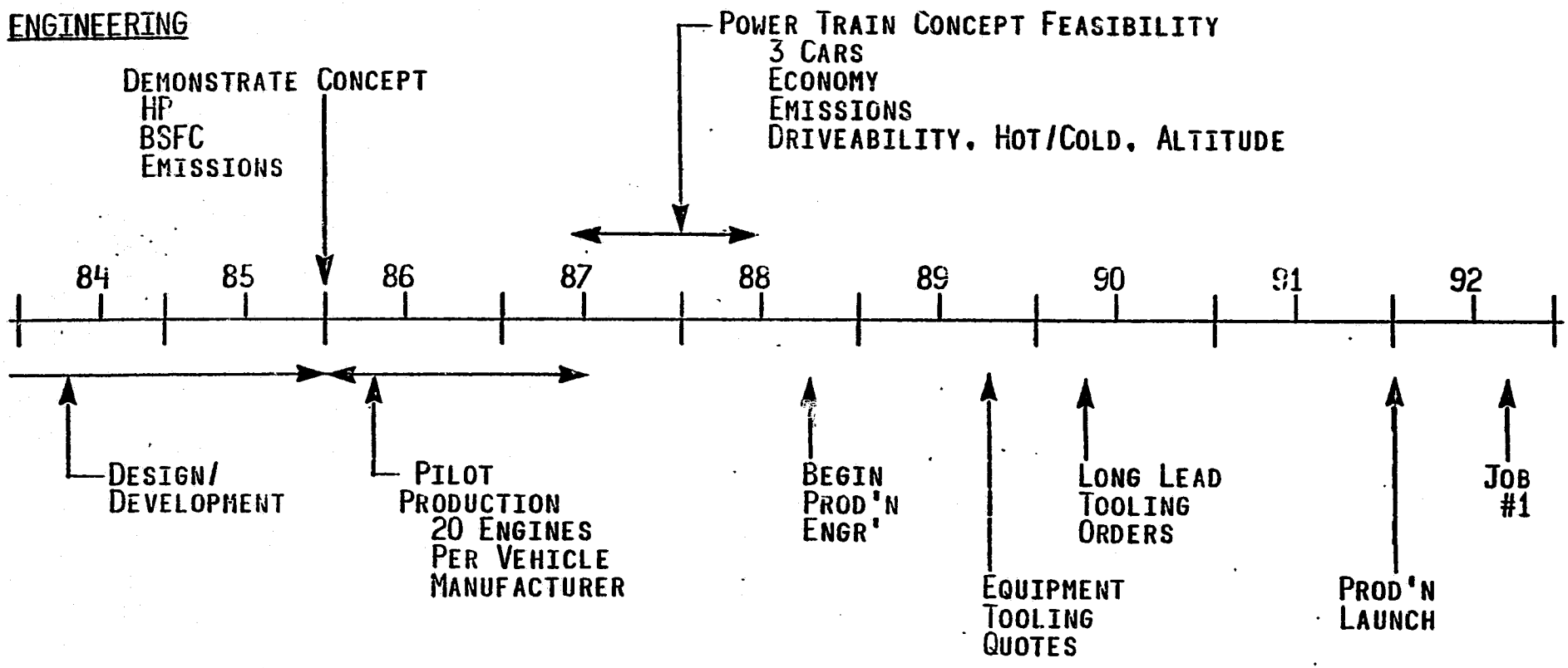

D9

APPENDIX 10

LONG TERM TECHNOLOGY DEVELOPMENT PROGRAM

R. SEKAR
L. TOZZI

In the Advanced Adiabatic Development program, the following technology have been identified as critical:

(1) Piston development for oil-less, adiabatic engine.

(2) Positive displacement compounding and charge system.

(3) Experimental evaluation of the preheat concept.

(4) Combustion system with positive ignition assist.

(5) Ceramic manufacturing technology.

Of these five areas, ceramic manufacturing technology is the pacing item, and is already being addressed by several organizations. therefore the four remaining areas need immediate attention. Since the lead time involved in engine development and production is long, this technology development should be done concurrently with the AAD engine development.

A four year program is outlined below which will simultaneously study these first four areas. This program requires two test rigs; 1) one single cylinder adiabatic engine; and 2) one multicylinder adiabatic turbocompound engine.

FIRST YEAR

Task 1 - Preparation of Test Beds

1. Prepare detailed drawings of adiabatic components:
   - Cylinder head
   - Piston
   - Liner
2. Order patterns and tools to make key components.
3. Prepare a complete list of standard and nonstandard components.
4. Inspect, modify, and assemble test engines.
5. Check out the engines in test cells.

This task is estimated to take up to 12 months.

Task 2 - Piston Designs for Oil-less, Adiabatic Engines

A gas bearing piston is currently being demonstrated under a TACOM program, and a ceramic piston-liner combination in a small gasoline engine has already been demonstrated. Specific activities under this task are:

1. Analytical study of gas bearing between piston and liner with emphasis on durability of components.

2. Make detailed design drawings.

3. Procure pistons for engines prepared in Task 1.

This task should take about 9 months.

Task 3 - Part Load Preheating Concept Study

Part load preheating coupled with a compounding system has shown improved fuel economy in a passenger car. This task proposed an analytical study be done to quantify the effects of this concept on one medium duty and one heavy duty application. Design of a heat exchanger for future testing is also included in this task.

Proposed activities are:

1. Generate fuel maps using Diesel Cycle Simulation (DCS) for medium and heavy duty applications with optimum levels of part load preheating.

2. Quantify the benefit in fuel consumption through Vehicle Mission Simulation (VMS).

3. Model and study thermal lag issues.

4. Determine if a "switching" mechanism is needed to switch from preheating to aftercooling.

5. Design a heat exchanger for multicylinder testing defined in Task 1.

This task is estimated to take 9 months.

Task 4 - Screw Compressor-Expander

A screw compressor-expander has shown potential for performance improvement. However, cost, producibility, and noise issues are unresolved at this time. This task consists of:

1. Detailed evaluation of Institute of Gas Technology reports, perhaps with some additional help from IGT.

2. Visit S.R.M., Sullair, Gardner-Denver, etc. to assess their interest and estimates for cost, producibility, and noise aspects.

3. Select a suitable manufacturer as a subcontractor to design and produce prototype expanders and compressors for the chosen engine. This includes a detailed design effort aimed at production.

This should be completed in 12 months.

Task 5 - Combustion System Technology with Ignition Assist

Spark assisted diesels have demonstrated satisfactory multifuel capability and emissions reduction. This task proposes two or three ignition assisted combustion systems be experimentally verified. The activities in this task consist of:

1. Visiting Michael May's Laboratories to see their tests and obtain some consulting advice.

2. Visiting Komatsu to observe their experimental program for spark assisted diesel.

3. Conduct initial lab experiments with a plasma generator and a single-cylinder engine.

4. Prepare special hardware needed for evaluating the selected means of ignition assist to be used in the engine prepared under Task 1.

This task should take 9 months.

SECOND YEAR

Task 6 - Baseline Tests of the Adiabatic

Test Engines

This task is primarily aimed at evaluating the suitability of adiabatic components for research programs.

1. Establish performance, emissions, and noise baselines.

2. Compare turbocompound and non-turbocompound test engine results.

Task 7 - Piston Design for Oil-less Operation

1. Use the single cylinder engine to screen the various piston designs for oil-less operation.

2. Endurance test the best design piston on a single cylinder engine for 250 hours.

3. If Step 2 is successful, endurance test the piston for 1000 hours.

This task would take 12 months.

Task 8 - Preheating Concept Testing

This is the first experimental phase of the preheating concept development. The activities are:

1. Procure proper heat exchanger and associated hardware.

2. Install it in the adiabatic turbocompound engine.

3. Run performance, emissions, and noise tests comparable to Task 6. If there is a measurable benefit, then proceed further.

This task should be completed in 6 months.

Task 9 - Screw Compressor-Expander

In this task, a matched helical compressor and expander would be made and bench tested for performance. Activities are:

1. Subcontractor completes the design and manufacturers prototypes.

2. Cummins will test for performance, response, and noise on component test stand.

This task should be completed in 12 months.

Task 10 - Experimental Test of Combustion Systems

This task will be the experimental phase of the various combustion systems. Single-cylinder engine tests with spark assist and plasma assist are proposed.

Activities are:

1. Component preparation.

2. Single-cylinder engine tests (performance and emissions).

3. Preparation for multicylinder engine tests.

THIRD YEAR

Task 11 - Compounding System Testing and Analysis

In this task, the adiabatic compounded engine configuration will be tested and compared to the Cummins turbocompound engine. The screw compressor-expander with part load preheating appears to be the main feature at this time. Activities are:

1. Full engine testing.

2. VMS analysis based on experimental fuel maps.

3. Cost analysis.

4. Market analysis.

This task should be completed in 12 months.

Task 12 - Applications of the Technologies Developed in this Program

All of the technologies developed in this program were included in the analytical study of the passenger car diesel. Medium and heavy duty diesel applications are likely to include some or all of these technologies depending on individual constraints. This task will identify some specific applications where these technologies could be successfully commercialized.

This task should be completed in 6 months.

Task 13 - Testing for Multi-fuel Capability

The selected ignition assist system will be tested for performance and emissions with at least three different fuels.

This task should be completed in 12 months.

Task 14 - Durability Testing

The configuration selected in Task 11 will be tested with and without oil for durability in a test cell for 1,000 hours.

This task should be completed in 12 months.

FOURTH YEAR

Task 15 - Durability Test in a Vehicle

The best configuration will be subject to a 100,000 mile durability test.

This task should be completed in 10 months.

Task 16 - Final Report

All the activities, conclusions, and recommendations will be compiled into a final report.

This task should be completed in 6 months.